Recovery of phosphorus from animal manure

Chris Schott

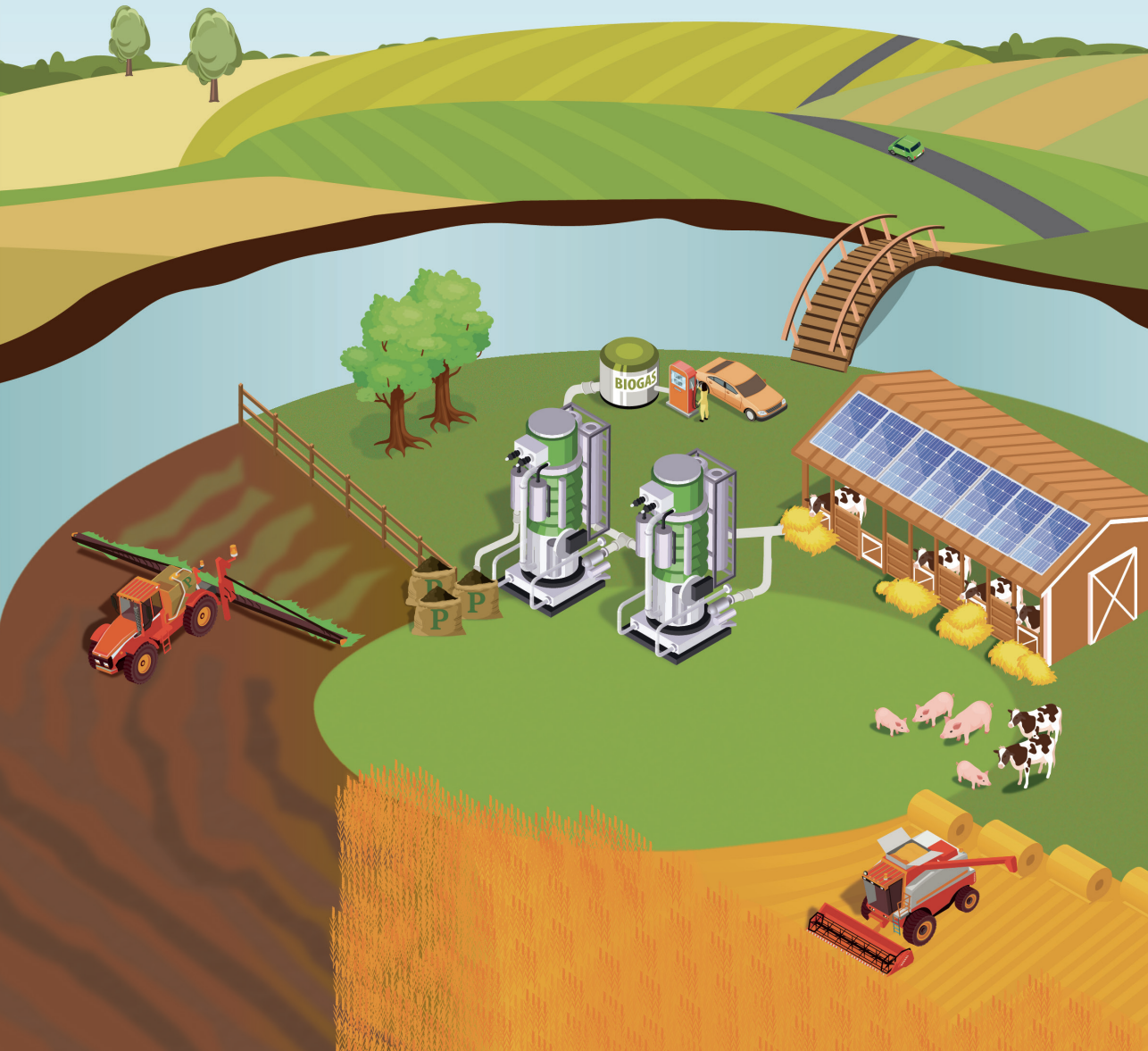

Propositions

1. Calcium phosphate granules form in manure in the same way bones form in the human body. (this thesis)

2. Inorganic carbon is the greatest obstacle to calcium phosphate granulation in manure. (this thesis)

3. Categorizing science into disciplines is helpful only at the beginning of a research career.

4. Amorphous thinking by scientists leads to crystal-clear perspectives on research.

5. Technological readiness depends more on demand than on the technology itself.

6. Unsustainable short-term solutions are tedious necessities.

7. As a society, we are as far from a circular economy as we are now from the neolithic revolution (10,000 BC).

8. Agricultural intensification has an optimum.

Propositions belonging to the PhD thesis, entitled
Recovery of phosphorus from animal manure
Chris Schott
Leeuwarden, 2 June 2023

RECOVERY OF PHOSPHORUS FROM ANIMAL MANURE

Chris Schott

Thesis committee

Promotor
Prof. Dr C.J.N. Buisman
Professor of Biological Recovery and Reuse Technology
Wageningen University & Research

Co-promotors
Dr R.D. van der Weijden
Researcher, Environmental Technology
Wageningen University & Research

Dr J.R.M.A. Cunha
Scientific advisor
IUTA, Institute for Energy and Environmental Technology

Other members
Prof. Dr P.W.G. Groot Koerkamp, Wageningen University & Research
Prof. Dr I. Angelidaki, Technical University of Denmark, Kongens Lyngby, Denmark
Prof. Dr J. Keller, The University of Queensland, Brisbane, Australia
Dr Ö.S. Türkmen, Koninklijke Oosterhof Holman, Grijpskerk

This research was conducted under the auspices of the Graduate School for Socio-Economic and Natural Sciences of the Environment (SENSE)

Recovery of phosphorus from animal manure

Chris Schott

Thesis

submitted in fulfilment of the requirements for the degree of doctor
at Wageningen University
by the authority of the Rector Magnificus,
Prof. Dr A.P.J. Mol,
in the presence of the
Thesis Committee appointed by the Academic Board
to be defended in public
on Friday 02 June 2023
at 4 p.m. in De Harmonie, Leeuwarden

Chris Schott
Recovery of phosphorus from animal manure,
214 pages.

PhD thesis, Wageningen University, Wageningen, the Netherlands (2023)
With references, with summary in English

ISBN 978-94-6447-606-4
DOI https://doi.org/10.18174/588466

Table of contents


P
P

1

Introduction

1.1. The Neolithic Revolution – From 4 million to 200 million people in 10,000 years

The history of animal husbandry and agriculture started about 12,000 years ago with the Neolithic Revolution or the First Agricultural Revolution. At the time, humans started to domesticate plants and animals in several places on earth [1]. About 7,000 years ago, agricultural practices came to Europe from the Middle East. People formed larger settlements, exploiting wild grains and herding animals [2, 3]. Crops and herded animals started to become the common source of food instead of foraging. Not long after, there is indication that cheese was produced and further integration of animals into agriculture began [4]. The increase of staple food consumption and production allowed one to produce an excess of food. The rise of agriculture transformed human demographics, environments, and statures. Agriculture was a more stable source of food than foraging and allowed the human population to grow. Humans started to design their environments so that the areas around settlements could efficiently provide crop growth and herd animals. Animal and human manure would go back to the land to provide nutrients to grow food and feed [5, 6]. However, the new, mainly grain-based diet caused the peoples' stature to change. People grew less in height, suffered from more chronic diseases such as osteoporosis and caries, and famines were more common than among their foraging ancestors [7, 8].

1.2. The Green Revolution – From 1.5 billion to 6 billion people in 100 years

Agriculture continued to develop over time by implementing the use of animals, irrigation systems, and planting methods and the world population slowly increased. However, the most drastic change and effect on the world population was during the Green Revolution, which brought about the invention and distribution of more efficient crop varieties, pesticides, and synthetic fertilizers [9, 10]. The new crop varieties offered higher yields, but needed more fertilizer input. Mining phosphorus and potassium and converting nitrogen gas into ammonia via the Haber Bosch process enabled the production of synthetic fertilizer [11]. Synthetic fertilizers allowed agricultural productivity to reach new heights in the twentieth century [12]. The intensification and enormous increase in productivity yielded enough food for the world population to quadruple to 6 billion people in the twentieth

century. The annual growth rate of the world population did not exceed 0.04% until 1700; however, in 1968, it peaked at 2.1% [13].

The Green Revolution enabled not only the production of more food but also more nutritious food. For the first time since the Neolithic Revolution, human stature was comparable with the stature of foraging ancestors. Part of this change in stature was due to the increased consumption of animal products [14]. From 1961 to 2001, global meat and dairy production increased by 245% and 70%, respectively. However, the land used for pasture and crop production only increased by 10% and 30%, respectively [15], indicating the dimensions of intensification in agriculture. The new required amounts of food necessitated stable agricultural production and optimizing production practices to keep high yields. Until the twentieth century, plowed-down legumes and manure provided the most nutrients for agriculture, but were overtaken by synthetic fertilizers to more easily meet nutrient requirements of crops. At the time, more nutrients seemed better for maximizing the production of food and feed. The intensification of livestock led to a higher abundance of manure, which was also mainly applied on land. The total application of nutrients from synthetic fertilizers and manure peaked in the 1980s beyond crop needs [16].

1.3. Consequences of intensification

The excessive application of nutrients on agricultural land soon caused pollution in surface and groundwater bodies, leading to counteractions during the end of the twentieth century. In the EU in 1991, the Nitrate Directive was implemented to protect water bodies from nitrogen pollution from agricultural sources [17]. The directive aimed to monitor and lower the application of nitrogen fertilizer and reduce the runoff of nitrogen to the environment. The actions included designating nitrate-vulnerable zones with special protection, soil analysis, implementation of nutrient-catching crops during and prohibiting the fertilizer application in periods with a high risk of runoff. From 1 October to 1 February or when the soil is soaked, frozen or covered with snow, the application of fertilizer became prohibited. Along with this action came the requirement to have enough manure storage capacity for 6–10 months, bridging the months when the application was prohibited. In 1998 and 2002, the application of manure was further limited to 210 and 170 kgN ha^{-1} $year^{-1}$, respectively [16]. The largest surpluses in nitrogen application and manure were in the Netherlands and Flanders, followed by the western regions of Germany and

Denmark [16]. The intense livestock farming in these regions, combined with the new regulations, required solutions for handling the manure. These regions of nutrient hotspots started to treat and or transport their manure to regions with lower livestock density where it could be applied on land according to the Nitrate Directive. However, the transport of manure in trucks for hundreds of kilometers opens the potential for more efficient approaches.

Today, the Netherlands still struggles to fully comply with the Nitrate Directive in terms of ground and surface water quality. In 2019, the Council of State ruled that the Dutch government's strategy to reduce excess nitrogen was in breach of the Nitrate Directive [18]. This forces the Dutch government to act and improve its strategy to reduce nitrogen emissions mainly from traffic and industry (NO_x), and agriculture (NH_3), and to protect nitrate-vulnerable zones better. The new goals are to reduce nitrogen emissions by 50% in regular zones and 75% in nitrate-vulnerable zones by 2030 [19]. An immense task that could follow in other nutrient hotspot regions.

1.4. Nutrient hotspots and livestock farming

Regions with intensive agriculture and especially livestock farming accumulate nutrients by importing them not only as fertilizer but also as feed. The import of nutrients in food and feed is not limited. The high yields of the livestock sector depend on feeding the animals on highly nutritious diets. While most feed for cattle is grass and corn and for pigs grains and corn, most dry weight and an important part of the nutrition comes from the concentrate feed [20, 21]. Concentrate feed often contains products rich in nutrients and even the addition of them in the form of powders. The largest concentrate feed legumes in the Netherlands are soybeans imported mainly from Latin America and the USA [22]. The oil of soybeans is extracted and the oilless fraction is roasted, resulting in soybean meal, which is fed as concentrate to livestock. It is rich in nitrogen, potassium and phosphorus [23]. While diets are primarily based on nitrogen and phosphorus, the supplementation of potassium is often in excess. The concentration of potassium in soybeans, for example, is higher than required for animals and causes an enrichment of potassium in animal manure. The application of manure on land can cause a further accumulation of potassium in the soil and crops, enriching potassium in the soils of countries with intensive livestock farming and extracting it from countries

with intensive feed production [24]. Similarly, nitrogen and phosphorus are also accumulating in countries with intensive livestock farming, but their accumulation is more proportional to the intensity of livestock farming compared to potassium.

The accumulation of nutrients in countries with intensive livestock farming makes exportation of manure nutrients a necessity. Especially, the demand for nutrients in regions with low nutrient input could make use of them. However, transport of manure over long distances is not desirable. Instead, the recovery of manure nutrients in concentrated form would allow for better local reuse and eventually longer distance transport. Currently, the limitation of using manure to supply nutrients is the inconsistent release of nutrients in soils and their concentration ratio. Although more nitrogen could be used on agricultural land from manure, the phosphorus content would exceed crop needs and likely runoff [25, 26]. Separating manure nutrients and recovering them in a concentrated form could replace synthetic fertilizers and the natural resources required to produce synthetic fertilizers, enabling the sustainable valorization of manure nutrients.

1.5. Key nutrient: phosphorus

From the three primary nutrients (i.e., nitrogen, potassium, and phosphorus), phosphorus is likely to have its natural sources depleted first. The natural phosphorus source, phosphate rock, is diminishing in quantity and quality. The remaining ores have higher degrees of pollution with heavy metals and radioactive material. Furthermore, most phosphate rock reserves are in a few countries, with 70% in the Western Sahara under the control of Morocco [27, 28]. The EU member states import their phosphorus from mines in Morocco and Russia. However, the geopolitical conflict in Ukraine and the consequential sanctions cut the supply of phosphorus from Russia, increasing the price of phosphorus fertilizer. The EU urges member states to enhance the recovery of phosphorus from secondary resources to become less dependent on primary sources [29].

Animal manure is the largest secondary source of phosphorus and can become more important as a resource if used more efficiently [30]. The recovery of phosphorus from animal manure would need to be sufficiently concentrated to qualify for fertilizer production. The separation of phosphorus from animal manure and its other nutrients (i.e., nitrogen and potassium) would allow the individual and

optimized use of the three primary nutrients. The question is: How to efficiently recover phosphorus from animal manure?

1.6. Phosphorus recovery

Pig and cattle manure are the most abundant types of manure in the EU and therefore the focus of this research [31]. From these manures, phosphorus can be recovered mechanically on size or density, biologically by growing organisms that are rich in phosphorus, such as algae, or chemically through precipitation and crystallization. The mechanical separation of phosphorus proves to be difficult because most of the phosphorus is in particles < 100 μm. The manure can be separated into a thick and a thin fraction, leaving most phosphorus in the thin fraction [32-34]. However, the phosphorus concentration in this fraction remains low (~0.05%P w/w). Additionally, most nitrogen and potassium are also in the thin fraction, inhibiting the individual recovery of phosphorus. More advanced mechanical separation equipment, such as centrifuges, could achieve a better separation efficiency with relatively good selectivity for phosphorus but are for the most part expensive and would require significant amounts of maintenance [35]. Biological recovery methods are limited with respect to phosphorus in solution [36]. Phosphate ions can be transported into living cells and used for biological growth and functioning. A biological recovery could be simple and inexpensive. However, in pig and cattle manure, approximately 80% and 90% of the phosphorus is present in suspended material, respectively [37, 38], being unavailable for biological recovery. For enabling biological recovery of more phosphorus from animal manure, pig and cattle manure would need to be diluted with significant amounts of water to increase the presence of phosphate ions [36]. This would dilute other nutrients and even increase the amount of manure. Chemical treatments based on precipitation also commonly require the presence of phosphate ions. Therefore, manure phosphorus is first solubilized with an acidification step before increasing the pH again so that it can precipitate as struvite or calcium phosphate. The pH swing from a high value to a low value and a high pH value again requires the addition of significant amounts of chemicals and a complex treatment process, making it hardly economically feasible [39].

The ideal treatment for the recovery of phosphorus from animal manure would probably combine the three approaches: A biologically assisted precipitation process

to save on chemicals that enables simple mechanical separation. A prospective process is calcium phosphate granulation, which was discovered during concentrated black water (toilet water) treatment [40]. During the anaerobic digestion of concentrated black water in up-flow anaerobic sludge blanket (UASB) reactors, the formation of granules with an inorganic core of calcium phosphate occurred. While the granulation of biomass in UASB reactors was a well-known phenomenon, the precipitation of calcium phosphate in these granules was new. The precipitation was triggered by a change in the hardness of the water by drinking water suppliers, increasing the calcium concentration. Calcium and phosphorus concentrations became high enough to precipitate on the inside of granules without negatively affecting methane production [41]. On the inside of the granules, the processes of anaerobic digestion caused a slight increase in pH compared to the bulk sludge bed. This microenvironment with an increased pH caused supersaturation and precipitation of calcium phosphate [42]. The longer solid retention time compared to the hydraulic retention time gave more time for the calcium phosphate core to grow. Over time, the calcium phosphate granules became heavier and settled to the bottom of the UASB reactor, where they could be harvested. Calcium phosphate granulation was optimized for concentrated black water treatment. Adding more calcium improved phosphorus removal to almost 90%, which would be recoverable as calcium phosphate granules over time [41].

1.7. Challenges for calcium phosphate granulation in black water and transition to animal manure

The challenges for calcium phosphate granulation in black water were mainly the availability of calcium ions for calcium phosphate formation and having calcium phosphate formation in granules and not on the wall of reactors or in the bulk of the sludge bed. The availability of calcium depended on the abundance of calcium ions and the abundance of inorganic carbon as bicarbonate ions [43]. Bicarbonate ions were binding to calcium ions to form calcium carbonate ($CaCO_3$). Thus, a high presence of inorganic carbon would reduce the availability of calcium to bind to phosphate and form calcium phosphate. Similarly, the availability of phosphate ions is probably important to induce calcium phosphate granulation but was never limiting in black water. A negative effect on the production of methane by forming precipitates was a concern, perhaps limiting the biological activity of the sludge bed. However, methane production was not affected.

Implementing calcium phosphate granulation for the recovery of phosphorus from animal manure might face similar challenges and more. Additional challenges might come with the significant higher concentrations of animal manure compared to black water. The solid content, COD, alkalinity, phosphorus, calcium, magnesium, and more are all approximately ten times more concentrated in pig and cattle manure than in black water. Calcium could preferably bind with the highly abundant inorganic carbon or adsorb to organic material and not be available for calcium phosphate formation. The low abundance of phosphate ions, especially in cattle manure, could inhibit the formation and subsequent granulation of calcium phosphate. The high solid content could limit granule formation and cause calcium phosphate to precipitate on solids outside granules, making its recovery more difficult. The abundance of other cations, such as magnesium, probably increases the competition for binding of phosphate ions, possibly limiting calcium phosphate formation. These possible challenges lead to the following research questions:

- How can calcium phosphate granulation be induced in animal manure treatment?
- How does the addition of calcium affect the recovery of phosphorus and methane production?
- What limits the availability of calcium and phosphate ions in animal manure for calcium phosphate granulation?
- How would calcium phosphate granulation be implemented for animal manure treatment in practice?
- Can calcium phosphate granulation efficiently and feasibly help to increase the reusability of manure and support sustainability in agriculture?

1.8. Scope and outline

The aim of this thesis is to introduce and possibly implement calcium phosphate granulation in the treatment of animal manure. The focus was on pig and cattle, but more so on dairy manure. The four research chapters show and discuss the continuous treatment of the thin fraction of manures in thermophilically operated UASB reactors. Separation was at 200 μm and led to > 90% of phosphorus and almost all nitrogen and potassium in the thin fraction. All reactors described in the thesis were started from their respective manure as inoculum.

The addition of calcium was decisive for calcium phosphate granulation in black water treatment and thus was tested for pig and dairy manure as the first parameter in Chapters 2 and 3, respectively. In **Chapter 2**, the addition of calcium caused a higher retention of phosphorus and induced calcium phosphate granulation. Calcium phosphate granulation occurred even though 80% of the phosphorus was natively present as struvite in pig manure. Instead of having small struvite crystals distributed throughout the sludge bed without calcium addition, calcium addition caused the formation of calcium phosphate granules, containing the majority of phosphorus (79%).

In **Chapter 3**, the addition of calcium to the UASB reactors that treat dairy manure caused greater removal of phosphorus and significantly improved methane production. However, calcium phosphate granulation did not occur because calcium was primary precipitated as $CaCO_3$. Additionally, the practical absence of phosphate ions and the abundance of magnesium also inhibited the formation of calcium phosphate.

The limitations for calcium phosphate granulation from dairy manure found in Chapter 3 were meant to be solved in **Chapter 4**. Before the UASB reactor, the addition of a continuously stirred tank reactor operating at low pH removed inorganic carbon and released phosphorus into solution. Subsequently, calcium phosphate granulation started in the UASB reactor and granules with the highest phosphorus content recovered from a UASB reactor were obtained. The low pH could be naturally increased in the UASB reactor because of the active anaerobic digestion. However, the pH regime was sensitive to changes in loading. An increase in loading quickly lowered the pH in the UASB reactor, causing a disturbance in the anaerobic digestion performance.

In **Chapter 5**, hydrogen gas was added to remove inorganic carbon from the UASB reactor and convert it into methane. By stimulating hydrogenotrophic methanogenesis, the biogas could be upgraded to contain more methane, and simultaneously calcium phosphate granulation could be induced by increasing the availability of calcium through potential carbonate removal. Hydrogen addition improved methane production, but calcium phosphate granulation was not induced. The conversion efficiency of hydrogen was low. However, the relative abundance of hydrogenotrophic methanogens increased in granules, indicating that the addition of hydrogen gas has potential to induce calcium phosphate granulation.

In **Chapter 6**, the challenges for calcium phosphate granulation in animal manure treatment are discussed regarding the research questions. On the basis of the remaining challenges, optimization and improvements of the process and the potential impact on recovery products such as calcium phosphate granules are discussed. Finally, the implementation and impact of phosphorus recovery through calcium phosphate granulation on livestock farming and agriculture as a whole are discussed.

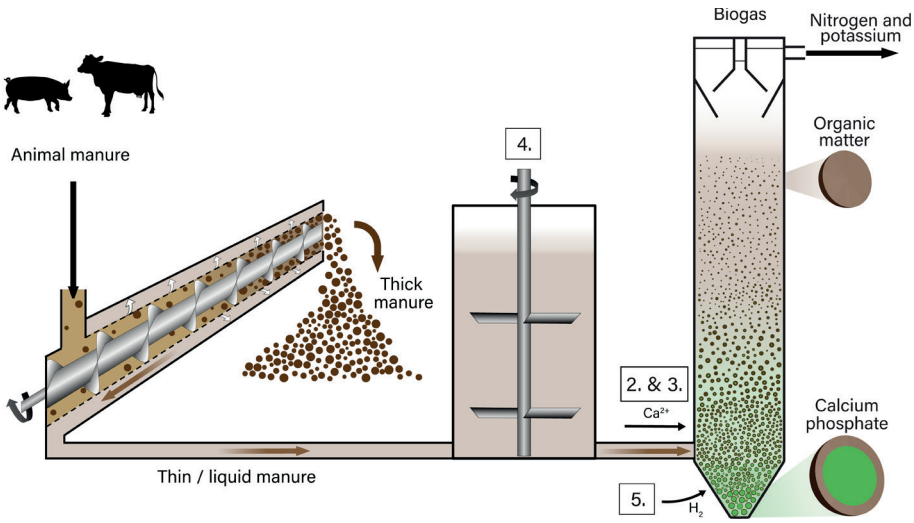

Fig. 1.1. Schematic representation of CaP granulation during anaerobic digestion with numbering corresponding to the research chapters mentioned in scope and outline.


P
P

2

Phosphorus recovery from pig manure: Dissolution of struvite and formation of calcium phosphate granules during anaerobic digestion with calcium addition

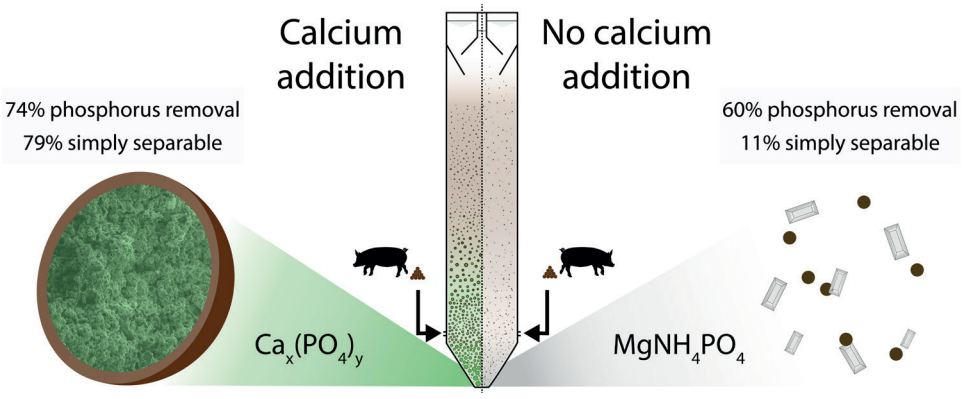

This chapter was published as:

C. Schott, J.R. Cunha, R.D. van der Weijden, C. Buisman, Phosphorus recovery from pig manure: Dissolution of struvite and formation of calcium phosphate granules during anaerobic digestion with calcium addition, Chemical Engineering Journal (2022) 135406. DOI: 10.1016/j.cej.2022.135406.

Abstract

Phosphorus is an essential but finite and scarce element, which is used extensively in pig farming. For recovering phosphorus from pig manure, we hypothesize that calcium addition during anaerobic treatment can trigger calcium phosphate granulation and enable efficient phosphorus recovery. In this study we tested the recovery of phosphorus from pig manure by adding calcium chloride during anaerobic treatment. Size-separated (< 200 μm) pig manure was treated in two identical up-flow anaerobic sludge blanket reactors for 456 days. Calcium was supplied to one of the reactors to study calcium phosphate granulation.

Calcium addition showed a positive effect on treatment stability and efficiency, increasing chemical oxygen demand and phosphorus removal. Phosphorus removal increased from on average 60% without calcium addition to 74% with calcium addition. The addition of calcium increased the phosphorus concentration in larger particles, calcium phosphate granules, (79% >0.4 mm compared with 11% without calcium addition) in the reactor with calcium addition, which enables separation and a transport reduction of 85% for the recovered phosphorus. The main phosphorus phase in the reactor sludge bed changed from struvite to calcium phosphate with calcium addition. The Mg:P molar ratio was 0.09 with calcium addition and 0.88 without calcium addition in particles larger than 2.5 mm. Thus, calcium addition enhances the treatment of pig manure and enables phosphate recovery as calcium phosphate granules.

2.1. Introduction

Phosphorus is a key nutrient to produce food, but its natural resources are finite [44]. Phosphorus has been mined for decades and brought to countries with intense agricultural activity to enhance soil fertility and crop yield [45]. In 2018, soils in the EU-27 received 1.1 million tons of imported mineral phosphorus fertilizer [46]. In regions with intense agricultural activity, the phosphorus accumulates in soils and waste streams, also called secondary phosphorus sources. The phosphorus from secondary phosphorus sources needs to be reused and redistributed geographically to avoid future phosphorus scarcity and pollution [47-49]. However, the phosphorus availability is often less predictable and varies more in secondary sources than in mineral fertilizer [50]. The unpredictability of phosphorus availability can lead to inferior fertilization with less crop growth if overestimated, and to a surplus of phosphorus and pollution of the environment if underestimated [51-54]. Furthermore, the redistribution of phosphorus from secondary sources is costly because of the low phosphorus concentrations and the distance between excessive phosphorus and arable land requiring phosphorus application [55].

Livestock manure is the largest secondary phosphorus source, but its application on soils is limited to protect the environment from nutrient leaching; this limitation leads to an excess of manure [48]. In the European Union, the application of livestock manure is limited to 170 kg of nitrogen per hectare per year, but there is no direct application limit for phosphorus from manure [56]. Only a few member states including the Netherlands have established a national regulation for limiting the phosphorus application from manure. In the Netherlands, the phosphorus application is limited to 75 kg P_2O_5 per hectare of grassland per year and 40 kg P_2O_5 per hectare of arable land per year [57, 58]. Any amount of manure exceeding the nutrient application limits for nitrogen and phosphorus needs to be transported to treatment facilities or areas where it can be applied. Furthermore, in the Netherlands, livestock farmers are obliged by law to treat 10 to 59% (dependent on the manure production of the region) of the excessive manure either themselves or have a contractor who agrees beforehand to treat or export their excess of manure [59, 60].

In the Netherlands, most pig farms have insufficient land for their produced manure, so they need to pay for the transportation and application or treatment of their excessive manure. In 2019, in the Netherlands, a pig farm had on average an excess of about 3100 tons of manure a year which cost about €64K (roughly €20 ton_{manure}^{-1}) for transport

and treatment, the largest manure-handling costs in the Dutch livestock sector [61]. However, each ton of pig manure (PM) contains about €10 worth of nutrients, which are of very low value when present in raw PM [61]. Therefore, more efficient recovery and reuse of nutrients from PM has enormous potential to provide relief for the pig-farming sector financially and significantly mitigates the environmental impact of those nutrients. Furthermore, in the Netherlands, in 2019, mineral phosphorus fertilizer made up about 13% of phosphorus fertilization, but mineral nitrogen fertilizer made up about 47% of nitrogen fertilization [61]. As a consequence, in the Netherlands, less mineral phosphorus fertilizer could be replaced by nutrients originating from PM than mineral nitrogen fertilizer. Separating the nutrients originating from PM could allow a more economical geographic redistribution of phosphorus to regions where it is needed and more application of nitrogen within the Netherlands.

This study aims to treat PM and recover phosphorus from PM as calcium phosphate granules during 456 days of anaerobic digestion in an up-flow anaerobic sludge blanket (UASB) reactor with calcium addition. This is an analogous strategy for treatment of black water and phosphorus recovery from black water [41]. We hypothesize that calcium addition will increase phosphorus removal in the UASB reactor by inducing particle aggregation. The aggregated particles are expected to be rich in calcium, leading to calcium phosphate precipitation and granulation. Increased particle size with higher phosphorus content will simplify phosphorus separation, ultimately improving recovery efficiency from PM. Calcium phosphate granulation in PM would open a large secondary source for efficient phosphorus recovery. Such recovered calcium phosphate could relieve the use of primary phosphorus sources as fertilizer in agriculture and allow individual use of phosphorus without other nutrients, which is an advantage over other recovery products such as struvite [62]. Furthermore, the recovered phosphorus can be reused and transported better and cheaper than raw PM because it is standardized and more concentrated.

2.2. Materials and methods

2.2.1. Experimental setup

Two similar double-walled 45 L UASB reactors were anaerobically digesting PM at 55 °C for 456 days (Fig. 2.1.). The PM was collected directly from a pit of a fattener stable accommodating 4400 animals in Marum, the Netherlands. Immediately after collection, the PM was manually sieved through a sieve bend with a grid size of 200 μm

(Estrad sieve bend, SI, Fig. S2.1.). After separation, the thin manure (filtrate) was stored in jerry cans in a climate room at 4 °C. This separated PM was used to fill a continuously stirred container placed inside a fridge next to the reactors. Both reactors were fed from the same influent container, and piping to the reactors was equal length.

The influent was pumped every 2 hours for 1 min to reach a feeding of 1200 mL day^{-1}, which corresponds to an organic loading rate (OLR) of 1 g chemical oxygen demand (COD) L^{-1} d^{-1}. A shared programmable logic controller (PLC; Siemens Logic) controlled master timer coordinated pumping. The effluent of each reactor was collected in 10 L jerry cans. The produced biogas went through a sampling point with a rubber septum towards a water lock followed by a drum gas flow meter before entering the gas exhaust.

For testing the effect of calcium addition, one UASB reactor was supplied with calcium addition (R_{Ca}), while the second served as a reference reactor (R_R) without calcium addition. The calcium in R_{Ca} was added as $CaCl_2 \cdot 2H_2O$ solution through a pipe with five 5 mm diameter openings. The openings were horizontally distributed for spreading the calcium inside the reactor. The added calcium solution was kept at 8% volume of the incoming PM to minimize dilution of the reactor content. The concentration of the calcium solution was adapted weekly, based on the influent total calcium and phosphorus concentrations, to supply a total molar ratio of Ca:P of 2. That molar ratio should ensure a supply of sufficient calcium to allow formation of the most stable calcium phosphate hydroxyapatite (HAP), which has a Ca:P molar ratio of 1.67. Previous research has shown that a total molar ratio Ca:P of at least 2 could induce calcium phosphate precipitation in black-water treatment [41]. The calcium solution was pumped for 30 sec every 2 hours together with the influent. The PLC timing the influent pumping also timed the calcium solution pumping to assure simultaneous inflow of both streams.

Both reactors had five vertically distributed sampling points for the sludge bed as shown in Fig. 2.1. During sludge bed sampling, the valves were briefly completely opened to sample 200 mL from sampling points 1 to 4 and 500 mL from sampling point 0. The order of sampling was from top to bottom, because sampling at the lower sampling locations affects sampling at the upper sampling points, but not vice versa.

pH, redox and temperature were measured online with three vertically distributed sensors that reached the reactor center with their tips (Memosens CPS16D-1014/0 Orbisint). The sensors entered the reactors through three 45° inclined valves with rubber tightening to enable maintenance without stopping the reactor's operation.

The online measurements were logged digitally every hour. The online measured temperature did not vary more than 1–2°C, at the three locations sensors were placed. The biological reactions could have led to little heat release but were likely inhibited and insignificant [63].

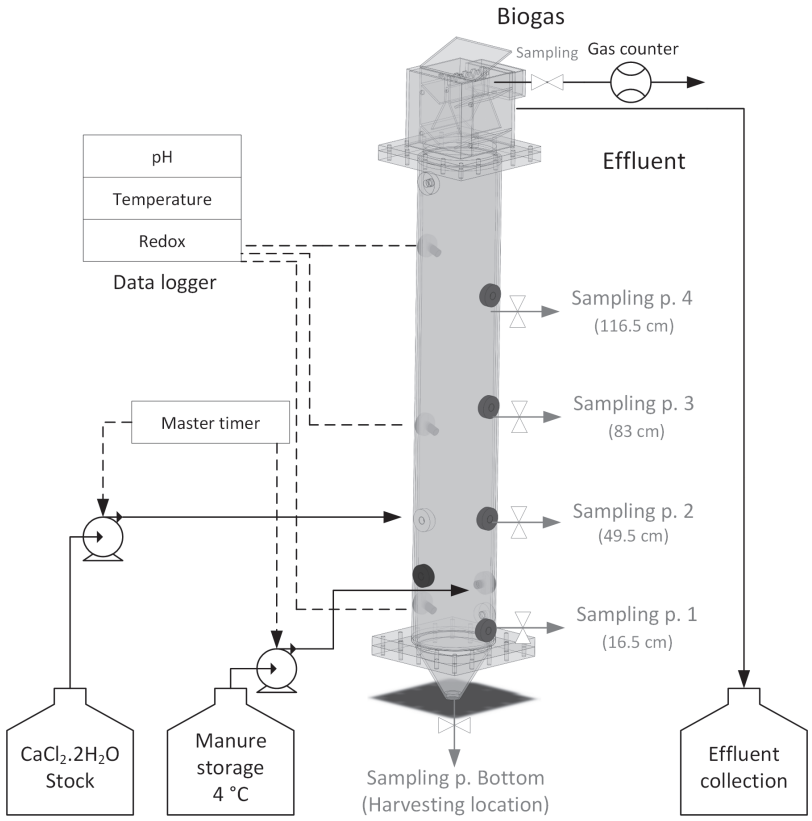

Fig. 2.1. Schematic representation of the setup including the UASB reactor with heating in a double wall. A cone-shaped bottom piece is for accumulation and harvesting of potential phosphorus-rich particles. On top, a gas-liquid solid separator was placed made from polypropylene. The gas was led towards the gas exhaust, the liquid towards the overflow and solids remain in the reactor through inclined plates. The reactor shown here represents R_{Ca} with calcium addition, while R_R is identical but without calcium addition. pH measurements in the sludge bed were in situ, while influent and effluent pH were measured at room temperature during weekly analysis.

2.2.2. Analysis and sampling program

The analysis and sampling program was designed to get detailed insights into both reactors and their differences in performance. The high frequency and variety

of measurements allows parameters to be cross-checked and their viability to be proofed for each reactor individually and in comparison.

The flows of effluent, calcium solution, and produced biogas were measured daily. The amount of produced effluent and consumed calcium solution were measured gravimetrically. The densities were tested but did not vary significantly from 1 kg L^{-1}. The produced biogas was noted from the drum flow meter.

The composition of influent, effluent, and biogas were analyzed weekly. The influent was sampled for analyses at a t-connection just before entering each reactor, to ensure an accurate representation of influent entering the reactors. For sampling, the reactor inlet valve was closed, and the sampling valve at the t-connection was opened before the inlet pumps were started. The effluent was collected in 1 L flasks over 24 hours to have fresh effluent, minimizing the loss of volatile and time-sensitive compounds before analyses. Temperature-sensitive compounds had been considered and none of them was significantly changed to influence our main goal of studying calcium phosphate granulation.

Both samples were analyzed in duplicate for pH, and total solids, volatile solids, total suspended solids and volatile suspended solids (TS, VS, TSS and VSS, respectively). The solids were incinerated at 550 °C to determine the volatile fraction according to the standard method [64]. The suspended solids were determined by using paper filtration with a black ribbon ashless filter (Whatman, Grade 589/1, 12-25 μm). The paper filtrate was collected and used for total carbon, total organic carbon, and inorganic carbon (TC, TOC, and IC, respectively) analyses with a Shimadzu TOC analyzer. Further, the paper filtrate was filtered with a 0.45 μm glass fiber Whatman filter. The membrane filtrate was used to determine:

- Soluble elements (phosphorus, calcium, magnesium, sulfur, iron, sodium and potassium [P_{sol} Ca_{sol} Mg_{sol} S_{sol} Fe_{sol} Na_{sol} and K_{sol}, respectively]) with inductive coupled plasma optic emission spectroscopy (ICP-OES; Perkin Elmer Optima 5300 DV with an internal yttrium standard);
- Anions and cations (PO_4^{3-}, SO_4^{3-} Cl^-, and Ca^{2+}, Mg^{2+} and NH_4^+, respectively) with ion chromatography (Metrohm 930 Compact IC flex with a conductivity detector and Metrosep A supp 5 150/4 mm column for anions and Metrosep C4 150/4 mm column for cations);
- Volatile fatty acids (VFA) such as acetic, propionic and butyric acid with IC (Metrohm 930 Compact IC flex with a conductivity sensor and a Phenomenex Synergi 4u hydro-RP 80A column).

COD was analyzed in the raw, paper filtrate, and membrane filtrate (COD_{tot}, $COD_{pap,}$ and COD_{sol}, respectively) with Hach Lange kits LCK014. Total elements (P_{tot}, Ca_{tot}, Mg_{tot}, S_{tot}, Fe_{tot}, Na_{tot}, and K_{tot}) were analyzed from raw samples with ICP-OES after performing a microwave-induced (Milestone Ethos Easy) acid digestion with 69% HNO_3.

On operation days 70, 98, 139, 165, 221, 229, 237, 244 and 341 and after stopping the operation, the sludge bed of both reactors was sampled and analyzed in duplicate for solids (TS, VS, TSS, and VSS) and total elements (P_{tot}, Ca_{tot}, Mg_{tot}, S_{tot}, Fe_{tot}, Na_{tot}, and K_{tot}) as described before. Furthermore, crystallographic characteristics were analyzed by X-ray diffraction (XRD) with a Bruker D8 Advance with a diffractometer of 280 mm measurement radius using Cu radiation, Linear PSD 3° detector opening, divergence slit at 0.58°, and a soller slit at 2.5°, scanning electron microscope (SEM) JEOL JSM-6480LV coupled with NORAN Systems SIX energy dispersive X-ray (EDX) and thermogravimetric analyses (TGA; Mettler Toledo, TGA 2). The TGA operated at a heating rate of 10°C per minute and under nitrogen atmosphere until 550°C, where it was switched to oxygen to combust organic material. Additionally, the liquid of the sludge bed was analyzed for the same analytes as during the weekly analysis on operation day 165. On day 165, the samples were prepared for analysis within 4 hours. After operation day 165, the sampling of the bottom of R_{Ca} (tap 0) was not representative because accumulation of large solids blocked the sampling port and only allowed sampling of liquid. The clogging of the lowest sampling valve must have happened between operation day 165 and 221 (see section 2.4.2). The sludge bed samplings considered as non-representative were not used for this study. For the solid retention time (SRT) determination of phase 3, the concentration of solids at tap 1 was used as estimate for tap 0 which could have led to an underestimation of the actual SRT during phase 3. After the operation stopped, both reactors were opened from the top and the sludge bed was removed stepwise from top to bottom with a large spoon to retrieve representative samples of each height. These samples underwent a particle size distribution analysis in addition to the previous mentioned analysis for sludge bed samples. For the particle size distribution, the sludge bed was sequentially sieved with analytical sieves of mesh sizes 2.5, 2, 1.4, 0.9 and 0.4 mm supplied by VWR. The separation experiment resulted in six fractions of > 2.5 mm, 2.5–2 mm, 2–1.4 mm, 1.4–0.9 mm, 0.9–0.4 mm and < 0.4 mm (Fig. S2.2).

2.2.3. Calculations

The OLR, SRT and methanization were calculated as described by Halalsheh et al. [65] and De Graaff et al. [66]. Suspended COD (COD_{sus}) was determined as the

difference of COD_{tot} and COD_{pap}. Colloidal COD (COD_{col}) was determined as the difference of COD_{pap} and COD_{sol}. The suspended species of elements (P_{sus}, Ca_{sus} and Mg_{sus}) were determined as the difference of total elements (P_{tot}, Ca_{tot} and Mg_{tot}) and soluble elements (P_{sol}, Ca_{sol} and Mg_{sol}).

For the cumulative removal, the daily flow data were multiplied with the respective weekly measured concentration of influent and effluent to receive the total amounts entering and leaving the reactors. The cumulative data were taken for influent and effluent, and the difference determined the removal. The deviation in cumulative removal was determined by cumulating the errors of measurement between the duplicates. The cumulative removal results were reset for each operational phase.

2.3. Results

2.3.1. Treatment performance

Anaerobic digestion

The experiment was carried out over 456 days where both reactors were continuously operated and fed with real PM collected from a local pig farm. Additionally, the experiment was long enough to include the seasonal impact on the manure composition. The operational time of both reactors was divided into four phases (Fig. 2.2, SI, A. b and c). Phase 1 (day 0–119) was the start-up phase of the reactors with PM collected during spring. The concentration of all analytes increased from early to later spring, represented by TS hereafter (59 ± 8 gTS L^{-1}). Phase 2 (day 120–175) coincided with PM collected during the summer, which was more concentrated in all analytes (68 ± 2 gTS/L) compared with PM collected during phase 1. Phase 3 (day 176–287) coincided with PM collected during autumn and start of winter, having lower concentration of all analytes compared with phases 1 and 2 (51 ± 12 gTS/L). Phase 4 (day 288–456) coincided with PM collected during the end of winter, spring and early summer, having higher concentration in all analytes than in phase 3 (61 ± 13 gTS/L). Both reactors received the same influent and the variation of analytes between influents measured just before entering the reactors was within 5%, assuring the comparability of both reactors.

The desired OLR was 1 $gCOD_{tot}\ L_{reactor}^{-1}\ d^{-1}$ for both reactors but fluctuated with the COD_{tot} concentration in PM because the HRT was kept close to 40 days. The removal of COD_{tot} remained below 50% for both reactors, but R_{Ca} had higher removals than

R_R (Tables S2.1 and S2.2). The COD_{tot} mostly corresponded to removed COD_{sus} in line with the high TSS removal. R_{Ca} removed more TSS and removed it in a more stable fashion than R_R as shown in the fluctuation of average effluent concentration and the cumulative TSS removal in Tables S2.1 and S2.2. Accordingly, the SRTs throughout the phases were higher in R_{Ca} than R_R (Tables S2.1 and S2.2).

The COD_{sol} consisted for both reactors partly of VFA that were produced but barely consumed to form CH_4 inside the reactors (Table S2.3 and S2.4). Accordingly, the methanization inside both reactors was only about 5% (Tables S2.1 and S2.2.). It is likely that the high ammonium concentration inhibited the methanization (Tables S2.3 and S2.4). Furthermore, R_{Ca} removed more IC than R_R (Tables S2.3. and S2.4). The pH dropped at the bottom of R_{Ca} during phases 3 and 4, which did not occur in R_R (Table S2.5 and S2.6).

Elemental flows (EF)

Phosphorus (EF)

The total phosphorus (P_{tot}) removal over the whole operation time was 60 ± 3% in R_R and 74 ± 2% in R_{Ca} (Fig. 2.2, Tables S2.7 and S2.8). Furthermore, the removal was more stable in R_{Ca} than in R_R, indicated by double the deviation of P_{tot} in the effluent of R_R (40%) compared with R_{Ca} (20%). For both reactors, the average concentration of P_{tot} in the effluent remained similar throughout phases 2–4 in both reactors, but the lower influent concentrations decreased the removal in phase 3 and 4. In the effluent of R_{Ca}, the P_{sol} and PO_4–P made up 7% and 16% less, respectively, of P_{tot} than in the effluent of R_R. The removal of PO_4–P was considerably better in R_{Ca} than in R_R.

Calcium (EF)

In R_{Ca} an average load of 1.5–4.0 gCa^{2+} L^{-1} of influent manure was supplied to stimulate accumulation of phosphorus by precipitating calcium phosphate and triggering calcium phosphate granulation (Tables S2.9 and S2.10). Despite the additional Ca^{2+}, the total calcium (Ca_{tot}) concentration in the effluent was lower and more stable for R_{Ca} (0.64 g L^{-1} with intrinsic standard deviation of 15%) when compared with R_R (0.85 g L^{-1} with intrinsic standard deviation of 48%) (Fig. 2.2). Notably, the soluble concentration of calcium (Ca_{sol}) in the effluent was similar for both R_{Ca} and R_R (0.35 ± 0.02 g L^{-1} and 0.35 ± 0.05 g L^{-1}, respectively). Overall, the calcium removal was higher for R_{Ca} (87 ± 2%) than for R_R (66 ± 3%).

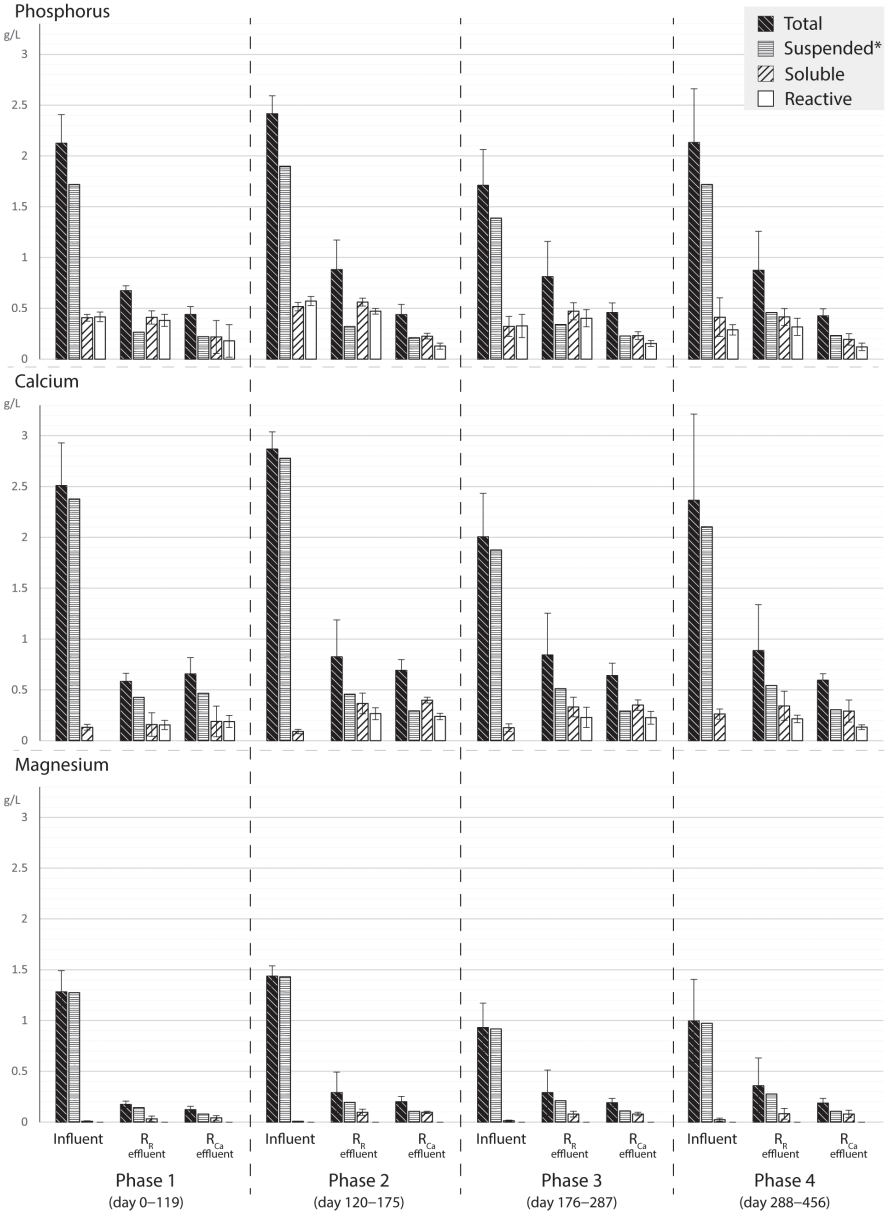

Fig. 2.2. Average influent, effluent of R_R and effluent of R_{Ca} concentrations of phosphorus, calcium, and magnesium over four operational phases where error bars represent the fluctuation in a phase. The elements are represented in total (P_{tot}, Ca_{tot}, Mg_{tot}), suspended (P_{sus}, Ca_{sus}, Mg_{sus}), soluble (P_{sol}, Ca_{sol}, Mg_{sol}) and reactive (PO_4-P, Ca^{2+}, Mg^{2+}). *The suspended fractions are calculated as the difference of total and soluble, but their variation is not shown because of the partly excessive size of the error bar due to the variation in the soluble fractions.

Magnesium (EF)

The influent magnesium was on average for 99% present as Mg_{sus}. The removal of total magnesium (Mg_{tot}) over the whole operation was 76 ± 3% in R_R and 82 ± 3% in R_{Ca} (Fig. 2.2, Tables S2.11 and S2.12). Once more, the variance of the effluent magnesium concentration was much higher for R_R than in R_{Ca}. Soluble magnesium (Mg_{sol}) in the influent was barely detected (7 ± 4 $mgMg_{sol}$ L^{-1}) for both reactors. However, a considerable increase to on average 85 ± 0.1 $mgMg_{sol}$ L^{-1} was observed in the effluent of both reactors, but the concentrations did not significantly differ between the effluents.

2.3.2. Distribution of solids and elements in sludge bed

Distribution of solids

The removed TSS accumulated in both UASB reactor sludge beds the most at the bottom and the least at the top of either reactor (Fig. 2.3). At the top of the reactors, the concentrations were similar: the sludge bed of R_{Ca} contained 49 ± 1 gTSS L^{-1} and the sludge bed of R_R 51 ± 1 gTSS L^{-1}. At the bottom of the reactors, however, the TSS concentration was higher in R_{Ca} (242 ± 1 gTSS L^{-1}) compared with R_R (163 ± 1 gTSS L^{-1}). The VSS made up 54% of TSS in R_{Ca} and 52% in R_R at the bottom and 58% for both reactors at the top.

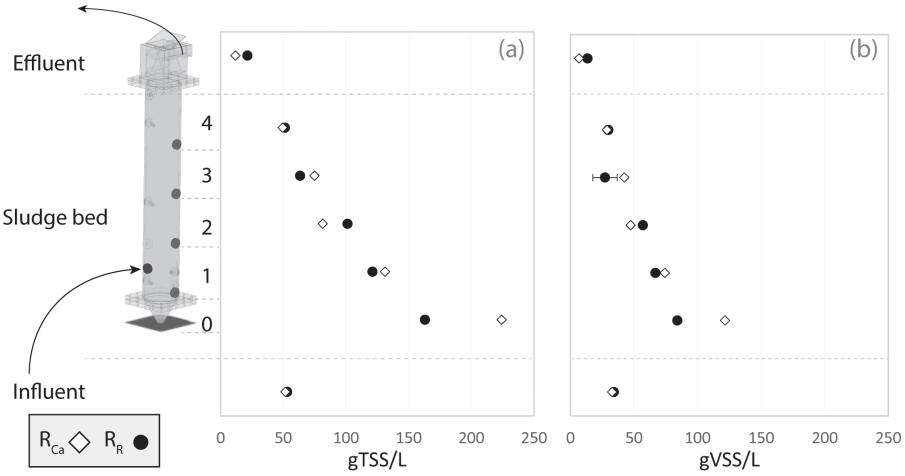

Fig. 2.3. The vertical distribution of TSS and VSS in the sludge bed of the UASB reactors R_R without and R_{Ca} with calcium addition together with the influent (bottom) and effluent (top) TSS and VSS concentrations at operation day 165 (phase 2).

Phosphorus distribution

A noticeable difference in the phosphorus distribution and concentration was observed between the two reactors (Fig. 2.4). In both, the highest fraction of phosphorus was found at the bottom, but a higher concentration was found in R_{Ca} (13.6 ± 0.5 gP_{tot} L^{-1}) when compared with R_R (11.1 ± 0.1 gP_{tot} L^{-1}). By contrast, a higher concentration was found at the top of R_R (3.4 ± 0.0 gP_{tot} L^{-1}) than at the top of R_{Ca} (2.1 ± 0.5 gP_{tot} L^{-1}). The enrichment of phosphorus at the bottom of the sludge bed compared with the influent was 4.5 times for R_R and 6.5 times for R_{Ca}. At the top, the P_{tot} concentration was 3.8 times higher in the sludge bed of R_R than in its effluent and 4.9 times for R_{Ca}, indicating the better removal of phosphorus by R_{Ca} than R_R. At the same time, P_{sol} is considerably less in the sludge bed of R_{Ca} than in the sludge bed of R_R. It can be concluded that addition of calcium promoted precipitation and accumulation of phosphorus in the sludge bed.

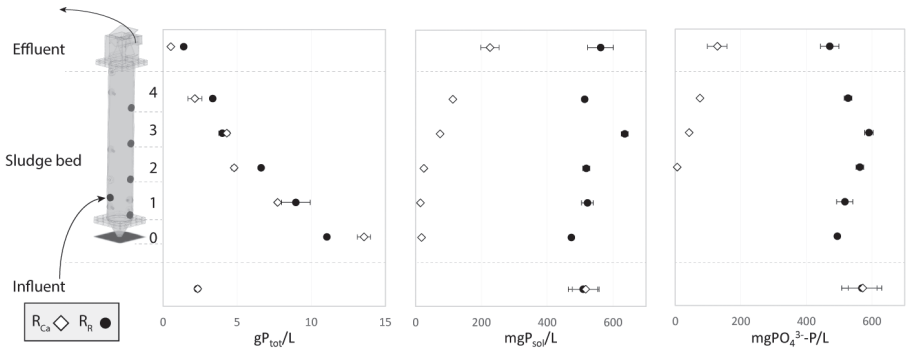

Fig. 2.4. The vertical distribution of total phosphorus (P_{tot}), soluble phosphorus (P_{sol}) and phosphorus as phosphate (PO_4^{3-}–P) in the sludge bed of the UASB reactors R_R without and R_{Ca} with calcium addition together with the influent (bottom) and effluent (top) concentration at operation day 165 (phase 2).

Calcium distribution

The removed calcium accumulated mostly at the bottom of the sludge beds of R_{Ca} and R_R and the least at the top of either reactor (Fig. 2.5). At the bottom of the sludge bed, the Ca_{tot} concentration was higher in R_{Ca} with 25.1 ± 0.8 gCa_{tot} L^{-1} than in R_R (11.5 ± 0.0 gCa_{tot} L^{-1}). At the top of the sludge bed, the Ca_{tot} concentration was higher in R_R (3.9 ± 0.0 gCa_{tot} L^{-1}) than in R_{Ca} (3.0 ± 0.7 gCa_{tot} L^{-1}). Notably, little Ca_{sol} and no Ca^{2+} was available in R_R, but in R_{Ca} both were mostly present at the bottom.

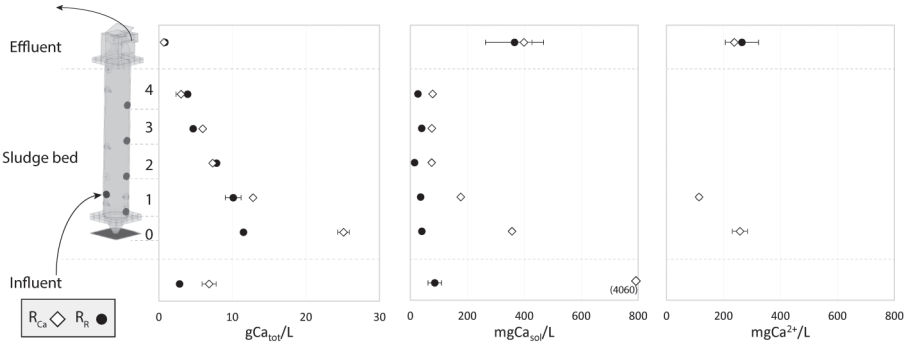

Fig. 2.5. The vertical distribution of total calcium (Ca_{tot}), soluble calcium (Ca_{sol}) and calcium ions (Ca^{2+}) in the sludge bed of the UASB reactors R_R without and R_{Ca} with calcium addition together with the influent (bottom) and effluent (top) concentration at operation day 165 (phase 2).

Magnesium distribution

The removed magnesium accumulated mostly at the bottom of the sludge beds of R_{Ca} and R_R and the least at the top of either reactor (Fig. 2.6). At the bottom of the sludge bed, the Mg_{tot} concentration was higher in R_{Ca} (8.9 ± 0.3 gMg_{tot} L^{-1}) than in R_R (7.8 ± 0.0 gMg_{tot} L^{-1}). Interestingly, at the bottom of R_{Ca}, magnesium was solubilized because Mg_{sol} and Mg^{2+} were detected even though no Mg_{sol} was in the influent or added. At the same positions, Ca_{sol} was detected.

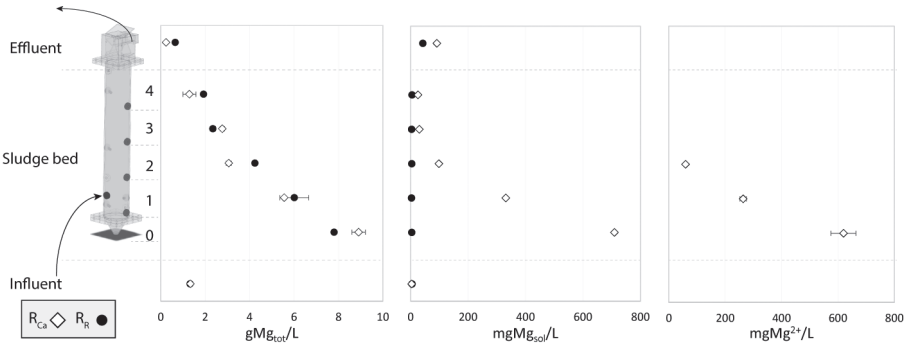

Fig. 2.6. The vertical distribution of total magnesium (Mg_{tot}), soluble magnesium (Mg_{sol}) and magnesium ion (Mg^{2+}) in the sludge bed of the UASB reactors R_R without and R_{Ca} with calcium addition together with the influent (bottom) and effluent (top) concentration at operation day 165 (phase 2).

2.3.3. Particle size distribution, elemental composition and characterization of precipitates at the bottom of the reactors

Particle size distribution at the bottom

After 456 days of operation, more and larger particles occurred at the bottom of R_{Ca} than at the bottom of R_R (Fig. 2.7). At the bottom of $R_{R,}$ 92% ± 1% of the particles were < 0.4 mm in diameter; however, at the bottom of R_{Ca}, only 37% ± 4% of the particles were < 0.4 mm in diameter. At the bottom of R_R, there was a negligible occurrence of size fractions between 0.4 mm and 2.5 mm, and particles > 2.5 mm made 6% ± 1% of the TSS. At the bottom of R_{Ca}, the size fraction between 0.4 mm and 2.5 mm made on average 19% ± 3% of the TSS, and particles > 2.5 mm made 44% ± 1%.

Phosphorus at the bottom

The phosphorus concentration was the lowest in the particles < 0.4 mm in diameter: 29.7 mgP $gTSS^{-1}$ for R_R and 17.8 ± 1.1 mgP $gTSS^{-1}$ for R_{Ca}. Particles > 2.5 mm contained 42.6 ± 5.5 mgP $gTSS^{-1}$ at the bottom of R_{Ca}. At the bottom of R_{Ca}, most phosphorus (59%) occurred in particles > 2.5 mm, and 21% occurred in particles < 0.4 mm. At the bottom of R_R, most phosphorus (89%) occurred in particles smaller than 0.4 mm (Fig. 2.7).

Calcium at the bottom

The particles recovered from the bottom of R_{Ca} contained more calcium than those from the bottom of R_R. Particles > 2.5 mm and < 0.4 mm from the bottom of R_{Ca} contained 178 ± 15 mgCa $gTSS^{-1}$ and 76 mgCa $gTSS^{-1}$, respectively (Fig. S2.3). Particles > 2.5 mm and < 0.4 mm from the bottom of R_R contained 59 ± 9 mgCa $gTSS^{-1}$ and 38 ± 6 mgCa $gTSS^{-1}$, respectively. The molar ratio of calcium to phosphorus for particles > 2.5 mm was 3.38 for R_{Ca} and 0.95 for R_R, based on the ICP measurement after acid digestion. The molar ratio of calcium to phosphorus for particles < 0.4 mm was 3.31 for R_{Ca} and 2.38 for R_R.

Magnesium at the bottom

The particles from the bottom of R_R contained more magnesium than those from the bottom of R_{Ca} (Fig. S2.4). Particles > 2.5 mm and < 0.4 mm from the bottom of R_{Ca} contained 2.87 ± 0.26 mgMg $gTSS^{-1}$ and 2.00 ± 0.03 mgMg $gTSS^{-1}$,

respectively. Particles > 2.5 mm and < 0.4 mm from the bottom of R_R contained 33.0 ± 5.4 mgMg gTSS^{-1} and 17.6 ± 0.3 mgMg gTSS^{-1}, respectively. The molar ratio of magnesium to phosphorus for particles > 2.5 mm was 0.09 for R_{Ca} and 0.88 for R_R. The molar ratio of magnesium to phosphorus for particles < 0.4 mm was 0.14 for R_{Ca} and 0.74 for R_R.

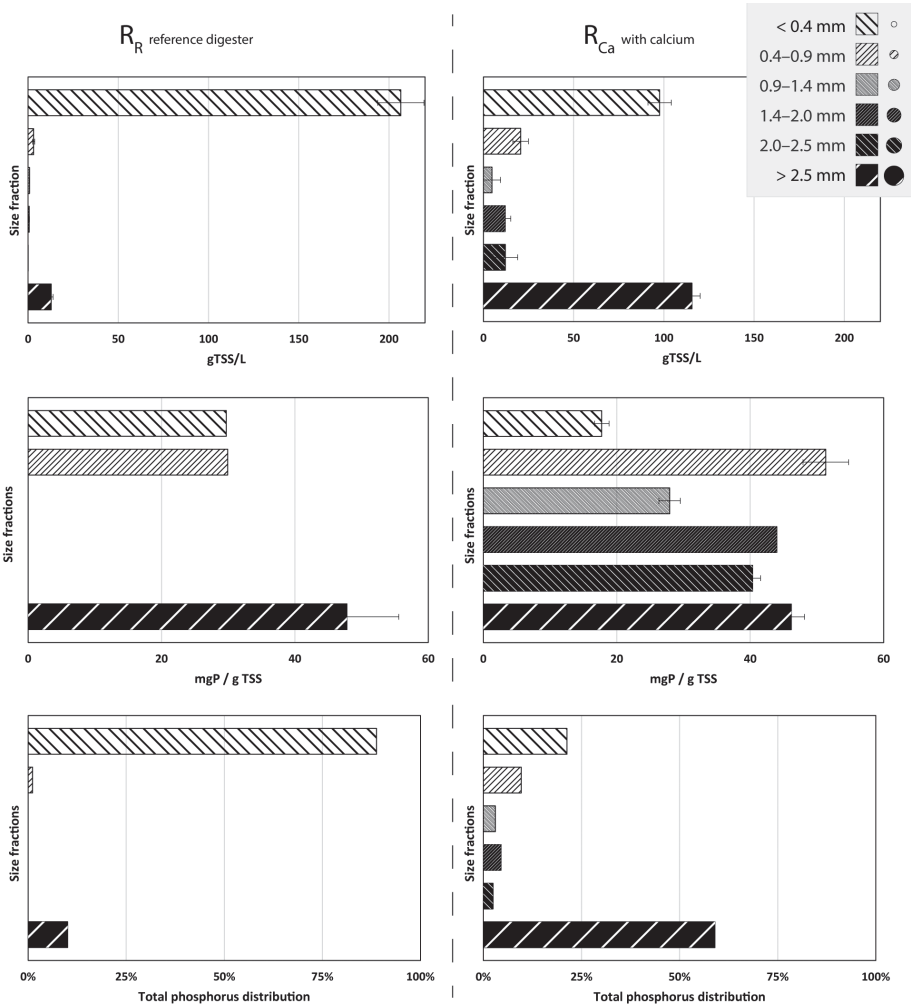

Fig. 2.7. Particle size distribution after sieving based on gTSS L^{-1} (top) with the phosphorus concentration for each size fraction (middle) and the total phosphorus distribution (bottom) based on the combination of abundancy of particle size fraction and its phosphorus concentration for R_R (left) and R_{Ca} (right)

2.3.4. Mineral and crystal characterization at the bottom

SEM–EDX

The phosphorus accumulated in R_R as struvite and in R_{Ca} as calcium phosphate according to the SEM-EDX analysis. In Fig. 2.8a and b, the SEM images showed the presence of coffin-shaped crystals of about 50 μm in size in particles smaller than 0.4 mm from R_R. The related EDX images showed the presence of phosphorus as yellow and magnesium as purple. Combined, the SEM-EDX images suggested the presence of $MgNH_4PO_4{\cdot}6H_2O$. In Fig. 2.8c and d, the SEM images show spherical precipitates of about 1 μm in size in particles larger than 2.5 mm from R_{Ca}. The related EDX images showed the presence of phosphorus as yellow and calcium as cyan. Combined, the overlap of phosphorus as yellow and calcium as cyan gave green, indicating the presence of $Ca_x(PO_4)_y$ species. Struvite crystals were not observed with SEM or EDX in particles from R_{Ca}. In Fig. S2.5, the green EDX image represented calcium phosphate in particles smaller than 0.4 mm from R_{Ca}.

XRD

The XRD analyses showed that the crystalline fraction at the bottom of R_R contained 70% struvite, but no struvite was detected in the sludge bed from R_{Ca}. $CaCO_3$ made up 24% of the crystalline phases at the bottom of R_R and 97% in R_{Ca} (Figs. S2.6–2.8). No crystalline calcium phosphate was detected, but broadened peaks on positions common for HAP were found in the sample from R_{Ca}, representing amorphous calcium phosphate (ACP).

TGA

The TGA indicated the presence of 9.8 wt% and 37.7 wt% struvite in particles larger than 2.5 mm in R_{Ca} and R_R, respectively (Fig. S2.9). The TGA overestimated the presence of struvite because of the loss of ammonia and crystal water, but also left-over sample moisture at 80-100°C. $CaCO_3$ made up 12 wt% at the bottom of R_R and 14 wt% at the bottom of R_{Ca} (Fig. S2.10).

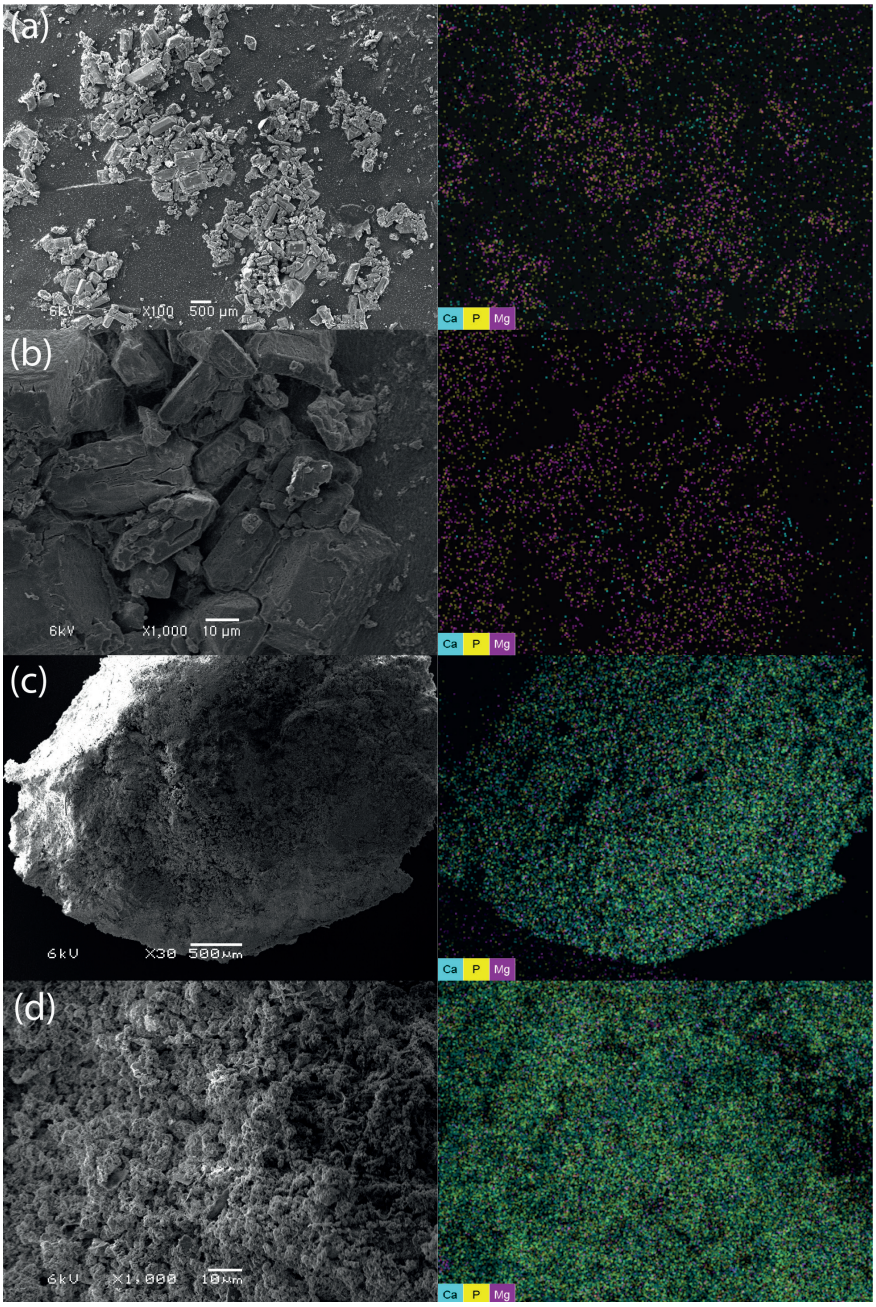

Fig. 2.8. Scanning electron microscope (left) and energy dispersive X-ray (right) of the most abundant size fractions from R_R (< 0.4 mm, a and b) and R_{Ca} (> 2.5 mm, c and d). (a) and (b), and (c) and (d) show the same particles, respectively, at different magnifications.

2.4. Discussion

2.4.1. Effect of calcium addition on treatment performance

Calcium addition enhances the treatment stability of the UASB reactors with lower fluctuation of phosphorus, solids and COD in the effluent. Without additional calcium, the effluent of R_R fluctuates because of the seasonal change in PM composition shown over 456 days of continuous operation. Throughout the seasons, changes in level in the manure storage pits below the stables are likely affecting the composition of the influent taken from the top of the pit. In a full pit during autumn and winter, when regulations forbid manuring, particles can settle and create a vertical concentration gradient, decreasing from bottom to top of the manure pit. In a nearly empty pit during summer, the concentration gradient is less, and the influent concentration is higher [67, 68]. The variation in influent concentration could cause loading shocks. According to literature, loading shocks can disturb removal efficiencies and microbial activities through physically washing out compounds meant to be retained or converted in the UASB reactor [69-71]. The retention is less affected by loading shocks in R_{Ca} than in R_R because calcium helps to retain compounds by inducing aggregation in R_{Ca} through bridging negatively charged species [72, 73]. This phenomenon is similar to that found by Yu et al. [74] and Cunha et al. [41], who described increased solid retention and aggregation in their UASB reactors with calcium addition. The resistance to loading shocks in R_{Ca} could indicate that the reactor ran under capacity and the loading rate could be increased without compromising its treatment performance.

Methanization is the conventional performance indicator for anaerobic digestion but was low (about 5% for both reactors) and not clearly enhanced by calcium addition in this study. Previous studies focusing on anaerobic digestion of PM show low methane yield because of the excessive ammonia concentration (>1.1 gNH3-N L^{-1}) and consequent toxicity [75-77]. While calcium addition improved the retention of solids and biodegradation, the high ammonium and consequent ammonia concentration (1.7 ± 0.5 gNH_3-N L^{-1}) in PM impedes methanization, leading to accumulation of organic acids (Tables S2.3 and S2.4). Conventionally applied anaerobic digesters treating PM are continuous stirred tank reactors (CSTRs), mainly focusing on methane production through co-digestion [78]. CSTRs barely retain nutrients and solids requiring additional treatment steps for nutrient removal or recovery [79-81]. Existing practices and research on phosphorus recovery from

PM focuses on chemical precipitation assisted by mechanical separation from digestate or raw PM [82-84]. However, in the present study, phosphorus recovery succeeded in a single UASB reactor while treating PM.

2.4.2. Effect of calcium on phosphorus recovery

The key for phosphorus recovery from PM is to concentrate phosphorus by optimizing solid–liquid separation, because most phosphorus is present in very fine particles in PM [85]. The UASB technology allows solid–liquid separation and enables accumulation and recovery of phosphorus from the sludge bed, which is not possible with conventional CSTR digesters [41, 79, 86]. Even without calcium addition, the UASB reactor R_R could already retain on average 60 ± 3% of the total phosphorus input in the sludge bed. By adding calcium, the retention of total phosphorus increased to 74 ± 2% in R_{Ca}. While calcium addition improves retention of solids and concentrated particulate phosphorus, this also induces precipitation of PO_4^{3-} and CO_3^{2-} as shown by the lower concentration of PO_4^{3-} and IC in the effluent of R_{Ca} than in R_R (Tables S2.7, S2.8, S2.3 and S2.4, respectively). In the sludge bed, the concentration of P_{sol} and PO_4^{3-} was lower in R_{Ca} than in R_R (Fig. 2.4), proving the precipitation of phosphorus. Cunha et al. [41] also reported phosphorus precipitation with calcium addition during treatment of source-separated black water. Similarly, the effluent contained less PO_4^{3-} with calcium addition during black-water treatment and most inorganic solids accumulated at the bottom of the reactor.

Calcium addition triggered calcium phosphate granulation, as demonstrated in previous research [41, 74, 87-89]. For instance, at the bottom of R_{Ca} 63% of the solids were present as particles > 0.4 mm diameter (of which 70% were > 2.5 mm diameter) while in R_R only 8% of the solids were > 0.4 mm diameter. The solids > 0.4 mm in R_{Ca} were possibly underestimated because the harvesting point clogged between operation day 165 and 221: the efficient working volume of the UASB reactor might have been reduced. The size of the reactor and harvesting valves are decisive to prevent clogging. Clogging is not likely to happen in a full-scale reactor. A full-scale reactor will possibly have more calcium phosphate granulation than the bench-scale UASB reactor of this study. Regarding the phosphorus distribution at the bottom of R_{Ca}, 79% of the phosphorus was in particles > 0.4 mm diameter compared with only 11% at the bottom of R_R. Accordingly, 1.19 gP L^{-1} of PM

(58%) could be recovered by sieving the sludge bed from the harvesting location as calcium phosphate granules (i.e., particles > 0.4 mm diameter).

The mechanisms behind the calcium phosphate granulation are likely aggregation of particles promoted by calcium bridging, calcium precipitation with PO_4^{3-} and CO_3^{2-} and subsequent crystal growth and maturation in the center of the granules. At the bottom of R_{Ca} during phase 3 and 4, the pH is 6 on average whereas the pH was 8.2 at the bottom of R_R (Table S2.6). The pH possibly dropped in R_{Ca} because of the CO_3^{2-} precipitating with added calcium and the consequent removal of its buffer capacity. Calcium addition can also lower the pH because calcium can complex with hydroxide ions, facilitating a release of protons [90]. At a pH of 6, the solubility of calcium phosphates increases and could reduce precipitation. However, high concentrations of calcium and phosphorus still can result in calcium phosphate supersaturation and precipitation [91, 92]. The amount of total calcium (including additional calcium) retained in R_{Ca} was 87%. Considering a Ca:P molar ratio of 1.67 for the formed calcium phosphate precipitate, 65% of the retained calcium was used for phosphorus precipitation. The other 35% likely precipitated as calcium carbonate as shown by the XRD measurements (Fig. S2.8). Although up to 4 gCa L^{-1} manure were additionally supplied to R_{Ca}, the calcium concentration in the effluent of R_{Ca} and R_R was similar. That indicates a large calcium uptake capacity of the sludge bed, leaving the calcium concentration in the effluent unaffected. In addition, hydrogenotrophic methanogenesis could support the formation of calcium phosphate by locally increasing the pH, because hydrogenotrophic methanogens are more resistant to ammonia toxicity and no H_2 was found in the biogas at any point [93]. Precipitation of calcium phosphate and carbonate and the involvement of calcium were similarly described in Cunha et al. [41, 42, 62, 94], Yu et al. [95] and Chen et al. [96] also showing the formation and growth of granules with high inorganic content. The ash content of granules larger than 2.5 mm diameter from R_{Ca} was 49%, which is higher than the common ash content of anaerobic granules (15–40% ash [97, 98]) and confirms the incorporation of precipitates.

2.4.3. Effect of calcium on phosphorus crystallization

Calcium addition caused the formation of larger particles, containing more phosphorus and calcium than smaller particles. In R_{Ca}, phosphorus and calcium enriched 2.3 and 2.0 times, respectively, in particles > 0.4 mm diameter (4.2 ± 0.8 wt% P and

15.2 ± 2.7 wt% Ca) compared with particles < 0.4 mm diameter (1.8 ± 0.1 wt% P and 7.6 ± 0.2 wt% Ca), confirming the calcium-induced precipitation and growth of calcium phosphate [41, 95]. However, in R_{Ca}, magnesium enriched only 1.2 times in particles > 0.4 mm diameter (0.25 ± 0.06 wt% Mg) compared with particles < 0.4 mm diameter (0.20 ± 0.01 wt% Mg). When comparing R_{Ca} with R_R, particles from R_R (2.5 ± 0.7 wt% Mg) contained considerably more magnesium than particles from R_{Ca}. The low concentrations of magnesium in R_{Ca} indicate the loss of magnesium from the solid phase, which is in line with the detected Mg^{2+} in the bulk liquid at the bottom of R_{Ca}. Similarly, Cunha et al. [41] reported an increase in magnesium leaving the reactor. The addition of calcium created a sufficient supersaturation for calcium minerals to dissolve magnesium minerals that are naturally occurring in PM.

Struvite was found in PM and in the sludge bed of R_R. Similarly, struvite was previously found in raw and treated PM [99-101]. In particles from the bottom of R_{Ca}, struvite crystals were not found with SEM-EDX nor with TGA analyses, which is in line with the low residual magnesium concentration (2.6 mgMg $gTSS^{-1}$) in particles from the bottom of R_{Ca}. In particles from the bottom of R_{Ca}, the molar ratio of Mg:P is significantly lower than in R_R (Mg:P 0.09 in R_{Ca} and 0.88 in R_R), indicating that magnesium phosphate precipitates dissolved. XRD confirmed the presence of an amorphous phase of calcium phosphate and the absence of struvite at the bottom of R_{Ca}. According to XRD, the main phosphate phase at the bottom of R_R was struvite (Fig. S2.6). Therefore, struvite certainly recrystallized to $Ca_x(PO_4)_y$ at the bottom of R_{Ca}, by releasing phosphate to solution and triggering $Ca_x(PO_4)_y$ formation.

Yet, the magnesium that was solubilized at the bottom of R_{Ca} did not leave with the effluent. The magnesium retention of R_{Ca} was about 6% higher than in R_R because more suspended magnesium was retained. Similarly, the release of ammonium from struvite dissolution was not notable in the effluent of R_{Ca} compared with R_R (5.2 $gNH_4\ L^{-1}_{effluent}$ at average pH 8.9 for both reactors). However, the ammonium concentration was 10.2 $gNH_4\ L^{-1}_{sludge\ bed}$ at average pH 7.5 (Fig. S2.11) at the bottom of R_{Ca}, while at the bottom of the sludge bed of R_R were only 7.5 $gNH_4\ L^{-1}_{sludge\ bed}$ at average pH 7.9. The influent for both reactors contained 6.0 $gNH_4\ L^{1}_{manure}$ at average pH 8.2, which is the same nitrogen concentration as the effluent when considering the pH. It is not likely that ammonia made part of the biogas stream.

The solubility of ammonia is considerably higher than the concentration in R_{Ca} and the low gas production provided low stripping forces [102]. The absence of the released ammonium (from dissolution of struvite and degradation of N-containing organic matter) and magnesium in the effluent of R_{Ca} suggests a reprecipitation of ammonium and magnesium at the upper part of the reactor, probably with carbonate as calcium and phosphate were not in solution at the top of the sludge bed. Magnesium ammonium carbonate was previously found under similar concentrations [103]. Coprecipitation of magnesium and calcium as $CaMg(CO_3)_2$ could also have occurred [104].

Calcium phosphate granulation and $Ca_x(PO_4)_y$ crystallization from struvite has not been previously reported to the best of our knowledge in a single unit treating PM. For forming $Ca_x(PO_4)_y$ during PM treatment, Szogi and Vanotti [39] acidified manure to a pH between 3 and 5 to solubilize all particulate phosphorus. In a second process step, the pH was increased through CaOH addition which also supplies calcium for $Ca_x(PO_4)_y$ precipitation. In a third process step, polymers were added to agglomerate the $Ca_x(PO_4)_y$ nuclei and enhance their size and sedimentation [84]. In R_{Ca}, the growth and sedimentation of $Ca_x(PO_4)_y$ particles (calcium phosphate granules) occur in a single step, facilitating efficient phosphorus recovery and enabling the application of simple processes based on size or density separation.

2.4.4. Mechanism for agglomeration and growth of $Ca_x(PO_4)_y$

Without calcium addition, struvite is the main phosphorus-containing mineral in PM, as shown in Fig. 2.7 and 2.8 for R_R, but the low particle size limits phosphorus extraction and recovery from the sludge bed [105, 106]. In synthetic and controlled solutions, struvite crystals grow mostly in needle shapes reaching sizes of 30 – 120 μm [107-109]. The size of struvite crystals barely surpasses 120 μm because of the crystal's negative zeta potential and smooth surface [110, 111]. Wei et al. [112, 113] and Li et al. [114] show that polymers such as humic substances and extracellular polymeric substances (EPS) commonly found in wastewater and especially in manure decrease the size of struvite crystals. The polymers increase the negativity of the zeta potential and block active growing sites, causing smaller, coffin-shaped crystals as seen in this study (Fig. 2.7 and 2.9, stage 1) and in Wei et al. [112, 113] and Li et al. [114].

Larger crystals appeared when Le Corre et al. [107] added calcium to the solution. Similarly to the current study, the added calcium caused an increase in soluble

magnesium and decreased the purity of struvite by precipitating ACP [115]. However, at a total molar ratio up to 0.5 Ca over Mg (Ca:Mg), struvite crystals could still grow with ACP on their surface. The spherical-shaped ACP precipitate possibly decreases the surface smoothness and mitigates the activation energy for crystal growth and aggregation (Fig. 2.9, stage 3) [116, 117]. In R_{Ca}, the growth of struvite was not observed, but $Ca_x(PO_4)_y$ formed at a total molar ratio close to 2.9 Ca:Mg. Yan and Shih [115] showed that addition of calcium stopped the growth of struvite at 1 Ca:Mg but enhanced the formation of ACP and eventually caused the dissolution of struvite at 2 Ca:Mg. Therefore, the abundance of calcium in R_{Ca} certainly led to dissolution of struvite and formation of ACP (Fig. 2.9, stage 4).

Phosphorus release from struvite dissolution promoted the formation of ACP in R_{Ca}. ACP is the first $Ca_x(PO_4)_y$ species precipitating before eventually maturing to HAP [118, 119]. Three aspects of the $Ca_x(PO_4)_y$ formation mechanism found in medical research are potentially relevant to this study:

1. ACP is known to accumulate on carboxylic groups of body fluids and simulated body fluids [120]. Body fluids barely occur in manure however it does contain plenty of polymers with carboxylic groups. The carboxylic groups of EPS, humic substances or organic acids could serve as calcium saturated sites to initiate ACP precipitation and later cluster formation [121].
2. Researchers found that magnesium ions can lower the solubility of ACP [122-124]. The Mg^{2+} found in solution at the bottom of R_{Ca} could have then induced ACP precipitation by lowering its solubility.
3. The carboxylic groups and other non-calcium cations such as magnesium, aluminum and iron can stabilize ACP and elongate the induction time of transitioning into HAP [125-127].

Thus, ACP formed on EPS and other polymers could continue growing, aggregating and finally agglomerating, allowing the formation of a large ACP precipitation cluster before transitioning towards crystalline HAP (Fig. 2.9, stage 5). The grown ACP cluster could transform into HAP through surface nucleation where a gel like layer of ACP turns into HAP [128] and result in a large, crystalline HAP cluster. Crystalline HAP clusters were previously observed in black water treatment [62]. In manure, however, the transitioning of ACP to HAP might be hindered by the high abundance of inhibitors such as organic polymers and magnesium.

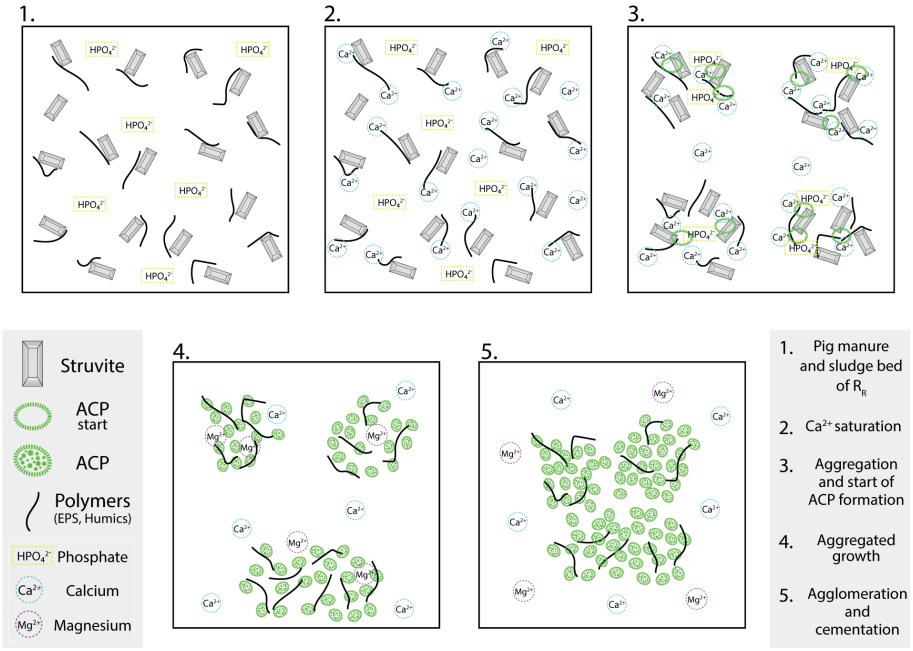

Fig. 2.9. Scheme of mechanism of calcium phosphate granulation in pig manure. (1) Representation of pig manure and sludge bed of R_R (without calcium). (2) Ca^{2+} addition and consequent saturation of binding sites. (3) Aggregation of polymers and particles including struvite crystals and start of ACP formation on polymers and recrystallization of struvite. (4) Aggregated growth (merging of aggregates). (5) Agglomeration and cementation of aggregates forming stronger and denser particles (calcium phosphate granules).

2.4.5. Recovered phosphorus and its use in agriculture

Considering the pig population and the available arable land for phosphorus application in the Netherlands, exporting phosphorus originating from PM is a necessity [61]. The transportation of phosphorus as phosphorus-rich sludge or CaP granules is a lot more economical and environmentally sustainable than as raw PM. The phosphorus is 6.5 times more concentrated in the sludge bed from the bottom of R_{Ca} than in raw PM. Thus, transporting sludge bed from the bottom of R_{Ca} reduces transportation by 85% compared to raw PM, considering the phosphorus concentration. Currently, the transport costs of excessive PM are about €20 per m^3. The reduction of transport by adding 2.9 kg of calcium per m^3 of PM could enable savings of roughly €14 (Table S2.13) per m^3 of PM (about €43k for an average-sized pig farm per year) treated in the UASB reactor [61, 129]. The UASB reactor with calcium addition treating PM enables 1.3 kgP $year^{-1}$ pig^{-1} to be recovered as

$Ca_x(PO_4)_y$. $Ca_x(PO_4)_y$ is similar to the natural resource of phosphorus, suiting current fertilizer production and agricultural needs better than struvite [62, 130].

Potassium and nitrogen as ammonia left the reactor as aqueous species in the effluent. Splitting phosphorus from nitrogen and potassium enables the individual application of phosphorus and the other two major plant nutrients. The three major nutrients are needed differently by crops. Crops mainly require different amounts and timing of nitrogen and phosphorus application, which is hard to control when applying raw manure [131, 132]. Raw manure contains all nutrients together; the state of nutrients varies, as they can be bound in organic material or be present as minerals or in solution, which affects nutrient ratios and availabilities. The treatment in the UASB standardized the form of the nutrients, overcoming one of the major complaints of crop farmers against fertilization with PM. Therefore, treated PM has the potential to be applied inside the Netherlands.

2.5. Conclusions

Calcium addition enhanced phosphorus removal from 60% to 74% and enabled the formation of calcium phosphate granules during anaerobic treatment of PM. Additional calcium induced the aggregation of particles and increased the phosphorus in particles > 0.4 mm from 11% to 79%. In the aggregated particles, struvite dissolved, and the released phosphate precipitated with calcium as ACP. Calcium phosphate granules are simple to recover by size separation and enable efficient phosphorus recovery from PM. The six times higher phosphorus concentration in calcium phosphate granules compared with raw PM could allow phosphorus to be redistributed with 85% less transport. The process proposed in this study has the potential to provide economical relief to farmers, reduce emissions during manure management and enhance nutrient, especially phosphorus, circularity.


P
P

3

Innovation in valorization of cow manure: Higher hydrolysis, methane production and increased phosphorus retention using UASB technology

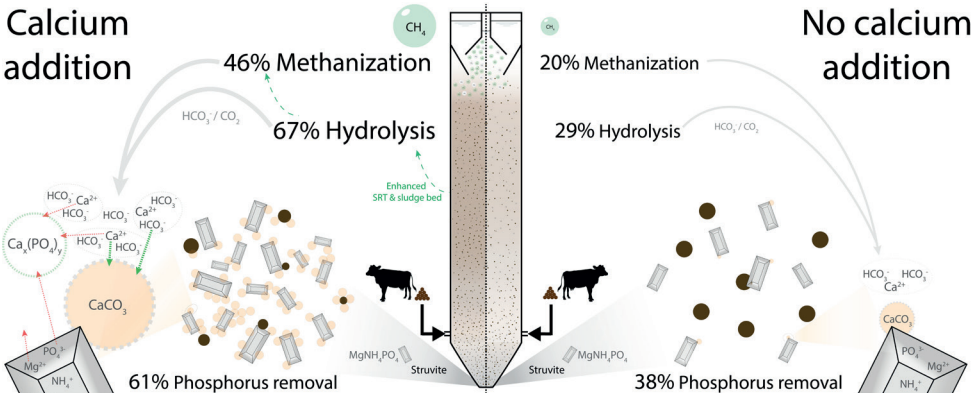

This chapter was published as:

C. Schott, J. R. Cunha, R.D. van der Weijden, C. Buisman, Innovation in valorization of cow manure: Higher hydrolysis, methane production and increased phosphorus retention using UASB technology, Chemical Engineering Journal (2022) 140294. DOI: 10.1016/j.cej.2022.140294.

Abstract

Cow manure has potential to serve as a sustainable secondary fuel and phosphorus resource and cut our reliance on finite primary resources. The efficient and sustainable valorization of cow manure faces compositional challenges because of a high solids content, the lack of soluble phosphorus, fine struvite particles being the main phosphorus species and high bicarbonate concentrations. Addition of calcium could result in higher methane production and conversion of struvite to calcium phosphate. To investigate this, cow manure was digested in two up-flow anaerobic sludge blanket reactors for 456 days, one with and one without $CaCl_2$ addition. A positive effect of calcium addition was found for hydrolysis (29% without calcium and 67% with calcium), methane production (136 L-CH_4 $kgVS^{-1}$ without calcium and 301 L-CH_4 $kgVS^{-1}$ with calcium) and sludge bed development. Although calcium was added in a 3:1 ratio to phosphorus, it did not result in recrystallization of struvite to calcium phosphate. Instead, it precipitated as calcium carbonate, which was further induced by additional bicarbonate production through higher hydrolysis and methane production. Still, calcium addition caused better phosphorous removal (from 38% to 61%), which is attributed to the enhanced sludge bed capturing and accumulating both the calcium carbonate and struvite fines. Higher methane production and improved phosphorus retention enables better valorization of cow manure. The access to resources from cow manure through this technology can contribute to the circularity of agriculture and save on finite natural resources.

3.1. Introduction

Natural resources for mineral phosphorus fertilizer and fossil energy are finite, geographically imbalanced and becoming scarce, which lead to governments urging the recovery and circular use of resources [29, 133]. Cow manure (CM) contains energy in the form of organic matter and phosphorus, as well as other nutrients, making it an interesting alternative resource. CM is the most abundant animal manure in Europe and makes up about 75% of all the 1.4 billion tons of animal manure produced annually [31]. In the Netherlands, the most common type of CM is a slurry (86% [134]), which is urine and feces falling through a slatted floor into a pit below the stable for storage [135]. The longer CM remains in the pit, the more it digests by itself, releasing methane and other volatile emissions; the ammonia released during storage represents 53% of the total ammonia emissions during manure management (44% during manure application) [135, 136].

CM is usually applied without treatment to agricultural soils for fertilization [31]. The application of animal manure is regulated by nitrogen limitations in the EU-27 area and in some countries (e.g. the Netherlands and Ireland) by phosphorus limitations [57, 137, 138]. The excess CM needs to be treated and redistributed to spare the environment and mitigate its effect on climate change [139]. In the Netherlands, the excess CM is brought from cattle farms to crop farms or frequently exported to neighboring countries. However, cattle farmers still apply artificial nitrogen fertilizer (32% of total nitrogen fertilization [25]) to achieve desired crop and grass yields because the N:P:K ratio (mainly N:P) of CM is not ideal for fertilization. The desired N:P ratio varies between crops, but often it is ~8 [137, 138], whereas CM has a N:P of 4. The intention of limiting manure application for environmental protection is biased as additional transport and application of artificial fertilizer are both economically and environmentally costly. Instead, the valorization of manure as energy and separated phosphorus and nitrogen fertilizers could effectively diminish the need for fossil fuel and finite and cost-intensive resources, while reaching sufficient and more flexible fertilization.

Anaerobic digestion of fresh CM can avoid unwanted emissions, produce biogas and potentially recover other resources such as nutrients and carbon [140]. Anaerobic digestion of CM could help achieve the goal of a 10-fold increase in the biogas production by 2030 and establishing a circular economy by 2050 in the Netherlands

[141, 142]. However, the economic viability is not yet convincing; therefore, only 2% of the CM was digested in 2018 in the Netherlands [143, 144]. The majority of digesters are co-digesters (> 50% animal manure), where energy crops are added to the manure to increase biogas production, whereas mono-digesters (> 95% animal manure) are a minority of mainly small units installed on farms [145]. Currently, the main advantage for farmers in installing anaerobic digesters is the income from energy production. The digestate (i.e. anaerobically digested CM) remains labeled as manure that still has the same limitation for applicability as raw manure [146]. Giving economic value and end-of-waste labels to products recovered from CM digestion would be an incentive to digest CM, recover nutrients and ultimately save on fossil fuel and finite natural resources such as phosphorus.

Improving methane production and phosphorus recovery from CM is often achieved with pre- or post-treatments for anaerobic digestion. Regarding methane production, chemical, mechanical and biological pretreatments are applied to enhance the hydrolysis of substances that are difficult and slow to hydrolyze biologically [147]. CM often contains predominantly slowly hydrolyzable organic material because of the type of animal feed and the efficient rumen digestion compared with monogastric digestions [135, 148]. Regarding phosphorus recovery, in CM phosphorus is often present in fine particles that have a relatively low phosphorus concentration. Mechanical separation can separate phosphorus from the solid or liquid fraction before and after digestion, but often the concentration of phosphorus remains low [149]. Biological treatments focus on the phosphorus in solution, requiring dilution with water for biomass such as fungi to take up the phosphorus [36]. Chemical treatments can be cost-intensive, as they depend on high chemical dosing for pH adjustment in a multi-step process because of the high pH buffering capacity in CM [135, 149]. One of the most studied phosphorus-recovery technology is struvite precipitation [150-152]. However, often the size of the struvite crystals limits the separation from manure solids, and co-existing cations can inhibit struvite crystallization, restricting its recovery potential [150]. Struvite contains besides phosphorus also nitrogen, which is best separately applied from phosphorus for ideal fertilization (N:P ratios). The current processes in the phosphate fertilizer industry are not based on struvite but on phosphate rock which is calcium phosphate. Another efficient route for phosphorus separation was achieved during anaerobic digestion in an up-flow anaerobic sludge blanket (UASB)

reactor by calcium addition for treatment of concentrated black water (BW) [41] and pig manure (PM) [37]. The formation of calcium phosphate granules (CaP granules) allowed for simple size separation and resulted in the removal of 89% and 74% phosphorus from BW and PM, respectively, in a single and simple treatment step. The addition of calcium can be beneficial for methane production as well [153]. However, adverse effects of calcium addition on methane production are also reported [74].

This study aims to simultaneously produce methane and recover phosphorus from CM during anaerobic digestion using UASB technology with calcium addition. The main challenge is the composition of CM, which is significantly different from BW and PM. CM has higher solid concentrations, harder (bio)-degradable organic material, a high bicarbonate content and phosphorus present as fine struvite particles. Furthermore, the composition also can vary seasonally. We hypothesize that calcium addition can improve methane production and phosphorus removal, which would enhance valorization of CM.

3.2. Materials and methods

3.2.1. Experimental setup

Two 45 L UASB reactors with double-walled heating at 55 °C anaerobically digested CM and operated for 456 days. The CM was collected after screw-press separation at 700 μm from the pit of a dairy farm with 150 lactating cows in Grijpskerk, the Netherlands. The stable had a slatted floor with combined urine and feces collection as a slurry in the pit. Immediately after collection, the CM was manually sieved through a sieve bend with a grid size of 200 μm (Estrad sieve bend). From a mixed and cooled storage tank (4°C), the CM was pumped every two hours for 1 min to reach a feed flow of 800 mL day^{-1} (peristaltic Masterflex pumps controlled by an external Siemens Logic PLC timer), corresponding to an organic loading rate (OLR) of 1 gCOD L^{-1} d^{-1} and a hydraulic retention time (HRT) of about 55 days (measured values in supplementary information [SI], Tables S3.1 and S3.2). The OLR of the reactors varied because the composition of the CM varied but the flow was kept the same. The composition of CM depended on the seasons throughout the operation. We separated the operation into four phases where the fluctuations in influent compositions were less (SI, Tables S3.1 and S3.2 and SI, Fig. S3.1). The

four phases correspond with spring (phase 1), summer (phase 2), fall (phase 3), and winter and spring (phase 4).

One UASB reactor operated without additional calcium (R_R); the other UASB reactor received additional calcium (R_{Ca}) as calcium chloride solution (Fig. 3.1). The calcium addition was based on the total calcium and phosphorus content measured in CM for reaching a Ca:P molar ratio of 3 (on average 2.4 gCa L_{manure}^{-1}). The Ca:P molar ratio of 3 was earlier found by Cunha et al. [41] to be optimal for calcium phosphate granulation. The calcium solution was pumped directly into the reactor through a pipe with 1 cm diameter and horizontally spaced openings for distributing the calcium into the reactor. The flow of calcium solution was 8% of the influent stream to avoid dilution and the pumping time was 30 sec every two hours to achieve a higher flow and better distribution inside the reactor. A shared master timer controlled the pumping of the calcium solution and the feed.

Both reactors had three vertically distributed sensors measuring online the pH, redox potential, and temperature at the center of the sludge bed (Fig. 3.1). The data were collected in a data logger and analyzed weekly to assure proper operation conditions and functioning of operation and monitoring equipment.

Both reactors had five vertically distributed sludge bed sampling valves (Fig. 3.1). The sludge bed was sampled (about 200 mL) from tap 1 to 4 and about 500 mL from tap 0 by briefly fully opening the sampling valve. Each sludge bed sampling started on top of the reactor and went toward the bottom (tap 4 to tap 0) to avoid the sampling of lower sampling points affecting the sample collected on upper sampling points (relocation of sludge bed).

3.2.2. Analysis and sampling program

The monitoring and sampling program consisted of (1) daily flow measurements of produced effluent (determined by weight, considering a density of 1 g mL^{-1}), formed biogas (measured with a gas counter from Ritter), and used calcium solution (estimated by weight, considering a density of 1 g mL^{-1}), (2) weekly compositional analysis of influent, fresh effluent and biogas and (3) (monthly planned) sludge bed analyses on operation days 70, 98, 139, 165, 221, 229, 237, 244 and 341 as well as after stopping the reactor operation (day 456). The sludge bed analyses

became more intense for research outside this study on days 221–244 and later less frequent because of limited accessibility (Covid-19). During all sampling sessions, similar amounts of sludge bed were sampled for R_{Ca} and R_R so that the active reactor volume was always similar and to ensure comparable reactor operation.

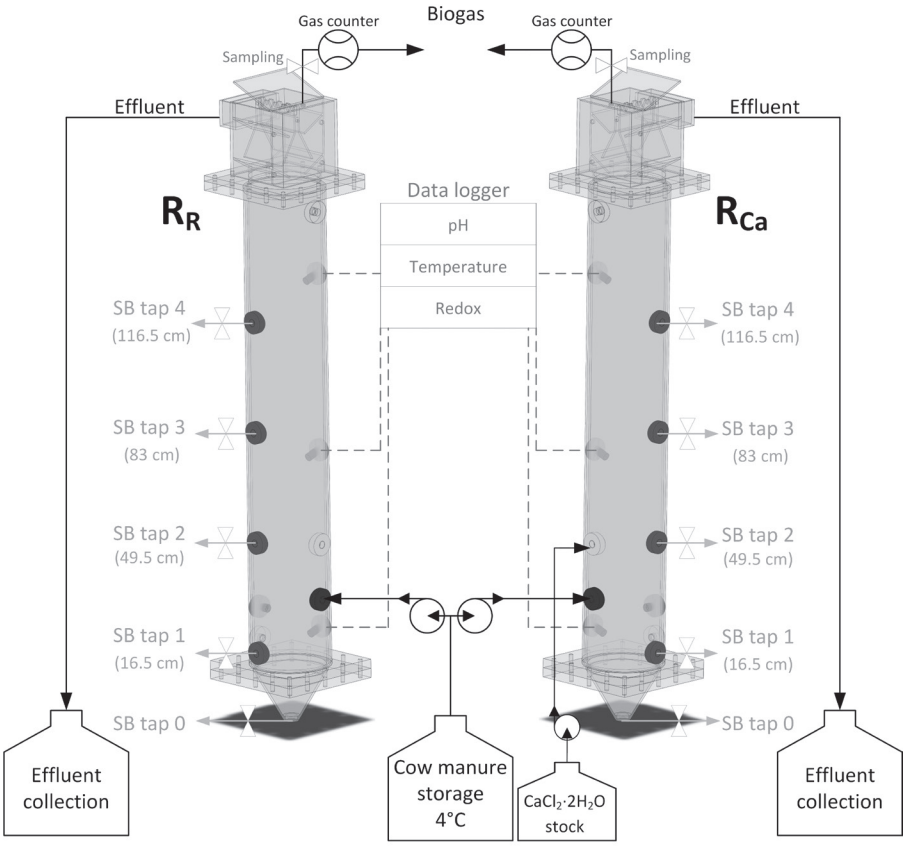

Fig. 3.1. Schematic representation of the setup, including the UASB reactors with heating in a double wall, a cone-shaped bottom piece for accumulating and harvesting potential phosphorus-rich particles and, on top, a gas–liquid–solid separator was placed made from polypropylene. The gas was led toward the gas exhaust through a sampling septum before going into a gas counter, the liquid toward the overflow, and solids remained in the reactor through inclined plates. pH measurements in the sludge bed were in situ, while influent and effluent pH were measured at room temperature during weekly analysis. The sludge bed taps show the vertically distributed sludge bed sampling taps for sludge bed analysis.

The analyzes for influent, effluent, and sludge bed, as well as the methodology and equipment, were as described in Schott et al. [37] and consisted of:

- pH measurements
- Gravimetric determination of total solids, fixed solids, volatile solids, total suspended solids, fixed suspended solids and volatile suspended solids (TS, FS, VS, TSS, FSS and VSS, respectively)
- Determination of total carbon, total organic carbon (TOC) and inorganic carbon (IC) of paper filtered (589/1 Whatman) sample using Shimadzu TOC analyzer
- Measurements of soluble elements (i.e. phosphorus [P_{sol}], calcium [Ca_{sol}], magnesium [Mg_{sol}], sulfur [S_{sol}], iron [Fe_{sol}], sodium [Na_{sol}] and potassium [K_{sol}]) with inductively coupled plasma optic emission spectroscopy (ICP-OES; with an internal yttrium standard; Perkin Elmer Optima 5300 DV) after membrane (0.45 μm Whatman) filtration
- Measurements of anions and cations (PO_4^{3-}, SO_4^{3-} and Cl^- and Ca^{2+}, Mg^{2+} and NH_4^+, respectively) using ion chromatography (Metrohm 930 compact IC flex) after membrane filtration
- Determination of acetic, propionic and butyric acid, which are considered the primary volatile fatty acids (VFAs) in the influent and effluent, using ion chromatography after membrane filtration
- Measurements of chemical oxygen demand (COD) as raw, paper (589/1 from Whatman) filtrate and membrane (0.45 μm Whatman) filtrate (COD_{tot}, $COD_{pap,}$ and COD_{sol}, respectively) with Hach-Lange kits
- Quantification of total elements (P_{tot}, Ca_{tot}, Mg_{tot}, S_{tot}, Fe_{tot}, Na_{tot} and K_{tot}) using ICP-OES after microwave-induced acid digestion (Milestone Ethos Easy) for 15 min at 180°C with 69% HNO_3

The sludge bed was analyzed for all parameters above on days 165 and 341. The sludge bed samples were also analyzed with a scanning electron microscope coupled with an energy dispersive X-ray (SEM-EDX) and X-ray diffraction (XRD) as described in Schott et al. [37]. On the other days, only the solids and total elemental composition were measured.

3.2.3. Calculations

The OLR, solid retention time (SRT), level of hydrolysis and methanization were calculated as described by Halalsheh et al. [65] and de Graaff et al. [66]. Suspended

and colloidal COD (COD_{sus} and COD_{col}, respectively) and the suspended species of elements (P_{sus}, Ca_{sus} and Mg_{sus}) were determined as the difference between the total and soluble fractions, and the cumulative removal and its errors were calculated based on the daily flow data combined with the weekly measured concentrations, where the errors in the cumulative data are resulting from the analytical errors.

3.2.4. Geochemical modeling with PHREEQC

The geochemical modeling was executed in PHREEQC Interactive version 3.5 [154]. The model included the composition of the liquid phase and solid phase based on the measured composition of CM (SI, Tables S3.1–S3.6 and SI, Fig. S3.1). All compounds started in solution and were allowed to form solids as "solid solutions." The precipitates allowed in the solid solution were based on the ones observed in SEM and XRD measurements and possible polymorphs.

We used the wateq4f.dat database (version from August 21, 2012) with the tipping hurley modifications to include humate and possible interactions with calcium [155]. The database was amended with master species and reactions for acetate, propionate and butyrate from the minteq.dat database to see their effect on cation activities. We included struvite and amorphous calcium phosphate (ACP) information in the database based on the data from Ohlinger et al. [156] and Musvoto et al. [157], respectively. We removed the abiotic carbonate reduction to methane because this reduction is not observed in anaerobic digesters and only happens in the presence of catalysts or in extreme environments with high pressure and/or high temperature [158-160]. All materials, consisting of the database used (including precipitation and complexation reactions), the scripts for the different iterations and scenarios as well as resulting raw datasets are given in the PHREEQC appendix as text in a Word file to support further studies.

3.3. Results and Discussion

3.3.1. The effect of calcium addition on methane production

Calcium addition resulted in 2.3 times higher methanization in R_{Ca} (46 ± 3%) compared with R_R (20 ±2%) over the whole operation period based on the COD mass balance and measured methane (Fig. 3.2). Both reactors received CM with a carbon to nitrogen ratio of 7.2 ± 1.3 (based on TOC and NH_4^+ measurements over

the entire operation period). The ammonia concentration in CM did not exceed 0.7 $gNH_3\ L^{-1}$ which is lower than the inhibiting concentration for methanogenesis of > 1.1 $gNH_3\ L^{-1}$ [75, 77]. R_{Ca} produced methane more stably and showed overall less intense and fewer fluctuations in the treatment than R_R (SI, Tables S3.1–S3.6). The latter was more sensitive to the seasonal fluctuations in the manure composition (especially in phase 3 [fall]). R_{Ca} produced even more methane than conventional anaerobic digestion in continuously stirred tank reactors (CSTRs) of CM and than reported in other studies digesting CM in CSTR [148, 161] (301 $L\text{-}CH_4\ kgVS^{-1}$ in R_{Ca}, 136 $L\text{-}CH_4\ kgVS^{-1}$ in R_R, and 200-230 $L\text{-}CH_4\ kgVS^{-1}$ conventionally [162, 163]). Angelidaki and Ahring [164] reported similar methane yields (300 $L\text{-}CH_4\ kgVS^{-1}$) as in R_{Ca} during thermophilic anaerobic digestion of CM, but in that case, the CM had a higher VS content. All the aforementioned studies and the conventional systems used CM with a VS:TS (fraction of volatile solids fed of total solids fed) of about 0.80, whereas in the current study the average VS:TS was 0.66 ± 0.02 for R_{Ca} and R_R. The lower VS:TS in the current study was due to the pre-treatment of CM with a 200 μm size separation removing mainly VS. The removed VS could have further increased methane production, but that stream was thought to find better use as soil amendment. A possible explanation for the exceptionally good methane production of R_{Ca} could be the following: (a) increased SRT and (b) higher concentration of biomass as well as respective substrates.

Effect of calcium addition on SRT and methanization

Adding calcium to CM treatment in a UASB reactor improved solids removal and, consequently, hydrolysis and methanization. The SRT doubled from R_R (123 days, 197 days and 224 days, in phases 2, 3 and 4, respectively; SI, Table S3.1) to R_{Ca} (252 days, 406 days and 450 days in phases 2, 3 and 4, respectively; SI, Table S3.2) because the calcium addition caused higher suspended and colloidal solid removal. The retention of suspended and colloidal material improved because calcium bridges between negatively charged species, stimulating the aggregation of particles [72, 73]. Calcium addition also can cause precipitation of minerals, further increasing the solid concentration in the sludge bed and consequently enlarging the SRT [41, 74]. In this study, the SRT was mainly affected by the retention of suspended materials (VSS and FSS) which doubled when adding calcium.

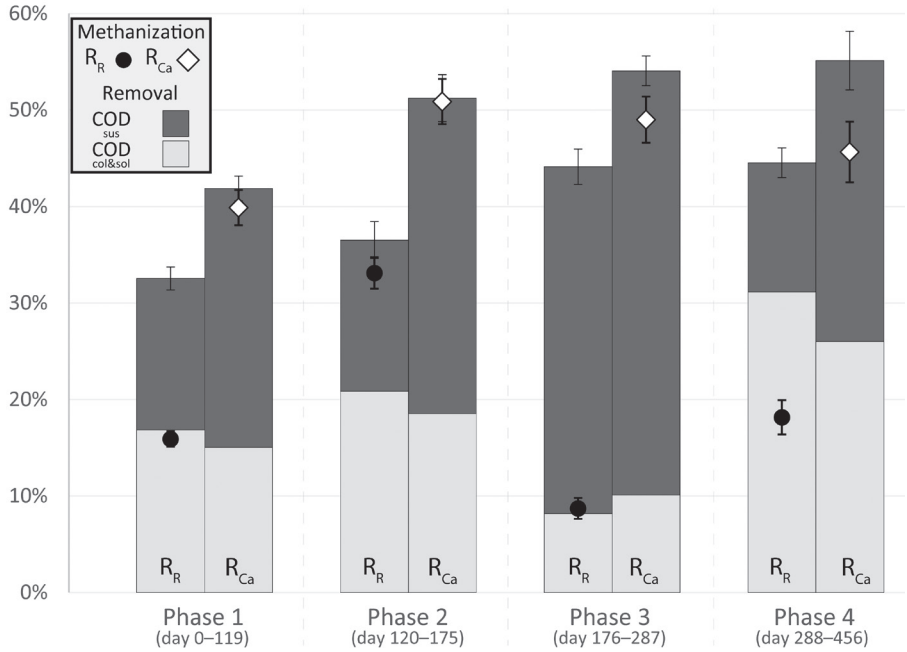

Fig. 3.2. The cumulative methanization as scatter plot combined with stacked columns for COD removal made of COD_{sus} and $COD_{col\&sol}$ for the reactor without (R_R) and with calcium addition (R_{Ca}) over the four operation phases. The methanization and removal values were based on cumulative in- and outflows. The error bars indicate analytical error percentages based on the standard deviations of influent and effluent measurements in duplicate.

Higher SRTs increased the contact time for hydrolysis of organic particles and consequently improved the conversion of COD_{sus} to methane in this study. More COD_{sus} was retained in R_{Ca} than in R_R (Fig. 3.2; 77 ± 4% and 50 ± 4%, respectively). In R_R, the methanization is probably mostly correlated to the easier degradable fraction of removed $COD_{col\&sol}$, which represented 20 ± 1% of the total COD entering the reactor and 49 ± 5% of the total removed COD over the whole operation period (Fig. 3.2). However, in R_{Ca}, the methanization exceeded the fraction of removed $COD_{col\&sol,}$ which represented 17 ± 1% of the total COD entering the reactor and 34 ± 4% of the total removed COD (Fig. 3.2). The level of hydrolysis was 29% in R_R and increased to 67% in R_{Ca} because of the calcium addition. Bahreini et al. [165] demonstrated that longer SRTs enhanced hydrolysis for waste-activated sludge (WAS) treatment. WAS is comparable with CM in (bio)degradability, especially

regarding hydrolysis [166]. Previous research on WAS [167, 168] showed improved hydrolysis, methanogenesis and treatment stability with increased SRTs. The SRTs were increased by increasing the recycling flow in pilot units or decreasing the feeding frequency in bench experiments. Enhancing the SRT by using the UASB technology and adding calcium avoids additional pumping for recycling while keeping a similar OLR and benefiting from improved hydrolysis and methanogenesis. Still, hydrolysis is commonly rate limiting for anaerobic digestion of particulate substrates [169], explaining the inferior methanization of COD_{sus} in R_R, conventional systems, and earlier-mentioned studies compared with R_{Ca} with the longer SRT.

Effect of biomass and substrate accumulation on methanization

The sludge bed developed faster (higher VSS enrichment) and had enhanced concentrations of biomass and substrates (higher VSS concentration in sludge bed) when calcium was added, resulting in higher conversion rates and methane production. Calcium addition improved the VSS removal in R_{Ca} (75 ± 7%) compared with R_R (61 ± 5%), helping the faster sludge bed development. The sludge bed of R_{Ca} also had a higher VSS concentration (55.9 ± 1.4 gVSS $L_{reactor}^{-1}$) than R_R (37.7 gVSS $L_{reactor}^{-1}$) at tap 1 during phase 1, demonstrating a denser sludge bed with higher proximity. The concentration of easily biodegradable VFA was higher in the sludge bed and in the effluent of R_R than in R_{Ca} (Fig. 3.3a; on average 1.83 gVFA L^{-1} and 0.25 gVFA L^{-1}, respectively). Acetate was present in the sludge bed and effluent of both reactors, but more for R_R than R_{Ca} (Fig. 3.3b; on average 0.55 gAcetate L^{-1} and 0.23 gAcetate L^{-1}, respectively), indicating improved methanogenesis in R_{Ca} and limited methanogenesis in R_R. Propionate made up most of the short-chain VFA in the sludge bed and effluent of R_R but barely occurred in R_{Ca} (Fig. 3.3c, 1.28 gPropionate L^{-1} and 0.06 gPropionate L^{-1}, respectively), indicating limited acetogenesis in R_R [170]. Still, the high alkalinity (as 14 $gCaCO_3$ L^1) primarily in the form of bicarbonate in CM (SI, Table S3.3 and S3.4) prevented a drop in pH in both reactors (SI, Table S3.5 and S3.6). Previous studies also reported enhanced substrate conversions when calcium was added to anaerobic treatment [171, 172]. The calcium-enhanced biomass retention and biomass proximity were previously found to be key for improved conversions by fermentative bacteria. Calcium could stimulate biofilm formation, which enhances retention and interactions of microorganisms [173]. In the case of propionate to acetate conversion, the proximity of symbiotic biomass is important to enhance the interspecies hydrogen transfer, which is produced by acetogens and consumed by methanogens [174]. If this symbiosis does not work due to lack of proximity then propionate accumulates [175] because of mass

transfer limitations. This would especially concern sludge beds of UASB reactors treating CM with low mixing. However, enhanced mixing could wash out biomass and other solids, possibly leading to lower treatment performance. Peces et al. [176] observed decreasing propionate degradation at shorter HRTs in stirred reactors, possibly resulting from washout of acetogens or a change of degradation pathways. While HRT is not a limiting factor in the reactors of the current study, the retention of acetogens capable of converting propionate would be higher in R_{Ca}.

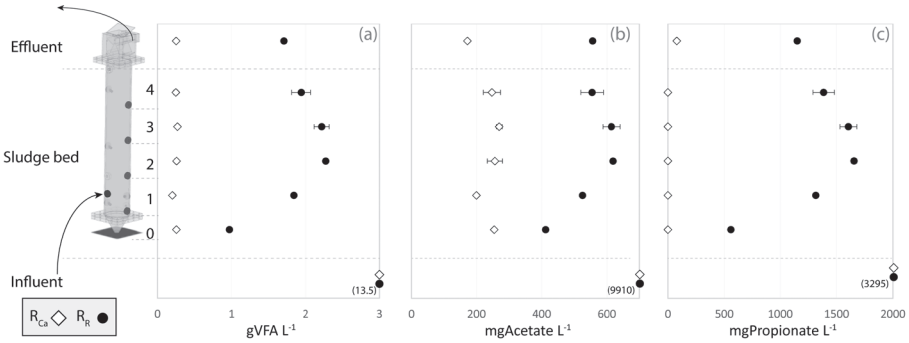

Fig. 3.3. The vertical distribution of (a) VFA (acetate, propionate and butyrate), (b) acetate and (c) propionate in the sludge bed of the UASB reactors R_R as reference and R_{Ca} with calcium addition together with the influent (bottom) and effluent (top) concentrations at operation day 165 (phase 2).

3.3.2. The relation between calcium and organic loading for methane production

Increased methane production with calcium addition had been reported in previous studies, but often the calcium concentration that was applied in this study (on average 2.4 gCa L^{-1}) apparently already inhibited methane production in other studies [74, 175, 177, 178]. Up to a certain concentration, calcium has a beneficial effect on the structure of the extracellular polymeric substance (EPS) matrix around microorganisms, thus improving mass transport [179]. Calcium can also enhance hydrolytic processes by improving enzyme activity or helping stabilize fermentation and anaerobic digestion [180]. When in excess, calcium can complex and precipitate with the substrates, increasing mass transfer limitations and slowing down biodegradation [153]. Calcium could also form inorganic precipitates and consequently limit the mass transport in the sludge, leading to slower degradation [95, 96]. When comparing studies, the calcium concentration seemingly needs to be

normalized for feed/substrate. The synthetic wastewater used in Chen et al. [175] had 2 gCOD L^{-1} and methane production slowed down with 0.4 gCa L^{-1}. Yu et al. [74] found that 0.3 gCa L^{-1} was the optimal amount of calcium addition for 4 gCOD L^{-1} in synthetic wastewater for UASB reactors. Above 0.3 gCa L^{-1}, the degradation of COD decreased. In this study, the CM contained on average 62 gCOD L^{-1}, and COD degradation and methane production increased even at 2.4 gCa L^{-1}. When comparing the calcium to COD concentration ratios (Ca:COD), the calcium added in R_{Ca} (Ca:COD of 0.04) was 5 and 2 times less than in Chen et al. [175] (Ca:COD of 0.2) and Yu et al. [74] (Ca:COD of 0.08), respectively. Although the Ca:COD value could indicate how calcium addition affects methane production, the calcium concentration as a parameter alone cannot fully predict the effect of adding calcium.

To our knowledge, the impact of the Ca:COD on methane production and/or anaerobic digestion had not been compared before between studies; yet, it could be essential for achieving optimum calcium addition effects. Ahn et al. [153], Dang et al. [181], and Zhou et al. [182] studied the effect of addition of calcium while monitoring methane production. They all found the highest methane production at a Ca:COD between 0.03 and 0.05 (Fig. 3.4a). At slightly lower or slightly higher Ca:COD (0–0.03 and 0.05–0.08), the effect of calcium was less significant, while the methane production decreased at Ca:COD > 0.08. It is striking that the greatest benefit for methane production occurred at similar Ca:COD in the three studies even though the added calcium concentration (Fig. 3.4b) and the feed for anaerobic digestion were significantly different. Ahn et al. [153] used PM, Dang et al. [181] used municipal solid waste leachate and Zhou et al. [182] used bagasse. In the current study, the Ca:COD was 0.04 with calcium addition and 0.02 without calcium addition, and the methanization increased by a factor of 2.3 by adding calcium. The reactor with calcium addition falls within the optimum (Fig. 3.4b, green area) deduced from Fig. 3.4a, affirming the beneficial effect of calcium at Ca:COD between 0.03 and 0.05. In Cunha et al. [41], the reactor without calcium (Ca:COD of 0.02) and with calcium addition (Ca:COD of 0.055) had similar methane production, and calcium addition had no significant effect on the methane production from BW. Both Ca:CODs were in ranges where other studies have not found a significant effect of calcium addition on methane production (Fig 3.4b, white area). From Ca:COD 0.05–0.08, the negative effects of calcium addition, as previously described, probably counterbalanced the positive effects of calcium addition. The negative effects were predominant in almost all studies when the Ca:COD exceeded 0.08 during the treatment, when calcification of sludge occurred or as a result of direct calcium toxicity.

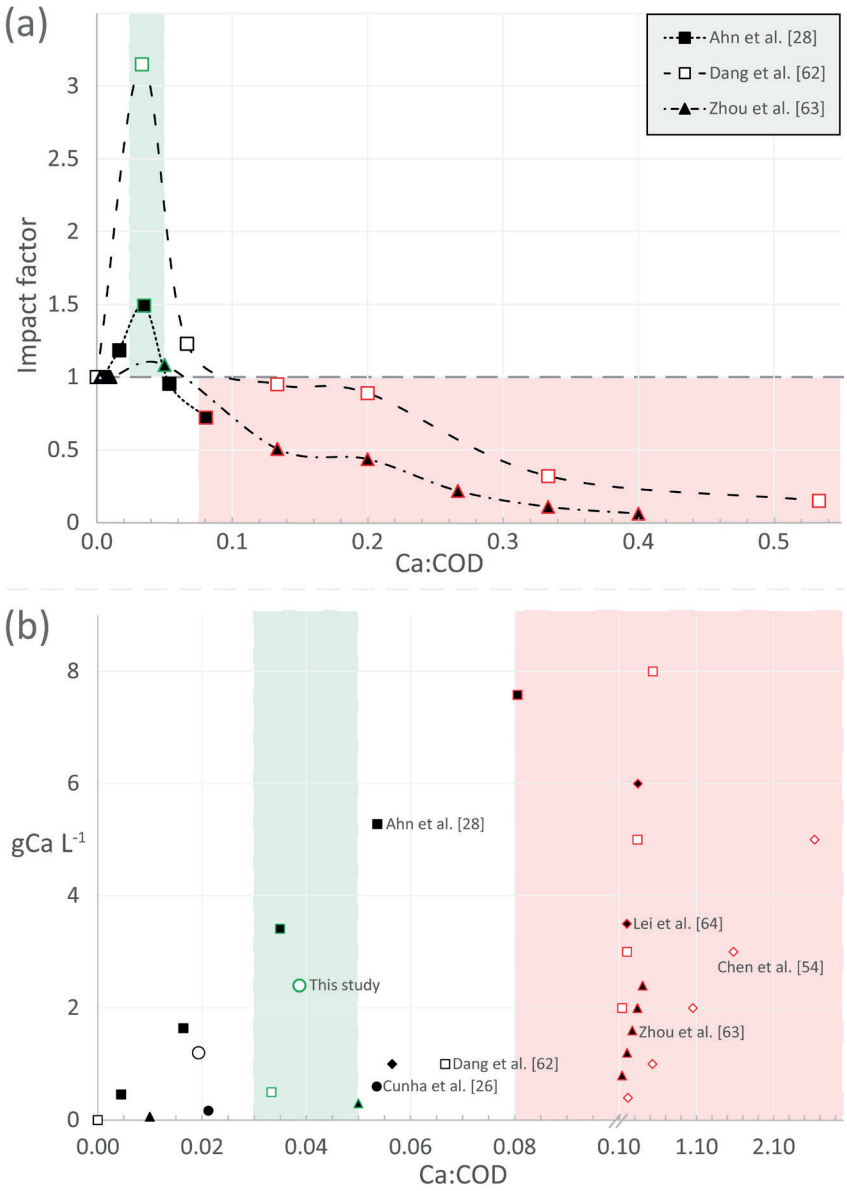

Fig. 3.4. (a) The relative impact factor of calcium addition based on the reference experiments conducted in each study over the Ca:COD mass ratio and (b) the calcium concentration used in this study (○), Ahn et al. [153] (■), Cunha et al. [41] (●), Chen et al. [175] (◊), Dang et al. [181] (□), Lei et al. [183] (♦), and Zhou et al. [182] (▲) against the Ca:COD. In (a) and (b), the zones and marker outlines highlight the positive impact of calcium in green, no significant impact in the white area and black outline, and negative impact in red.

The age and the level of calcification of sludge influences the sludge response to added calcium even at optimum Ca:COD. Chen et al. [54] found that sludge with a higher level of calcification was more sensitive to calcium addition than non-calcified, fresh sludge, which could benefit from higher Ca:COD. Similarly, Yu et al. [29] reported that the specific methanogenic activity (SMA) of fresh sludge benefitted from a Ca:COD of 0.2 during the first 30 days. However, continuous calcium accumulation at the bottom of the sludge bed in all the UASB reactors tested resulted in a decrease of SMA over time. Even at optimum Ca:COD value of 0.038, the positive effect of adding calcium became detrimental after 90 days. Calcification over time at the bottom of the reactors was the cause for the reduction in SMA, and the speed of calcification depended on the calcium concentration. Still, timely removal of calcified sludge from the bottom could prevent deterioration of the local SMA. For instance, growing and harvesting CaP granules by size separation could prevent the reduction in local SMA, prolonging the beneficial effect of calcium addition during anaerobic digestion and simultaneously recovering phosphorus.

3.3.3. The effect of calcium addition on phosphorus removal and speciation

Calcium addition enhanced the total phosphorus removal from 38% (R_R) to 61% (R_{Ca}) over the entire operation time. The phosphorus was almost only present in suspended form (> 90%), and its removal was highly correlated with the removal of suspended solids. Higher solids removal went along with higher phosphorus removal (Fig. 3.5). The removal of suspended phosphorus (R_R 43 ± 3% and R_{Ca} 70 ± 3% over the whole operation) contributed the most to the total phosphorus removal and increased by calcium addition. Therefore, the UASB technology, which allows a different HRT and SRT, is essential to enable phosphorus removal.

Calcium addition likely induced aggregation and cementation of small phosphorus-containing particles (< 125 μm) originating from CM and enhanced the retention of phosphorus-rich solids in R_{Ca} [32, 33]. Possibly, phosphorus-rich particles aggregated for size ranges below 0.4 mm (the lower threshold for particle size analysis in this study), which was seemingly significant in improving phosphorus retention in R_{Ca}. The phosphorus-rich particles were identified as struvite particles by XRD measurements (SI, Figs. S3.12 and S3.13), which explains why phosphorus remained as small particles. Struvite barely forms crystals larger than 120 μm because the crystals have a smooth surface and a negative zeta potential [107, 111]. Barzee et

al. [184] reported that the majority of phosphorus remains in small particles (0.45–75 μm) even after CM was digested, which would be the case for the digestion in R_R without calcium addition. With calcium addition, a possible co-precipitation cemented the phosphorus-rich particles and allowed for removal in R_{Ca}.

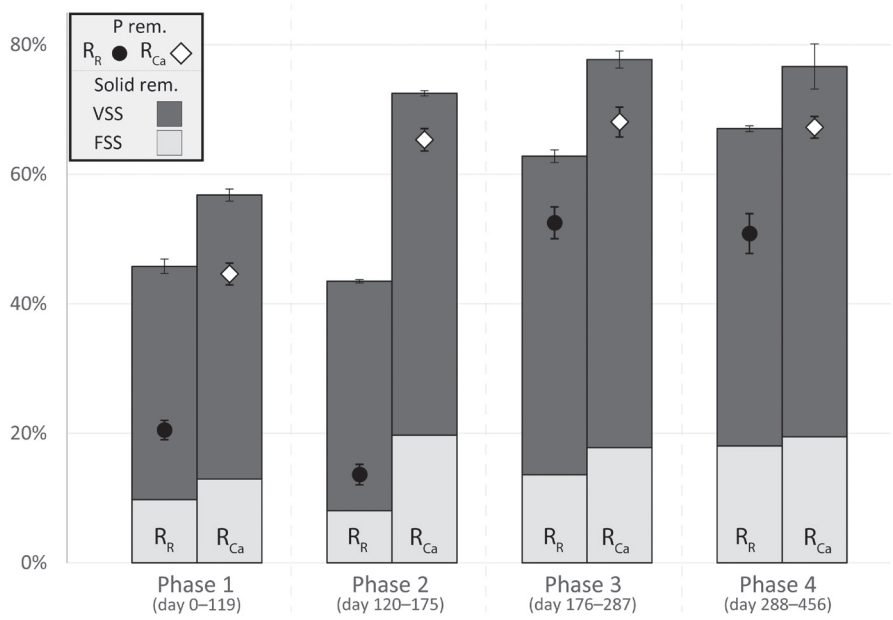

Fig. 3.5. Phosphorus removal as scatter plot combined with stacked columns for TSS removal made of FSS and VSS removal for R_R and R_{Ca} over four operational phases. The removal values were based on cumulative in- and outflows. The error bars indicate analytical error percentages based on the standard deviations of influent and effluent measurements in duplicate.

The phosphorus and other solids accumulated mainly at the bottom of both reactors (Fig. 3.6a and b). The particles that accumulated in R_{Ca} had a lower VSS content, and a gradient of increasing VSS content from bottom to top was found in both reactors (Fig. 3.6c). These findings were in line with our previous research on BW and PM [37, 41]. In this study, however, the gradient of phosphorus and calcium concentration in the sludge bed was considerably less pronounced in both reactors, especially in $R_{Ca,}$ compared with previous studies (tap 0 7.7 ± 0.1 gCa L^{-1} and tap 1 8.2 ± 0.2 gCa L^{-1}, SI, Fig. S3.4). It seemed that the phosphorus, calcium and solids content at the bottom of the sludge bed reached its maximum capacity and, therefore, also a lot of solids were present at tap 1 sampling day 165 (Fig. 3.6, phase 2). During a later sampling of R_{Ca} on operation day 340 (phase 4), the

gradient was more pronounced (Tap 0 9.0 ± 0.7 gCa L^{-1} and tap 1 7.9 ± 0.1 gCa L^{-1}, Figs. S3.6–S3.11). The settling of particles and accumulation of phosphorus at the bottom of the sludge bed might be considerably slower with CM than with BW and PM. According to studies investigating the physical properties of different wastewater types, the viscosity of CM was higher than the viscosity of PM and BW [185, 186]. Possibly the higher viscosity caused slower settling in the sludge bed when treating CM than when treating PM and BW. The particle size remained at 96% < 0.4 mm in R_R and R_{Ca}. The smaller particles combined with a higher viscosity compared with PM and BW can cause a lower settleability during CM treatment and, consequently, results in a less pronounced phosphorus gradient.

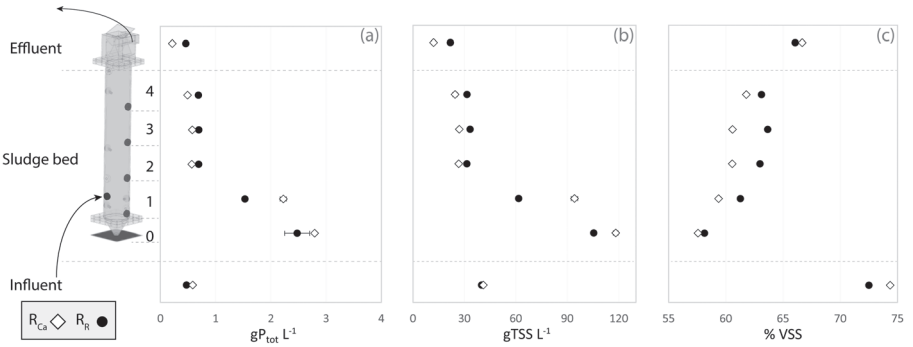

Fig. 3.6. The vertical distribution of (a) total phosphorus concentration (P_{tot}), (b) TSS concentration and (c) the VSS content in the sludge bed of the UASB reactors R_R as a reference and R_{Ca} with calcium addition together with the influent (bottom) and effluent (top) concentration at operation day 165 (phase 2).

The phosphorus in the CM fed to the reactors was mainly in the form of struvite, and the bulk of retained phosphorus was also present as struvite in the sludge beds of both reactors. In both reactors, the molar ratio of magnesium to phosphorus (Mg:P; on average 1.2 in R_{Ca} and 1.3 in R_R on sampling days 165 and 340) based on the measured elemental composition was sufficient to form struvite (struvite Mg:P 1). The presence of struvite was observed with SEM (Fig. 3.7) and confirmed by XRD (SI, Figs. S3.12–S3.14). Calcium addition in R_{Ca} caused the occurrence of two broadened peaks in the XRD spectra at theta angle 27.5, 29 and 30.5, which could not be identified and might indicate the presence of amorphous precipitates (SI, Fig. S3.13). Le Corre et al. [107] described that struvite formation becomes inhibited when calcium ions were added to the solution. When enough calcium ions were added to struvite-containing streams, struvite started to dissolve, and calcium phosphate precipitated [115]. Still, contrary to

our hypothesis, struvite remained the dominant phosphorus species even with calcium addition in R_{Ca} and calcium to phosphorus (Ca:P) molar ratios up to 4 in the solids of R_{Ca}. Calcium phosphate did precipitate at the cost of struvite when calcium was added in PM and BW treatment [37, 41]. However, in the current study, struvite crystals were incorporated into a heterogeneous cluster of mostly calcium carbonate and possibly a little calcium phosphate (Fig. 3.7b). Güngör et al. [187] found that most phosphorus was present as dicalcium phosphate anhydrous (57%), and the rest was struvite in raw CM. After digestion, struvite was the dominant phosphorus solid (78%), and the more stable calcium phosphate phase, hydroxyapatite, was the other solid present [187]. However, in raw CMs and digestates, previous studies have reported and predicted different dominant phosphorus species, mainly consisting of either calcium- or magnesium phosphates [188-191]. Precipitation of phosphorus with either calcium or magnesium seems partly dependent on their abundance but also on their availability and ion activity, as shown in this study when struvite prevailed even though additional calcium was supplied.

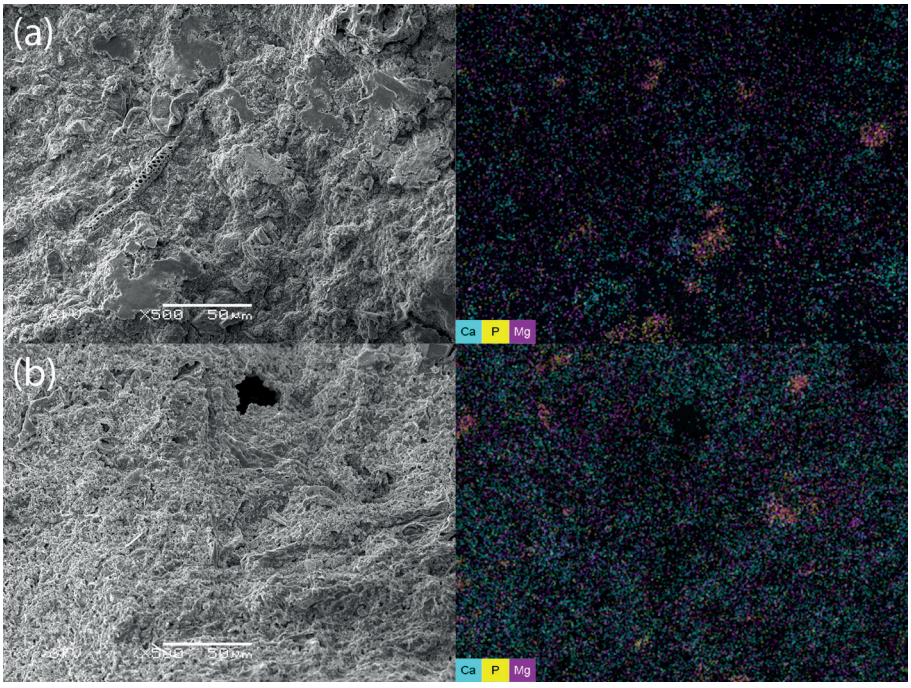

Fig. 3.7. SEM (left) and EDX (right) images of sludge bed from the bottom of R_R (a) and R_{Ca} (b). In the EDX image calcium is represented as cyan, phosphorus as yellow and magnesium as purple. The overlap of phosphorus (yellow) and magnesium (purple) appears as orange and indicates the presence of struvite. The overlap of phosphorus (yellow) and calcium (cyan) appears as green and indicates the presence of calcium phosphate.

3.3.4. The competition for calcium is inhibiting calcium phosphate granulation

The added calcium in R_{Ca} did help phosphorus removal compared with R_R but did not clearly induce calcium phosphate precipitation or granulation as in previous studies. The relatively higher concentration of magnesium in CM compared with the other streams (SI, Fig. S3.1) might have caused struvite to remain and inhibit calcium phosphate precipitation and granulation. Fig. 3.8a shows the Ca:Mg molar ratio after calcium addition for CM (1.79), PM (2.91), and BW treatment (7.43). At Ca:Mg molar ratios ≥1, calcium should be capable of binding more phosphate than magnesium, according to Yan and Shih [115]. Huchzermeier and Tao [192] found that calcium phosphate became the dominant phosphorus species over struvite at Ca^{2+}:Mg^{2+} molar ratios of 0.5 in synthetic, filtered, anaerobically digested CM. In synthetic digestate, the orthophosphate removal as calcium phosphate was very efficient (99.9%), but when the real, filtered digestate was tested, the precipitation dropped to insignificant percentages (0.8%). The recipe of the synthetic digestate contained mainly calcium, magnesium, phosphorus and ammonium ions with chloride and potassium as counter ions, respectively. It is likely that the influence of organic material and its derivates when digested, such as bicarbonate, were underestimated in the tests of Huchzermeier and Tao with synthetic digestate; this explains better recovery results in the synthetic digestate with less calcium-capturing bicarbonate than can be obtained in the real digestate with higher presence of bicarbonate. The limitation of precipitation for Huchzermeier and Tao [192] and the inhibition of struvite recrystallization to calcium phosphate in the current study could be in both cases because of anaerobic digestion resulting in high bicarbonate concentrations which contributed to the alkalinity and that can also precipitate with calcium. Calcium carbonate was previously identified as the main impurity in CaP granules from BW and PM treatment, but calcium phosphate was the primary precipitate [37, 62]. Chen et al. [96] found calcium carbonate as the primary precipitate in granules when treating synthetic wastewater and testing the addition of calcium. Zhang et al. [89] could not qualify calcium carbonate with XRD measurements during the treatment of BW without calcium addition but found CaP granules. Identifying the drivers for calcium carbonate formation during the treatment of waste streams would allow developing strategies to avoid its precipitation. The possible main drivers for calcium carbonate to precipitate over calcium phosphate are most likely as follows:

- The abundance of inorganic carbon in solution together with calcium ions or precursors of inorganic carbon. Cunha et al. [43] saw a negative relation between the abundance of inorganic carbon and the removal of phosphate. In Zhang et al. [89] and Chen et al. [96], it was not clear how much inorganic carbon was in the solution, but Chen et al. [96] had a higher COD concentration entering the reactor. The higher COD concentration might have caused higher production of inorganic carbon and consequently triggered calcium carbonate over calcium phosphate formation. Similarly, the higher COD conversion in R_{Ca} almost doubled the calcium carbonate precipitation (99gC in R_{Ca} and 52gC in R_R) and inhibited calcium phosphate precipitation and granulation.
- The absence of phosphate as an ion. In CM, phosphate is mainly present in suspended form as struvite (> 90%). In BW and PM treatment of previous studies, we saw the presence of phosphate ions (28% and 21%, respectively) [37, 41]. The presence of phosphate ions allows calcium phosphate precipitation at lower activation energies and consequent homogeneous growth at even lower activation energy compared with a situation where phosphate was bound in a precipitate only [116]. Thus, the activation energy might have been too high to initiate the dissolution of struvite and reprecipitation of phosphate as calcium phosphate in CM. Consequently, the available calcium is bound to abundantly present inorganic carbon.

In the geochemical model (PHREEQC) presented in Fig. 3.8b, struvite was predicted to be the dominant phosphorus species without calcium addition in CM (100% struvite) and PM (70% struvite) but not in BW (39% struvite) (Ca:Mg 1.05 in CM, 1.31 in PM and 1.94 in BW, Fig. 3.8a). In Fig. 3.8b, the model showed the presence of ACP for PM (22% ACP) and BW (43% ACP) even without calcium addition. However, in CM, struvite dominantly prevailed even when calcium was added (99% struvite), whereas in PM and BW, 43% and 83% of the phosphorus, respectively, was present as ACP. In PM and BW, the model showed that 56% and 16% of the phosphorus, respectively, remained as struvite, which was not actually observed in the sludge bed of PM nor BW treatment with calcium addition [37]. This discrepancy probably comes from the model predicting the precipitates based on the concentrations in the raw waste streams but not in the sludge bed during the treatment. In the sludge bed, calcium accumulated over time in complexed form with other compounds (bicarbonate, EPS, organic matter) and consequently will cause supersaturation of ACP at some point [121]. The formation of ACP in

granules probably led to energetically favorable surface precipitation of more ACP and recrystallization of struvite [116]. Thus, over time, the sludge bed became rich in calcium, creating a local supersaturation where almost all struvite became ACP [37]. A similar process could have happened in CM treatment, but possibly over a significantly longer time, as struvite is dominant in Fig. 3.8b. The limited ACP formation in CM treatment thus was probably related to the lower Ca:Mg ratio, but may also be caused by the relatively higher competition for calcium by bicarbonate in CM treatment than in PM and BW treatment.

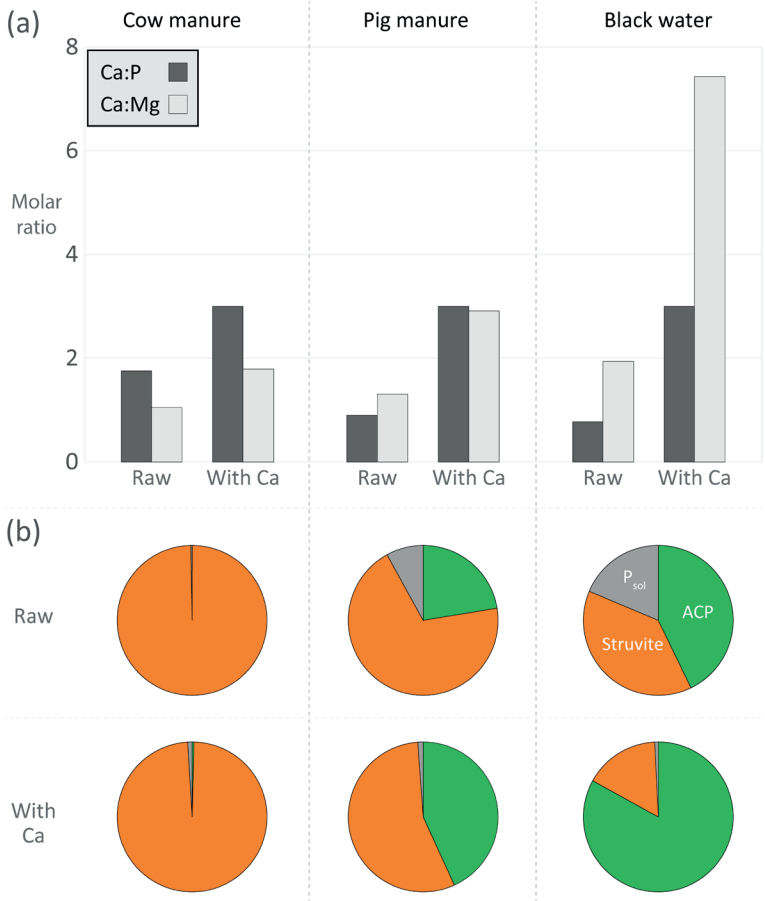

Fig. 3.8. (a) The molar ratios of calcium over phosphorus (Ca:P) in dark grey and calcium over magnesium (Ca:Mg) in light grey and (b) the phosphorus distribution in struvite (orange), ACP (green) and soluble phosphorus (grey) according to geochemical modeling with PHREEQC in pie charts with and without calcium addition in cow manure, pig manure and black water.

Sommer et al. [135] also pointed to calcium carbonate as a likely precipitate when calcium was added to manure. Over the entire operation time of our reactors, the retained 330 gCa would bind 99 g of inorganic carbon in R_{Ca} compared with 52 g of inorganic carbon in R_R. Still, inorganic carbon was produced in both reactors (SI, Tables S3.3 and S3.4). However, in R_{Ca}, the inorganic carbon concentrations in the liquid phase were lower throughout the sludge bed than in R_R (SI, Fig. S3.8). The CO_2 content in the biogas of R_{Ca} (phase 1, 38%; phase 2, 38%; phase 3, 36%; and phase 4, 34%; based on cumulative production data) was also lower than in the biogas of R_R (phase 1, 43%; phase 2, 41%; phase 3, 40%; and phase 4, 35%; based on cumulative production data). The mass balance for carbon on day 340 (last sludge bed sampling) was missing 4% carbon in R_{Ca} and had an overestimation of 1% in R_R (SI, Fig. S3.15). The mass balance agreed with double the calcium carbonate formation in the sludge bed of R_{Ca} compared with R_R. This was qualitatively examined with SEM-EDX (Fig. 3.7) and XRD (SI, Figs. S3.12 and S3.13) measurements. The geochemical model PHREEQC also predicted that all calcium precipitated as either calcite, vaterite or aragonite. The combined results indicate that bicarbonate is the most significant and abundant competitor for reacting with calcium and not struvite or phosphate. A competitor that still has a beneficial effect as the formed calcium carbonate can cement struvite particles together and thus increase overall particle size and enhance sedimentation.

3.3.5. The potential of recovering methane and phosphorus from cow manure

The technology is easy to implement and maintain, which makes it suitable for farms. At an averagely sized farm (150 cows) in the Netherlands, the reactor unit would need to be of about 200-300m^3, depending on the farm-specific CM characteristics. Such a farm-scale reactor could produce about 37k m^3 of CH_4 per year based on the treatment efficiency of R_{Ca}. That is enough energy to heat a full-scale reactor to 55°C and allow 28 dwellings to be supplied with energy for space heating. When extrapolating for the entire country of the Netherlands, about 0.5 million dwellings of the 7.9 million dwellings in the Netherlands could be heated on digested CM if all the CM would be digested (estimated based on numbers from [31]). A current waste could thus be turned into a significant contribution for energy supply.

While digesting the CM in a UASB reactor with calcium addition, the removal of phosphorus would allow for a higher application of nutrients originating from CM.

Dairy farmers are commonly limited in applying the manure on their land, because of phosphorus application limit regulations. Removing 61% phosphorus would allow for more than double the nitrogen application on the same area originating from CM. This would diminish the need for artificial nitrogen fertilizer in dairy farming and substantially reduce economic and environmental costs [25] while contributing toward a circular economy. The phosphorus in the sludge bed could be transported in higher concentrations than in untreated CM to regions where phosphorus is needed. Thus, the transportation costs and CO_2 emissions could be reduced when transporting phosphorus as sludge bed instead of as untreated CM. The removal, recovery and reuse of phosphorus could be further improved if higher phosphorus concentrations and quantities would be present as easy to separate CaP granules.

3.4. Conclusions

Calcium addition increased the phosphorus removal from 38% to 61% and the methanization from 20% to 46%. Additional calcium stimulated the conversion of suspended material to methane and enhanced the sludge bed development. Hydrolysis improved from 29% to 67% because of calcium addition. We found that calcium concentration alone did not describe the effect of calcium addition well enough and found an optimum of calcium addition in the range of 0.03–0.05 in Ca:COD when comparing this study and the literature. The optimum Ca:COD range demonstrated across multiple digester and substrate types suggests that the Ca:COD can generally help to optimize methane production during anaerobic digestion. More particles and phosphorus were retained with calcium addition, but phosphorus remained in the form of struvite. Struvite could prevail because the Ca:Mg molar ratio was low (1.8) compared with previous studies (2.9 in PM and 7.4 in BW) and because bicarbonate captured calcium. Most of the calcium precipitated as calcium carbonate, limiting the calcium availability for calcium phosphate formation and granulation. The presence of inorganic carbon and the Ca:Mg molar ratio are two indicators to predict the success of CaP granulation, granting the possibility to identify new waste streams for CaP granulation. Still, the higher methane production and removal of phosphorus by adding calcium improves the valorization of CM. The phosphorus-rich sludge bed and the nitrogen-rich digestate can be used separately, saving on mined and artificial fertilizer.


P
P

4

Enabling efficient phosphorus recovery from cow manure: Liberation of phosphorus through acidification and recovery of phosphorus as calcium phosphate granules

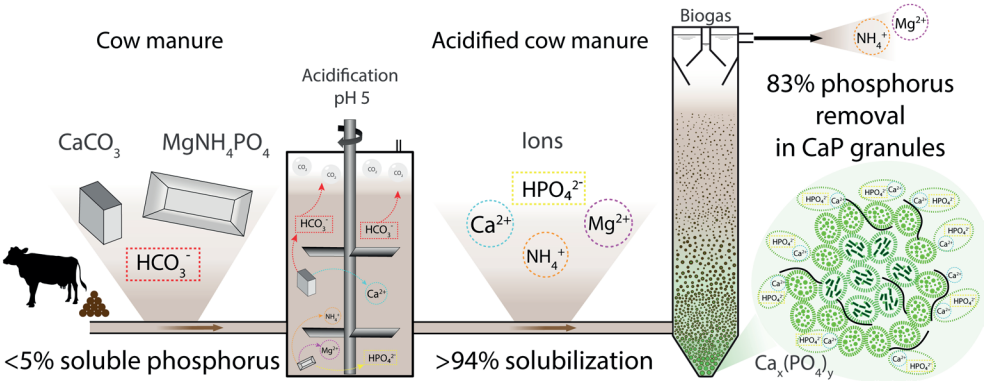

This chapter was published as:

C. Schott, L. Yan, U. Gimbutyte, J.R. Cunha, R.D. van der Weijden, C. Buisman, Enabling efficient phosphorus recovery from cow manure: Liberation of phosphorus through acidification and recovery of phosphorus as calcium phosphate granules, Chemical Engineering Journal 460 (2023) 141695. DOI: 10.1016/j.cej.2023.141695.

Abstract

Cow manure (CM) is one of the largest secondary sources of phosphorus, while mined phosphorus rock is becoming scarce and diminishing in quality. Phosphorus recovery from CM is essential for increasing the phosphorus use efficiency and, therefore, securing future food production. Calcium phosphate (CaP) granulation can enable efficient phosphorus recovery during anaerobic digestion. However, in CM, the absence of phosphorus in the ionic form and the high presence of inorganic carbon and magnesium inhibits CaP granulation. In this study, CaP granulation was achieved for the first time during CM treatment, using an up-flow anaerobic sludge blanket (UASB) reactor preceded by an acidifying continuously stirred tank reactor (CSTR). The UASB reactor and CSTR ran for 190 days at organic loading rates of 1 and 22.5 gCOD $L_{reactor}^{-1}$ d^{-1}, respectively. The acidification of CM at pH 5 dissolved struvite and calcium carbonate, causing more than 94% of phosphorus, calcium and magnesium to be present as ions. In the UASB reactor fed with the CSTR effluent, 83 ± 3% of phosphorus was removed and mainly present as CaP granules > 2.5 mm in diameter. The CaP granules had a phosphorus content of 8.4 ± 1.3 w/w% with amorphous and crystalline calcium phosphate being the dominant phases. The formation of large and concentrated CaP granules causes accumulation at the bottom of the reactor and allows for simple size separation leading to efficient phosphorus recovery. The recovery of CaP granules improves CM valorization and can reduce the transport of manure by up to 87%. The acidification prior to digestion thus promotes a more efficient use of phosphorus from CM in agriculture and can replace phosphorus from primary phosphorus sources.

4.1. Introduction

Phosphorus is an essential nutrient for food production, but its finite natural reserves are rapidly diminishing and geographically imbalanced, necessitating the circular use of phosphorus from secondary sources [29, 44]. The largest secondary and renewable source of phosphorus is animal manure [30] of which cow manure (CM) and, more specifically, cow slurry (CS) is the most abundant animal manure in the EU [31]. In the EU and especially in the Netherlands, there is an excess of CM and it is currently regarded as a waste stream and a threat to the environment. For pollution prevention, the application of CM to land is regulated by phosphorus and nitrogen field-application limits in the Netherlands [137, 138]. On cow farms in the Netherlands, the limits for phosphorus application have already been reached with CM as the only phosphorus source [26]. However, on cow farms, only 2/3 of the total applied nitrogen application comes from CM, whereas 1/3 comes from artificial nitrogen fertilizer [25]. This means the excessive phosphorus in CM is the cause for its required redistribution and transportation. When recovering phosphorus separately from the nitrogen in CM, more nitrogen, water and other substances originating from CM and of importance for soils could be applied on farmland in the Netherlands; at the same time, the recovered phosphorus could be transported cheaper and more sustainably to locations with a phosphorus deficit.

Resource recovery from CM is often primarily focused on biogas production by anaerobic digestion [193, 194]. A simultaneous recovery of phosphorus and nutrients from CM could improve the efficient valorization of CM. Phosphorus recovery from CM is often limited by the size of phosphorus-containing particles. In CM, phosphorus is often present as struvite [38, 195], these individual crystals hardly aggregate or grow larger than 120 μm [107-109] because of its defined and smooth crystalline surface [110, 111]. The size of struvite crystals makes their separation from CM difficult [150, 192], complicating the recovery of a product with high phosphorus concentration [32, 38]. The addition of calcium can induce calcium phosphate (CaP) granulation, causing the accumulation of phosphorus in particles that can easily be separated from CM.

In Cunha et al. [41] and Schott et al. [37], this was proven for concentrated black water (BW; separated human toilet water) and pig manure (PM) digestion, resulting in 89% and 74% potential phosphorus recovery, respectively. In CM,

calcium addition enhanced phosphorus removal but CaP granulation did not occur when creating similar calcium to phosphorus molar ratios (Ca:P) of 3:1 as was done in BW and PM [38]. In Schott et al. [38], it became clear that the magnesium to phosphorus molar ratio (Mg:P), the abundance of bicarbonate (HCO_3^-), and the availability of the phosphate ion (HPO_4^{2-}) were limiting for CaP granulation in CM. The added calcium as $CaCl_2$ was precipitated with HCO_3^- to form $CaCO_3$ and the phosphorus remained mainly as fine struvite ($MgNH_4PO_4$) particles. A decrease in HCO_3^- and liberation of phosphorus from struvite to increase the presence of aqueous HPO_4^{2-} could allow for CaP granulation in CM.

Acidification of CM can remove inorganic carbon from solution and from calcium carbonate as CO_2, and liberate bound phosphorus from struvite into solution as HPO_4^{2-}. At a pH lower than the HCO_3^-/carbonic acid (H_2CO_3) pKa of 6.4, HCO_3^- is removed as CO_2 [196, 197] and struvite will likely dissolve already at pH values below 7 [198]. This could enable CaP granulation. However, the amount of carbonates and other pH buffering substances (NH_3/NH_4, HPO_4^{2-}, volatile fatty acids [VFA] and more) is commonly high in CM [38, 135], requiring relatively large quantities of acids to achieve sufficient acidification. The high costs of lowering the pH using acid, motivated researchers to explore alternative solutions. Szogi et al. [199] co-digested PM with peach waste to lower the pH because of the quick degradation of the latter, resulting in acid formation. The pH buffering effect of PM hence was overcome, and mineral phosphorus was released. A subsequent increase of pH with addition of CaOH required less base than acid because the buffers had been removed which allowed for calcium phosphate [$Ca_x(PO_4)_y$] precipitation. However, extra polymer addition was required in an extra treatment step to separate the formed $Ca_x(PO_4)_y$ fines in settleable aggregates. Another strategy to lower pH was investigated by Yilmaz and Demirer [200]. They achieved partial manure acidification by increasing the organic loading rate (OLR) of their reactor. This "overfeeding" enhanced the quicker acidogenic and acid-forming metabolism and outpaced the slower methanogenic metabolism [63]. Consequently, organic acids started accumulating, causing the pH to decrease. At pH values of 6 and below, the acidogenic activity increased, but the methanogenic activity was found to be reduced or eliminated [201, 202].

In this study, the acidification of CM and subsequent recovery of CaP granules during anaerobic digestion was tested with a two-reactor system. This separates

acid and methane production, taking advantage of the characteristics of acidogenic and methanogenic microorganisms. This could enable efficient and economic CaP granulation from CM. In the first reactor, a continuously stirred tank reactor (CSTR) with a high OLR, acid was added and acid formation stimulated to achieve removal of inorganic carbon and liberation of phosphorus. The effluent was fed to a second reactor (up-flow anaerobic sludge blanket [UASB] reactor), operating at a lower OLR to allow VFA to methane conversion. At a higher pH and by addition of calcium, this can induce CaP granulation. The goal was to study the ideal conditions for liberation of phosphorus with as little acid addition as possible in the CSTR and subsequent formation of recoverable and re-usable CaP granules in the UASB reactor. This would promote the efficient use of phosphate in agriculture and significantly reduce economic and environmental costs during transportation.

4.2. Materials and methods

4.2.1. Experimental setup

Reactor setup: CSTR and UASB reactor in series

A 2 L glass CSTR working at an acidic pH and a 45 L acrylic UASB reactor working at a neutral pH were continuously treating CM in series at 55°C for 190 days. Two types of CM were fed to the system: first (until operation day 53), a CS consisting of urine and feces falling through a slatted floor collected from a dairy farm in Grijpskerk, the Netherlands, and later gradually added dairy cow feces (CF; operation day 53–123, 10% increase per week with two weeks at 90% because of national holidays and from operation day 123–190 at 100% CF) collected from a dairy farm in Hardenberg, the Netherlands. The CF were separated from urine by a stable floor system with channels and holes for urine and a floor scraper to move feces in a separate pit. Both manure types went through a screw press at the farm and were separated on the day of collection with a sieve bend of 200 μm (Estrad sieve). The manure was stored in a climate chamber (4°C), after which it entered the stirred and cooled (4°C) storage tank before entering the treatment system. Both reactors were double-walled for heating to 55°C with individual heating systems. The CSTR was continuously fed at 0.5 mL min^{-1} and the UASB reactor at 60 mL min^{-1} (Masterflex pumps) but only every 2 hours for 1 minute; this led to a daily inflow of 720 mL d^{-1} for both reactors, aiming for an OLR of 1 gCOD $L_{reactor}^{-1}$ d^{-1} in the UASB reactor which resulted in an OLR of 22.5 gCOD $L_{reactor}^{-1}$ d^{-1} in the CSTR.

A buffer tank was placed between the reactors to allow for buffering eventual flow fluctuations and sampling of CSTR effluent. The buffer tank was emptied daily, and only fresh effluent was measured. The UASB reactor effluent was collected in a 10 L container. For analyses, the UASB reactor effluent was collected in a 1 L bottle overnight to ensure fresh effluent was measured

The CSTR was operated with an individual pump for the inflow and outflow, where frequent calibration ensured similar in- and outflows over the reactor, keeping the variation below 5%. The CSTR was operated anaerobically and closed so the gas could be sampled through a rubber septum, and its flow was measured (Ritter gas flow meter). The stirring bar was stirred through a magnetic connection and stabilized at the bottom with a Teflon bearing situated in a PVC inlay at the bottom of the CSTR.

The pH in the CSTR was controlled at pH value 5 by adding 5M HCl at a flow of 10 mL min^{-1} when the pH rose above 5. The acid concentration was chosen to remain below 10% dilution of the CM, which was based on estimations from titrations tests. The value was set in a transmitter unit from Endress+Hauser, which controlled the acid addition pump (Masterflex). The pH was measured with a pH and temperature probe (Endress+Hauser) entering from the top of the CSTR. The acid was added from the top of the CSTR and dripped into the reactor liquid.

The UASB reactor received additional calcium as $CaCl_2 \cdot H_2O$ solution based on the calcium-to-phosphorus concentration in the manure to achieve a Ca:P molar ratio of 3. The calcium solution was pumped every 2 hours for 30 sec to add 8% in volume of the influent, avoiding dilution of the manure. The calcium was sprayed into the UASB reactor through a horizontal pipe crossing the reactor horizontally with five horizontally distributed 5 mm openings.

The UASB reactor had five vertically distributed sludge bed sampling valves (tap 0 to 4, bottom to top, Fig. 4.1). The sludge bed was sampled from top to bottom to avoid moving the sludge bed of other taps before sampling it. The valves were briefly completely opened to sample 500 mL of sludge bed from tap 0 and 200 mL from tap 1 to 4.

The pH, temperature and redox were measured online at three vertically distributed locations. The probes (Memosens CPS16D-1014/0 Orbisint) were long enough to reach the horizontal center of the sludge bed and entered the reactor through 45°

angled openings to assure probe functioning. The probes were connected to a data logger for data collection.

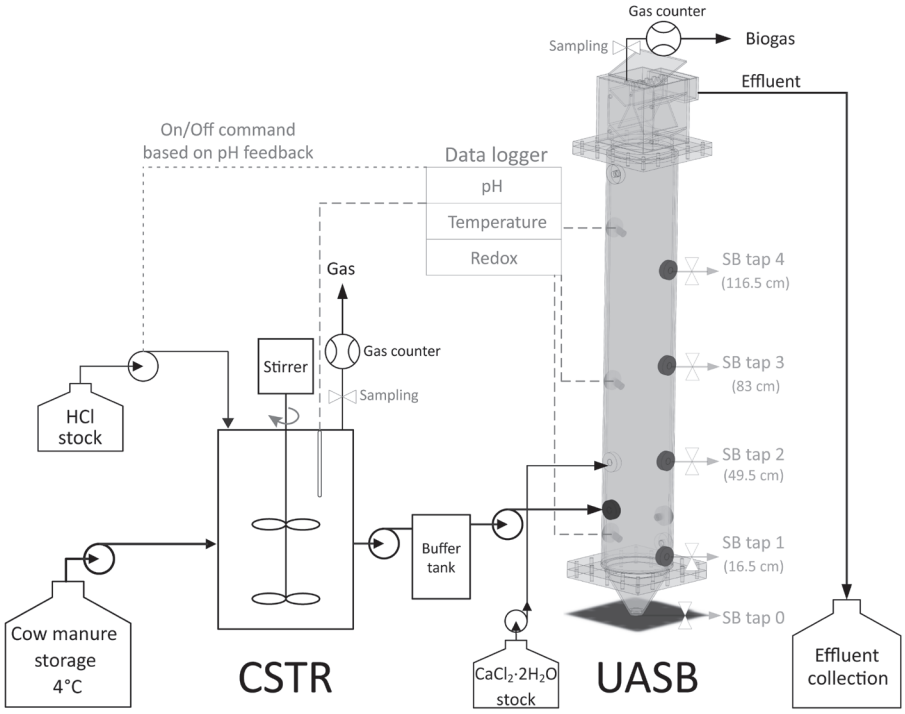

Fig. 4.1. Schematic of the two-reactor setup. First, the CM entered the 2 L continuously stirred tank reactor (CSTR) for acidification where the pH was measured online; once the pH value exceeds the set value, a pH-based feedback system started the pump adding HCl. The effluent of the CSTR is pumped into a buffer tank, where it becomes the influent for the 45 L up-flow anaerobic sludge blanket (UASB) reactor. The $CaCl_2$ solution was added separately to the UASB reactor. The effluent of the UASB reactor was collected in an external container. The UASB reactor had five vertically distributed sludge bed (SB) sampling taps. Both reactors were gas tight and had a gas collection system with a sampling point and gas counter. Note that the size representations are not accurate.

Titration and batch test acidification and phosphorus recovery

The alkalinity of CM was determined with automated titrations (888 Titrando, Metrohm with TIAMO 2.2 software) with 0.1M, 1M and 5M HCl for optimization. The titration vessel was stirred with a magnetic stirrer during the titration, and the acid was added at 1 mL min^{-1}. The addition rate was slowed down when foam formation occurred to avoid excessive foaming and failure of the titration.

In the acidification batch tests, CS (60 mL, all taken from the same mother sample of 10 L) was acidified in duplicate in 200 mL pressure-resistant bottles (Duran) to a pH of 4, 5, 5.5 and 6 with 5M HCl to avoid excessive dilution of the samples (<10% v/v). The added acid amount was based on the acid titration to reach the pH values. The batch bottle was stirred during the acid addition, and the pH was measured to be within ±0.1 of the desired pH. Afterward, the bottles were sealed and flushed with nitrogen. The batches of pH 4, 5 and 6 were incubated (New Brunswick Scientific) at 150 rpm for 30, 60 and 120 min at 25°C and 55°C with new batches for each parameter combination. The targeted pH increased by up to 0.5 pH units after incubation time, possibly because the dissolution of solid phases consumed protons. Therefore, the measured pH values after 30 min incubation were more suitable for predicting solubilization. Another set of batch tests was done with acetic acid (glacial ≥ 99.7%, 16.6 mol L^{-1} from VWR) for 30 min at 55°C. The focus of the batch tests was on solubilization of phosphorus.

In the phosphorus recovery batch tests, acidified CS (pH 5) was mixed with UASB reactor sludge bed in 200 mL pressure-resistant bottles (Duran). The ratio of acidified CS and sludge bed was changed between 1:10, 1:3 and 1:2 to simulate reactor loadings (ratios and volumes). The addition of calcium was based on Ca:P molar ratios of 1.85 (in raw CS), 2.5 and 5. The time for incubation was 5, 10 and 20 days. Each parameter combination was executed in individual bottles and with a reference bottle. The batch tests focused on the pH recovery and the phosphorus precipitation.

4.2.2. Analysis and sampling program

The flows over the reactor systems were monitored daily: the produced CSTR and UASB reactor effluent were weight (accumulation in buffer tank for CSTR and effluent container of UASB reactor), the biogas production read from the flow meters, and the weight of the HCl and $CaCl_2 \cdot H_2O$ solution. The influent and fresh effluent were analyzed weekly, and the biogas composition determined. The biogas was sampled with a gas syringe from the rubber septa of the sampling points described in Fig. 4.1. The sampling and analysis was done in duplicate in a Micro GC (Varian CP4900 Micro GC equipped with a Molsieve 5Å [MS5] and a PoraPLOT U [PPU] column). Each column is connected to its own micro thermal conductivity detector [μTCD]). The sludge bed sampling was done on operation days 34, 93, 147 and 181.

The analyses of influent, effluent and sludge bed included measurements for:

- pH determination with a Mettler Toledo Inlab Expert Pro-ISM after calibration with standard solutions from VWR at pH 4, 7 and 10.
- Total solids, volatile solids, fixed solids (TS, VS and FS, respectively) and total suspended solids, volatile suspended solids and fixed suspended solids (TSS, VSS and FSS) according to standard methods [64]
- Total, paper filtered (589/1 ashless Whatman) and soluble (0.45 μm Whatman filtration) chemical oxygen demand (COD_{tot}, COD_{pap}, and COD_{sol}, respectively) using Hach-Lange kits (LCK014)
- Total carbon, total organic carbon and total inorganic carbon (TC, TOC and TIC, respectively) from paper filtered samples (589/1 ashless Whatman) using a Shimadzu TOC analyzer
- Soluble elements in solution (phosphorus [P_{sol}], calcium [Ca_{sol}], magnesium [Mg_{sol}], sulfur [S_{sol}], iron [Fe_{sol}], sodium [Na_{sol}] and potassium [K_{sol}]) from 0.45 μm filtered (Whatman) samples using inductively coupled plasma optic emission spectroscopy (ICP-OES, with an internal yttrium standard; Perkin Elmer Optima 5300 DV)
- Anions (PO_4^{3-}, SO_4^{3-} and Cl^-), cations (Ca^{2+}, Mg^{2+} and NH_4^+) and VFA (acetate, propionate and butyrate) using ion chromatography (IC, Metrohm 930 compact IC flex) from 0.45 μm filtered samples
- Total elements (P_{tot}, Ca_{tot}, Mg_{tot}, S_{tot}, Fe_{tot}, Na_{tot}, and K_{tot}) using ICP-OES after microwave-induced acid digestion (Milestone Ethos Easy) with 69% HNO_3 for 15 min at 180°C.

The sludge bed samples underwent a particle size distribution (PSD) with sieves (analytical sieves from VWR). The grid size of the sieves was 0.4 mm, 0.9 mm, 1.4 mm, 2 mm, and 2.5 mm. A sample of about 30 g was consecutively sieved through the largest mesh size sieve and stepwise toward the smallest. The smallest fraction was collected in a crucible and dried together with the sieves at room temperature to determine the TSS and elemental composition of each fraction. The PSD and analyses were executed in duplicate. The sieved sludge bed samples were also analyzed with a scanning electron microscope coupled with an energy dispersive X-ray (SEM-EDX; JEOL JSM-6480LV coupled with NORAN Systems SIX energy dispersive X-ray) and X-ray diffraction (XRD; Bruker D8 Advance with a diffractometer of 280 mm measurement radius using Cu radiation, Linear PSD 3◦ detector opening, divergence slit at 0.58◦, and a soller slit at 2.5°) as described in Schott et al. [37].

The analyzes for the acidification batch tests included P_{tot}, P_{sol}, PO_4^{3-}, and solid analyses. The phosphorus recovery batch tests underwent the full analyses described for influent, effluent, and sludge bed.

4.2.3. Calculations

The OLR, solid retention time (SRT), level of hydrolysis and methanization were calculated as described by Halalsheh et al. [65] and de Graaff et al. [66]. Suspended and colloidal COD (COD_{sus} and COD_{col}, respectively) and the suspended species of elements (P_{sus}, Ca_{sus} and Mg_{sus}) were determined as the difference between the total and soluble fractions, and the cumulative removal and its errors were calculated as described in Schott et al. [37]. The solubilization was the percentage of a total element present as soluble element (E_{sol} E_{tot}^{-1}). Supersaturation calculations were based on similar procedure as described in Schott et al. [38].

4.3. Results and discussion

4.3.1. Pre-acidification of cow manure enables calcium phosphate granulation in the UASB reactor

Lowering the pH in CM resulted in the release of phosphorus and calcium into solution. Titration and acidification batch tests were used to find the optimum pH for phosphorus dissolution in CM. Lowering the pH to 5.2 ± 0.1 resulted in dissolution of 94 ± 11% of the solid phosphorus in CM; therefore, pH 5 was set in the acidification CSTR to acidify CM before entering the UASB reactor, ensuring phosphorus enters the UASB reactor as phosphate ion only. At pH 6.3 ± 0.1, there was no significant dissolution (6 ± 2%) and at pH 4.5 ± 0.1, the dissolution (91 ± 9%) did not significantly increase compared to pH 5. Along with phosphorus, calcium and magnesium were solubilized at pH 5.2 ± 0.1 (95 ± 10% and 109 ± 13%, respectively; supplementary information (SI), Fig. S4.1). Magnesium was mainly bound to phosphorus as struvite (SI, Figs. S4.2 and S4.3). Struvite dissolution contributed to an increase in the ammonium concentration in the effluent of the CSTR (1.6 g L^{-1} in influent to 3.3 g L^{-1} in effluent). However, the majority of released ammonium (78%) did not originate from struvite based on the molar balance of released phosphorus, but must have originated from organic compound degradation. Still, no detrimental effect of ammonium on anaerobic digestion of CM was observed. Calcium was mainly present as $CaCO_3$ in untreated

CM (SI, Figs. S4.2 and S4.3). The carbonate in $CaCO_3$ was stripped as CO_2 gas during acidification, freeing calcium and enabling $Ca_x(PO_4)_y$ precipitation. The CO_2 production matched the inorganic carbon removal, confirming its release as CO_2 from the system. $Ca_x(PO_4)_y$ precipitation was previously inhibited by the abundance of inorganic carbon [38, 198]. By removing CO_2 and dissolving struvite through acidification in a CSTR, calcium and phosphorus became available to form CaP granules in the UASB reactor that follows (Fig. 4.1).

In the UASB reactor, 83 ± 3% of the total phosphorus in CM could be retained in the sludge bed. The phosphorus precipitated with calcium (65 ± 3% calcium removed) and not again with magnesium as struvite. The dissolved magnesium (98 ± 3% Mg_{sol} of the total) remained in solution throughout the sludge bed and in the effluent of the UASB reactor. The total amount of phosphorus, calcium and magnesium removed in the UASB reactor gave molar ratios of 1.89 Ca:P and 0.11 Mg:P. The Mg:P molar ratio was too low for struvite to be present. The Ca:P molar ratio was high enough for $Ca_x(PO_4)_y$ to be present (1–1.67 Ca:P molar ratio [18]), but a Ca:P molar ratio above 1.67 indicated co-precipitation of $CaCO_3$. The concentration of inorganic carbon entering the UASB reactor was 102 ± 28 mgC L^{-1}, which probably was mostly CO_2/H_2CO_3 at the given pH [197] and seemed low for inducing $CaCO_3$ precipitation. The inorganic carbon concentration in the effluent of UASB reactor was 211 ± 42 mgC L^{-1}, where the difference with the influent indicates the production of HCO_3^- during methanogenesis. The additional production of inorganic carbon in the UASB reactor might have induced the observed $CaCO_3$ formation and an increase in Ca:P molar ratio [19]. However, this would still be considerably less than in raw CM where the concentration of inorganic carbon was 2419 ± 145 mgC L^{-1}. Combined with XRD analysis (SI, Figs. S4.4–S4.6), these results confirm that $Ca_x(PO_4)_y$ is the dominant calcium and phosphorus phase in the UASB reactor when fed with acidified CM.

The accumulation of phosphorus and calcium as $Ca_x(PO_4)_y$ in the sludge bed of the UASB reactor led to the formation of aggregates and later CaP granules (Fig. 4.2). To our knowledge, this is the first time that CaP granulation has been observed in CM treatment. Previously, even after 456 days of continuous CM treatment, using a similar UASB reactor with calcium addition did not yield CaP granulation [38]. By acidifying CM, the amount of CaP granules (particles > 2.5 mm in diameter) in the sludge bed of the UASB reactor rapidly increased (Fig. 4.3a). The broadened peaks at positions 31 and 34.5 θ in XRD analysis and the calculated crystallinity (SI, Fig.

S4.5 and Table S4.1) indicate that $Ca_x(PO_4)_y$ in CaP granules was also amorphous. The spherical morphology of the 1–5 μm $Ca_x(PO_4)_y$ precipitates (Fig. 4.2b) was previously observed and confirmed as $Ca_x(PO_4)_y$ [18]. The formation of $Ca_x(PO_4)_y$ spheres enabled the aggregation of precipitate clusters [203], which evolved over time into CaP granules. The CaP granules >2.5 mm in diameter had the highest phosphorus content (8.4 ± 1.3%P w/w), also higher than CaP granules from BW (7.6 ± 0.8%P w/w) [21] and PM treatment (4.1 ± 0.8%P w/w) [6].

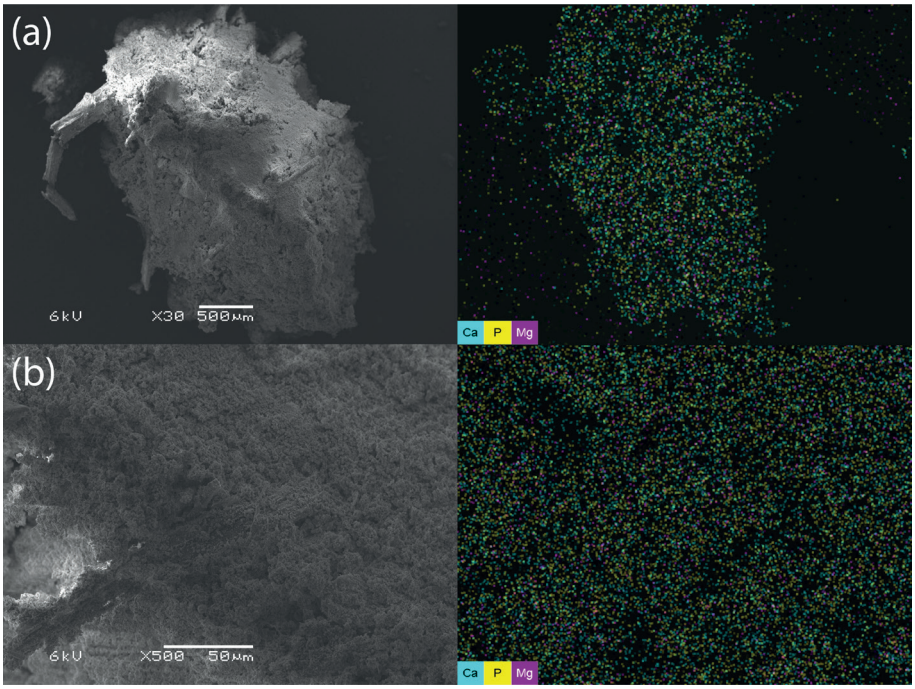

Fig. 4.2. SEM (left) and EDX (right) images of (a) a CaP granule >2.5 mm sampled on operation day 93 at 30x magnification and (b) 500x magnification. In the EDX images, calcium is represented as cyan, phosphorus as yellow and magnesium as purple. The overlap of calcium and phosphorus appears as green [$Ca_x(PO_4)_y$] and the overlap of magnesium and phosphorus as orange (struvite).

4.3.2. The sludge bed development of the UASB reactor and the fate of phosphorus.

The concentration of solids in the sludge bed increased over time at all sampled heights (Fig. 4.3a). Particles > 0.4 mm were especially present at taps 0 and 1. At taps

0 and 1, the bulk phosphorus concentration (2.7±0.6 and 3.1±0.8 gP L^{-1} averages of all sampling days) and the FSS content (37±4% and 33±1%, respectively) was the highest and decreased toward the top of the reactor, similar to previous studies with calcium addition [37, 41, 94]. At tap 0, the fraction > 2.5 mm in diameter increased the most (from 7% on day 34 to 21% on day 181). While the abundance of particles > 2.5mm was similar at taps 0 and 1 throughout the operation, the phosphorus concentration in particles > 2.5 mm in diameter was a factor 1.5 higher at tap 0 compared with tap 1 (9.1%P w/w and 5.9%P w/w, respectively on day 181). This is in line with a higher density of particles when containing more $Ca_x(PO_4)_y$ precipitates, settling to the bottom of the reactor. At tap 0, the phosphorus content in particles > 2.5 mm in diameter was on average 8.4 ± 1.3%P w/w, whereas in particles < 2.5 mm, the concentration was on average 1.4–1.9 ± 0.5%P w/w (day 34, 93, 147 and 181; Fig. 4.3b). Over time, not only the highest concentration was found in particles > 2.5 mm in diameter, but also most of the phosphorus was present in particles > 2.5 mm at tap 0 (57%, Fig. 4.3c). This trend can continue when the sludge bed of the UASB reactor, and especially at tap 0, would be regularly harvested for CaP granules. The faster accumulation of TSS in particles with > 2.5 mm in diameter than in the other size fractions as well as the high phosphorus content allows for efficient and selective phosphorus recovery with simple size separation methods.

The preferential distribution of phosphorus in particles > 2.5 mm in diameter compared with particles < 2.5 mm in diameter (factor 4.4 based on phosphorus content) was not previously observed. In BW and PM treatment, the particles > 0.4 mm in diameter all have a higher phosphorus content (7.6 ± 0.8%P w/w and 4.1 ± 0.8%P w/w for BW and PM, respectively) than the particles < 0.4 mm in diameter (4.4 ± 0.4%P w/w and 1.8 ± 0.1%P w/w for BW and PM, respectively) [37, 94]. Still, all phosphorus in particles was almost exclusively present as $Ca_x(PO_4)_y$ in BW and PM treatment. In the current study, on operation day 34, the XRD measurements found that $Ca_x(PO_4)_y$ made up 81% and 46% of the phosphorus in particles > 2.5 mm and < 2.5 mm in diameter, respectively. The other phosphorus was present as struvite, which was in line with the Mg:P molar ratio found in the particles. Particles < 2.5 mm in diameter had a Mg:P molar ratio of 1.29 ± 0.04 on operation day 34, while particles > 2.5 mm in diameter had a Mg:P molar ratio of 0.26 (Fig. 4.4). This confirms a higher presence of struvite (Mg:P molar ratio is 1) in

smaller particles than in larger particles. The struvite in smaller particles must have been mainly legacy struvite from the inoculum, because struvite is entirely dissolved in acidified manure and therefore not fed to the UASB reactor.

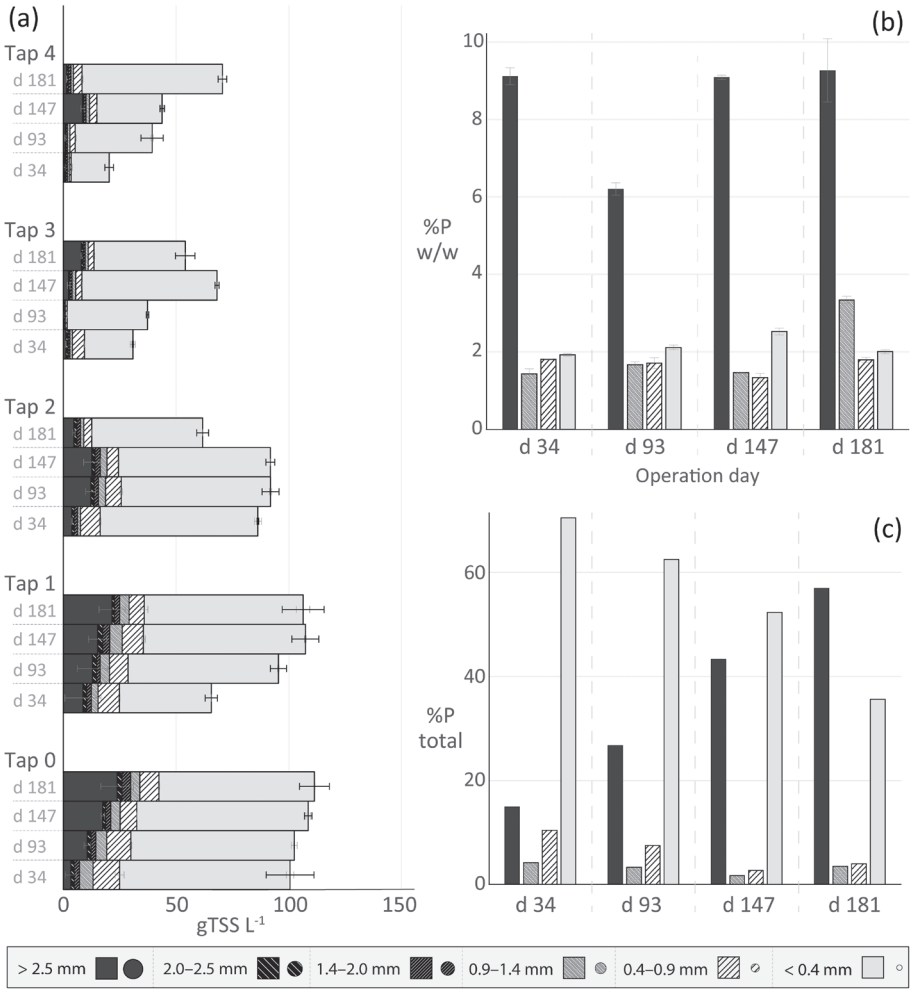

Fig. 4.3. (a) Particle size distribution in the sludge bed of the up-flow anaerobic sludge blanket (UASB) reactor over the height of the reactor and over time. The black error bars represent the deviation of the total TSS measurement and the grey error bars the deviation for each size fraction. (b) The phosphorus weight percentage based on dry matter in size fractions collected from tap 0 over time and (c) the distribution of the total amount of phosphorus at tap 0 based on dry matter over the same size fractions over time. Note that particles in the fractions 1.4–2 mm and 2–2.5 mm were not enough to do the elemental analyses described in (b) and (c).

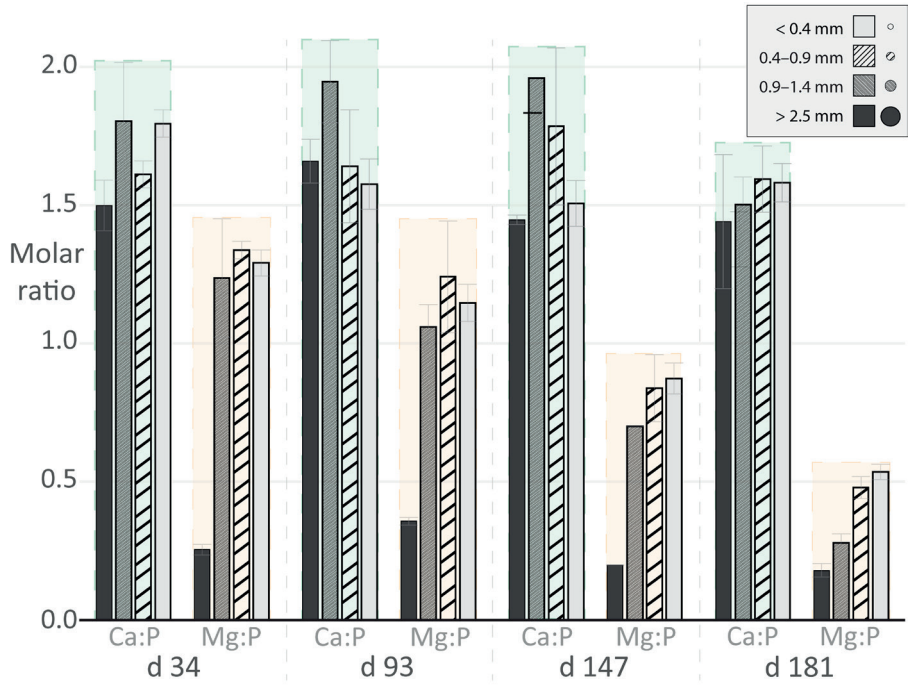

Fig. 4.4. Molar ratios of calcium to phosphorus (Ca:P, green background) and magnesium to phosphorus (Mg:P, orange background) in particle size fractions from tap 0 of the UASB reactor over time.

The magnesium content decreased over time in particles of all sizes in the sludge bed, indicating the dissolution of legacy struvite. In particles < 2.5 mm in diameter, the Mg:P molar ratio decreased from 1.29 ± 0.04 on day 34 to 0.43 ± 0.11 on day 181 (Fig. 4.4). In particles < 0.4 mm in diameter, the XRD detected only 7% of the phosphorus as struvite on day 181, but 93% as $Ca_x(PO_4)_y$ (SI, Fig. S4.6). In particles > 2.5 mm in diameter, the XRD detected $Ca_x(PO_4)_y$ as the only phosphorus species. The low Mg:P molar ratio, the decrease of measured struvite with XRD, and the high magnesium concentration in the effluent of the UASB reactor confirm the dissolution of legacy struvite. The reason for struvite dissolution is the high abundance of calcium in ionic form entering the UASB reactor from the effluent of the CSTR (1.93 ± 0.34 $gCa^{2+}\ L^{-1}$) with barely any inorganic carbon present (< 0.1 $gC\ L^{-1}$). Thus, the calcium entering the UASB reactor from the CSTR effluent and the calcium added directly (1.63 ± 0.50 $gCa^{2+}\ L_{manure}^{-1}$) to the UASB reactor was freely available to bind phosphate and as consequence dissolve struvite.

Additionally, the reduction of urine in the CM used as influent from operation days 53 to 123 reduced the concentration of ammonium and consequently, further lowered the supersaturation of struvite and promoted its dissolution. After day 123, only CF were fed to the CSTR. CF contained less ammonium (28% less) and a higher phosphorus concentration (33% more) compared with CS.

The mechanism behind the preferential phosphate distribution, the growth of granules, the maturation of granules and the recrystallization of struvite can be explained in six steps as illustrated in Fig. 4.5a and b, representing the sludge bed on days 34 and 181, respectively.

1. The acidified CM entering the UASB reactor contains phosphorus, calcium and magnesium primarily in ionic form (Fig. 4.5a.1). Additionally, the inorganic carbon concentration is extremely low (102 ± 28 mgC L^{-1}) when compared with raw CM (2419 ± 145 mgC L^{-1}).
2. The magnesium ions are not retained in the sludge bed (93 ± 3% present in the effluent of the UASB reactor), indicating higher supersaturation of $Ca_x(PO_4)_y$ than of struvite (supersaturation index based on PHREEQC: amorphous calcium phosphate [ACP] 13.1, struvite 0.7). The difference in supersaturation is likely caused by the high abundance of Ca^{2+} from the pre-acidification and added $CaCl_2$, boosting the competitiveness of calcium with magnesium to precipitate with phosphate. $Ca_x(PO_4)_y$ precipitation is preferable at the surface of existing particles over bulk precipitation. Silverman and Boskey [204] evaluated diffusion systems for biomineralization of $Ca_x(PO_4)_y$. Their setup consisted of a flow system connecting two separate reservoirs with calcium and phosphate ions and specific locations for creation of supersaturation and precipitation. They noticed a decrease in concentration of both ions at the precipitation locations, creating a concentration gradient between the reservoirs and these locations. Consequently, the concentration gradient induced diffusion of ions toward the existing precipitate surface where more ions precipitated. Ion diffusion especially becomes important in systems with little mixing, like the UASB reactor in which mixing was mainly induced while pumping the influent every 2 hours. This mechanism could explain the transport of ions entering with the influent to the existing CaP granules where they precipitate over bulk $Ca_x(PO_4)_y$ precipitation in the UASB reactor (Fig. 4.5a.2).

3. At the surface of CaP granules (Fig. 4.5a.3), the ions can undergo secondary nucleation which allows precipitation at lower supersaturation, because of the presence of already existing $Ca_x(PO_4)_y$ [116, 205]. Polymers with negatively charged functional groups could have functioned as a site (such as extracellular polymeric substances [EPS] or humics) for calcium complexation and triggering supersaturation of $Ca_x(PO_4)_y$. During the formation of $Ca_x(PO_4)_y$, ACP is often the first precipitate to form, because of its favorable kinetics over other more stable $Ca_x(PO_4)_y$ [206]. The kinetics of ACP are favorable because the phosphate and calcium ions pre-arrange in pre-nucleation clusters similar to the structure of ACP [207]. The pre-nucleation clusters of ACP were first described by Posner and Betts [208] and are therefore also known as Posner's clusters. Posner's clusters have a centered calcium ion surrounded by phosphate ions that are again surrounded by calcium ions, resulting in a composition of $Ca_9(PO_4)_6$ and a Ca:P molar ratio of 1.5 [208]. The Ca:P molar ratio in the CaP granules (1.51 ± 0.09) was close to 1.50, agreeing with the presence of ACP in the granules. Several ACP particles commonly form spherical ACP precipitate-clusters [209]. Spherical clusters of approximately 1 μm in size were observed with SEM in this study (Fig. 4.2b). The inclusion of new ACP particles into existing ACP precipitate-clusters is an aggregated growth [209]. Aggregated growth is key for the growth of CaP granules and explains the relatively fast increase in size.
4. The CaP granules mature over time, transitioning from ACP to a more crystalline phase (Fig. 4.5a.4). Hydroxyapatite (HAP) is the thermodynamically most stable crystalline phase of $Ca_x(PO_4)_y$ and is therefore, likely to form over time. The "sharpening" over time of the peaks at positions 31 and 34.5 θ for the XRD spectra (SI, Figs. S4.5 and S4.7) and the increase in crystallinity from 23% to 34% (SI, Table S4.1) over the operation time indicates the transition from ACP to HAP. Similarly, in BW treatment, the XRD peaks sharpened in more mature granules [62], even though to a lesser extent compared with the current study. During the phase transition, the precipitate clusters dissolve and rearrange into continuous crystalline lattices of HAP as shown in transmission electron microscopy (TEM) images by Roohani et al. [209]. Posner and Betts [208] predicted already when introducing the Posner's clusters that they could be incorporated into the lattice of HAP. Yin and Stott [210] supported this theory and generalized that Posner's clusters could be the building blocks for apatites and α- and ß-tricalcium phosphate (TCP). Most studies predict an

autocatalytic dissolution-recrystallization process of ACP to HAP [211-213], which might be the same on the inside of the CaP granules.

5. In the bulk of the sludge bed, struvite was the dominant phosphorus species, but dissolved to form $Ca_x(PO_4)_y$ over time (Fig. 4.5a.5). Qin et al. [214] closely followed the dissolution of struvite and reprecipitation as $Ca_x(PO_4)_y$ in a $CaCl_2$ solution. The conversion of struvite to $Ca_x(PO_4)_y$ resulted in different precursor phases of HAP (e.g., acidic ACP [$(CaHPO_4)_n$], crystalline monetite [CaHPO], ß-TCP and whitlockite [$Ca_{29}Mg(HPO_4)_3(PO_4)_{18}$)], depending on the formation location of $Ca_x(PO_4)_y$ on the surface of the struvite crystal. The orientation of the struvite crystal lattice toward the newly forming $Ca_x(PO_4)_y$, caused different structures and phases of $Ca_x(PO_4)_y$. In the current study, the presence of different $Ca_x(PO_4)_y$ phases in fine particles might have slowed down the precipitation of ACP in particles < 0.4 mm in diameter. Additionally, magnesium ions released from struvite might have increased the competition for phosphate precipitation and prolonged the induction time for the phase transition from ACP to HAP [125, 128, 215]. This is in line with the lower degree of crystallinity (SI, Table S4.1) that was observed for particles < 0.4 mm in diameter when compared with CaP granules (> 2.5 mm in diameter) at day 181, indicating a more dominant presence of ACP and other precursor phases.
6. Once all struvite in the sludge bed recrystallized to $Ca_x(PO_4)_y$ (after day 181), a more similar phosphorus content over the size fractions > 0.4 mm in diameter would be expected (Fig. 4.5b). The particles < 2.5 mm in diameter should also mainly consist of ACP and allow for formation of new ACP on their surfaces. The presence of more homogeneous $Ca_x(PO_4)_y$ phases would allow better aggregated growth and particle agglomeration to form together larger CaP granules. This would also equalize the difference in phosphorus content over the size fractions, which is partially visible in this study as the phosphorus content in particles between 0.4 and 2.5 mm diameter increases from 1.6 %P w/w on day 34 to 2.6 %P w/w on day 181. However, longer operation time is needed for confirmation.

The possibility of starting CaP granulation in a sludge bed already containing struvite and transforming it into $Ca_x(PO_4)_y$ demonstrates the applicability of this process for existing digestion units. This means that existing CM digesters can also be adapted by feeding acidified CM to form CaP granules and efficiently recover phosphorus.

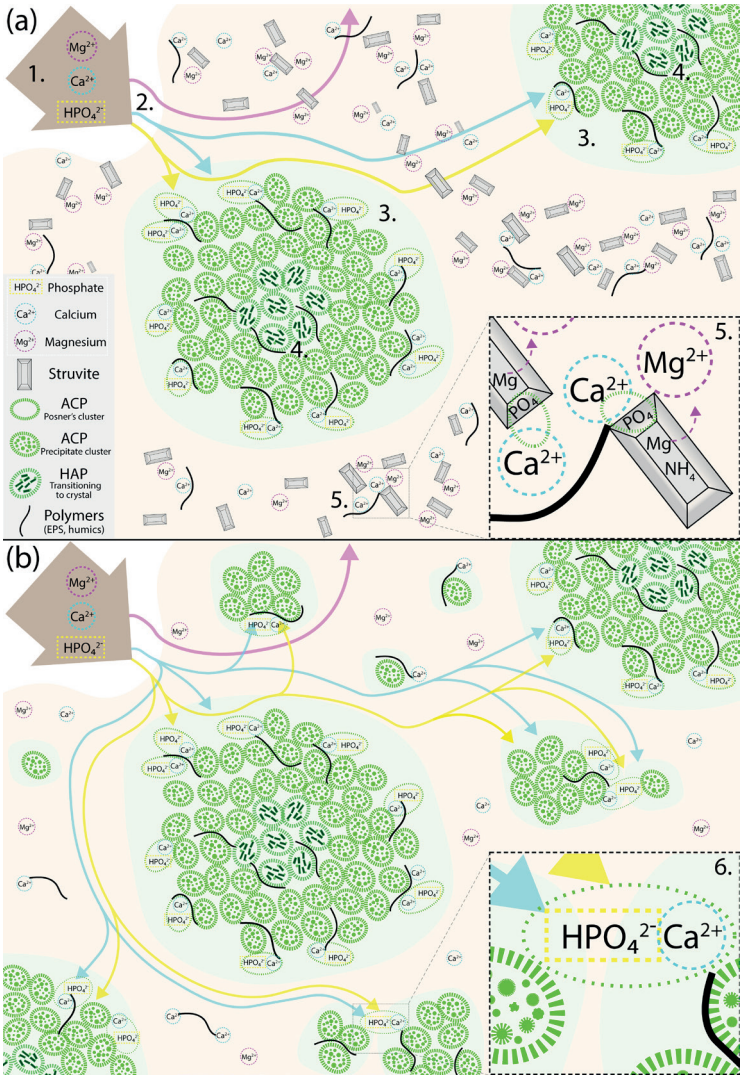

Fig. 4.5. Schematic representation of the sludge bed at (a) day 34 and (b) day 181 and after. In the schematics: (1) receiving acidified influent with (2) elemental distribution of influent (arrows) and (3) preferential precipitation areas for calcium and phosphate (green), while magnesium leaves the sludge bed as ion. (4) The ACP at the center of the CaP granules transitions through dissolution/rearrangement and recrystallization into crystalline structures and agglomerates of hydroxylapatite (HAP). (5) The dissolution of small struvite crystals to reprecipitate as calcium phosphate [$Ca_x(PO_4)_y$] in the bulk and the lower Ca:Mg molar ratio due to the release of magnesium from struvite dissolution. (6) Once struvite was fully dissolved and only $Ca_x(PO_4)_y$ phases are present (after day 181), the distribution of incoming ions will be more equal and induce also aggregated growth of small particles to eventually grow into larger CaP granules.

4.3.3. Optimization of sequenced phosphorus liberation and CaP granulation

Four key aspects for optimization could be identified: (1) the decrease of acid addition and replacing it by biologically produced acid in the CSTR; (2) an optimal pH regime: a CSTR pH low enough to liberate phosphorus and a UASB reactor pH high enough to have methane production and CaP granulation; (3) an improved mixing in the UASB reactor to distribute the influent and bring small particles back into the sludge bed from tap 0; and (4) the decrease of calcium addition by defining a new Ca:P ratio required when no inorganic carbon is present.

Lowering the acid addition in the CSTR would make the process more cost efficient. The production of organic acids inside the CSTR could replace the addition of external acid. Organic acid production can be increased by optimizing the process conditions in the CSTR. Wang et al. [216, 217] achieved low pH values (6.1) in dairy manure digestate by co-fermenting beet root pulp and potato peels. Wang et al. [218] reported a 1.4-fold increase in VFA yield when running anaerobically digesting food waste at pH 6 instead of pH 5. In the current study, the VFA production increased at pH 5.6 and kept increasing with increasing pH until pH 6.6 in the CSTR (Fig. 4.6a). However, at pH 6.6, the CH_4 production was 121 mL d^{-1}, whereas at pH 5 and below, the CH_4 production did not exceed 20 mL d^{-1}. Production of CH_4 meant conversion of organic acids, removing their acidity and, thus, was not desired in the CSTR. Still, the presence of VFA, and especially acetate, was higher at pH 6.6 than at pH 5 and below. However, the solubilization of phosphorus only began at pH 6 and below and worked best at pH values closer to 5 (Fig. 4.6b). Accordingly, the pH in the CSTR cannot be much higher than 5.5. At a higher pH, not enough phosphorus would be dissolved, nor enough inorganic carbon removed, which jeopardizes CaP granulation and the possibility of efficient phosphorus recovery.

The pH in the UASB reactor should allow methane production and CaP granulation. A neutral pH is ideal for both, but with the acidified manure entering the reactor, the pH in the sludge bed of the UASB reactor can decrease. When testing a loading rate increase (from OLR 1 to 1.5 gCOD $L_{reactor}$ d^{-1}) in the UASB reactor on operation days 144–158, the pH decreased to 5.2 at taps 2 and 3 in the sludge bed. This caused phosphorus dissolution in the sludge bed (Fig. 4.6c)

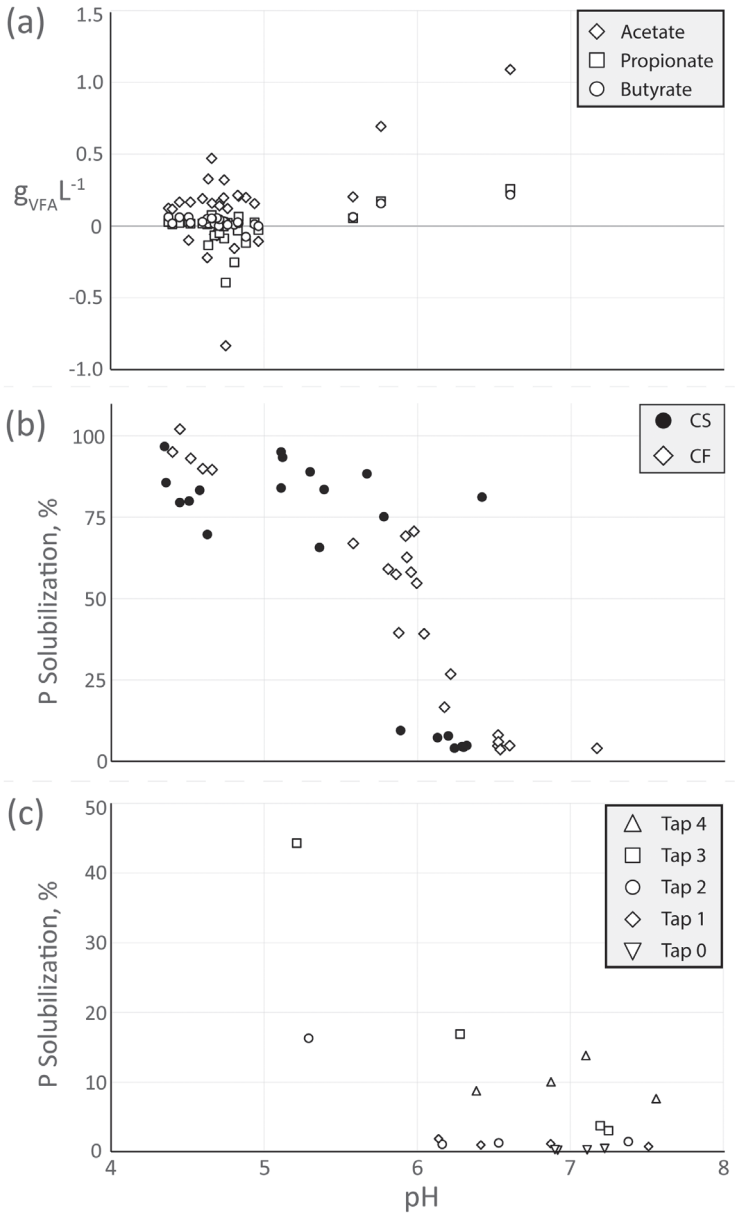

Fig. 4.6. (a) Production (positive) and consumption (negative) of volatile fatty acids (VFA) over the continuously stirred tank reactor (CSTR) at different pH values. (b) The solubilization of phosphorus in cow manure (CM) at different pH values and (c) the solubilization of phosphorus in the sludge bed of the up-flow anaerobic sludge blanket (UASB) reactor at different pH values.

and could cause washout of phosphorus. The decrease of pH in the sludge bed depended on the proton loading rate (PLR) versus the buffer production, mainly inorganic carbon from acetate conversion. From day 144 to day 158, the PLR increased from 9.85 μmol L^{-1} d^{-1} to 16.82 μmol L^{-1} d^{-1} while the buffer production did not increase, explaining the decrease in pH. If the majority of acid would be of organic nature and produced in the CSTR, then that organic acid could be converted to methane in the UASB reactor and mitigate the acidity, while producing more pH buffer. This would allow for a loading increase, optimizing the efficiency of the complete process and emphasizing that acidification with organic acids is beneficial.

The increased PLR had the most effect on taps 2 and 3, which indicates that the actual PLR was the highest in the sludge bed at these taps. A better mixing could prevent a local decrease in pH by distributing the low pH influent and the PLR better. Additionally, mixing of the bottom part of the UASB reactor can lift smaller particles that are lighter and less dense back into the sludge, where they can accumulate more phosphorus. In the batch tests with acidified CM and sludge bed, the phosphorus was precipitated within 5 days. Accordingly, the hydraulic retention time currently applied to the UASB reactor is not necessary for phosphorus precipitation, but for pH recovery and organic material degradation. This supports that mixing of at least part of the sludge bed could be beneficial for CaP granulation and the pH stability of the UASB reactor.

CaP granulation worked in previous studies for BW and PM with a Ca:P ratio of 3 and most calcium was removed (78% and 87%, respectively). In the current study, CaP granulation occurred with a was lower removal of calcium (65%) than in previous CaP granulation studies, while the magnesium liberation was higher [37, 41]. This indicates that the needed Ca:P ratio (previously thought to be 3) and, thus, the amount of additional calcium for CaP granulation in the UASB reactor could be lower. The removal of inorganic carbon during acidification lowers the potential for formation of $CaCO_3$, leaving more calcium for $Ca_x(PO_4)_y$ formation. Based on the calcium leaving the UASB reactor in solution, calcium addition could be decreased by up to 74%.

4.3.4. Potential and perspective of CaP granulation with an acidification step from cow manure

The acidification in the CSTR enabled the recovery of CaP granules with the highest phosphorus content (8.4 ± 1.3%P w/w) that has been directly recovered

from a UASB reactor thus far [37, 41, 94]. For the Netherlands, the phosphorus recovered as CaP granules from CM could annually save up to 32 million kg of mined phosphorus [219]. Replacing the mined phosphorus with CM-phosphorus would also reduce mining and transport emissions while simultaneously producing biogas. Because of the phosphorus application limits, currently, CM is transported from areas with high livestock density to areas with a lower density to apply it on land. If the phosphorus is extracted as CaP granules, their transport would be almost negligible compared to CM because of the much higher phosphorus content. This would significantly mitigate the economic and environmental costs.

Separating phosphorus and nitrogen in the UASB reactor allows for separate use of the two main plant nutrients. The nitrogen in the effluent of the UASB reactor was in the form of ammonium and can be applied on land as such or be recovered separately. The recovery by stripping or even by electrochemical recovery processes becomes an option because the originally organically bound nitrogen was mineralized to ammonium during the process. In current full-scale manure co-digestions treatment plants in Belgium (Am-Power and Waterleau), the nitrogen and phosphorus remain in the same stream, leading to the disapproval by farmers of the recovered nutrients [220, 221]. The relatively high phosphorus content together with high nitrogen makes the nutrient application unfavorable. In a full-scale treatment plant of PM in the Netherlands (Groot Zevert), phosphorus and nitrogen were successfully separated into individual recovery products (i.e. calcium phosphate sludge and reverse osmosis ammonium and potassium concentrate) from the digestate in pilot tests [222]. The digestate underwent a solid-liquid separation in a decanter to separate the nitrogen (78%) into the liquid fraction from the phosphorus (60%) into the solid fraction. The solid fraction was then acidified to pH 5 in two acidification steps with sulfuric acid and separated again with a screw press to have the phosphorus in the liquid fraction. The resulting liquid fraction went into a precipitation reactor where the pH was increased to 8 with $CaOH_2$ to form $Ca_x(PO_4)_y$. This was dewatered again with a decanter to obtain 98% of the ingoing 60% (59% of the phosphorus in digestate) as the phosphorus recovery product with 6.8%P w/w. The overall phosphorus recovery and phosphorus content in the recovery product was higher in the current study. A significant difference was the use of digestate for phosphorus recovery in the cited study compared with the recovery during digestion from raw manure in the current study. The direct recovery from raw manure in digesters includes the recovery of phosphorus which accumulated in the digester, minimizing losses.

The feasibility and viability of the two-phased process described in this study rely mainly on the added value of CaP granulation versus the costs of acidification compared to previous studies. Without optimization, the addition of the acidification step increased the phosphorus recovery from 61% [38] to 83% and enabled the formation of CaP granules. Consequentially, the transport of CaP granules (8.4%P w/w) could save up to 87% compared with CM (0.05%P w/w) and ~45% compared to phosphorus-rich sludge (0.4%P w/w) as presented in Schott et al. [38], based on the phosphorus content. At applied conditions without optimization, the acidification required an addition of 0.41 ± 0.05 mol H^+ L^{-1}_{manure}, leading to a cost of technical grade HCl [223] of ~7.5 € kg^{-1} of phosphorus, based on current prices. The phosphorus recovery process at the Groot Zevert installation would require ~30 € kg^{-1} of phosphorus in sulfuric acid and $CaOH_2$ addition, based on current prices. Besides the higher cost of chemical usage, only 60% of the phosphorus from the digestate was added to the recovery process, while in this study 90–95% of the phosphorus in cow manure was fed to the CSTR. Furthermore, base addition is not required to increase the pH due to the natural pH increase during anaerobic digestion in the UASB reactor. Other costs and savings are too uncertain to be considered at this technology readiness level (TRL); therefore, we focus only on the cost of chemical use.

According to the phosphorus content, the recovered CaP granules (8.4% w/w) from CM are a potential alternative to phosphate rock (7–18% w/w), which is currently priced at ~3 € kg^{-1}P [224, 225]. Furthermore, because the CaP granules are a recovery product, constraints with phosphorus availability from geopolitical events, scarcity of primary sources, and the required long-distance transport are reduced, while promoting efficient CM-phosphorus use.

4.4. Conclusions

The acidification in the CSTR successfully dissolved struvite and $CaCO_3$ particles, releasing more than 94% of phosphorus, calcium and magnesium into solution. In the subsequent UASB reactor, the majority of phosphorus and calcium (83 ± 3% and 65 ± 3%, respectively) was retained and precipitated as $Ca_x(PO_4)_y$. The $Ca_x(PO_4)_y$ aggregated and formed phosphorus-rich CaP granules. The CaP granules were > 2.5 mm in diameter with a phosphorus content of 9.6 ± 0.4 %P w/w and represented 57% of all phosphorus at the bottom of the sludge bed. The high phosphorus content

and the abundance of CaP granules allows for efficient phosphorus recovery from CM with simple size separation. The solubilized magnesium entering the UASB reactor also left the reactor in soluble form. More magnesium left the UASB reactor; this magnesium originated from dissolving legacy struvite in the sludge bed, which originated from the inoculum. The phosphorus from the dissolved legacy struvite precipitated again as $Ca_x(PO_4)_y$ in the same small particles, demonstrating the possibility to adapt a running digestion unit to the CaP granule-producing process. The acidification of CM enabled selective recovery of phosphorus in concentrated form, thus, improving the efficiency of the phosphorus as fertilizer or resource for fertilizer production.


P
P

5

Potential impact on calcium phosphate recovery by hydrogen in anaerobic digestion of cow manure

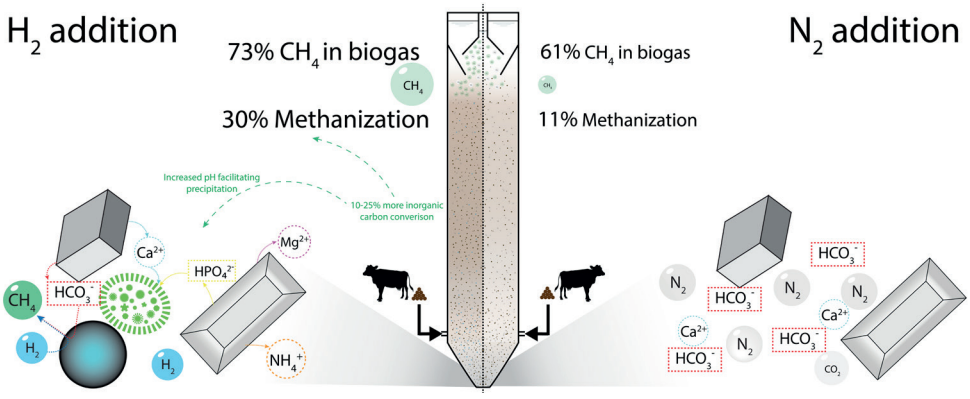

This chapter is in preparation for submission to a scientific journal as:

C. Schott, R. Pekusek, A. Guerrero, H.P.J. van Veelen, J.R. Cunha, R.D. van der Weijden, C. Buisman, Potential impact on calcium phosphate recovery by hydrogen in anaerobic digestion of cow manure

Abstract

The use of secondary source phosphorus is essential to secure a future phosphorus supply. Animal manure is the largest secondary source of phosphorus source, and cow manure (CM) is the most abundant animal manure in the European Union. Efficient phosphorus recovery from CM is essential to enable feasible valorization of phosphorus from CM. Calcium phosphate (CaP) granulation has a high potential to recover phosphorus in concentrated form during anaerobic digestion. The presence of inorganic carbon can inhibit CaP granulation, because calcium can precipitate as calcium carbonate in the presence of inorganic carbon instead of forming calcium phosphate [$Ca_x(PO_4)_y$]. In this study, hydrogen gas was added to stimulate hydrogenotrophic methanogenesis (HM) to convert inorganic carbon into methane and possibly induce CaP granulation. The performance of the UASB reactor with hydrogen gas addition was compared with a reactor with nitrogen gas addition with similar mixing conditions but without stimulated HM. The addition of hydrogen gas increased production of methane from 74 to 198 L-CH_4 $kgVS^{-1}$ and the overall production of biogas from 5 ± 2 to 9 ± 2 L d^{-1}. This resulted in a 10–25% removal of inorganic carbon from the sludge bed. The relative abundance of the microorganisms responsible for HM significantly increased in granules > 2.5 mm. The removal of phosphorus increased slightly from 30% to 34% with the addition of hydrogen gas, but no $Ca_x(PO_4)_y$ formed. A PHREEQC simulation indicated that the removal of inorganic carbon would need to be increased 6-fold to induce $Ca_x(PO_4)_y$ precipitation. Optimizing the availability of hydrogen gas for HM by increasing the reactor height could increase the inorganic carbon removal and eventually induce CaP granulation.

5.1. Introduction

Primary sources of phosphorus are finite, which puts a foreseeable end to their linear use [30, 47]. The linear use needs to be turned into a circular use by stimulating and improving the recovery from secondary sources [45]. Secondary sources, such as animal manure, are increasing in abundance since agriculture is becoming more intensive [226]. Animal manure contains significant amounts of phosphorus and energy in the form of organic material [135]. Phosphorus and energy from animal manure could substantially contribute to supplying resources to a circular and renewable economy.

In the EU, cow manure (CM) is the most abundant animal manure [31] and one of the largest secondary sources of phosphorus, energy and other nutrients [30, 163]. Currently, however, CM is for the most part directly used on land as fertilizer, while its fertilization capacity and nutrient availability vary. This can lead to nutrient runoff and harm the environment. For environmental protection, the application of CM is regulated by application limitations for nitrogen in the EU and additionally phosphorus in the Netherlands [137-139]. The abundance of phosphorus is the limiting factor for CM application, necessitating the transportation of CM including exportation to neighboring countries [227]. An efficient and well-integrated phosphorus recovery process for CM could avoid transportation and inadequate use of resources and instead produce resources that can mitigate reliance on primary resources.

The treatment of choice for CM is often anaerobic digestion to produce biogas and supply a green energy source. The biogas which is produced generally contains about 60% methane (CH_4) and 40% carbon dioxide (CO_2) and can be turned into heat or electricity [162]. Alternatively, biogas can be upgraded to the higher value biomethane, which mainly contains CH_4 by removing CO_2 or converting it into CH_4. Biomethane can replace natural gas in the general gas grid or vehicle fuel [228]. Whereas heat and electricity production are most beneficial when used close to the production site, biomethane can be distributed using existing natural gas networks [229]. Commercially, biogas upgrading is commonly done with membranes that separate CO_2 from the CH_4 in a unit after the digester. For the conversion of CO_2 into CH_4, a source of hydrogen (H_2) is required. CO_2 and H_2 can be abiotically converted into CH_4 and water by the Sabatier reaction under high pressure and temperature [230]. The same conversion can be executed biologically by hydrogenotrophic methanogens (HM) during anaerobic digestion without the need for increased temperature and pressure [231].

The biological conversion of CO_2 into CH_4 depends on the syntrophic partnership between acetogens and HM; the former requires the latter to consume its metabolic products such as H_2 and CO_2 and vice versa for feed availability. To ensure the consumption of H_2 by HM, the syntrophic partners need to be in proximity. The proximity provided in a biofilm or biological granule is often beneficial for syntrophic microorganisms [232]. The same syntrophic process can locally increase pH by converting (i.e., removing) CO_2 or HCO_3^- [43]. A higher pH can induce precipitation of calcium phosphate [$Ca_x(PO_4)_y$] but also calcium carbonate [38]. However, as HM can remove CO_2 when supplied with H_2, $Ca_x(PO_4)_y$ precipitation as granules can be stimulated with CH_4 production [43, 88]. CaP granulation has been shown to allow efficient recovery of phosphorus from concentrated human toilet water, also called black water (BW), pig manure (PM), and acidified cow manure (CM) [37, 41, 233]. For CaP granulation in CM, the CM had to be acidified to liberate phosphorus from struvite and calcium from calcium carbonate ($CaCO_3$). Without the acidification, even additionally supplied calcium was bound by inorganic carbon and precipitated as $CaCO_3$ and phosphate remained as struvite. The conversion of CO_2 to CH_4 via HM might have a positive effect on CaP granulation as acidification by lowering the presence of inorganic carbon.

This study aims to simultaneously improve CH_4 production and allow efficient recovery of phosphorus from CM by stimulating HM through H_2 addition, which removes inorganic dissolved carbon. This could make calcium available for $Ca_x(PO_4)_y$ formation and locally increase the pH, doubly benefiting CaP granulation. We hypothesize that H_2 addition stimulates the growth of HM which consequently benefits CaP granulation. In this study, this was tested in two UASB reactors with gas addition treating CM, where one reactor received nitrogen gas (N_2) and the other H_2. The addition of N_2 was supposed to create similar mixing conditions, but without the possibility of stimulating HM.

5.2. Materials and Methods

5.2.1. Experimental setup

Continouos UASB reactor set up with gas addition

Two UASB reactor of 45 L were operated for 200 days (prior 120 days start up not included) at 55°C to anaerobically digest CM (Fig. 5.1). The CM was collected from a dairy farm in Grijpskerk, the Netherlands. At the farm, the dairy feces and

urine fell through a slatted floor and were collected as a slurry in the manure pit below the stable. On the farm, the manure was separated with a screw press at 700 µm. On the day of collection, the manure was again manually sieved at 200 µm with a sieve bend (Estrad). The thin/liquid fraction was stored at 4°C and stirred when fed to the UASB reactors. The feeding was timed to pump for one minute every two hours to reach a daily flow of 800 mL, aiming for an organic loading rate (OLR) of 1 gCOD L^{-1} d^{-1} and a hydraulic retention time (HRT) of about 55 days (measured values in Table 1). The effluent was collected in a 10 L container.

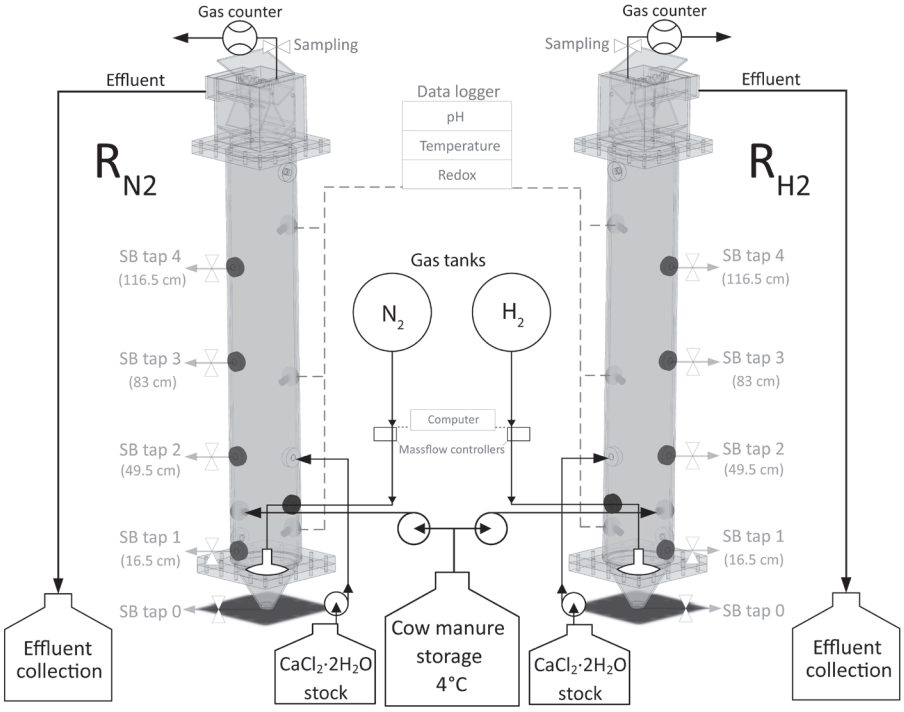

Fig. 5.1. Schematic representation of the setup, including the two 45 L UASB reactors fed with cow manure (CM) from a shared storage tank, calcium addition for both reactors, a gas-liquid-solids separator (GLS) on top of the reactors with a gas sampling spot before a gas flow meter and the effluent leaving the reactor after an overflow. The GLS contained inclined plates to improve the retention of solids. Both reactors received gas through a sintered metal gas sparger (2 µm pores) positioned at the bottom of the reactor. R_{N2} received nitrogen (N_2) gas from the gas line at 2 bars pressure and R_{H2} received hydrogen (H_2) gas from a gas bottle at 2 bars of pressure controlled by mass flow controllers. The pH temperature and redox were measured online with three vertically distributed sensors. The reactors had five vertically distributed sampling valves to sample the sludge bed.

Both reactors were equipped with a sintered metal gas dispenser for gas addition (Fig. 5.1). The openings in the sintered metal dispenser were 2 μm to add fine bubbles to the reactor. One UASB reactor received N_2 gas (R_{N2}) and the second received H_2 gas (R_{H2}). The addition was timed and controlled with mass flow controllers (Bruker). Every 20 minutes the gas valves opened for 30 sec at a flow of 300 mL min^{-1} to ensure an even distribution of gas bubbles. The addition of H_2 was based on matching the CO_2 production (~3 L-CO_2 d^{-1}) observed in Schott et al. [38] with a 4:1 H_2:CO_2 molar ratio, supplying enough H_2 to theoretically convert all CO_2 into CH_4. The addition of N_2 was based on the values of H_2 to have a reference reactor with similar gas-induced mixing. In both reactors, the gas left through the gas-liquid-solid (GLS) separator on top, where it went through a sampling point toward a gas flow meter (Ritter).

Both reactors received additional calcium based on a Ca:P molar ratio of 3:1 to induce $Ca_x(PO_4)_y$ formation. The Ca:P molar ratio of 3:1 was based on previous research with BW, PM and CM [37, 41]. The calcium was added as a $CaCl_2$ solution through a horizontally entering pipe with openings distributed over the width of the reactors. Calcium was pumped at the same timing as the influent, but only for 30 seconds to reach higher velocities and better spread of the calcium. The calcium solution was adapted to add only 8% in volume of the influent volume, avoiding dilution of the sludge bed.

Both reactors had three vertically distributed sensors (Memosens CPS16D-1014/0 Orbisint) for online measurements of pH, temperature, and redox at the center of the sludge bed. The measurements were collected in a data logger (Endress Hauser) and analyzed on a weekly basis to ensure proper reactor functioning.

Both reactors had five vertically distributed sampling valves for sludge bed sampling. The sludge bed sampling started from the top of the reactors (tap 4) and continued toward the bottom of the reactor (tap 0) to avoid relocation of the sludge bed before taking a sample. At taps 4-1 (in that order), samples of 200 mL were taken and at tap 0 a sample of 500 mL.

Batch tests to characterize hydrogenotrophic methanogenesis in cow slurry

In the batch experiments, H_2 availability was tested in combination with the Ca:P ratio, incubation temperature and incubation time. CM (100mL, all taken from the same mother sample) was incubated in 250 mL pressure-resistant bottles (Duran). The H_2 availability was changed between 25% and 75%. The Ca:P ratio was changed

between 2.5 and 3. Calcium was added in the form of $CaCl_2$. The incubation was carried out at 35°C (mesophilic conditions) or 55°C (thermophilic conditions) at 120 rpm. The incubation time was 2 days or 4 days. Each parameter combination was executed in individual bottles in duplicate and with a reference bottle. All bottles were first filled with 100mL CM, then the appropriate amount of $CaCl_2$ was added. After that, the bottles were sealed and flushed with a gas mixture of H_2 and N_2, with the help of mass flow controllers. The gas composition of each flushed bottle was collected in 5 L gas sampling bags (Tedlar) and analysed with a Micro GC (Varian CP4900 Micro GC equipped with a Molsieve 5Å [MS5] and a PoraPLOT U [PPU] column). Batch tests focused on CH_4 production and H_2 use in combination with inorganic carbon.

5.2.2. Analysis and sampling program

Sampling program and physico- chemical analyses

The sampling and analysis program included daily gravimetrical measurements of produced effluent and added calcium, and readings of the gas flow meters and mass flow controllers for biogas formation and gas addition. Weekly, the influent, fresh effluent and gas composition of both reactors were analyzed. For analysis, the effluent was collected in a 1 L flask over not more than 24 hrs to endure fresh effluent was used for analyses. Monthly, the sludge bed was sampled at all taps and analyzed on operation days 2, 57, 105, and 197. The physico-chemical analyses for influent, effluent and sludge bed were similar to Schott et al. [38] and comprised:

- pH measurements with a Mettler Toledo Inlab, which was calibrated with pH standards from VWR at pH 4, 7 and 10.
- Gravimetric determination of total solids, fixed solids, volatile solids, total suspended solids, fixed suspended solids, and volatile suspended solids (TS, FS, VS, TSS, FSS, and VSS, respectively)
- Total carbon, total, total organic carbon and total inorganic carbon (TC, TOC and TIC, respectively) from paper-filtered samples (Whatman 589/1) with the Shimadzu TOC analyzer
- Soluble elements including phosphorus (P_{sol}), calcium (Ca_{sol}), magnesium (Mg_{sol}), sulfur (S_{sol}), iron (Fe_{sol}), aluminum (Al_{sol}), sodium (Na_{sol}) and potassium (K_{sol}) from membrane filtered sampled (Whatman 0.45μm) with inductively coupled optic emission spectroscopy (ICP-OES; Perkin Elmar Optima 5300 DV) working with a yttrium standard

- Anions (PO_4^{3-}, SO_4^{2-} and Cl^-), cations (Ca^{2+}, Mg^{2+} and NH^{4+}) and volatile fatty acids (VFA; acetate, propionate and butyrate) from membrane-filtered samples (Whatman 0.45μm) with ion chromatography (Metrohm 930 compact IC flex)
- Chemical oxygen demand (COD) of the raw sample (COD_{tot}), paper filtered sample (COD_{pap}; Whatman 589/1) and membrane-filtered samples (COD_{sol}; Whatman 0.45 μm) with Hach Lange kits and a Hach Lange spectrophotometer
- Total elements including phosphorus (P_{tot}), calcium (Ca_{tot}), magnesium (Mg_{tot}), sulfur (S_{tot}), iron (Fe_{tot}), aluminum (Al_{tot}), sodium (Na_{tot}) and potassium (K_{tot}) from raw sample undergoing microwave-induced acid digestion (Milestone Ethos Easy) at 180°C for 15 min with 69% HNO_3 and measured with ICP-OES

For the sludge bed samples from tap 0, the particles size distribution (PSD) was gravimetrically determined with sieves of 0.4, 0.9, 1.4, 2.0 and 2.5 mm grid size (VWR analytical sieves). The dominant size fractions were analyzed with a scanning electron microscope coupled with energy-dispersive X-ray (SEM-EDX; JEOL JSM-6480LV and NORAN Systems SIX) and X-ray diffraction (XRD; Bruker D8 Advance).

DNA extraction and bioinformatic analyses

PSD samples of < 0.4 and > 2.5 mm in diameter for DNA extraction were collected (1.5 mL mixed liquor), centrifuged at maximum speed, and stored at -20 °C after supernatant removal. Defrosted subsamples (~400mg granule) were pre-processed by washing with 1mL sterile 1xPBS, 1 min centrifugation at maximum speed, and supernatant removal. The pellet was then suspended in SPB buffer of the FastSpin Kit for Soil (MP Biomedicals, OH, USA) by 15-30 min homogenization at 37 °C on a shaker at 150 rpm. Samples were subsequently sonicated for 30-40 s at 40 kHz in a water bath. DNA was then extracted using the FastSpin Kit for Soil (MP Biomedicals, OH, USA) following manufacturer's instructions with two minor adjustments. First, 40 μL polyA was added with 122 μL MT buffer. Second, homogenization was performed by 4 cycles of 40 s bead beating (Precellys Evolution, Bertin) at 7200 rpm with alternated 30 s pauses. Eluted DNA (60 μL) was further cleaned with Zymo Clean and Concentrator-5TM (Zymo Research, CA, USA).

Normalized DNA samples (5 ng/ul) were sent to MrDNAlab (Shallowater, TX, USA) for 16S rRNA gene amplicon sequencing. In summary, DNA amplicon

libraries were constructed with PCR using universal primers targeting the V4-V5 region of the 16S rRNA gene of bacteria and archaea. PCR was performed with primers 515F [234] and 926R [235] and a HotStarTaq Plus Master Mix Kit (Qiagen). Initial denaturation at 94°C for 3 min was followed by 30 cycles of 94°C for 30 s, 53°C for 40 s and 72°C for 1 min, with a final elongation at 72°C for 5 min. Amplicon sizes were confirmed on a 2% agarose gel, and amplicons were equimolarly pooled, and purified using Ampure XP beads (Beckman Coulter). Subsequent Illumina library preparation was followed by 2x300 bp paired-end sequencing on a MiSeq using V3 chemistry (Illumina).

Sequence data processing was carried out with QIIME2 (v. 2019.10) [236]. Briefly, the demultiplexed sequences were quality filtered by removal of primers and subsequent trimming of bases with a median Phred < 30. Accordingly, the first five bases of all reads were removed, and forward and reverse reads were trimmed at 200 and 190 bp, respectively. Then, DADA2 [237] error correction was applied, followed with inference of exact amplicon sequence variants (ASVs): the read pairs were merged and then dereplicated into ASV representative sequences. An alignment of representative sequences was created with MAFFT [238] and used to construct a phylogenetic tree using FastTree2 [239]. The taxonomic classification of ASVs was achieved with a naive Bayes classifier trained on primer set-specific sequences from the SILVA 132 reference database [240].This resulted in approximately 1.82 mio high-quality sequences and a median sequencing depth of 120578 reads per sample (range = 102619 – 143372). ASVs merged to genus level taxonomy to calculate genus relative abundances. Statistical (FDR $p < 0.001$) identification of differentially abundant bacterial groups (genus level) was obtained with ANCOM-BC modeling [241]. Sequence data are deposited into the European Nucleotide Archive (PRJEB60017). The microbial community analyses can be reproduced from the following link.

https://github.com/pietervanveelen/CSCH_UASB_granule_microbiome.

5.2.3. Calculations

The OLR, solid retention time (SRT), level of hydrolysis and methanization were calculated as described by Halalsheh et al. [65] and de Graaff et al. [66]. The suspended and colloidal COD (COD_{sus} and COD_{col}, respectively) and the

suspended elements species (P_{sus}, Ca_{sus} and Mg_{sus}) were determined as the difference between the total and soluble fractions, and the cumulative removal and its errors were calculated as described by Schott et al. [37].

5.2.4. Geochemical modeling with PHREEQC

Geochemical modeling was executed in PHREEQC Interactive version 3.5 [154]. The model included the composition of the liquid phase and the solid phase according to the measured composition of the sludge bed at tap 0 in R_{H2}. All compounds started in solution and were allowed to form solids as "solid solutions." The precipitates allowed in the solid solution were based on those observed in SEM and XRD measurements and possible polymorphs (e.g. calcite, aragonite and vaterite).

We used the wateq4f.dat database (version from August 21, 2012) with tipping hurley modifications to include humate and possible interactions with calcium [155]. The database was amended with master species and reactions for acetate, propionate, and butyrate from the minteq.dat database to see their effect on cation activities. We included information on struvite and amorphous calcium phosphate (ACP) in the database based on the data from Ohlinger et al. [156] and Musvoto et al. [157], respectively. We removed the abiotic reduction of carbonate into CH_4 because this reduction is not observed in anaerobic digesters and only occurs in the presence of catalysts or in extreme environments with high pressure and/or high temperature [158-160]. All materials, consisting of the database used (including precipitation and complexation reactions), the scripts for the different iterations and scenarios, and the resulting raw data sets are given in the PHREEQC appendix to support further studies.

5.3. Results and discussion

5.3.1. The effect of hydrogen addition on methane production from cow manure

The CH_4 yield increased from 74 L-CH_4 $kgVS^{-1}$ with N_2 addition to 198 L-CH_4 $kgVS^{-1}$ with H_2 addition. However, the CH_4 yield was higher in previous research (Table 5.1, R_{Ca}), because more VS was removed. Methanization was higher in R_{H2}

than in R_{N2} (30% and 11%, respectively). This combined with the higher CH_4 content in the biogas (on average 73% instead of 61% CH_4) of R_{H2} indicates the successful conversion of CO_2 to CH_4 when adding H_2. The overall biogas production (subtracting added gases) was also enhanced by H_2 addition from on average 5 ± 2 L d^{-1} with N_2 to 9 ± 2 L d^{-1} with H_2. The addition of H_2 can increase the CH_4 content, but the increase in biogas production cannot be simply explained by CO_2 gas conversions. Consumption of H_2 and CO_2 to form CH_4 should lead to a decrease in gas volume according to the ideal gas law. This was observed as a decrease in pressure in the batch experiments. Therefore, the increased biogas production was not only the result of CO_2 gas conversion, but must have been affected by the inorganic carbon from solution or the acetoclastic methanogenesis.

Table 5.1, Overview of reactor operation and performance in averages and deviation over time.

Parameter	Unit	R_{H2}	R_{N2}	R_{Ca} [38]
HRT	*d*	58 ± 9	56 ± 9	57 ± 7
OLR	$gCOD\ L^{-1}\ d^{-1}$	1	1	1
Methane production	$L\text{-}CH_4\ kgVS^{-1}$	198	74	301
Biogas production	$L\ d^{-1}$	9 ± 2	5 ± 2	11 ± 3
Methane content	%	73 ± 5	61 ± 4	62 ± 3
VFA removal	%	98	97	98
VS removal	%	38	42	51

CH_4 production through acetoclastic methanogenesis seemingly did not differ enough to explain the difference in biogas production. The COD_{tot} removal was 45% and 49% in R_{N2} and R_{H2}, respectively. The removal of VFA was similar in both reactors (~98%). If the biogas did not increase through the acetoclastic pathway, then it was probably induced by HM. The carbon source was probably inorganic carbon in solution in the form of HCO_3^-. In the sludge bed of R_{H2}, the concentration of inorganic carbon in solution was on average 25% lower at tap 0 and 10% lower at taps 1, 2, 3 and 4 than in the sludge bed of R_{N2} (Fig. 5.2a). The removal of HCO_3^- increased the pH because HCO_3^- is a weak acid. In the sludge bed of R_{H2}, the pH was significantly higher than in the sludge bed of R_{N2} (Fig. 5.2b). Treu et al. [242] also observed a significant increase in pH when adding H_2 gas to upgrade the biogas from CM digestion. This higher pH can influence the precipitation of elements.

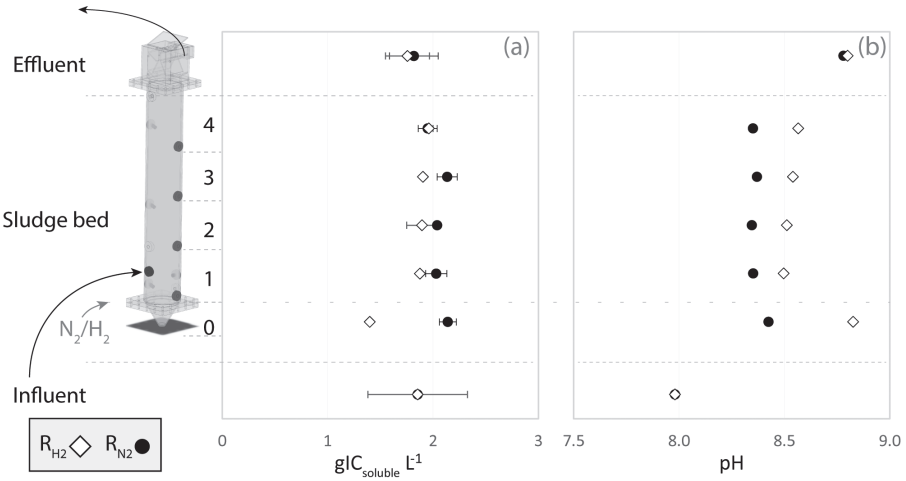

Fig. 5.2. The vertical distribution of (a) inorganic carbon in solution concentration and (b) the pH in the sludge bed of the UASB reactors R_{H2} and R_{N2} together with the influent (bottom) and effluent (top) concentration. Note that the N_2/H_2 line marks the location of gas addition in the UASB reactors.

5.3.2. The chemical composition in the sludge bed and the fate of phosphorus

The retained phosphorus was in the form of struvite and did not dissolve and form $Ca_x(PO_4)_y$ with the added calcium in either reactor. Although the removal of phosphorus and magnesium was slightly increased with H_2 addition (from 30 to 34% and from 31 to 35%, respectively), the removal of calcium, including the added calcium, was 67% in both reactors. Calcium probably primarily precipitated with inorganic carbon as $CaCO_3$. The removal of inorganic carbon by HM likely was not high enough to sufficiently decrease the competition for calcium ions and increase their availability for phosphate to induce CaP granulation. In Schott et al. [38], struvite also remained in the sludge bed and CaP granules could not form, because calcium precipitated as $CaCO_3$. However, in Schott et al. [233], the dissolution of struvite and the removal of inorganic carbon through acidification in a step prior to the UASB reactor enabled the formation of CaP granules in the UASB reactor. The acidification removed inorganic carbon as CO_2 gas to less than 100 mgC L^{-1}, boosting the availability of calcium ions for $Ca_x(PO_4)_y$ precipitation. The reduction in soluble inorganic carbon was 96% in the sludge bed by prior acidification, while in the current study, the reduction was only 10–25%. The 10–25% reduction in

inorganic carbon was probably not enough to limit $CaCO_3$ formation and induce struvite dissolution with consequent $Ca_x(PO_4)_y$ precipitation.

The removal of inorganic carbon necessary to induce $Ca_x(PO_4)_y$ precipitation and granulation is likely between 25% and 96%. In Fig. 5.3, the removal of inorganic carbon was simulated in PHREEQC with the composition of the sludge bed at tap 0 of R_{H2}. The concentration of total inorganic carbon includes the carbon estimated to be precipitated with $CaCO_3$. To estimate the amount of $CaCO_3$, we assumed that all calcium precipitated as $CaCO_3$, as indicated by the XRD measurements (Figs. S5.1–S5.4). The removal of total inorganic carbon at tap 0 was about 10% when compared with R_{N2} (3.9 and 4.4gIC_{total} L^{-1}). The simulation predicted that the 25% removal of total inorganic carbon (3 gIC_{total} L^{-1}) reduced $CaCO_3$ precipitation and would allow calcium to precipitate as $Ca_x(PO_4)_y$. This would lead to the phosphorus not being present solely as struvite and could potentially start the formation of CaP granulation. At 60% total inorganic carbon removal, all phosphorus at tap 0 of R_{H2} should be present as $Ca_x(PO_4)_y$, indicating that a situation similar to Schott et al. [233] could be achieved. Increasing the removal from 10% to 60% would also require an increase in H_2 conversion. Currently, 21% of the added H_2 was consumed, indicating that a 6-fold increase in the removal of inorganic carbon would require an increase in consumption of H_2 and a higher amount of H_2 addition. In an ideal situation, that would lead to 50% of CH_4 coming from HM (i.e., produced CO_2 and inorganic carbon in solution) and another 50% from acetoclastic methanogenesis.

The absence of phosphate ions could be detrimental to CaP granulation. In the current and previous CM study without acidification, barely any phosphate ions (< 10% phosphorus) were entering the UASB reactor. Studies with successful CaP granulation from BW and PM had ~21–28% of the phosphorus present as phosphate ions. The presence of phosphate ions allows for the formation of $Ca_x(PO_4)_y$ without needing to dissolve struvite. Once the first $Ca_x(PO_4)_y$ precipitates are formed, the lowered activation energy for secondary nucleation could favor the dissolution of struvite and continue the precipitation of $Ca_x(PO_4)_y$. The addition of H_2 caused an increase in pH in the sludge bed and partly removed inorganic carbon, but did not cause struvite dissolution and subsequent $Ca_x(PO_4)_y$ precipitation. Both precipitates form preferably at an elevated pH (8–9), which means that the pH

increase could have stabilized the struvite in R_{H2} and inhibit the dissolution of struvite and subsequent formation of $Ca_x(PO_4)_y$.

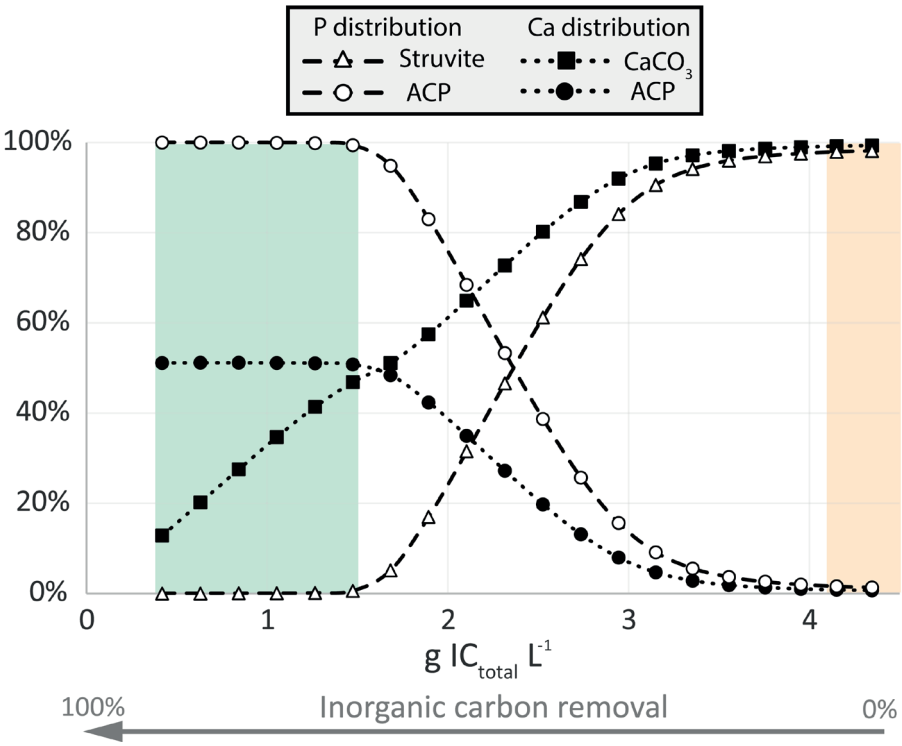

Fig. 5.3. PHREEQC simulation of the distribution of phosphorus and calcium distribution in precipitates in the sludge bed of R_{H2} at tap 0 at pH 8.8 over the presence of total inorganic carbon (IC; including inorganic carbon in solution and estimation of inorganic carbon present as $CaCO_3$ based on the assumption that all precipitated calcium is present as $CaCO_3$). The measured and estimated concentration of total inorganic carbon is 4 gIC_{total} L^{-1} (0% removal), and any decrease in that concentration is a possible removal, simulating the conversion of inorganic carbon by HM. The green and orange areas indicate where phosphorus is precipitated mainly as ACP and struvite, respectively. The simulation input (2.2 gP L^{-1}, 8.4 gCa L^{-1}, and 2.6 gMg L^{-1}, full information in PHREEQC Appendix) is based on the measurements at tap 0 in R_{H2}.

The formation of $Ca_x(PO_4)_y$ and CaP granulation may need more time in the given conditions. The sludge bed in R_{H2} and R_{N2} matured faster at tap 0 than higher in the sludge bed based on TSS and phosphorus accumulation. Above tap 0, the addition of gas as fine bubbles caused a strong buoyancy, washing out particles, which resulted

in a significant concentration difference between tap 0 (92 ± 6 gTSS L^{-1}) and the sludge bed at taps 1 to 4 (33 ± 6 gTSS L^{-1}) in both reactors (Fig. 5.4). Over time, the concentrations at tap 1 began to increase (from 43 ± 4 – 56 ± 1 gTSS L^{-1}) and could have reached higher concentration after the formation of an adapted sludge bed with denser and heavier particles. The low accumulation of solids at taps 1–4 explains the low phosphorus removal, indicating the washout of sludge bed. The washout led to a low SRT of 90 days in R_{N2} and 156 days in R_{H2}, probably giving too little time for the formation of CaP granules. In PM, the SRT was ~580 days and the dissolution of struvite and subsequent reprecipitation as $Ca_x(PO_4)_y$ took more than a year, while the current operation was about 200 days [37]. At taps 0, 1 and 2 in the UASB reactor treating PM with calcium addition, no inorganic carbon was found in solution. The added calcium completely precipitated the inorganic carbon as $CaCO_3$, resulting in a high $CaCO_3$ content in CaP granules with a lower phosphorus content (4.1%P w/w). Similarly, the process could have continued in R_{H2} and led to CaP granulation once the sludge bed matured and the SRT increased. However, the CaP granules would probably also have a low phosphorus content and remained inferior compared with the CaP granules recovered after acidification (8.4%P w/w). While the process is promising, a more efficient use of hydrogen and conversion of inorganic carbon needs to be achieved to have a positive effect on CaP granulation (Fig. 5.5d).

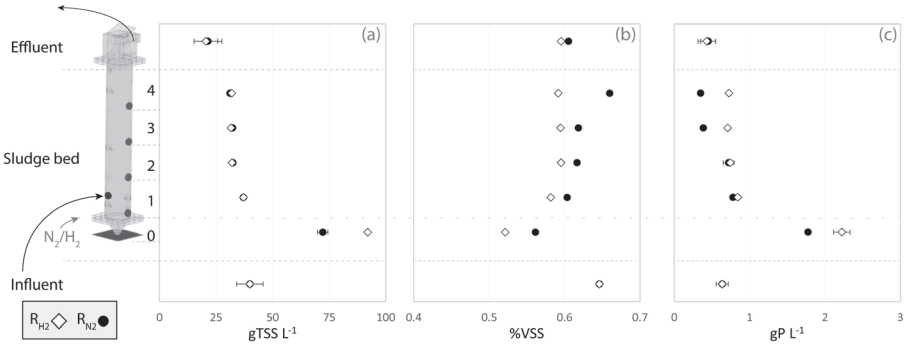

Fig. 5.4. The vertical distribution of (a) TSS concentration, (b) VSS content and (c) phosphorus concentration in the sludge bed of the UASB reactors R_{H2} and R_{N2} together with the influent (bottom) and effluent (top) concentration. Note that the N_2/H_2 line marks the location of gas addition in the UASB reactors.

5.3.3. Changes in the microbial community with hydrogen addition and their potential for CaP granulation

CM contains a highly diverse microbial community and native HM. While HM can generally be advantageous for CaP granulation by removing inorganic carbon and increasing the pH, the focus was on the group accumulating in larger particles when hydrogen was added. This allows categorizing the microbial communities within the sludge beds of R_{H2} and R_{N2} into organisms found in particles > 2.5 mm (granules) and particles < 0.4 mm.

The granules in R_{H2} hosted a significantly different microbial community compared with the granules from R_{N2} and the smaller particles from both reactors (Fig. S5.5). The relative abundance of a group of fermentative microorganisms was lower in granules from R_{H2} than in other sample groups (Fig. 5.5). The fermenters belong to the class of *Clostridium* and *Bacteroides*, including *Ruminiclostridium* and unclassified genera of *Rikenelleceae*, and the *Bacteroidales UCG-001* group, respectively [174]. They are known to hydrolyze cellulose and hemicellulose and ferment the resulting sugars into acetate, propionate, butyrate, CO_2 and H_2 [174]. When H_2 was added to R_{H2}, the increase in partial pressure likely made their conversion reactions unfavorable, triggering feedback inhibition. However, the removal of COD was not significantly affected by H_2 addition, indicating that the inhibited fermenters were probably active in the smaller particles of the sludge bed of R_{H2}. Interestingly, the relative abundance of these fermenters was similar in particles < 0.4 mm from both reactors. This indicates that they were specifically excluded from the granules, possibly by other H_2-producing microorganisms.

Syntrophic organisms rely on proximity and simple substrate exchange. In R_{H2} and R_{N2}, syntrophic acetogens preferably accumulated in biofilms or granules where their syntrophic relations were simpler to maintain [232]. Specifically, an unclassified genus of *Syntrophomonadaceae* increased in relative abundance in granules from R_{H2}. Its conversion of intermediate products into acetate produces H_2 that needs to be consumed to keep the metabolism energetically feasible. The HM are the syntrophic partners for keeping the H_2 concentration low by consuming the H_2 produced. They were also preferably accumulating in granules. The syntrophic partnership might have supported the *Syntrophomonadaceae* to outcompete earlier mentioned fermenters in granules. The HM population differed between R_{N2} and R_{H2}. In R_{N2}, *Methanobrevibacter* was dominant, which was reported to be naturally

dominant in untreated CM, suggesting their presence and involvement in ruminal processes [243, 244]. In this study, *Methanobrevibacter* were also the most abundant HM in the inoculum CM. In R_{H2}, *Methanoculleus* were the dominant HM. Previous researchers reported *Methanoculleus* to be the dominant HM when hydrogen was added to anaerobic digestion and biomethanation units [245, 246]. More HM, such as *Methanoplasma* and *Methanocorpusculum*, also had an increased abundance in granules from R_{H2}. The predominant presence of HM in the granules over the bulk sludge indicates that the addition of H_2 had the intended effect of having HM locally in the granules (Fig. 5.5a). However, the extent or quantity of conversion would need to be increased to impact or induce CaP granulation (Fig. 5.5d).

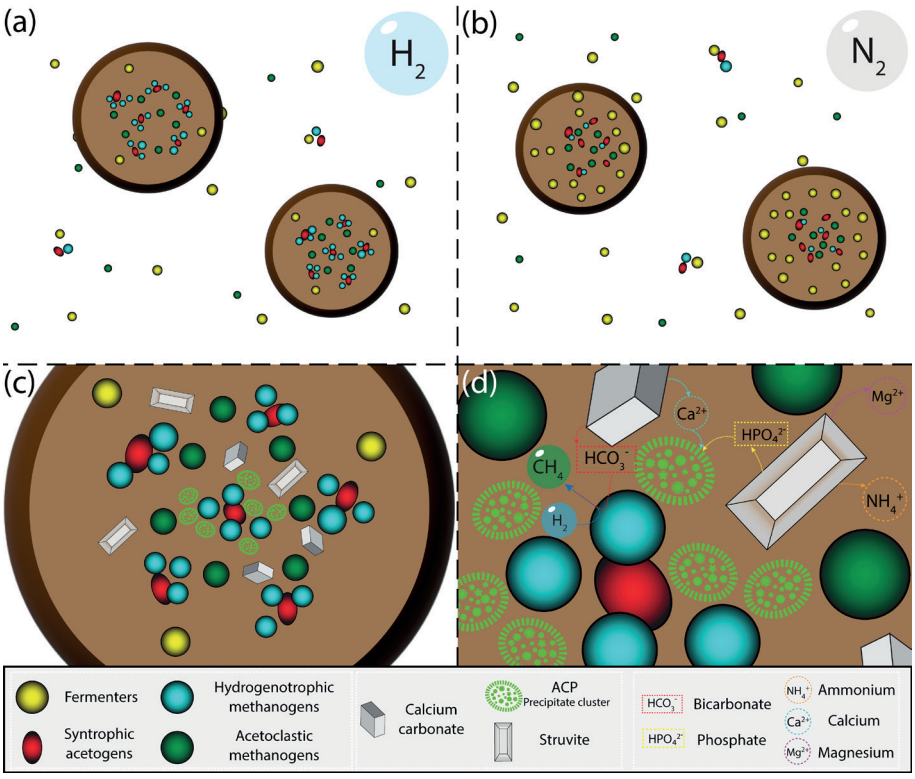

Fig. 5.5. Schematic representation of microbial communities based on relative abundances in bulk sludge and granules from tap 0 of (a) R_{H2} and (b) R_{N2}. (c) a zoom in of a granule from R_{H2} with potential distribution of crystals and possibly ACP accumulation and (d) the mechanism of how HM could be involved in ACP formation and struvite dissolution by freeing calcium from calcium carbonate.

The availability of H_2 for consumption by HM seems to be limiting, because H_2 and CO_2 can be found in the off gas. Although the amount of H_2 added to R_{H2} should be sufficient to convert all CO_2 into CH_4, only part of it (21%) was used, leaving CO_2 in the biogas and inorganic carbon as HCO_3^- in the liquid phase. The transfer of H_2 from the gas to the liquid phase was probably limiting. Other biomethanation studies used gas recirculation, biofilms at the gas-liquid interface, or a headspace with H_2 to achieve high conversion rates [246-248]. This indicates that the manner of adding H_2 gas to the UASB reactor needs to be improved. The in-situ biomethanation need to work similar to the syntrophic acetogens and HM. The H_2 produced or added should be immediately consumed when produced, to keep local H_2 concentrations low and within the range of its solubility. Otherwise, the H_2 escapes and is not used. H_2 in excess is not only not used, but can possibly also inhibit fermenting organisms and disrupt anaerobic digestion. Although the reactor performance did not show this kind of disturbance, the lower relative abundance of fermenting organisms in granules from R_{H2} was an indication of H_2 induced inhibition.

The addition of H_2 could be optimized by introducing lower flow rates continuously instead of higher flow rates with frequent injections. In the current study, the higher flow rates every 20 minutes were meant to introduce H_2 gas as small bubbles, increasing the surface area and the gas to liquid transfer. However, the high flow rates probably caused a brief overload in H_2, reducing the uptake capacity of the liquid phase. A continuous addition of H_2 at lower flow rates might result in overall higher uptake efficiency. An increased contact time by increasing the height of the reactor or recirculation of the biogas containing H_2 gas could further improve the conversion of H_2 and CO_2 into CH_4.

5.3.4. Integration of CaP granulation and green gas production in a hydrogen economy

The use of H_2 to improve phosphorus recovery possibly as CaP granules and to produce green gas is a step toward an integrated circular economy of and nutrient recovery. When the production of H_2 will increase the storage of H_2 could become a bottle neck. Converting it into CH_4 enables its storage and use in widely tested and commonly implemented gas systems. Simultaneously, CO_2 emissions can be reduced and the value of biogas increased. Production of CaP granules with H_2

addition allows the recovery of secondary source phosphorus with a fuel that could be made from renewable resources.

At the farm level or in a rural resource recovery and energy production sites, renewable energy sources such as wind and solar could be used to power electrolyzers for H_2 production. The H_2 produced could be used for biomethanation in a local digester where the area manure is treated. The manure-phosphorus could possibly be recovered as CaP granules and reused for efficient phosphorus fertilization in the area. The upgraded biogas or green gas could meet local energy demands of dwellings or supply the general gas distribution network.

5.4. Conclusions

The addition of H_2 increased the CH_4 yield from 74 to 198 L-CH_4 $kgVS^{-1}$ and the overall biogas production from 5 ± 2 to 9 ± 2 L d^{-1}. The CO_2 content in the biogas and the inorganic carbon concentration in the sludge bed decreased with the addition of H_2. This resulted in an increased pH, which slightly increased the removal of phosphorus (from 30 to 34%). The improvement in CH_4 production and the change in the chemical composition of the sludge bed could be correlated to an increase in relative abundance of HM in R_{H2}. The relative abundance of HM was markedly increased in granules over small particles. This was a promising indication for HM to eventually induce $Ca_x(PO_4)_y$ precipitation in the granules and trigger CaP granulation, when sufficient H_2 would be available. The availability of H_2 for consumption by HM seemed to be limiting in this study. An optimization could be to enhance the transfer from the gas to the liquid phase by increasing the contact time with a higher reactor.


P
P

6

General discussion and outlook

The future of agriculture depends on improving resource utilization efficiency. The effective recovery and reuse of resources from secondary sources, such as animal manure, is an essential part of that. To make better use of animal manure nutrients and improve their valorization, their separation to allow individual reuse could be valuable. The removal and recovery of phosphorus enables the valorization of phosphorus and nitrogen from manure, because often the ratio of nitrogen and phosphorus concentrations limits the application of manure as natural fertilizer on land. Calcium phosphate granulation proved itself to be a prospective technology for efficient recovery of phosphorus from animal manure as can be concluded from the research described in this thesis. Here, the key findings of the research and their impact on the understanding of the calcium phosphate granulation mechanism during anaerobic digestion and the applicability and feasibility of the process in the agricultural sector will be discussed.

6.1. Anaerobic digestion of animal manure using UASB technology

Anaerobic digestion of animal manure commonly takes place in continuously stirred tank reactors (CSTRs) for homogenization and for maximizing contact between substrate and biomass. Because of the good mixing, the hydraulic retention time (HRT) is equal to the solid retention time (SRT), which implies that no separation between the solid and liquid phases occurs [249]. In a UASB reactor, solids can settle and stay longer in the reactor than the liquid, resulting in higher biomass concentrations in the sludge blanket [86]. The highly concentrated sludge blanket can treat low-strength wastewater with primary soluble COD and a small solid content at a high rate. Typically, the organic loading rate (OLR) is at least 5 kgCOD $m^{-3}_{reactor}$ d^{-1} to have sufficient feeding and to create an upflow velocity (0.5–1.0 m h^{-1}) that induces the formation of a sludge bed with high settleability [250]. The selective pressure for well-settling biomass often leads to the formation of granules. In this thesis, the UASB reactors treat animal manure which contains about 50% suspended COD, requiring to operate at lower OLRs of 1 kgCOD $m^{-3}_{reactor}$ d^{-1}. That corresponds to HRTs of about 40 and 50 days for pig manure (PM) and cow manure (CM), respectively. Due to pulse feeding (every two hours), the upflow velocities reached 0.02 and 0.01 m h^{-1} in PM and CM treatment, respectively. The low upflow velocities and OLR remind more of a UASB septic tank configuration

[249]. This configuration and process conditions allowed for longer SRTs than HRTs (up to ten times longer) in the UASB reactors of this thesis research.

The long SRTs allowed enough contact time for the degradation of more suspended COD. The addition of calcium further improved the SRTs in the UASB reactors by enhancing the solid removal. In PM treatment, solid removal was higher, but COD removal was lower than in CM treatment. In PM treatment, conversion of VFA into methane failed because of the high ammonia concentration (1.7 gNH_3-N L^{-1}), leading to VFA in the effluent (Chapter 2). In CM treatment with calcium addition (Chapter 3), the removed solids were converted into methane. Methane production outperformed commonly applied CSTR reactors by 1/3 (~300 and ~200 L-CH_4 $kgVS^{-1}$ from CM, respectively). The longer SRT (450 days) caused by calcium addition allowed for higher hydrolysis (from 29% to 67%) and consequently higher methanization. The opposite happened when the SRT was shortened (150 days), because the addition of hydrogen gas (H_2) caused wash out of solids. The conversion of suspended COD was considerably lower compared with the UASB reactor without H_2 gas addition.

6.2. Phosphorus recovery and calcium phosphate granules

Phosphorus removal was closely correlated with solid removal in all chapters and improved when calcium was added. The addition of calcium improved phosphorus removal from 60% to 74% and from 38% to 61% in PM and CM, respectively. To recover phosphorus, simple separation in the sludge bed is not sufficient, but the formation of granules enabling simple mechanical recovery is desired. CaP granulation succeeded in animal manure, but the recovered CaP granules differed from another and from those recovered from BW. In concentrated BW treatment, CaP granules were evenly distributed over size fractions > 0.4 mm and had a phosphorus content of 7.8 ± 0.6%P w/w. The CaP granules recovered from PM treatment were mainly > 2.5 mm and had the lowest phosphorus content (4.3 ± 0.6%P w/w) among all streams, because of their high calcium carbonate ($CaCO_3$) content (38%). After 450 days, the granules contained 59% of all phosphorus present at the bottom of the reactor. In CM treatment, simple calcium addition did not trigger CaP granulation. However, it increased the removal of phosphorus by aggregation of struvite crystals (containing most of the phosphorus in CM) and cementation by precipitation of $CaCO_3$. Only after acidifying the CM and feeding the acidified CM to the UASB reactor did CaP granulation occur. CaP

granules recovered from acidified CM treatment were primarily > 2.5 mm (21% of all TSS) and had the highest phosphorus content (8.4 ± 1.3%P w/w) observed in CaP granules from UASB reactors thus far. After 181 days, CaP granules (> 2.5 mm) contained the most phosphorus (from 15% on day 34 to 57% on day 181) at the bottom of the sludge bed. This enabled selective and efficient phosphorus recovery and may have become more selective considering the trend in phosphorus content.

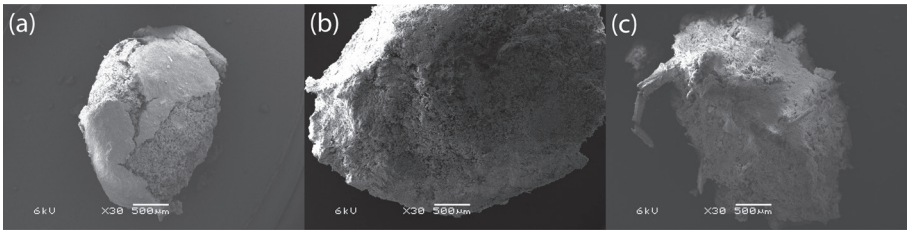

Fig. 6.1. Scanning electron microscope images of calcium phosphate granules from (a) concentrated black water treatment, (b) pig manure treatment, and (c) cow manure treatment.

In all recovered CaP granules, calcium phosphate was mainly amorphous. The XRD measurements showed broadened peaks at θ angles 31 and 34.5. In measurements of granules from PM treatment, these peaks remained broadened. For granules from BW treatment, this broadening was reduced with time, indicating the transition into a crystalline phase [62]. For granules from CM treatment, the peaks were the most defined and sharpened over time as well, indicating that they were the most crystalline of all granules.

6.3. Mechanisms for calcium phosphate granulation in animal manure

Mechanisms of CaP granulation in animal manure and black water have a common cause: calcium phosphate supersaturation. In one way or another, calcium phosphate must be supersaturated at some point in a certain environment to induce precipitation. At the same time, the supersaturation cannot be too high because if so, there would be primary nucleation of fine precipitates throughout the sludge bed. Understanding how the supersaturation of calcium phosphate is reached and how the mechanism of CaP granulation works in BW, PM and CM would

potentially allow one the introduction of CaP granulation in a phosphorus recovery technology.

6.3.1. Biologically induced CaP granulation in BW

The first CaP granulation occurred in the UASB reactors treating BW [40]. The addition of calcium stimulated CaP granulation in the BW treatment [41]. Based on the experience with CaP granulation in BW treatment, the calcium addition chapters of this thesis (Chapters 2 and 3) were designed. In BW treatment, the inorganic core was more defined and covered in an outer layer of biomass. Meanwhile, in CaP granules from animal manure, the precipitation clusters did not stick to a defined core but were present throughout the entire granule. The mechanisms for CaP granulation seem different. In BW treatment, the start of CaP granulation was thought to be one of two possibilities [42]: (1) primary nucleation of calcium phosphate followed by attachment of biomass, creating conditions facilitating secondary nucleation and growth of the inorganic core; or (2) biological granule formation through conditions created in the UASB reactors and the presence of calcium, creating a microenvironment for heterogeneous nucleation inside granules on organic material. Neither was proven or disproven, nor does one exclude the other. However, both theories are based on the idea of a well-defined inner inorganic core that becomes more dense over time. The defined inner core could form because of the methanogenic conversion of organic acids to methane, increasing the local pH. The diffusion of calcium and phosphate ions to the inner part of the granules enabled the continued secondary nucleation on the existing calcium phosphate precipitation clusters. The granules also incorporated suspended phosphorus present as struvite crystals and possibly an organic substrate to dissolve, degrade, and supply phosphate ions to the calcium phosphate core.

6.3.2. More chemically induced CaP granulation in PM

In PM treatment, CaP granulation was less biologically induced than in BW treatment, because ammonia toxicity inhibited methanogenic activity (Chapter 2). Consequently, the pH of the core was not increased by methanogenic activity. The co-precipitation of $CaCO_3$ was significantly higher than in BW. At the bottom of the sludge bed in PM treatment, inorganic carbon was below the detection limit of 100 mg L^{-1} in solution, indicating extensive precipitation of $CaCO_3$. The formation

of CaP granules from PM probably started from natively present phosphate ions that precipitated with the added calcium ions while $CaCO_3$ coprecipitated. It is unlikely that biomass facilitated the formation of CaP granules in PM except perhaps as heterogeneous nucleation surface. Calcium may have enriched on negatively charged sites of organic material, which can induce local supersaturation of calcium phosphate. Fig. 6.2b shows organic material, probably a fiber, serving as a heterogeneous nucleation surface for the spherical precipitation clusters of calcium phosphate. Once calcium phosphate precipitates were present, precipitation became easier through secondary nucleation, allowing calcium phosphate precipitation clusters to grow by continuing precipitation from soluble phosphorus and calcium. The phosphorus present as phosphate ions was only 20%, though, while 80% was in the form of struvite, which dissolved to form calcium phosphate. At least some soluble phosphorus or phosphate ions seem essential to initiate calcium phosphate precipitation and granulation in PM.

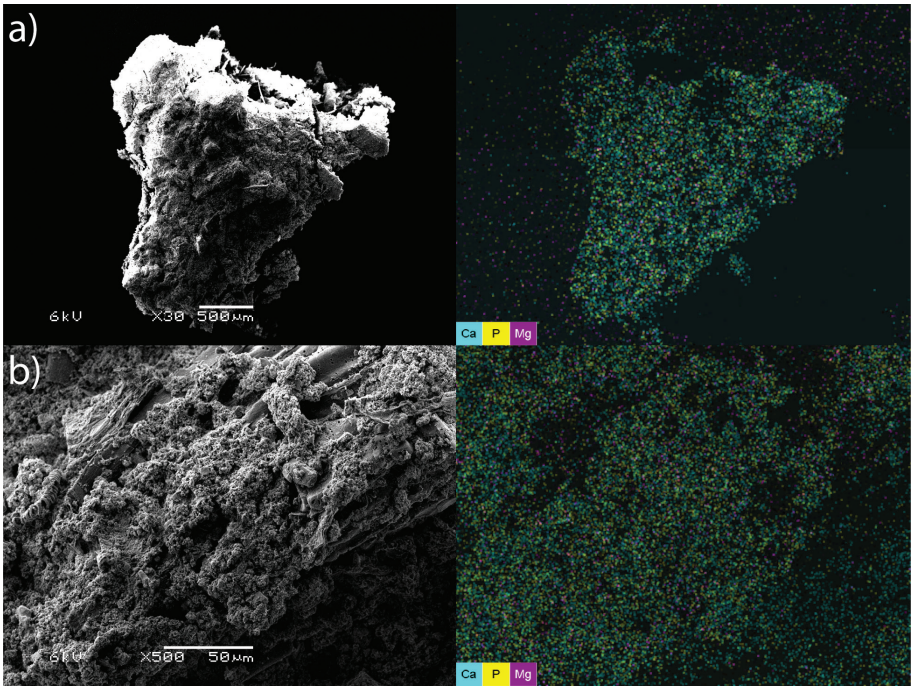

Fig. 6.2. Scanning electron microscope with energy-dispersive X-ray image of (a) calcium phosphate aggregates from PM treatment and (b) a zoom-in of it.

6.3.3. CaP granulation inhibiting factors in CM

In CM, almost no phosphorus is in solution. This is a problem for CaP granulation in CM treatment, unless phosphorus is released from the solids. In fact, the addition of calcium did not induce CaP granulation in 450 days of reactor operation and therefore was not considered a successful application (Chapter 3). However, comparing CM with PM and BW, the relative abundance of magnesium compared to calcium and phosphorus is much higher than in BW and PM. The higher abundance of magnesium increases the supersaturation of struvite, which proves that it is a competitor to bind phosphate. CM was the stream with the highest biogas production, meaning that inorganic carbon production was also highest in CM treatment. That leads to three factors contributing to inhibition of calcium phosphate granulation in CM treatment as identified in Chapter 3: (1) the abundance of inorganic carbon; (2) the absence of phosphate ions; and (3) the competition with magnesium. However, we could not yet identify which impacts CaP granulation in animal manure the most.

The acidification of CM before entering the UASB reactor removed inorganic carbon and dissolved struvite (Chapter 4). This induced CaP granulation by eliminating two out of three inhibition factors. Competition between calcium and magnesium was not directly altered, but removing inorganic carbon increased the availability of calcium and caused a preferred precipitation with phosphate over magnesium. However, calcium phosphate formed first in the large granules, and only over a longer time was it found in particles < 0.4 mm. These small particles contained struvite still from the inoculum, which probably slowed down the formation of calcium phosphate. The dissolution of struvite probably increases the concentration of magnesium and the competition for phosphate ions locally where struvite dissolves. That probably made it less favorable for the calcium phosphate to form in small particles and incorporate the phosphorus from struvite at first. So, secondary nucleation mostly occurred in larger particles. After acidification, the UASB reactor had more calcium and magnesium in the effluent than UASB reactors without prior acidification. This indicates that calcium is already in excess and outcompeting magnesium when inorganic carbon is removed, and phosphorus is solubilized through acidification.

The addition of hydrogen gas (Chapter 5) also removed inorganic carbon, but not to the same extent as acidification. CaP granulation was not induced. A

PHREEQC simulation indicates that more removal of inorganic carbon would induce precipitation of calcium phosphate because more calcium would be available to enhance the dissolution of struvite and precipitation of calcium phosphate. The question remains: Is the presence of inorganic carbon or the absence of phosphate ions dominating the inhibition of CaP granulation in animal manure?

At this point, it seems that overcoming one of the two limiting factors could lead to CaP granulation in animal manure. Chapters 2 and 5 indicate that the presence of phosphate ions and the removal of inorganic carbon can each induce CaP granulation, respectively. Both affect calcium phosphate supersaturation, which is decisive for calcium phosphate precipitation. The simulation predicted supersaturation based on concentrations measured in the sludge bed. However, the supersaturation, which is decisive for CaP granulation, is a local one. In PM treatment, calcium ions probably accumulate in granules, binding all inorganic carbon and free phosphate ions. Likely, calcium kept accumulating on negatively charged sites of organic material within the granules, locally inducing a higher supersaturation for calcium phosphate. Similarly, the idea for adding H_2 gas was to locally increase calcium availability by stimulating the conversion of inorganic carbon into methane in granules, inducing local supersaturation. Inside the granules, this could increase the supersaturation of calcium phosphate, which can lead to struvite dissolution and calcium phosphate precipitation.

6.4. Process optimization

Optimizing the process ideally considers aspects for improving the CaP granulation and their recovery while facilitating the sustainable valorization of other resources from animal manure. Currently, the primary aspects are phosphorus and methane. Still, the separation of phosphorus affects the reusability of nitrogen and possibly potassium. With that in mind, the following suggestions for process optimization were considered.

6.4.1. Temperature for CaP granulation and anaerobic digestion

Ideally, CaP granules are significantly larger and denser than the bulk sludge and have a high phosphorus content. A significant size and density difference from the bulk sludge allows for simple separation. A high phosphorus content improves

its reusability and reduces the harvesting of unwanted substances. In PM, CaP granulation occurred, and large granules formed, which contained most of the phosphorus at the bottom of the sludge bed. However, the phosphorus content could be higher. The high amount of $CaCO_3$ impurities in the granules decreases the phosphorus content. A solution could be to run the PM reactors at a lower temperature. At a lower temperature (25–30°C), the supersaturation of calcium phosphate increases, and the supersaturation for $CaCO_3$ decreases. Additionally, the almost entirely inhibited methanogenesis might be able to work under mesophilic conditions; the ammonium/ammonia equilibrium would shift toward ammonium compared to thermophilic conditions (0.6 and 1.7 gNH_3-N L^{-1}, respectively). When decreasing the free ammonia presence, its toxicity could be lowered enough (< 1.1 gNH_3-N L^{-1} [76]) to activate methane production from PM while having CaP granulation. Acidification or H_2 gas addition might work to improve CaP granulation from PM.

6.4.2. Better pH regime and less acid addition

The costs of acidification could be reduced by lowering the acid addition. The latter could be lowered by stimulating biological acid production, replacing the externally added acid. Furthermore, the pH might not need to be lowered to 5, as 5.8 might be enough. At pH 5.8, most inorganic carbon would be already removed and most phosphorus solubilized in CM. Less removal of inorganic carbon might be enough to increase the availability of calcium sufficiently to cause struvite dissolution. That would allow for keeping the pH around the equilibrium of bicarbonate and carbonic acid of 6.3. Additionally, the acidified CM entering the UASB reactor causes a slightly lower pH (6.9) in the sludge bed, which favors calcium phosphate over $CaCO_3$ precipitation. PHREEQC indicates that at a lower pH (6.9) in the UASB sludge bed calcium phosphate would form with even more inorganic carbon present (Fig. 6.3). Once calcium phosphate is formed, the increased supersaturation on the surface of calcium phosphate precipitates could stimulate further precipitation, similar to the mechanism described for CaP granulation during PM treatment. However, too strong a pH decrease in the UASB reactor was not tolerable for the methanogens. The methane production decreased from 301 to 33 L-CH_4 $kgVS^{-1}$ when the pH decreased to 5.2 at the vertical center of the UASB reactor.

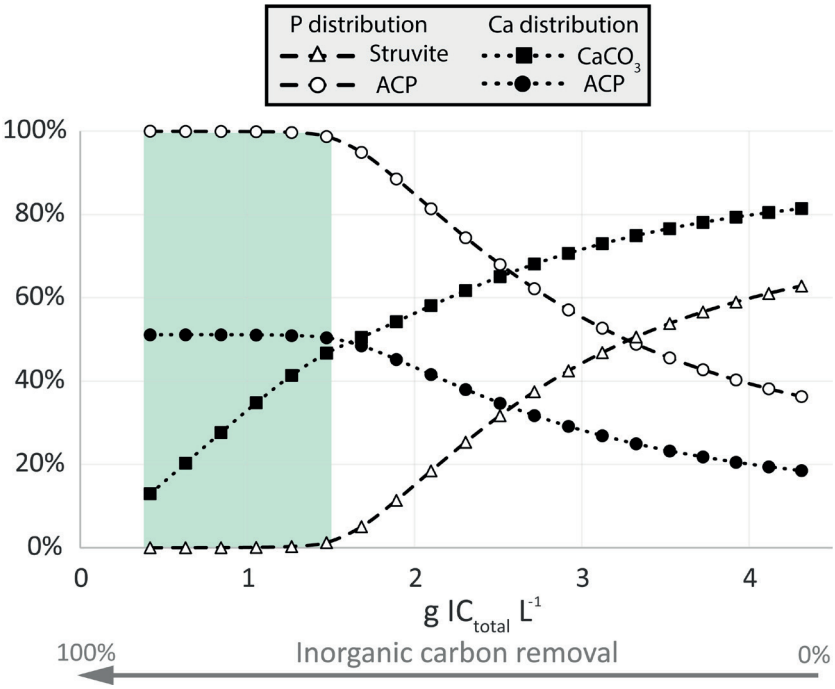

Fig. 6.3. PHREEQC simulation of calcium phosphate precipitation at the bottom of the UASB reactor at a pH of 6.9 against the presence of inorganic carbon (IC). The grey arrow represents the removal percentage of inorganic carbon from the bottom of the reactors for CM (Where 0% is about 4.2 gIC L^{-1}). The lines describe the distribution of phosphorus in struvite and ACP and calcium in CaCO3 and ACP. The simulation input data are based on the measurements from Chapter 5.

6.4.3. Combining acidification and hydrogen gas addition

For maintaining adequate methane production while taking advantage of the acidified CM, the combination of acidification and H_2 gas addition could be ideal. The pre-acidification led to CaP granulation with a high phosphorus content, but the pH regime was fragile, partly leading to a decrease in pH in the UASB reactor. The addition of H_2 caused an increase in pH and could stabilize the pH in the UASB reactor. If hydrogenotrophic methanogenesis was specifically active in granules as described in Chapter 5, the CaP granules would likely be of even higher purity because of the preferential local pH for the precipitation of calcium phosphate and additional removal of inorganic carbon. Acidification may not need to reach a pH as low as without the addition of H_2, because part of the inorganic carbon

could still be removed in the UASB reactor, saving acid addition. The combination of acidification and H_2 addition could make the process cheaper and deliver CaP granules of higher purity. Additionally, the biogas produced would have a higher methane content, and increasing its value especially if the green electricity was produced locally.

6.4.4. Inoculating seed crystals for secondary nucleation

An alternative approach could be the addition or inoculation of calcium phosphate seed precipitates or granules. This would provide a calcium phosphate phase for secondary nucleation, which could initiate struvite dissolution. It may be that no initial soluble phosphorus would need to be present to induce calcium phosphate granulation. This could be especially helpful for inducing CaP granulation during CM treatment and could be an alternative or addition to acidification and H_2 gas addition.

6.5. Applicability and feasibility

6.5.1. The process in modules and their technological readiness

CaP granulation during anaerobic digestion could help solve the problem of excess manure and facilitate circular use of resources. Manure treatment is obligatory for areas with intensive livestock farming in the EU. Simultaneously, the supply of resources from primary resources is fragile and dependent on imports from outside the EU [29]. In the Netherlands, the pressure on the livestock sector to reduce emissions is among the highest in the world. In the coming three years, the derogation for manure application will decrease and end, reducing the allowed amount of manure applied on land by one-third [251]. This means that almost every livestock farm in the Netherlands will require manure treatment when the derogation ends in 2026 (73% dairy farms and 93% pig farms in 2021 [252]). The demand for efficient manure valorization in the Netherlands is very high and urgent, as it probably soon will be in more countries and areas with intensive livestock farming.

The technological applicability of CaP granulation during anaerobic digestion can best be discussed in separate modules. Modules would be manure-specific treatment and recovery-based. (1) the recovery of phosphorus as CaP granules from PM with calcium addition; (2) the removal of phosphorus with enhanced

methane production from CM treatment with calcium addition; (3) the recovery of CaP granules with enhanced methane production from CM with acidification and calcium addition; and (4) the recovery of phosphorus and the production of green gas from CM with the addition of calcium and H_2.

The first two modules were tested over 450 days and showed robust treatment with good performance. The treatment of CM described in module (2) was carried out in a pilot on a dairy farm. This leaves modules (1) and (2) at a technology readiness level (TRL) between 6 and 7. The next step would be to demonstrate of full-scale units for these modules. The third module yielded the highest phosphorus recovery of CaP granules with the highest phosphorus content, but showed that pH control could be a challenge that requires optimization. The TRL falls between 4 and 5, requiring pilot testing next. The addition of H_2 gas showed a higher methane content and the removal of inorganic carbon, possibly leading to CaP granulation. However, the bioconversion of H_2 needs optimization and the formation of CaP granules remains still to be shown, leaving this module at a TRL of 2 to 3.

6.5.2. Economic assessment

The economic feasibility is situational and best described per module for the case of the Netherlands. The treatment of PM costs, on average, ~€70k annually per farm (roughly €20 ton^{-1}_{manure}; status 2020 [253]). The capital expenditures (CAPEX) to install a UASB reactor as described in module (1) for one pig farm would require around €200k (based on offers requested in summer 2022 for tank, pumps, heating, separation and installation). This includes the reactor and the required pumping, but no combined heat and power (CHP) unit or dihydrogen sulfide (H_2S) scrubbing from the biogas, because the biogas production was minimal for the time being. Operational expenditures (OPEX) would consist of costs of the added calcium (€3 m^{-3}_{manure} for ~3100 m^3 $year^{-1}$ thin fraction of PM) and the maintenance of the reactor. The simplicity of the reactor without any moving parts keeps its maintenance costs low at an estimated 5% of the CAPEX on average. Recovery of CaP granules would probably still require transportation of recovered CaP granules of roughly €1 m^{-3}_{manure}. Combined, the OPEX would amount to about €23k $year^{-1}$ for one farm. This assumes that the digestate could be applied locally as a nitrogen fertilizer, which must meet the requirements discussed in the next chapter. The current costs of pig farms for their manure treatment compared with the OPEX of the UASB reactors

show a saving of €47k $year^{-1}$. This results in a return on investment (ROI) in about 4.5 years. In these calculations, the value of nutrients is not considered. However, the formation of CaP granules allows for individual reuse that saves on costs for synthetic fertilizers and their raw materials. With the increase in prices for synthetic fertilizers due to supply restrictions, recovered nutrients could create additional revenue. This revenue could be up to €12 m^{-3}_{manure} (status 2021 [253]). If all nutrients could be recovered at that value, then the ROI would be about two years. However, more realistic estimations for including revenue for recovered nutrients, also considering the current phosphorus content of CaP granules and the concentration of nutrients recovered from PM, would be €3 m^{-3}_{manure}, resulting in an ROI of 3.5 years.

The situation for dairy farmers is very different from that for pig farmers. The yearly treatment costs about €5k per farm (status 2020 [253]) and is much lower than for pig farms because dairy farms have much more land to apply their manure. Thus, the possible cost reduction is much smaller than for PM. However, CM treatment involves methane production, changing the business case. The CAPEX would amount to about €300k (based on offers requested in summer 2022 for module 1 plus CHP unit) for CM produced by a single farm, including the costs considered in module (1) plus the costs for the biogas treatment. The OPEX would roughly be €2 m^{-3}_{manure} (~3100 m^3 $year^{-1}$ thin fraction of CM) for calcium addition plus about 7.5% of the CAPEX per year, due to the more maintenance-demanding biogas equipment. The total OPEX would amount to about €30k $year^{-1}$ for an average farm. Such a unit would produce about 37k m^3-CH_4 $year^{-1}$. Without separating the thick fraction before entering the UASB reactor, the CH_4 production could be further increased, but the effect on CaP granulation could be negative. The methane could be converted into heat and power with the CHP, heating the UASB reactor, and having an additional 850 GJ $year^{-1}$ of heat (60%) and electricity (40%) worth about €70k (based on energy prices and governmental price caps in the Netherlands in February 2023 [254]). The profit would amount to €40k $year^{-1}$ and result in an ROI of about 7.5 years. Alternatively, upgrading biogas to green gas is an option by separating CO_2 from methane in biogas. However, this would require a minimum amount of 320 thousand m^3-CH_4 $year^{-1}$ (40 m^3 h^{-1} green gas production current minimum for suppliers) to be considered economically feasible.

The integration of acidification described in module (3) induced CaP granulation, enabling efficient reuse of nutrients from CM. The CAPEX would increase slightly

by about €10k (Based on offers requested in summer 2022) compared with module (2) by adding the CSTR for acidification. The OPEX would probably be again around 7.5%, but the costs for acid addition of €6 m^{-3}_{manure} (~3100 m^3 $year^{-1}$ thin CM) would need to be added. The OPEX and costs for acid would amount to €20k $year^{-1}$ for one dairy farm. The added revenue of recovering the CaP granules with a high phosphorus content could be compared with the value of phosphate rock with €3 kgP^{-1} and would result in €2.5 m^{-3}_{manure}. The value of other reusable nutrients in CM enabled by CaP granulation is around €3 m^{-3}_{manure}. The €5k $year^{-1}$ treatment costs might not be necessary with this system applied if the recovery products qualify as fertilizer products, leading to a revenue of €24k $year^{-1}$. This is a less convincing business case with a profit of €4k $year^{-1}$ and an ROI of 7.5 years, but that could quickly change with the optimization of the acid addition.

Module (4) is in TRL that is too low to make a reasonable economic assessment. The H_2 gas market is developing quickly, which could make it more feasible in the future. Then it could become a competitive alternative to CO_2 separating technologies for upgrading biogas to biomethane if the efficiency can be improved.

6.6. Implementation and impact

6.6.1. Single farm or collective of farms

The implementation of the technology would be at farm sites, treating the manure of each farm separately or having a collective of a few farms and treating their manure together. The unit per farm would eliminate manure transport and allow the most local resource reuse. The recovered nutrients and energy could be reused on the farm as much as possible, and additional nutrients and energy could ideally be used locally. Overview of influent composition and the adjustment of process conditions would be simple because of the common origin of manure. The manure could be added directly to the treatment unit and digested in a fresh state to obtain the highest methane production, also creating a beneficial pH regime for CaP granulation. Treatment for a collective of farms might make the adjustment of process conditions more challenging due to possibly more significant fluctuations in influent composition and less fresh manure. However, the use of biogas in a CHP unit or a biogas upgrading unit comes with a higher CAPEX and a minimum treatment capacity. This might make a collective manure treatment financially more feasible, possibly making a collective with a treatment unit for 5 to 10 farms more

interesting. The farms could still have a UASB reactor per farm to have simpler feeding conditions, fresher manure and no raw manure transport, but the biogas treatment could be centralized. From this centralized location, heat and electricity or green gas could be brought to urban areas and support the public energy requirements. This would fit nicely into the plan to reach the Dutch government's green gas production ambitions by 2030.

6.6.2. Reusability of nutrients

The recovered nutrients could make a notable contribution to the required nutrients, decreasing the dependence on primary sources and possibly the costs. These costs recently increased immensely in the EU, because of a supply cut from sources in Russia and Belarus. To qualify as recovered fertilizer products in the EU, the products made from recovered nutrients must fulfill the Fertilizing Products Regulation (FPR) criteria [255]. Under the FPR, CaP granules fall under the product function category (PFC) "straight solid inorganic macronutrient fertilizer" (PFC 1 [C][I][a][i]), because of their phosphorus and calcium content as primary and secondary macronutrient, respectively (minimum of 3% w/w and 1.5% w/w as P_2O_5 and CaO, respectively). The sum of their masses also exceeds the requirement of an 18% mass of the main macronutrients. Additionally, this category has criteria for a low presence of *Salmonella* spp. and *Escherichia coli* and *Enterococcae*., which are likely fulfilled by the long SRTs in the UASB reactor at 55°C. Preliminary tests showed that the removal of *Escherichia coli* would be sufficient [256]. The limits for heavy metals such as chromium, cadmium, lead, and especially copper and zinc would need to be tested. However, in Cunha et al. [62] heavy metals tended to remain in the organic fraction of the bulk sludge bed over accumulating in CaP granules. The digestate does not reach 1.5% w/w of nitrogen and potassium oxide to fulfill the criteria under "compound liquid inorganic macronutrient fertilizer" (PFC 1 [C][I][b][ii]). It could almost fulfill the "liquid organic fertilizer" category because it contains carbon and nutrients of solely biological origin. However, the concentration of nitrogen and potassium oxide would still be below the 1% w/w (~0.7% and ~0.9%).

The recovered CaP granules could directly go to land application as a slow-release phosphorus fertilizer. The presence of mainly amorphous phosphorus species in granules improves its availability. The size ensures it is not flushed out of the soil and entering surface water bodies or other environments where it is not wanted.

The granules recovered throughout this work might find different ideal fertilization purposes. The CaP granules recovered from PM have a lower phosphorus content because of their high $CaCO_3$ content. $CaCO_3$ is one of the most applied minerals in agriculture, mainly for increasing the pH of acidic soils [257]. The CaP granules from PM might be a good product for supplying phosphorus and $CaCO_3$ for pH stabilization to acidic soils. The granules recovered in Chapter 4 had the highest phosphorus content, allowing them to compete with phosphate rock as a phosphorus raw material for synthetic fertilizers. However, when envisioning an ideal situation, the reuse remains local within the same farms or neighboring farms to minimize transportation and further processing, avoiding additional use of resources. In the future, the CaP granules could even be an option for organic farming when the chemical addition can be minimized and the process could be steered more biologically.

Nitrogen and potassium remain in the digestate in the current process. The nitrogen leaving the UASB reactor was mainly present as ammonium because organically bound nitrogen comes free during digestion. The standardized presence of ammonium simplifies the following application and recovery of nitrogen. It could be separated and concentrated via a stripping process or, eventually, through an electrochemical process (likely reaching the requirements for PFC 1 [C][I][b][ii]). Alternatively, the direct application of the digestate on land could supply nitrogen, usually applied as synthetic fertilizers. For this, the digestate would need to have an end-of-waste status and fall in a fertilizer category instead of still being categorized as animal manure. The potassium would stay in the digestate and be applied on land as well, because there currently is no technological solution for feasibly separating and concentrating the potassium from the digestate. The separation or regulation of potassium would probably need to be regulated with the feed of animals. The current nutrient concentrations would restrict the direct application of digestate and require a change in composition.

6.6.3. A look at soils

The impact of recovery products on soils might be more than simply nutrition. The application of digestate and possibly CaP granules brings along the microorganisms that grow in the UASB reactor. In the agricultural sector, there is the belief that the application of digestate could negatively affect soils, decreasing their biodiversity

and excluding beneficial microorganisms. Long-term field experiments disprove this belief and show that digestate or manure does not negatively affect soil biodiversity and microorganisms' functioning [258]. However, the integration of digestate and inhabiting microorganisms enhances the production of extracellular polymeric substances (EPS) [259], a sticky substance that can provide structure and facilitate aggregation. The enhancement of aggregation in soils provides much-needed structure. Intensively worked soils erode, meaning they lose structure and become more and more vulnerable to droughts due to the lower water holding capacity, leading to more nutrient runoff. The provision of microorganisms and other substances that can re-establish soil structure could be essential to maintain soil functionality for agriculture. The addition of organic amendments could be an additional way of improving soil structure and its resilience [260]. The thick fraction of animal manure from the separation with a screw press before the UASB reactor is already added to the soils of farms. Treatment of this thick fraction could possibly improve its impact on soil structure by, for example, increasing the abundance of microorganisms that can enhance soil structure or providing more carbon in a form that specific soils require to improve their structure.

The impact of CaP granulation during anaerobic digestion promotes the resilience of livestock farming and mitigation of emissions while turning them into resources. The impact goes beyond the livestock sector, possibly affecting broader agriculture by providing resources that induce better soil structure, and even the domestic energy supply could be supported with this technology. At the same time, the transport of 12 million tons of CM and 8 million tons of PM annually in the Netherlands [227] would no longer be needed, saving immense amounts of fossil fuels and emissions. The implementation of this technology could reduce the pressure of intensive agriculture on primary resources, soil, and the environment, and help to make agriculture more sustainable.


P
P

Summary

The world's growing population and the intensification of agriculture require more efficient resource use to sustain food production and protect the environment. To achieve this, it is essential to reuse resources from secondary sources, such as animal manure. Animal manure is a large secondary resource that contains organic matter and the three primary plant nutrients (nitrogen, phosphorus, and potassium). However, the primary sources of phosphorus may become depleted first. One promising process for efficient resource utilization is the granulation of calcium phosphate (CaP) during anaerobic digestion. This process can convert organic matter into methane for energy and separate phosphorus from nitrogen and potassium for balanced application and improved nutrient reusability. CaP granulation was first observed during anaerobic digestion of concentrated black water (BW) in up-flow anaerobic sludge blanket (UASB) reactors, where calcium was limiting. Further research demonstrated that adding calcium can induce CaP granulation in BW and enable efficient phosphorus recovery. This study investigated CaP granulation for recovering phosphorus from cow and pig manure. The thin fraction (< 200 μm) containing > 90% of the nutrients was digested thermophilically in UASB reactors, which were inoculated with their respective manures.

The addition of calcium was found to induce CaP granulation in the treatment of black water (BW), which led to its testing as the first parameter for inducing CaP granulation in pig and cow manure. In **Chapter 2**, the effect of calcium addition to a UASB reactor treating pig manure was studied for 456 days. This addition induced CaP granulation in the pig manure treatment, increasing phosphorus removal from 60% to 74%, with 79% of the removed phosphorus accumulating in CaP granules at the bottom of the UASB reactor. In these granules, amorphous calcium phosphate (ACP) formed, while struvite (a native phosphorus species in pig manure) dissolved. Recovering CaP granules from pig manure could save 85% of transportation costs.

In **Chapter 3**, the addition of calcium to UASB reactors treating cow manure for 456 days did not induce CaP granulation. However, it did enhance phosphorus removal from 38% without calcium addition to 61% with calcium addition, as well as methane production from 136 L-CH_4 $kgVS^{-1}$ without calcium addition to 301 L-CH_4 $kgVS^{-1}$. The increased solid retention and cementation of struvite crystals in calcium carbonate precipitates enhanced phosphorus removal. Longer solid retention times resulted in higher hydrolysis, with 29% without calcium and 67% with calcium, resulting in more suspended material being converted into methane. Calcium phosphate did not form because most calcium precipitated as calcium carbonate. The absence of phosphorus in solution also limited the formation of calcium phosphate.

In **Chapter 4**, to overcome limitations found in chapter 3, a treatment at low pH in a continuously stirred tank reactor (CSTR) was conducted prior to the UASB reactor to liberate phosphorus and remove inorganic carbon from cow manure. The system operated for 190 days with an organic loading rate (OLR) of 22.5 and 1 gCOD $L_{reactor}^{-1}$ d^{-1} in the CSTR and UASB reactor, respectively. In the CSTR, the treatment at pH 5 solubilized over 94% of phosphorus, calcium and magnesium and removed almost all inorganic carbon as CO_2. The high OLR partly stimulated organic acid production, but further optimization is necessary. In the UASB reactor, 83 ± 3% of phosphorus was removed, mainly as CaP granules > 2.5 mm in diameter. The recovered CaP granules had a phosphorus content of 8.4 ± 1.3%P w/w, primarily present as ACP and a few crystalline phases. The removal of inorganic carbon eliminated calcium carbonate precipitation, resulting in high-purity CaP granules with a phosphorus content comparable to primary sources of phosphorus.

In **Chapter 5**, the addition of hydrogen (H_2) gas at the bottom of a UASB reactor treating cow manure was found to stimulate hydrogenotrophic methanogenesis (HM), which converts H_2 and CO_2 into CH_4. A parallel UASB reactor with nitrogen (N_2) gas addition was run alongside the H_2 gas reactor for 200 days to compare the effect. H_2 gas addition led to a significant increase in CH_4 production, from 74 to 198 L-CH_4 $kgVS^{-1}$, and overall biogas production, from 5 ± 2 to 9 ± 2 L d^{-1}. The conversion of CO_2 and inorganic carbon by HM resulted in 10–25% less inorganic carbon in the sludge bed. However, this was insufficient to induce CaP granulation, which would require a 60% reduction in inorganic carbon, as per a PHREEQC simulation of the bottom of the sludge bed. HM was primarily stimulated in granules > 2.5 mm, suggesting potential for inducing CaP granulation, but the uptake and availability of H_2 gas need to be improved, perhaps by increasing contact times with a taller reactor or introducing gas recirculation.

In **Chapter 6**, the results from the previous chapters are compared with each other and with prior research. The various compositions and formation mechanisms of CaP granules in BW, pig, and cow manure are discussed and compared. The optimization of the process, including reducing ammonia toxicity, minimizing acid addition, stabilizing the pH regime, and possibly inducing CaP granulation through seed particles, is also discussed, and potential areas for further research are highlighted. The technological readiness of the process is considered in the context of its implementation in livestock farming. An economic assessment based on the current situation in the Netherlands is presented, demonstrating that the process is economically feasible. Finally, the implementation of the process and the recovery products under EU regulations and their impact on the soil are discussed.


P
P

References

[1] D.Q. Fuller, T. Denham, M. Arroyo-Kalin, L. Lucas, C.J. Stevens, L. Qin, R.G. Allaby, M.D. Purugganan, Convergent evolution and parallelism in plant domestication revealed by an expanding archaeological record, Proceedings of the National Academy of Sciences 111(17) (2014) 6147-6152. https://doi.org/10.1073/pnas.1308937110.

[2] D.Q. Fuller, E. Kingwell-Banham, L. Lucas, C. Murphy, C. Stevens, Comparing pathways to agriculture, Archaeology International 18(1) (2015) 61. https://doi.org/10.5334/ai.1808.

[3] G. Larson et al., Current perspectives and the future of domestication studies, Proceedings of the National Academy of Sciences 111(17) (2014) 6139-6146. https://doi.org/10.1073/pnas.1323964111.

[4] M. Salque, P.I. Bogucki, J. Pyzel, I. Sobkowiak-Tabaka, R. Grygiel, M. Szmyt, R.P. Evershed, Earliest evidence for cheese making in the sixth millennium bc in northern europe, Nature 493(7433) (2013) 522-525. https://doi.org/10.1038/nature11698.

[5] J.C.K. Wells, J.T. Stock, Life history transitions at the origins of agriculture: A model for understanding how niche construction impacts human growth, demography and health, Front Endocrinol (Lausanne) 11 (2020) 325. https://doi.org/10.3389/fendo.2020.00325.

[6] J.C. Scott, Against the grain: A deep history of the earliest states, Yale University Press, New Haven, 2017.

[7] C.S. Larsen, The agricultural revolution as environmental catastrophe: Implications for health and lifestyle in the holocene, Quaternary International 150(1) (2006) 12-20. https://doi.org/10.1016/j.quaint.2006.01.004.

[8] G.J. Armelagos, A.H. Goodman, K.H. Jacobs, The origins of agriculture: Population growth during a period of declining health, Population and Environment 13(1) (1991) 9-22. https://doi.org/10.1007/bf01256568.

[9] J.R. Stevenson, N. Villoria, D. Byerlee, T. Kelley, M. Maredia, Green revolution research saved an estimated 18 to 27 million hectares from being brought into agricultural production, Proceedings of the National Academy of Sciences 110(21) (2013) 8363-8368. https://doi.org/10.1073/pnas.1208065110.

[10] N. Borlaug, Feeding a hungry world, Science 318(5849) (2007) 359-359. https://doi.org/doi:10.1126/science.1151062.

[11] D.A. Russel, G.G. Williams, History of chemical fertilizer development, Soil Science Society of America Journal 41(2) (1977) 260-265. https://doi.org/10.2136/sssaj1977.03615995004100020020x.

[12] H. Ritchie, Yields vs. Land use: How the green revolution enabled us to feed a growing population, Our World in Data (2017).

[13] M. Roser, H. Ritchie, E. Ortiz-Ospina, L. Rodes-Guirao, World population growth, Our World in Data (2013).

[14] F. Collantes, Why did the industrial diet triumph? The massification of dairy consumption in spain, 1965–90, The Economic History Review (2017). https://doi.org/10.1111/ehr.12702.

[15] H. Steinfeld, P. Gerber, Livestock production and the global environment: Consume less or produce better?, Proceedings of the National Academy of Sciences 107(43) (2010) 18237-18238. https://doi.org/10.1073/pnas.1012541107.

[16] G.J. Monteny, The eu nitrates directive: A european approach to combat water pollution from agriculture, The Scientific World JOURNAL 1 (2001) 927-935. https://doi.org/10.1100/tsw.2001.377.

[17] European-Comission, Directive 91/676/eec. Council directive of 12 december 1991 concerning the protection of waters against pollution caused by nitrates from agricultural sources., in: European-Comission (Ed.) Official Journal of European Community, 1991.

[18] Raad van State [Court of State], Programma aanpak stikstof (pas) mag niet als toestemmingsbasis voor activiteiten worden gebruikt [program approach nitrogen cannot serve as basis for activity permits], in: R.v.S.C.o. State] (Ed.) Den Haag, 2019.

[19] C. van der Wal-Zeggelink, Hoofdlijnen van de gecombineerde aanpak van natuur, water en klimaat in het landelijk gebied, en van het bredere stikstofbeleid [guidelines of the combined approch of nature, water and climate in rural areas, and the borader nitrogen directive], Rijksoverheid, Den Haag, 2022.

[20] Nederlandse Zuivel Organisatie [Dutch Dairy Association], Cattle feed, Den Haag, 2016.

[21] J.P. Holen, R.D. Goodband, M.D. Tokach, J.C. Woodworth, J.M. Derouchey, J.T. Gebhardt, Effects of increasing soybean meal in corn-based diets on the growth performance of late finishing pigs, Translational Animal Science 7(1) (2023). https://doi.org/10.1093/tas/txac165.

[22] Centraal Bureau voor de Statistiek [Central bureau of Statistics] CBS, Dutch soybean imports, Den Haag, 2022.

[23] T. Banaszkiewicz, Nutritional value of soybean meal, InTech2011. https://doi.org/10.5772/23306.

[24] D.L. Jones, P. Cross, P.J.A. Withers, T.H. Deluca, D.A. Robinson, R.S. Quilliam, I.M. Harris, D.R. Chadwick, G. Edwards-Jones, Review: Nutrient stripping: The global disparity between food security and soil nutrient stocks, Journal of Applied Ecology 50(4) (2013) 851-862. https://doi.org/10.1111/1365-2664.12089.

[25] Agrimatie, Stikstofbemesting per ha - melkveehouderij [nitrogen fertilization per ha - dairy farming], Wageningen University, agrimatie.nl, 2022.

[26] Agrimatie, Fosfaatbemesting per ha - melkveehouderij [phosphate fertilization per ha - dairy farming], Wageningen University, agrimatie.nl, 2022.

[27] J.J. Elser, Phosphorus: A limiting nutrient for humanity?, Current Opinion in Biotechnology 23(6) (2012) 833-838. http://dx.doi.org/10.1016/j.copbio.2012.03.001.

[28] D. Cordell, S. White, Life's bottleneck: Sustaining the world's phosphorus for a food secure future, Annual Review of Environment and Resources 39(1) (2014) 161-188. https://doi.org/10.1146/annurev-environ-010213-113300.

[29] European-Commission, Safeguarding food security and reinforcing the resilience of food systems, Communication from the commission to the European parliament, the European council, the council, the European economic and social committee and the committee of the regions, Brussels, 2022.

[30] D. Cordell, S. White, Sustainable phosphorus measures: Strategies and technologies for achieving phosphorus security, Agronomy 3(1) (2013) 86-116. https://doi.org/10.3390/agronomy3010086.

[31] J. Köninger, E. Lugato, P. Panagos, M. Kochupillai, A. Orgiazzi, M.J.I. Briones, Manure management and soil biodiversity: Towards more sustainable food systems in the eu, Agricultural Systems 194 (2021) 103251. https://doi.org/10.1016/j.agsy.2021.103251.

[32] D. Meyer, P.L. Ristow, M. Lie, Particle size and nutrient distribution in fresh dairy manure, Applied Engineering in Agriculture 23(1) (2007) 113-118.

[33] K. Peters, M. Hjorth, L.S. Jensen, J. Magid, Carbon, nitrogen, and phosphorus distribution in particle size-fractionated separated pig and cattle slurry, Journal of Environmental Quality 40(1) (2011) 224-232. https://doi.org/10.2134/jeq2010.0217.

[34] L. Masse, D.I. Massé, V. Beaudette, M. Muir, Size distribution and composition of particles in raw and anaerobically digested swine manure, American Society of Agricultural Engineers 48(5) (2005) 1943-1949.

[35] E. Martín-Hernández, A.M. Sampat, V.M. Zavala, M. Martín, Optimal integrated facility for waste processing, Chemical Engineering Research and Design 131 (2018) 160-182. https://doi.org/10.1016/j.cherd.2017.11.042.

[36] Q. He, A. Rajendran, J. Gan, H. Lin, C.A. Felt, B. Hu, Phosphorus recovery from dairy manure wastewater by fungal biomass treatment, Water and Environment Journal 33(4) (2019) 508-517. https://doi.org/10.1111/wej.12421.

[37] C. Schott, J.R. Cunha, R.D. van der Weijden, C. Buisman, Phosphorus recovery from pig manure: Dissolution of struvite and formation of calcium phosphate granules during anaerobic digestion with calcium addition, Chemical Engineering Journal (2022) 135406. https://doi.org/10.1016/j.cej.2022.135406.

[38] C. Schott, J. Ricardo Cunha, R.D. van der Weijden, C. Buisman, Innovation in valorization of cow manure: Higher hydrolysis, methane production and increased phosphorus retention using uasb technology, Chemical Engineering Journal (2022) 140294. https://doi.org/10.1016/j.cej.2022.140294.

[39] A.A. Szogi, M.B. Vanotti, Removal of phosphorus from livestock effluents, Journal of Environmental Quality 38(2) (2009) 576-586. https://doi.org/10.2134/jeq2007.0641.

[40] T. Tervahauta, R.D. van der Weijden, R.L. Flemming, L. Hernández Leal, G. Zeeman, C.J.N. Buisman, Calcium phosphate granulation in anaerobic treatment of black water: A new approach to phosphorus recovery, Water Research 48 (2014) 632-642. http://dx.doi.org/10.1016/j.watres.2013.10.012.

[41] J.R. Cunha, C. Schott, R.D. van der Weijden, L.H. Leal, G. Zeeman, C. Buisman, Calcium addition to increase the production of phosphate granules in anaerobic treatment of black water, Water Research 130 (2018) 333-342. https://doi.org/10.1016/j.watres.2017.12.012.

[42] J.R. Cunha, T. Tervahauta, R.D. van der Weijden, H. Temmink, L. Hernández Leal, G. Zeeman, C.J.N. Buisman, The effect of bioinduced increased ph on the enrichment of calcium phosphate in granules during anaerobic treatment of black water, Environ Sci Technol (2018). https://doi.org/10.1021/acs.est.8b03502.

[43] J.R. Cunha, T. Tervahauta, R.D. van der Weijden, L. Hernández Leal, G. Zeeman, C.J.N. Buisman, Simultaneous recovery of calcium phosphate granules and methane in anaerobic treatment of black water: Effect of bicarbonate and calcium fluctuations, Journal of Environmental Management (2017). https://doi.org/10.1016/j.jenvman.2017.09.013.

[44] D. Cordell, Global phosphorus scarcity: A food secure future?, Journal of Nutrition & Intermediary Metabolism 8 (2017) 61-62. https://doi.org/10.1016/j.jnim.2017.04.005.

[45] D. Cordell, J.-O. Drangert, S. White, The story of phosphorus: Global food security and food for thought, Global Environmental Change 19(2) (2009) 292-305. https://doi.org/10.1016/j.gloenvcha.2008.10.009.

[46] Eurostat, Consumption of inorganic fertilizers (aei_fm_usefert), Eurostat, Brussels, 2021.

[47] W. Steffen et al., Planetary boundaries: Guiding human development on a changing planet, Science 347(6223) (2015) 1259855. https://doi.org/10.1126/science.1259855.

[48] D. Cordell, S. White, Peak phosphorus: Clarifying the key issues of a vigorous debate about long-term phosphorus security, Sustainability 3(10) (2011) 2027-2049.

[49] M. van den Berg, K. Neumann, D.P. van Vuuren, A.F. Bouwman, T. Kram, J. Bakkes, Exploring resource efficiency for energy, land and phosphorus use: Implications for resource scarcity and the global environment, Global Environmental Change 36 (2016) 21-34. https://doi.org/10.1016/j.gloenvcha.2015.09.016.

[50] T. Klammsteiner, V. Turan, M. Fernández-Delgado Juárez, S. Oberegger, H. Insam, Suitability of black soldier fly frass as soil amendment and implication for organic waste hygienization, Agronomy 10(10) (2020) 1578. https://doi.org/10.3390/agronomy10101578.

[51] S. Rahimpour Golroudbary, M. El Wali, A. Kraslawski, Rationality of using phosphorus primary and secondary sources in circular economy: Game-theory-based analysis, Environmental Science & Policy 106 (2020) 166-176. https://doi.org/10.1016/j.envsci.2020.02.004.

[52] S.C. Sheppard, Elemental composition of swine manure from 1997 to 2017: Changes relevant to environmental consequences, Journal of Environmental Quality 48(1) (2019) 164-170. https://doi.org/10.2134/jeq2018.06.0226.

[53] M.D. Miller, H.E. Gall, A.R. Buda, L.S. Saporito, T.L. Veith, C.M. White, C.F. Williams, K.J. Brasier, P.J.A. Kleinman, J.E. Watson, Load-discharge relationships reveal the efficacy of manure application practices on phosphorus and total solids losses from agricultural fields, Agriculture, Ecosystems & Environment 272 (2019) 19-28. https://doi.org/10.1016/j.agee.2018.11.001.

[54] O. Sönmez, V. Turan, C. Kaya, The effects of sulfur, cattle, and poultry manure addition on soil phosphorus, 40 (2022). https://dergipark.org.tr/en/pub/tbtkagriculture/issue/34740/384164.

[55] S.M. Powers, R.B. Chowdhury, G.K. MacDonald, G.S. Metson, A.H.W. Beusen, A.F. Bouwman, S.E. Hampton, B.K. Mayer, M.L. McCrackin, D.A. Vaccari, Global opportunities to increase agricultural independence through phosphorus recycling, Earth's Future 7(4) (2019) 370-383. https://doi.org/10.1029/2018EF001097.

[56] European-Commission, Report from the commission to the council and the european parliament on the implementation of council directive 91/676/eec concerning the protection of waters against pollution caused by nitrates from agricultural sources based on member state reports for the period 2012–2015, Brussel, 2018.

[57] B. Garske, J. Stubenrauch, F. Ekardt, Sustainable phosphorus management in european agricultural and environmental law, Review of European, Comparative & International Environmental Law 29(1) (2020) 107-117. https://doi.org/10.1111/reel.12318.

[58] Rijksdienst voor Ondernemend Nederland [Netherlands Enterprise Agency] RVO, Fosfaat bemesting (phosphate fertilization), in: R.v.O. Nederland (Ed.) 2021.

[59] Meststoffenwet, Meststoffenwet (fertilizers act), in: N.a.F. Ministry of Agriculture (Ed.) Dutch Government, 2016.

[60] Rijksdienst voor Ondernemend Nederland [Netherlands Enterprise Agency] RVO, Mestverwerkingsplicht veehouder (manure treatment obligation), Rijksdienst voor Ondernemend Nederland, 2021.

[61] Agrimatie, Pig farming: Manure treatment costs, Wageningen University, agrimatie.nl, 2021.

[62] J.R. Cunha, C. Schott, R.D. van der Weijden, L.H. Leal, G. Zeeman, C. Buisman, Calcium phosphate granules recovered from black water treatment: A sustainable substitute for mined phosphorus in soil fertilization, Resources, Conservation and Recycling 158 (2020) 104791. https://doi.org/10.1016/j.resconrec.2020.104791.

[63] G. Tchobanoglous, F.L. Burton, H.D. Stensel, Metcalf, I. Eddy, Wastewater engineering: Treatment and reuse, McGraw-Hill Education2003.

[64] Clesceri, Greenberg, Eaton, Standard methods for the examination of water and wastewater, Washington [etc.], US: American Public Health Association [etc.]1998.

[65] M. Halalsheh, J. Koppes, J. den Elzen, G. Zeeman, M. Fayyad, G. Lettinga, Effect of srt and temperature on biological conversions and the related scum-forming potential, Water Research 39(12) (2005) 2475-2482. https://doi.org/10.1016/j.watres.2004.12.012.

[66] M.S. De Graaff, H. Temmink, G. Zeeman, C.J.N. Buisman, Anaerobic treatment of concentrated black water in a uasb reactor at a short hrt, Water 2(1) (2010) 101.

[67] D. N. Miller, R. P. McGhee, Two new designs for manure solids and liquids sampling from tank, pit, and lagoons at various depths, Applied Engineering in Agriculture 27(5) (2011) 847-854. https://doi.org/10.13031/2013.39555.

[68] M. Barret, N. Gagnon, E. Topp, L. Masse, D.I. Massé, G. Talbot, Physico-chemical characteristics and methanogen communities in swine and dairy manure storage tanks: Spatio-temporal variations and impact on methanogenic activity, Water Research 47(2) (2013) 737-746. https://doi.org/10.1016/j.watres.2012.10.047.

[69] J. Li, H. Yan, Q. Chen, J. Meng, J. Li, Y. Zhang, A.K. Jha, Performance of anaerobic sludge and the microbial social behaviors induced by quorum sensing in a uasb after a shock loading, Bioresource Technol 330 (2021) 124972. https://doi.org/10.1016/j.biortech.2021.124972.

[70] S.P. Lohani, R. Bakke, S.N. Khanal, Load limit of a uasb fed septic tank-treated domestic wastewater, Water Science and Technology 72(8) (2015) 1455-1461. https://doi.org/10.2166/wst.2015.358.

[71] K.M. Wang, A. Soares, B. Jefferson, H.Y. Wang, L.J. Zhang, S.F. Jiang, E.J. Mcadam, Establishing the mechanisms underpinning solids breakthrough in uasb configured anaerobic membrane bioreactors to mitigate fouling, Water Research 176 (2020) 115754. https://doi.org/10.1016/j.watres.2020.115754.

[72] A. Pevere, G. Guibaud, E.D. van Hullebusch, W. Boughzala, P.N.L. Lens, Effect of na+ and ca2+ on the aggregation properties of sieved anaerobic granular sludge, Colloids and Surfaces A: Physicochemical and Engineering Aspects 306(1-3) (2007) 142-149. https://doi.org/10.1016/j.colsurfa.2007.04.033.

[73] H. Li, Y. Wen, A. Cao, J. Huang, Q. Zhou, P. Somasundaran, The influence of additives (ca2+, al3+, and fe3+) on the interaction energy and loosely bound extracellular polymeric substances (eps) of activated sludge and their flocculation mechanisms, Bioresource Technol 114 (2012) 188-194. https://doi.org/10.1016/j.biortech.2012.03.043.

[74] H.Q. Yu, J.H. Tay, H.H.P. Fang, The roles of calcium in sludge granulation during uasb reactor start-up, Water Research 35(4) (2001) 1052-1060. https://doi.org/10.1016/S0043-1354(00)00345-6.

[75] I. Angelidaki, B.K. Ahring, Thermophilic anaerobic digestion of livestock waste: The effect of ammonia, Appl Microbiol Biot 38(4) (1993) 560-564. https://doi.org/10.1007/BF00242955.

[76] K.H. Hansen, I. Angelidaki, B.K. Ahring, Anaerobic digestion of swine manure: Inhibition by ammonia, Water Research 32(1) (1998) 5-12. https://doi.org/10.1016/s0043-1354(97)00201-7.

[77] O. Yenigün, B. Demirel, Ammonia inhibition in anaerobic digestion: A review, Process Biochemistry 48(5-6) (2013) 901-911. https://doi.org/10.1016/j.procbio.2013.04.012.

[78] T.L.I. Vergote, A.E.J. De Dobbelaere, B. Willems, J. Leenknegt, J. Buysse, E.I.P. Volcke, E. Meers, Stability of thermophilic pig manure mono-digestion: Effect of thermal pre-treatment and separation, Frontiers in Energy Research 8(40) (2020). https://doi.org/10.3389/fenrg.2020.00040.

[79] A. Chini, C.E. Hollas, A.C. Bolsan, F.G. Antes, H. Treichel, A. Kunz, Treatment of digestate from swine sludge continuous stirred tank reactor to reduce total carbon and total solids content, Environment, Development and Sustainability 23(8) (2021) 12326-12341. https://doi.org/10.1007/s10668-020-01170-6.

[80] W. Zeng, D. Wang, Z. Wu, L. He, Z. Luo, J. Yang, Recovery of nitrogen and phosphorus fertilizer from pig farm biogas slurry and incinerated chicken manure fly ash, Science of The Total Environment 782 (2021) 146856. https://doi.org/10.1016/j.scitotenv.2021.146856.

[81] F. Corona, D. Hidalgo, J.M. Martín-Marroquín, E. Meers, Study of pig manure digestate pre-treatment for subsequent valorisation by struvite, Environ Sci Pollut R (2020). https://doi.org/10.1007/s11356-020-10918-6.

[82] S. Montalvo, C. Huiliñir, A. Castillo, J. Pagés-Díaz, L. Guerrero, Carbon, nitrogen and phosphorus recovery from liquid swine wastes: A review, Journal of Chemical Technology & Biotechnology 95(9) (2020) 2335-2347. https://doi.org/10.1002/jctb.6336.

[83] M. Zubair, S. Wang, P. Zhang, J. Ye, J. Liang, M. Nabi, Z. Zhou, X. Tao, N. Chen, K. Sun, J. Xiao, Y. Cai, Biological nutrient removal and recovery from solid and liquid livestock manure: Recent advance and perspective, Bioresource Technol 301 (2020) 122823. https://doi.org/10.1016/j.biortech.2020.122823.

[84] A.A. Szögi, M.B. Vanotti, P.G. Hunt, Phosphorus recovery from pig manure solids prior to land application, Journal of Environmental Management 157 (2015) 1-7. https://doi.org/10.1016/j.jenvman.2015.04.010.

[85] M.L. Christensen, K. Keiding, P.V. Christensen, Phosphorus removal from manure by mechanical separation using salt and polymers: Theoretical simulations and experimental data, Applied Engineering in Agriculture 36(2) (2020) 175-185. https://doi.org/10.13031/aea.13726.

[86] G. Lettinga, A.F.M. van Velsen, S.W. Hobma, W. de Zeeuw, A. Klapwijk, Use of the upflow sludge blanket (usb) reactor concept for biological wastewater treatment, especially for anaerobic treatment, Biotechnology and Bioengineering 22(4) (1980) 699-734.

[87] E.P.A. van Langerak, H. Ramaekers, J. Wiechers, A.H.M. Veeken, H.V.M. Hamelers, G. Lettinga, Impact of location of caco3 precipitation on the development of intact anaerobic sludge, Water Research 34(2) (2000) 437-446. https://doi.org/10.1016/S0043-1354(99)00154-2.

[88] D.J. Batstone, J. Landelli, A. Saunders, R.I. Webb, L.L. Blackall, J. Keller, The influence of calcium on granular sludge in a full-scale uasb treating paper mill wastewater, Water Science and Technology 45(10) (2002) 187-193.

[89] L. Zhang, A. Mou, H. Sun, Y. Zhang, Y. Zhou, Y. Liu, Calcium phosphate granules formation: Key to high rate of mesophilic uasb treatment of toilet wastewater, Science of The Total Environment 773 (2021) 144972. https://doi.org/10.1016/j.scitotenv.2021.144972.

[90] J. McMurry, R. Fay, Chemistry, Sixth ed., Pearson2012.

[91] F. Ozdemir, I. Evans, O. Bretcanu, Calcium phosphate cements for medical applications, Clinical applications of biomaterials, Springer International Publishing2017, pp. 91-121. https://doi.org/10.1007/978-3-319-56059-5_4.

[92] K. Ishikawa, Bone substitute fabrication based on dissolution-precipitation reactions, Materials (Basel) 3(2) (2010) 1138-1155. https://doi.org/10.3390/ma3021138.

[93] H. Wang, Y. Zhang, I. Angelidaki, Ammonia inhibition on hydrogen enriched anaerobic digestion of manure under mesophilic and thermophilic conditions, Water Research 105 (2016) 314-319. https://doi.org/10.1016/j.watres.2016.09.006.

[94] J.R. Cunha, C. Schott, R.D. van der Weijden, L.H. Leal, G. Zeeman, C. Buisman, Recovery of calcium phosphate granules from black water using a hybrid upflow anaerobic sludge bed and gas-lift reactor, Environmental Research 178 (2019) 108671. https://doi.org/10.1016/j.envres.2019.108671.

[95] T. Yu, L. Tian, X. You, L. Wang, S. Zhao, D. Kang, D. Xu, Z. Zeng, M. Zhang, P. Zheng, Deactivation mechanism of calcified anaerobic granule: Space occupation and pore blockage, Water Research 166 (2019) 115062. https://doi.org/10.1016/j.watres.2019.115062.

[96] L. Chen, Y. Ji, Z. Yu, C. Wang, P.J.J. Alvarez, X. Xu, L. Zhu, Uncover the secret of granule calcification and deactivation in up-flow anaerobic sludge bed (uasb) reactor with long-term exposure to high calcium, Water Research 189 (2021) 116586. https://doi.org/10.1016/j.watres.2020.116586.

[97] M.M. Ghangrekar, S.R. Asolekar, S.G. Joshi, Characteristics of sludge developed under different loading conditions during uasb reactor start-up and granulation, Water Research 39(6) (2005) 1123-1133. https://doi.org/10.1016/j.watres.2004.12.018.

[98] J. Liang, Q. Wang, B.A. Yoza, Q.X. Li, C. Chen, J. Ming, J. Yu, J. Li, M. Ke, Rapid granulation using calcium sulfate and polymers for refractory wastewater treatment in up-flow anaerobic sludge blanket reactor, Bioresource Technol 305 (2020) 123084. https://doi.org/10.1016/j.biortech.2020.123084.

[99] T. Komiyama, T. Ito, The characteristics of phosphorus in animal manure composts, Soil Science and Plant Nutrition 65(3) (2019) 281-288. https://doi.org/10.1080/00380768.2019.1615384.

[100] M.L. Christensen, M. Hjorth, K. Keiding, Characterization of pig slurry with reference to flocculation and separation, Water Research 43(3) (2009) 773-783. https://doi.org/10.1016/j.watres.2008.11.010.

[101] P. W. Westerman, K. E. Bowers, K. D. Zering, Phosphorus recovery from covered digester effluent with a continuous-flow struvite crystallizer, Applied Engineering in Agriculture 26(1) (2010) 153-161. https://doi.org/10.13031/2013.29471.

[102] M.J. O'Neil, The merck index - an encyclopedia of chemicals, drugs, and biologicals., Cambridge, UK, 2013.

[103] C. Deng, W. Liu, G. Chu, D. Luo, G. Zhang, L. Wang, H. Yue, B. Liang, C. Li, Aqueous carbonation of mgso4 with (nh4)2co3 for co2 sequestration, Greenhouse Gases: Science and Technology 9(2) (2019) 209-225. https://doi.org/10.1002/ghg.1840.

[104] X. Cao, W. Harris, Carbonate and magnesium interactive effect on calcium phosphate precipitation, Environ Sci Technol 42(2) (2008) 436-442. https://doi.org/10.1021/es0716709.

[105] C. González-Morales, B. Fernández, F.J. Molina, D. Naranjo-Fernández, A. Matamoros-Veloza, M.A. Camargo-Valero, Influence of ph and temperature on struvite purity and recovery from anaerobic digestate, Sustainability 13(19) (2021) 10730.

[106] N. Park, H. Chang, Y. Jang, H. Lim, J. Jung, W. Kim, Critical conditions of struvite growth and recovery using mgo in pilot scale crystallization plant, Water Science and Technology 81(12) (2020) 2511-2521. https://doi.org/10.2166/wst.2020.306.

[107] K.S. Le Corre, E. Valsami-Jones, P. Hobbs, S.A. Parsons, Impact of calcium on struvite crystal size, shape and purity, Journal of Crystal Growth 283(3-4) (2005) 514-522. https://doi.org/10.1016/j.jcrysgro.2005.06.012.

[108] Z.-G. Liu, X.-B. Min, F. Feng, X. Tang, W.-C. Li, C. Peng, T.-Y. Gao, X.-L. Chai, C.-J. Tang, Development and simulation of a struvite crystallization fluidized bed reactor with enhanced external recirculation for phosphorous and ammonium recovery, Science of The Total Environment 760 (2021) 144311. https://doi.org/10.1016/j.scitotenv.2020.144311.

[109] D. Kim, C. Olympiou, C.P. Mccoy, N.J. Irwin, J.D. Rimer, Time-resolved dynamics of struvite crystallization: Insights from the macroscopic to molecular scale, Chemistry – A European Journal 26(16) (2020) 3555-3563. https://doi.org/10.1002/chem.201904347.

[110] K.S. Le Corre, E. Valsami-Jones, P. Hobbs, S.A. Parsons, Impact of reactor operation on success of struvite precipitation from synthetic liquors, Environ Technol 28(11) (2007) 1245-1256. https://doi.org/10.1080/09593332808618885.

[111] M. Fromberg, M. Pawlik, D.S. Mavinic, Induction time and zeta potential study of nucleating and growing struvite crystals for phosphorus recovery improvements within fluidized bed reactors, Powder Technology 360 (2020) 715-730. https://doi.org/10.1016/j.powtec.2019.09.067.

[112] L. Wei, T. Hong, H. Liu, T. Chen, The effect of sodium alginate on struvite crystallization in aqueous solution: A kinetics study, Journal of Crystal Growth 473 (2017) 60-65. https://doi.org/10.1016/j.jcrysgro.2017.03.039.

[113] L. Wei, T. Hong, K. Cui, T. Chen, Y. Zhou, Y. Zhao, Y. Yin, J. Wang, Q. Zhang, Probing the effect of humic acid on the nucleation and growth kinetics of struvite by constant composition technique, Chemical Engineering Journal 378 (2019) 122130. https://doi.org/10.1016/j.cej.2019.122130.

[114] H. Li, T.-L. Zhao, F.-J. Qian, H.-F. Jiang, Q.-Z. Yao, Y. Luo, S.-Q. Fu, G.-T. Zhou, A model of extracellular polymeric substances on crystal growth and morphogenesis of struvite: Effects of sodium alginate, Powder Technology 380 (2021) 80-88. https://doi.org/10.1016/j.powtec.2020.11.037.

[115] H. Yan, K. Shih, Effects of calcium and ferric ions on struvite precipitation: A new assessment based on quantitative x-ray diffraction analysis, Water Research 95 (2016) 310-318. https://doi.org/10.1016/j.watres.2016.03.032.

[116] J.W. Mullin, 6 - crystal growth, in: J.W. Mullin (Ed.), Crystallization (fourth edition), Butterworth-Heinemann, Oxford, 2001, pp. 216-288. https://doi.org/10.1016/B978-075064833-2/50008-5.

[117] A. Mersmann, Crystallization technology handbook, Marcel Dekker, New York, 2001.

[118] J.L. Meyer, C.C. Weatherall, Amorphous to crystalline calcium phosphate phase transformation at elevated ph, Journal of Colloid and Interface Science 89(1) (1982) 257-267. https://doi.org/10.1016/0021-9797(82)90139-4.

[119] A. Mañas, M. Pocquet, B. Biscans, M. Sperandio, Parameters influencing calcium phosphate precipitation in granular sludge sequencing batch reactor, Chemical Engineering Science 77 (2012) 165-175. https://doi.org/10.1016/j.ces.2012.01.009.

[120] S. Jiang, W. Jin, Y.-N. Wang, H. Pan, Z. Sun, R. Tang, Effect of the aggregation state of amorphous calcium phosphate on hydroxyapatite nucleation kinetics, RSC Advances 7(41) (2017) 25497-25503. https://doi.org/10.1039/c7ra02208e.

[121] P. Ustriyana, F.M. Michel, M.C. Wilson, E. Harmon, J. Chen, T. Liu, N. Sahai, Oligo(l-glutamic acids) in calcium phosphate precipitation: Mechanism of delayed phase transformation, The Journal of Physical Chemistry B 124(29) (2020) 6288-6298. https://doi.org/10.1021/acs.jpcb.0c01690.

[122] J. Yun, B. Holmes, A. Fok, Y. Wang, A kinetic model for hydroxyapatite precipitation in mineralizing solutions, Crystal Growth & Design 18(5) (2018) 2717-2725. https://doi.org/10.1021/acs.cgd.7b01330.

[123] E. Loste, R.M. Wilson, R. Seshadri, F.C. Meldrum, The role of magnesium in stabilising amorphous calcium carbonate and controlling calcite morphologies, Journal of Crystal Growth 254(1-2) (2003) 206-218. https://doi.org/10.1016/s0022-0248(03)01153-9.

[124] Y. Politi, D.R. Batchelor, P. Zaslansky, B.F. Chmelka, J.C. Weaver, I. Sagi, S. Weiner, L. Addadi, Role of magnesium ion in the stabilization of biogenic amorphous calcium carbonate: A structure–function investigation, Chemistry of Materials 22(1) (2010) 161-166. https://doi.org/10.1021/cm902674h.

[125] Y. Chen, W. Gu, H. Pan, S. Jiang, R. Tang, Stabilizing amorphous calcium phosphate phase by citrate adsorption, CrystEngComm 16(10) (2014) 1864-1867. https://doi.org/10.1039/c3ce42274g.

[126] H. Ding, H. Pan, X. Xu, R. Tang, Toward a detailed understanding of magnesium ions on hydroxyapatite crystallization inhibition, Crystal Growth & Design 14(2) (2014) 763-769. https://doi.org/10.1021/cg401619s.

[127] S. Jiang, Y. Cao, C. Zong, Y. Pang, Z. Sun, Appropriate regulation of magnesium on hydroxyapatite crystallization in simulated body fluids, CrystEngComm 23(3) (2021) 678-683. https://doi.org/10.1039/d0ce01421d.

[128] X. Yang, B. Xie, L. Wang, Y. Qin, Z.J. Henneman, G.H. Nancollas, Influence of magnesium ions and amino acids on the nucleation and growth of hydroxyapatite, CrystEngComm 13(4) (2011) 1153-1158. https://doi.org/10.1039/c0ce00470g.

[129] L. Zhonghong-Chemical Co., China supplier anhydrous calcium chloride food grade for food processing, 2022. https://cnlygzha.en.made-in-china.com/product/nONftwJCgGha/China-China-Supplier-Anhydrous-Calcium-Chloride-Food-Grade-for-Food-Processing.html. (Accessed 02.02.2022 2022).

[130] J.J. Weeks, G.M. Hettiarachchi, A review of the latest in phosphorus fertilizer technology: Possibilities and pragmatism, Journal of Environmental Quality 48(5) (2019) 1300-1313. https://doi.org/10.2134/jeq2019.02.0067.

[131] B. Davies, J.A. Coulter, P.H. Pagliari, Timing and rate of nitrogen fertilization influence maize yield and nitrogen use efficiency, PLOS ONE 15(5) (2020) e0233674. https://doi.org/10.1371/journal.pone.0233674.

[132] B. J.Shelp, W. J.Sutton, E. J.Flaherty, BrianBeres, Strategic timing and rate of phosphorus fertilization improves phosphorus-use efficiency in two contrasting cultivars of subirrigated greenhouse-grown chrysanthemum, Canadian Journal of Plant Science 100(3) (2020) 264-275. https://doi.org/10.1139/cjps-2019-0173.

[133] D. Cordell, T.S.S. Neset, Phosphorus vulnerability: A qualitative framework for assessing the vulnerability of national and regional food systems to the multi-dimensional stressors of phosphorus scarcity, Global Environmental Change 24 (2014) 108-122. https://doi.org/10.1016/j.gloenvcha.2013.11.005.

[134] Centraal Bureau voor de Statistiek [Central bureau of Statistics] CBS, Dierlijke mest [Animal manure]; productie en mineralenuitscheiding [Production and excreted minerals], diercategorie [Animal category], regio, 2022.

[135] S.G. Sommer, M.L. Christensen, T. Schmidt, L.S. Jensen, Animal manure recycling: Treatment and management, Wiley2013.

[136] Agrimatie, Ammoniakemissie melkveehouderij [ammonia emission from dairy farming], Wageningen University, 2022.

[137] Rijksdienst voor Ondernemend Nederland [Netherlands Enterprise Agency] RVO, Mestbeleid 2022: Stikstofgebruiksnormen [nitrogen use norms], Den Haag, 2022.

[138] Rijksdienst voor Ondernemend Nederland [Netherlands Enterprise Agency] RVO, Mestbeleid 2022: Fosfaatgebruiksnormen [phosphate use norms], Den Haag, 2022.

[139] Rijksdienst voor Ondernemend Nederland [Netherlands Enterprise Agency] RVO, Mestverwerkingsplicht veehouder [manure treatment obligation livestockfarmer], Rijksdienst voor Ondernemend Nederland, 2022.

[140] D.L. Hoang, B. Wiersema, H.C. Moll, S. Nonhebel, The impact of biogas production on the organic carbon input to the soil of dutch dairy farms: A substance flow analysis, Journal of Industrial Ecology 26(2) (2022) 491-508. https://doi.org/10.1111/jiec.13197.

[141] R. Jetten, Beantwoording kamervragen over de opschaling van de groen gas productie in nederland [answers to parliament questions about the scale-up of green gas production in nl], Rijksoverheid, 2022.

[142] Rijksoverheid [Dutch government], Nederland circulair in 2050, Het ministerie van Infrastructuur en Milieu en het ministerie van Economische Zaken, mede namens het ministerie van Buitenlandse Zaken en het ministerie van Binnenlandse Zaken en Koninkrijksrelaties., 2016.

[143] Nederlandse Vereniging Duurzame Energie [Dutch Association Sustainable Energy] NVDE, Groen gas: Feiten & cijfers [green gas: Facts and numbers], 2020, p. 14.

[144] Centraal Bureau voor de Statistiek [Central bureau of Statistics] CBS, Elektriciteits- en groen gasproductie mestvergisters 2020 [electricity and green gas prdocution from animal manure digesters 2020], 2021.

[145] Rijksdienst voor Ondernemend Nederland [Netherlands Enterprise Agency] RVO, Feiten en cijfers sde(+)(+) [facts and numbers sde(+)(+)], Den Haag, 2022.

[146] Rijksoverheid [Dutch government], Meststoffenwet [fertilizers act], in: N.a.F. Ministry of Agriculture (Ed.) Dutch Government, 2016.

[147] H. Carrere, G. Antonopoulou, R. Affes, F. Passos, A. Battimelli, G. Lyberatos, I. Ferrer, Review of feedstock pretreatment strategies for improved anaerobic digestion: From lab-scale research to full-scale application, Bioresource Technol 199 (2016) 386-397. https://doi.org/10.1016/j.biortech.2015.09.007.

[148] H.B. Møller, S.G. Sommer, B.K. Ahring, Methane productivity of manure, straw and solid fractions of manure, Biomass and Bioenergy 26(5) (2004) 485-495. https://doi.org/10.1016/j.biombioe.2003.08.008.

[149] A.M. Sampat, E. Martín-Hernández, M. Martín, V.M. Zavala, Technologies and logistics for phosphorus recovery from livestock waste, Clean Technologies and Environmental Policy 20(7) (2018) 1563-1579. https://doi.org/10.1007/s10098-018-1546-y.

[150] W. Tao, K.P. Fattah, M.P. Huchzermeier, Struvite recovery from anaerobically digested dairy manure: A review of application potential and hindrances, Journal of Environmental Management 169 (2016) 46-57. https://doi.org/10.1016/j.jenvman.2015.12.006.

[151] E. Wagner, K.G. Karthikeyan, Precipitating phosphorus as struvite from anaerobically-digested dairy manure, Journal of Cleaner Production 339 (2022) 130675. https://doi.org/10.1016/j.jclepro.2022.130675.

[152] K. Brown, J. Harrison, K. Bowers, Struvite precipitation from anaerobically digested dairy manure, Water Air and Soil Pollution 229(7) (2018). https://doi.org/10.1007/s11270-018-3855-5.

[153] J.-H. Ahn, T.H. Do, S.D. Kim, S. Hwang, The effect of calcium on the anaerobic digestion treating swine wastewater, Biochemical Engineering Journal 30(1) (2006) 33-38.

[154] D.L. Parkhurst, C.A.J. Appelo, Description of input and examples for phreeqc version 3—a computer program for speciation, batch-reaction, one-dimensional transport, and inverse geochemical calculations: U.S. Geological survey techniques and methods, 2013.

[155] E. Tipping, Humic ion-binding model vi: An improveddescription of the interactions of protons and metalions with humic substances, Aquatic Geochemistry 4(1) (1998) 3-47. https://doi.org/10.1023/a:1009627214459.

[156] K.N. Ohlinger, P.E., T.M. Young, E.D. Schroeder, Kinetics effects on preferential struvite accumulation in wastewater, Journal of Environmental Engineering 125(8) (1999)730-737.https://doi.org/doi:10.1061/(ASCE)0733-9372(1999)125:8(730).

[157] E.V. Musvoto, M.C. Wentzel, G.A. Ekama, Integrated chemical–physical processes modelling—ii. Simulating aeration treatment of anaerobic digester supernatants, Water Research 34(6) (2000) 1868-1880. https://doi.org/10.1016/S0043-1354(99)00335-8.

[158] H.P. Scott, R.J. Hemley, H.-K. Mao, D.R. Herschbach, L.E. Fried, W.M. Howard, S. Bastea, Generation of methane in the earth's mantle: In situ high pressure–temperature measurements of carbonate reduction, Proceedings of the National Academy of Sciences 101(39) (2004) 14023-14026. https://doi.org/10.1073/pnas.0405930101.

[159] W. Peng, L. Zhang, S. Tumiati, A. Vitale Brovarone, H. Hu, Y. Cai, T. Shen, Abiotic methane generation through reduction of serpentinite-hosted dolomite: Implications for carbon mobility in subduction zones, Geochimica et Cosmochimica Acta 311 (2021) 119-140. https://doi.org/10.1016/j.gca.2021.07.033.

[160] C. Mesters, N. Rahimi, D. Van Der Sloot, J. Rhyne, F. Cassiola, Direct reduction of magnesium carbonate to methane, ACS Sustainable Chemistry & Engineering 9(33) (2021) 10977-10989. https://doi.org/10.1021/acssuschemeng.1c01439.

[161] V. Moset, M. Poulsen, R. Wahid, O. Højberg, H.B. Møller, Mesophilic versus thermophilic anaerobic digestion of cattle manure: Methane productivity and microbial ecology, Microbial Biotechnology 8(5) (2015) 787-800. https://doi.org/10.1111/1751-7915.12271.

[162] T.A.S. Biosantech, D. Rutz, R. Janssen, B. Drosg, 2 - biomass resources for biogas production, in: A. Wellinger, J. Murphy, D. Baxter (Eds.), The biogas handbook, Woodhead Publishing2013, pp. 19-51. https://doi.org/10.1533/9780857097415.1.19.

[163] N. Scarlat, F. Fahl, J.-F. Dallemand, F. Monforti, V. Motola, A spatial analysis of biogas potential from manure in europe, Renewable and Sustainable Energy Reviews 94 (2018) 915-930. https://doi.org/10.1016/j.rser.2018.06.035.

[164] I. Angelidaki, B.K. Ahring, Anaerobic thermophilic digestion of manure at different ammonia loads: Effect of temperature, Water Research 28(3) (1994) 727-731. https://doi.org/10.1016/0043-1354(94)90153-8.

[165] G. Bahreini, E. Elbeshbishy, J. Jimenez, D. Santoro, G. Nakhla, Integrated fermentation and anaerobic digestion of primary sludges for simultaneous resource and energy recovery: Impact of volatile fatty acids recovery, Waste Management 118 (2020) 341-349. https://doi.org/10.1016/j.wasman.2020.08.051.

[166] R.A. Labatut, L.T. Angenent, N.R. Scott, Characterizing the influence of wastewater composition and lignin content on anaerobic biodegradability, Environmental Science: Water Research & Technology 8(7) (2022) 1507-1520. https://doi.org/10.1039/d2ew00077f.

[167] M.N. Young, R. Krajmalnik-Brown, W. Liu, M.L. Doyle, B.E. Rittmann, The role of anaerobic sludge recycle in improving anaerobic digester performance, Bioresource Technol 128 (2013) 731-737. https://doi.org/10.1016/j.biortech.2012.11.079.

[168] I.-S. Lee, P. Parameswaran, B.E. Rittmann, Effects of solids retention time on methanogenesis in anaerobic digestion of thickened mixed sludge, Bioresource Technol 102(22) (2011) 10266-10272. https://doi.org/10.1016/j.biortech.2011.08.079.

[169] Y. Miron, G. Zeeman, J.B. van Lier, G. Lettinga, The role of sludge retention time in the hydrolysis and acidification of lipids, carbohydrates and proteins during digestion of primary sludge in cstr systems, Water Research 34(5) (2000) 1705-1713. https://doi.org/10.1016/S0043-1354(99)00280-8.

[170] W. Gujer, A.J.B. Zehnder, Conversion processes in anaerobic digestion, Water Science and Technology 15(8-9) (1983) 127-167. https://doi.org/10.2166/wst.1983.0164.

[171] V.M.C. Blanco, L.T. Fuess, M. Zaiat, Calcium dosing for the simultaneous control of biomass retention and the enhancement of fermentative biohydrogen production in an innovative fixed-film bioreactor, International Journal of Hydrogen Energy 42(17) (2017) 12181-12196. https://doi.org/10.1016/j.ijhydene.2017.02.180.

[172] G.-J. Xie, B.-F. Liu, H.-Q. Wen, Q. Li, C.-Y. Yang, W.-L. Han, J. Nan, N.-Q. Ren, Bioflocculation of photo-fermentative bacteria induced by calcium ion for enhancing hydrogen production, International Journal of Hydrogen Energy 38(19) (2013) 7780-7788. https://doi.org/10.1016/j.ijhydene.2013.04.099.

[173] B.T. Somerton, Effect of cations on biofilm formation by geobacillus species and anoxybacillus flavithermus dairy isolates : A thesis presented in partial fulfilment of the requirements for the degree of doctor of philosophy in food technology at massey university, palmerston north, new zealand, Massey University, 2013.

[174] M.T. Madigan, J.M. Martinko, K.S. Bender, D.H. Buckley, D.A. Stahl, Brock biology of microorganisms, Pearson2014.

[175] L. Chen, H. Chen, D. Lu, X. Xu, L. Zhu, Response of methanogens in calcified anaerobic granular sludge: Effect of different calcium levels, Journal of Hazardous Materials 389 (2020) 122131. https://doi.org/10.1016/j.jhazmat.2020.122131.

[176] M. Peces, S. Astals, P.D. Jensen, W.P. Clarke, Transition of microbial communities and degradation pathways in anaerobic digestion at decreasing retention time, New Biotechnology 60 (2021) 52-61. https://doi.org/10.1016/j.nbt.2020.07.005.

[177] E.P.A. van Langerak, G. Gonzalez-Gil, A. van Aelst, J.B. van Lier, H.V.M. Hamelers, G. Lettinga, Effects of high calcium concentrations on the development of methanogenic sludge in upflow anaerobic sludge bed (uasb) reactors, Water Research 32(4) (1998) 1255-1263. https://doi.org/10.1016/S0043-1354(97)00335-7.

[178] Y. Chen, J.J. Cheng, K.S. Creamer, Inhibition of anaerobic digestion process: A review, Bioresource Technol 99(10) (2008) 4044-4064. https://doi.org/10.1016/j.biortech.2007.01.057.

[179] H. Ma, C. Guo, M. Yao, M. Wu, Z. Wang, S. Wang, Calcium ions affect sludge digestion performance via changing extracellular polymeric substances in anaerobic bioreactor, Biomass and Bioenergy 137 (2020) 105548. https://doi.org/10.1016/j.biombioe.2020.105548.

[180] J. Yang, J. Zhang, J. Zhang, J. Zhang, Y. Yang, L. Zang, Roles of calcium-containing alkali materials on dark fermentation and anaerobic digestion: A systematic review, International Journal of Hydrogen Energy 46(78) (2021) 38645-38662. https://doi.org/10.1016/j.ijhydene.2021.09.129.

[181] Y. Dang, R. Zhang, S. Wu, Z. Liu, B. Qiu, Y. Fang, D. Sun, Calcium effect on anaerobic biological treatment of fresh leachate with extreme high calcium concentration, International Biodeterioration & Biodegradation 95 (2014) 76-83. https://doi.org/10.1016/j.ibiod.2014.05.016.

[182] J.H. Zhou, X.N. Shang, Z.W. Wang, C.C. Zhu, S.F. Wang, Effects of calcium concentration on up-flow multistage anaerobic reactor performance in treating bagasse spraying wastewater, Bioresources 14(2) (2019) 4254-4269. https://doi.org/10.15376/biores.14.2.4254-4269.

[183] Y. Lei, Y. Dang, Z. Lan, D. Sun, Effects of multiple inhibitory components on anaerobic treatment processes in municipal solid waste incineration leachate, Appl Microbiol Biot 100(11) (2016) 5123-5130. https://doi.org/10.1007/s00253-016-7341-y.

[184] T.J. Barzee, A. Edalati, J.L. Rapport, H.M. El-Mashad, R. Zhang, Characterization of nutrients and pilot biofertilizer production from food waste and dairy manure digestates, Trans. ASABE 64(4) (2021) 1153-1164. https://doi.org/10.13031/trans.13767.

[185] H. Landry, C. Laguë, M. Roberge, Physical and rheological properties of manure products, Applied Engineering in Agriculture 20(3) (2004) 277-288. https://doi.org/https://doi.org/10.13031/2013.16061.

[186] A.K. Thota Radhakrishnan, J.B. van Lier, F.H.L.R. Clemens, Rheological characterisation of concentrated domestic slurry, Water Research 141 (2018) 235-250. https://doi.org/10.1016/j.watres.2018.04.064.

[187] K. Güngör, K.G. Karthikeyan, Phosphorus forms and extractability in dairy manure: A case study for wisconsin on-farm anaerobic digesters, Bioresource Technol 99(2) (2008) 425-436. https://doi.org/10.1016/j.biortech.2006.11.049.

[188] B. Li, K. Dinkler, N. Zhao, M. Sobhi, W. Merkle, S. Liu, R. Dong, H. Oechsner, J. Guo, Influence of anaerobic digestion on the labile phosphorus in pig, chicken, and dairy manure, Science of The Total Environment 737 (2020) 140234. https://doi.org/10.1016/j.scitotenv.2020.140234.

[189] K. Güngör, K. G. Karthikeyan, Probable phosphorus solid phases and their stability in anaerobically digested dairy manure, Transactions of the ASAE 48(4) (2005) 1509-1520. https://doi.org/10.13031/2013.19188.

[190] Z. He, C.W. Honeycutt, T.S. Griffin, B.J. Cade-Menun, P.J. Pellechia, Z. Dou, Phosphorus forms in conventional and organic dairy manure identified by solution and solid state p-31 nmr spectroscopy, Journal of Environmental Quality 38(5) (2009) 1909-18.

[191] Z. He, T.S. Griffin, C.W. Honeycutt, Phosphorus distribution in dairy manures, Journal of Environment Quality 33(4) (2004) 1528. https://doi.org/10.2134/jeq2004.1528.

[192] M.P. Huchzermeier, W. Tao, Overcoming challenges to struvite recovery from anaerobically digested dairy manure, Water Environ Res 84(1) (2012) 34-41. https://doi.org/10.2175/106143011x13183708018887.

[193] Y. Li, J. Zhao, J. Krooneman, G.J.W. Euverink, Strategies to boost anaerobic digestion performance of cow manure: Laboratory achievements and their full-scale application potential, Science of The Total Environment 755 (2021) 142940. https://doi.org/https://doi.org/10.1016/j.scitotenv.2020.142940.

[194] N. Bhatnagar, D. Ryan, R. Murphy, A.M. Enright, A comprehensive review of green policy, anaerobic digestion of animal manure and chicken litter feedstock potential – global and irish perspective, Renewable and Sustainable Energy Reviews 154 (2022) 111884. https://doi.org/10.1016/j.rser.2021.111884.

[195] K. Güngör, A. Jürgensen, K.G. Karthikeyan, Determination of phosphorus speciation in dairy manure using xrd and xanes spectroscopy, Journal of Environmental Quality 36(6) (2007) 1856-1863. https://doi.org/10.2134/jeq2006.0563.

[196] R. Sander, Compilation of henry's law constants (version 4.0) for water as solvent, Atmospheric Chemistry and Physics 15(8) (2015) 4399-4981. https://doi.org/10.5194/acp-15-4399-2015.

[197] X. Wang, W. Conway, R. Burns, N. McCann, M. Maeder, Comprehensive study of the hydration and dehydration reactions of carbon dioxide in aqueous solution, The Journal of Physical Chemistry A 114(4) (2010) 1734-1740. https://doi.org/10.1021/jp909019u.

[198] M. Iqbal, H. Bhuiyan, D.S. Mavinic, Assessing struvite precipitation in a pilot-scale fluidized bed crystallizer, Environ Technol 29(11) (2008) 1157-1167. https://doi.org/10.1080/09593330802075452.

[199] A.A. Szogi, M.B. Vanotti, P.D. Shumaker, Economic recovery of calcium phosphates from swine lagoon sludge using quick wash process and geotextile filtration, Frontiers in Sustainable Food Systems 2(37) (2018). https://doi.org/10.3389/fsufs.2018.00037.

[200] V. Yilmaz, G.N. Demirer, Improved anaerobic acidification of unscreened dairy manure, Environmental Engineering Science 25(3) (2008) 309-317. https://doi.org/10.1089/ees.2006.0222.

[201] I. Vanwonterghem, P.D. Jensen, K. Rabaey, G.W. Tyson, Temperature and solids retention time control microbial population dynamics and volatile fatty acid production in replicated anaerobic digesters, Sci Rep-Uk 5(1) (2015) 8496. https://doi.org/10.1038/srep08496.

[202] D.P. Ho, P.D. Jensen, D.J. Batstone, Methanosarcinaceae and acetate-oxidizing pathways dominate in high-rate thermophilic anaerobic digestion of waste-activated sludge, Applied and Environmental Microbiology 79(20) (2013) 6491-6500. https://doi.org/10.1128/aem.01730-13.

[203] H. Füredi-Milhofer, L. Brečević, B. Purgarić, Crystal growth and phase transformation in the precipitation of calcium phosphates, Faraday Discuss. Chem. Soc. 61(0) (1976) 184-193. https://doi.org/10.1039/dc9766100184.

[204] L. Silverman, A.L. Boskey, Diffusion systems for evaluation of biomineralization, Calcified Tissue International 75(6) (2004) 494-501. https://doi.org/10.1007/s00223-004-0019-y.

[205] A. Mersmann, Crystallization technology handbook (second edition), Marcel Dekker, New York, 2001.

[206] W.J.E.M. Habraken, J. Tao, L.J. Brylka, H. Friedrich, L. Bertinetti, A.S. Schenk, A. Verch, V. Dmitrovic, P.H.H. Bomans, P.M. Frederik, J. Laven, P. van der Schoot, B. Aichmayer, G. de With, J.J. DeYoreo, N.A.J.M. Sommerdijk, Ion-association complexes unite classical and non-classical theories for the biomimetic nucleation of calcium phosphate, Nature Communications (2013). https://doi.org/10.1038/ncomms2490.

[207] G. Mancardi, C.E. Hernandez Tamargo, D. Di Tommaso, N.H. De Leeuw, Detection of posner's clusters during calcium phosphate nucleation: A molecular dynamics study, Journal of Materials Chemistry B 5(35) (2017) 7274-7284. https://doi.org/10.1039/c7tb01199g.

[208] A.S. Posner, F. Betts, Synthetic amorphous calcium phosphate and its relation to bone mineral structure, Accounts of Chemical Research 8(8) (1975) 273-281. https://doi.org/10.1021/ar50092a003.

[209] I. Roohani, S. Cheong, A. Wang, How to build a bone? - hydroxyapatite or posner's clusters as bone minerals, Open Ceramics 6 (2021) 100092. https://doi.org/10.1016/j.oceram.2021.100092.

[210] X. Yin, M.J. Stott, Biological calcium phosphates and posner's cluster, The Journal of Chemical Physics 118(8) (2003) 3717-3723. https://doi.org/10.1063/1.1539093.

[211] E.D. Eanes, I.H. Gillessen, A.S. Posner, Intermediate states in the precipitation of hydroxyapatite, Nature 208(5008) (1965) 365-367. https://doi.org/10.1038/208365a0.

[212] E.D. Eanes, A.S. Posner, A note on the crystal growth of hydroxyapatite precipitated from aqueous solutions, Materials Research Bulletin 5(6) (1970) 377-383. https://doi.org/10.1016/0025-5408(70)90075-9.

[213] A.L. Boskey, A.S. Posner, Magnesium stabilization of amorphous calcium phosphate: A kinetic study, Materials Research Bulletin 9(7) (1974) 907-916. https://doi.org/10.1016/0025-5408(74)90169-X.

[214] L. Qin, C.V. Putnis, L. Wang, Facet-specific dissolution–precipitation at struvite–water interfaces, Crystal Growth & Design 21(7) (2021) 4111-4120. https://doi.org/10.1021/acs.cgd.1c00400.

[215] X. Li, Y. Xu, S. Shen, T. Guo, H. Dai, X. Lu, Effects of dissolved organic matter on phosphorus recovery via hydroxyapatite crystallization: New insights based on induction time, Science of The Total Environment 822 (2022) 153618. https://doi.org/10.1016/j.scitotenv.2022.153618.

[216] L. Wang, L. Chen, S.X. Wu, A. Krosuri, Non-airtight fermentation of dairy manure with waste potato peels and subsequent phosphorus recovery via struvite precipitation, Appl Biochem Biotech (2019). https://doi.org/10.1007/s12010-019-03133-8.

[217] L. Wang, L. Chen, S.X. Wu, J. Ye, Non-airtight fermentation of sugar beet pulp with anaerobically digested dairy manure to provide acid-rich hydrolysate for mixotrophic microalgae cultivation, Bioresource Technol 278 (2019) 175-179. https://doi.org/10.1016/j.biortech.2019.01.075.

[218] K. Wang, J. Yin, D.S. Shen, N. Li, Anaerobic digestion of food waste for volatile fatty acids (vfas) production with different types of inoculum: Effect of ph, Bioresource Technol 161 (2014) 395-401. https://doi.org/10.1016/j.biortech.2014.03.088.

[219] Agrimatie, Mestproductie - veehouderij [manure production - livestockfarming], Wageningen University, Wageningen, the Netherlands, 2022.

[220] Systemic, Waterleau new energy, belgium (demonstration plant), Systemic-Project, 2018.

[221] Systemic, Am-power, flanders, belgium (demonstration plant), Systemic-Project, 2018.

[222] I. Regelink, P. Ehlert, G. Smit, S. Everlo, A. Prinsen, O. Schoumans, Phosphorus recovery from co-digested pig slurry - development of the repeat process, Wageningen, the Netherlands, 2019.

[223] Chemanalyst, Hydrochloric acid price trend and forecast, Chemanalyst, 2022.

[224] indexmundi, Rock phosphate monthly price - euro per metric ton, 2022.

[225] IFA, (International-fertilizer-association), Phosphate products, IFA, Paris, France, 2022.

[226] A. Buckwell, E. Nadeau, Nutrient recovery and reuse (nrr) in european agriculture. A review of the issues, opportunities, and actions, The RISE Foundation, Brussels, 2016.

[227] Rijksdienst voor Ondernemend Nederland [Netherlands Enterprise Agency] RVO, Overzicht vervoer dierlijke mest per kwartaal [overview transport of animal manure per quarter], Den Haag, 2022.

[228] N. Keogh, D. Corr, R. O'Shea, R.F.D. Monaghan, The gas grid as a vector for regional decarbonisation - a techno economic case study for biomethane injection and natural gas heavy goods vehicles, Applied Energy 323 (2022) 119590. https://doi.org/10.1016/j.apenergy.2022.119590.

[229] N. Keogh, D. Corr, R.F.D. Monaghan, Biogenic renewable gas injection into natural gas grids: A review of technical and economic modelling studies, Renewable and Sustainable Energy Reviews 168 (2022) 112818. https://doi.org/10.1016/j.rser.2022.112818.

[230] S. Rönsch, J. Schneider, S. Matthischke, M. Schlüter, M. Götz, J. Lefebvre, P. Prabhakaran, S. Bajohr, Review on methanation – from fundamentals to current projects, Fuel 166 (2016) 276-296. https://doi.org/10.1016/j.fuel.2015.10.111.

[231] I. Angelidaki, D. Karakashev, D.J. Batstone, C.M. Plugge, A.J.M. Stams, Chapter sixteen - biomethanation and its potential, in: A.C. Rosenzweig, S.W. Ragsdale (Eds.), Methods in enzymology, Academic Press2011, pp. 327-351. https://doi.org/10.1016/B978-0-12-385112-3.00016-0.

[232] A.C. Trego, S. O'Sullivan, C. Quince, S. Mills, U.Z. Ijaz, G. Collins, Size shapes the active microbiome of methanogenic granules, corroborating a biofilm life cycle, mSystems 5(5) (2020) e00323-20. https://doi.org/doi:10.1128/mSystems.00323-20.

[233] C. Schott, L. Yan, U. Gimbutyte, J.R. Cunha, R.D. van der Weijden, C. Buisman, Enabling efficient phosphorus recovery from cow manure: Liberation of phosphorus through acidification and recovery of phosphorus as calcium phosphate granules, Chemical Engineering Journal 460 (2023) 141695. https://doi.org/10.1016/j.cej.2023.141695.

[234] A.E. Parada, D.M. Needham, J.A. Fuhrman, Every base matters: Assessing small subunit rrna primers for marine microbiomes with mock communities, time series and global field samples, Environmental Microbiology 18(5) (2016) 1403-1414. https://doi.org/10.1111/1462-2920.13023.

[235] C. Quince, A. Lanzen, R.J. Davenport, P.J. Turnbaugh, Removing noise from pyrosequenced amplicons, BMC Bioinformatics 12(1) (2011) 38. https://doi.org/10.1186/1471-2105-12-38.

[236] E. Bolyen et al. Reproducible, interactive, scalable and extensible microbiome data science using qiime 2, Nature Biotechnology 37(8) (2019) 852-857. https://doi.org/10.1038/s41587-019-0209-9.

[237] B.J. Callahan, P.J. McMurdie, M.J. Rosen, A.W. Han, A.J.A. Johnson, S.P. Holmes, Dada2: High-resolution sample inference from illumina amplicon data, Nature Methods 13(7) (2016) 581-583. https://doi.org/10.1038/nmeth.3869.

[238] K. Katoh, D.M. Standley, Mafft multiple sequence alignment software version 7: Improvements in performance and usability, Molecular Biology and Evolution 30(4) (2013) 772-780. https://doi.org/10.1093/molbev/mst010.

[239] M.N. Price, P.S. Dehal, A.P. Arkin, Fasttree 2 – approximately maximum-likelihood trees for large alignments, PLoS ONE 5(3) (2010) e9490. https://doi.org/10.1371/journal.pone.0009490.

[240] C. Quast, E. Pruesse, P. Yilmaz, J. Gerken, T. Schweer, P. Yarza, J. Peplies, F.O. Glöckner, The silva ribosomal rna gene database project: Improved data processing and web-based tools, Nucleic Acids Research 41(D1) (2012) D590-D596. https://doi.org/10.1093/nar/gks1219.

[241] H. Lin, S.D. Peddada, Analysis of compositions of microbiomes with bias correction, Nature Communications 11(1) (2020). https://doi.org/10.1038/s41467-020-17041-7.

[242] L. Treu, P.G. Kougias, B. de Diego-Díaz, S. Campanaro, I. Bassani, J. Fernández-Rodríguez, I. Angelidaki, Two-year microbial adaptation during hydrogen-mediated biogas upgrading process in a serial reactor configuration, Bioresource Technol 264 (2018) 140-147. https://doi.org/10.1016/j.biortech.2018.05.070.

[243] Y. Xie, H. Sun, M. Xue, J. Liu, Metagenomics reveals differences in microbial composition and metabolic functions in the rumen of dairy cows with different residual feed intake, Animal Microbiome 4(1) (2022). https://doi.org/10.1186/s42523-022-00170-3.

[244] C. Greening et al., Diverse hydrogen production and consumption pathways influence methane production in ruminants, The ISME Journal 13(10) (2019) 2617-2632. https://doi.org/10.1038/s41396-019-0464-2.

[245] B. Kakuk, R. Wirth, G. Maróti, M. Szuhaj, G. Rakhely, K. Laczi, K.L. Kovács, Z. Bagi, Early response of methanogenic archaea to h2 as evaluated by metagenomics and metatranscriptomics, Microbial Cell Factories 20(1) (2021). https://doi.org/10.1186/s12934-021-01618-y.

[246] K. Maegaard, E. Garcia-Robledo, M.V.W. Kofoed, L.M. Agneessens, N. De Jonge, J.L. Nielsen, L.D.M. Ottosen, L.P. Nielsen, N.P. Revsbech, Biogas upgrading with hydrogenotrophic methanogenic biofilms, Bioresource Technol 287 (2019) 121422. https://doi.org/10.1016/j.biortech.2019.121422.

[247] D.G. Mulat, F. Mosbæk, A.J. Ward, D. Polag, M. Greule, F. Keppler, J.L. Nielsen, A. Feilberg, Exogenous addition of h2 for an in situ biogas upgrading through biological reduction of carbon dioxide into methane, Waste Management 68 (2017) 146-156. https://doi.org/10.1016/j.wasman.2017.05.054.

[248] Y.-M. Yun, S. Sung, S. Kang, M.-S. Kim, D.-H. Kim, Enrichment of hydrogenotrophic methanogens by means of gas recycle and its application in biogas upgrading, Energy 135 (2017) 294-302. https://doi.org/10.1016/j.energy.2017.06.133.

[249] J.B. van Lier, N. Mahmoud, G. Zeeman, Anaerobic wastewater treatment, in: G. Chen, G.A. Ekama, M.C.M. van Loosdrecht, D. Brdjanovic (Eds.), Biological wastewater treatment: Principles, modeling and design, IWA Publishing2020, p. 0. https://doi.org/10.2166/9781789060362_0701.

[250] G. Lettinga, L.W.H. Pol, I.W. Koster, W.M. Wiegant, W.J.D. Zeeuw, A. Rinzema, P.C. Grin, R.E. Roersma, S.W. Hobma, High-rate anaerobic waste-water treatment using the uasb reactor under a wide range of temperature conditions, Biotechnology and Genetic Engineering Reviews 2(1) (1984) 253-284.

[251] H. Staghouwer, Stand van zaken derogatie van de nitraatrichtlijn [status of the derogation from the nitrate directive], in: N.e.V. Ministerie van Landbouw (Ed.) Den Haag, 2022.

[252] Centraal Bureau voor de Statistiek [Central bureau of Statistics] C B S , Dierlijke mest; productie en mineralenuitscheiding, diercategorie, regio [animal manure; production and mineral excretion, animal category, region], 2022.

[253] Agrimatie, Mestafzetkosten - veehouderij [animal manure treatment costs - livestock farming], Wageningen University, Wageningen, 2022.

[254] Rijksdienst voor Ondernemend Nederland [Netherlands Enterprise Agency] RVO, Price cap for gas, electricity and district heating, Rijksoverheid, Den Haag, 2023.

[255] European-Comission, Regulation (eu) 2019/1009 of the european parliament and of the council of 5 june 2019, laying down rules on the making available on the market of eu fertilising products and amending regulations (ec) no 1069/2009 and (ec) no 1107/2009 and repealing regulation (ec) no 2003/2003, in: European-Comission (Ed.) Official Journal of the European Union, 2019.

[256] G. Macedo, Manure-based spread of antimicrobial resistance in soil and water ecosystems, Utrecht University, Utrecht, 2021.

[257] Agrimatie, Verbruik kalk en kunstmest [use of lime and synthetic fertilizer], Wageningen University, Wageningen, 2022.

[258] G. Iepema, E. Elferink, M. Jelsma, Resultaten onderzoek bokashi [results bokashi research], Van Hall Larenstein - University of applied sciences, Leeuwarden, 2021.

[259] Y. Luo, Influence of organic amendments on soil microbiomes, Wageningen University, Wangeningen, 2022.

[260] V.S. Chavez-Rico, P.L.E. Bodelier, M. van Eekert, V. Sechi, A. Veeken, C. Buisman, Producing organic amendments: Physicochemical changes in biowaste used in anaerobic digestion, composting, and fermentation, Waste Management 149 (2022) 177-185. https://doi.org/10.1016/j.wasman.2022.06.005.


P
P

SI

Supplementary information

Appendix Chapter 2

a. Methods

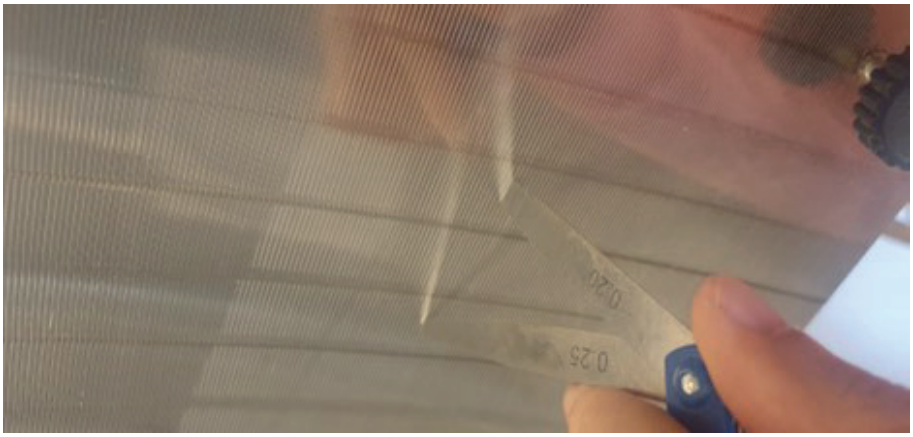

Fig. S2.1. Sieve bend from Estrad with 200 μm grid size. The grid size was tested with a "feel measure" (translated from Dutch) in mm.

b. Anaerobic digestion

i. Retention times, COD and solids

Table S2.1. Average and deviation over time of organic loading rate (OLR), hydraulic retention time (HRT), solid retention time (SRT), TSS and COD_{tot} in- and effluent concentrations, cumulative TSS and COD_{tot} removal and methanization of COD_{tot} over four operation phases of R_R.

R_R without Calcium			Phase 1 (Start-up)		Phase 2 (Summer)		Phase 3 (Winter)		Phase 4 (Spring)	
Parameter		**Unit**	**Aver.**	**Dev.**	**Aver.**	**Dev.**	**Aver.**	**Dev.**	**Aver.**	**Dev.**
OLR		*gCOD/L*d*	1.1	±0.3	1.4	±0.3	1.0	±0.2	0.8	±0.3
HRT		*Days*	46	±6	44	±9	43	±6	55	±18
SRT			n.a.		414		376		463	
In	**TSS**	*g/L*	46	±7	53	±2	37	±8	52	±19
	COD_{tot}		53	±8	63	±3	44	±8	47	±11
Out	**TSS**		9	±4	10	±7	12	±7	15	±11
	COD_{tot}		32	±2	42	±5	33	±6	31	±3
TSS removal			79	±6	80	±8	67	±10	70	±17
COD removal			40	±1	34	±3	25	±2	31	±6
Methanization			4	±1	5	±1	5	±2	9	±5

Table S2.2. Average and deviation over time of organic loading rate (OLR), hydraulic retention time (HRT), solid retention time (SRT), TSS and COD_{tot} in- and effluent concentrations, cumulative TSS and COD_{tot} removal and methanization of COD_{tot} over four operation phases of R_{Ca}.

R_{Ca} with Calcium			Phase 1 (Start-up)		Phase 2 (Summer)		Phase 3 (Winter)		Phase 4 (Spring)	
Parameter		**Unit**	**Aver.**	**Dev.**	**Aver.**	**Dev.**	**Aver.**	**Dev.**	**Aver.**	**Dev.**
OLR		*gCOD/L*d*	1.1	±0.3	1.5	±0.2	1.1	±0.3	1.0	±0.5
HRT		*Days*	45	±5	43	±4	42	±6	47	±9
SRT			n.a.		594		473		583	
In	**TSS**	*g/L*	47	±7	52	±2	37	±8	48	±19
	COD_{tot}		53	±7	63	±2	44	±8	46	±13
Out	**TSS**		6	±3	8	±3	9	±3	10	±3
	COD_{tot}		29	±1	35	±3	30	±5	30	±6
TSS removal		*%*	85	±5	83	±7	74	±7	77	±15
COD removal			47	±2	44	±2	33	±3	32	±4
Methanization			5	±3	5	±1	6	±2	12	±6

ii. Inorganic carbon, ammonium and volatile fatty acids

Table S2.3. Average inorganic carbon (IC), ammonium (NH_4), and volatile fatty acids (VFA, acetate, propionate, and butyrate) concentrations with variations over time in the influent and effluent and cumulative removal of R_R for four operation phases.

R_R without Calcium			Phase 1 (Start-up)		Phase 2 (Summer)		Phase 3 (Winter)		Phase 4 (Spring)	
Parameter		Unit	Aver.	Dev.	Aver.	Dev.	Aver.	Dev.	Aver.	Dev.
In	IC	*g/L*	5.3	±0.8	6.1	±0.6	4.9	±1.1	4.4	±1.1
	NH_4		6.6	±2.2	7.2	±0.9	4.9	±1.1	5.8	±1.0
	VFA		2.4	±2.7	2.2	±2.4	0.7	±0.7	5.4	±3.7
Out	IC	*g/L*	3.7	±0.6	3.5	±0.5	3.5	±0.5	4.4	±2.2
	NH_4		5.2	±0.5	5.6	±0.6	5.3	±1.2	5.4	±1.0
	VFA		3.5	±0.8	5.0	±2.1	3.8	±1.4	5.2	±1.8
IC removal		%	32	±4	43	±4	13	±6	-18	±15
NH_4 removal			29	±5	22	±6	-8	±6	6	±5
VFA removal			-41	±2	-128	±2	-452	±3	-5	±4

Table S2.4. Average inorganic carbon (IC), ammonium (NH_4), and volatile fatty acids (VFA, acetate, propionate, and butyrate) concentrations with variations over time in the influent and effluent and cumulative removal of R_{Ca} for four operation phases.

R_{Ca} with Calcium			Phase 1 (Start-up)		Phase 2 (Summer)		Phase 3 (Winter)		Phase 4 (Spring)	
Parameter		Unit	Aver.	Dev.	Aver.	Dev.	Aver.	Dev.	Aver.	Dev.
In	IC	*g/L*	5.4	±0.8	6.2	±0.5	4.6	±1.4	4.5	±1.1
	NH_4		7.0	±1.0	7.1	±0.8	4.9	±1.0	6.5	±1.5
	VFA		2.3	±2.3	2.2	±2.4	0.6	±0.6	6.9	±6.1
Out	IC	*g/L*	2.8	±0.4	2.5	±0.5	2.6	±0.4	2.8	±0.3
	NH_4		5.2	±0.2	5.8	±0.6	4.9	±1.0	4.7	±0.8
	VFA		3.5	±0.8	4.4	±1.7	3.4	±0.9	2.6	±0.6
IC removal		%	49	±4	60	±7	41	±5	39	±15
NH_4 removal			25	±4	17	±4	2	±5	29	±29
VFA removal			-48	±5	-105	±3	-454	±3	59	±3

iii. pH in influent, effluent and sludge bed

Table S2.5. Average and deviation over time of pH in the influent, effluent, and at three vertically distributed locations inside R_R over four operation phases.

R_R without calcium			Phase 1 (Start-up)		Phase 2 (Summer)		Phase 3 (Winter)		Phase 4 (Spring)	
Parameter		Unit	Aver.	Dev.	Aver.	Dev.	Aver.	Dev.	Aver.	Dev.
Effluent			8.75	±0.16	8.93	±0.15	8.89	±0.07	8.88	±0.29
Reactor	Top	*pH*	n.a.		7.70	±0.04	7.66	±0.23	7.57	±0.22
	Middle		n.a.		7.64	±0.03	7.83	±0.06	7.96	±0.01
	Bottom		n.a.		7.91	±0.06	8.10	±0.05	8.19	±0.01
Influent			8.27	±0.21	8.20	±0.06	8.35	±0.19	8.12	±0.25

Table S2.6. Average and deviation over time of pH in the influent, effluent, and at three vertically distributed locations inside R_{Ca} over four operation phases.

R_{Ca} with calcium			Phase 1 (Start-up)		Phase 2 (Summer)		Phase 3 (Winter)		Phase 4 (Spring)	
Position		Unit	Aver.	Dev.	Aver.	Dev.	Aver.	Dev.	Aver.	Dev.
Effluent			8.75	±0.16	8.82	±0.13	8.99	±0.27	8.88	±0.20
Reactor	Top	*pH*	n.a.		7.48	±0.03	7.74	±0.19	8.01	±0.07
	Middle		n.a.		7.46	±0.04	7.60	±0.09	7.44	±0.01
	Bottom		n.a.		7.45	±0.23	6.17	±0.52	5.84	±0.02
Influent			8.26	±0.21	8.22	±0.06	8.37	±0.16	7.89	±0.22

c. Elemental flows

i. Phosphorus (EF)

Table S2.7. Average phosphorus concentrations with variations over time in the influent and effluent and removal of cumulative phosphorus entering and leaving the reactor R_R for four operation phases.

R_R without calcium			Phase 1 (Start-up)		Phase 2 (Summer)		Phase 3 (Winter)		Phase 4 (Spring)	
Parameter		Unit	Aver.	Dev.	Aver.	Dev.	Aver.	Dev.	Aver.	Dev.
In	P_{tot}	*mg/L*	2191	±313	2447	±151	1680	±368	1752	±490
	P_{sus}[1]		1781	±537	1938	±291	1354	±799	1416	±792
	P_{sol}		410	±65	509	±45	326	±121	336	±94
	PO_4^{3-}-P		422	±38	569	±61	333	±137	301	±68
Out	P_{tot}	*mg/L*	674	±48	882	±290	812	±346	874	±384
	P_{sus}[1]		264	±61	320	±127	341	±206	459	±292
	P_{sol}		410	±65	562	±39	471	±84	415	±82
	PO_4^{3-}-P		382	±60	471	±28	403	±84	318	±85
P_{total} removal		*%*	68	±1	64	±3	53	±2	58	±4
PO_4^{3-} removal			9	±3	17	±3	-21	±3	-6	±3

[1]Calculated values

Table S2.8. Average phosphorus concentrations with variations over time in the influent and effluent and removal of cumulative phosphorus entering and leaving the reactor R_{Ca} for four operation phases.

R_{Ca} with Calcium			Phase 1 (Start-up)		Phase 2 (Summer)		Phase 3 (Winter)		Phase 4 (Spring)	
Parameter		Unit	Aver.	Dev.	Aver.	Dev.	Aver.	Dev.	Aver.	Dev.
In	P_{tot}	*mg/L*	2125	±281	2415	±177	1710	±353	2131	±530
	P_{sus}[1]		1718	±366	1898	±290	1388	±709	1718	±1222
	P_{sol}		407	±33	517	±41	322	±98	413	±191
	PO_4^{3-}-P		416	±48	572	±44	327	±115	289	±51
Out	P_{tot}	*mg/L*	440	±78	437	±101	459	±95	426	±70
	P_{sus}[1]		221	±202	211	±75	228	±86	232	±106
	P_{sol}		219	±161	226	±28	231	±39	194	±57
	PO_4^{3-}-P		179	±160	128	±30	154	±29	121	±37
P_{total} removal		*%*	77	±2	80	±1	70	±2	71	±3
PO_4^{3-} removal			57	±3	78	±3	53	±2	58	±3

[1]Calculated values

ii. Calcium (EF)

Table S2.9. Average calcium concentrations with variations over time in the influent and effluent and removal of cumulative calcium entering and leaving the reactor R_R for four operation phases.

R_R without calcium			Phase 1 (Start-up)		Phase 2 (Summer)		Phase 3 (Winter)		Phase 4 (Spring)	
Parameter		Unit	Aver.	Dev.	Aver.	Dev.	Aver.	Dev.	Aver.	Dev.
In	Ca_{tot}	*mg/L*	2426	±325	2822	±171	2042	±408	2351	±608
	Ca_{sus} [1]		2298	±703	2736	±929	1910	±888	2205	±1582
	Ca_{sol}		128	±22	86	±24	132	±35	146	±67
	Ca^{2+}		<100	±	<100	±	<100	±	<100	±
Out	Ca_{tot}	*mg/L*	584	±80	824	±364	844	±410	885	±452
	Ca_{sus} [1]		425	±209	458	±210	512	±339	542	±365
	Ca_{sol}		159	±116	366	±102	332	±96	343	±143
	Ca^{2+}		155	±45	265	±58	229	±99	214	±36
Ca_{total} removal		%	76	±1	71	±3	59	±2	63	±4

[1]Calculated values

Table S2.10. Average calcium concentrations with variations over time in the influent, effluent and the calcium addition per liter of manure added and removal of cumulative phosphorus entering and leaving the reactor R_{Ca} for four operation phases.

R_{Ca} with Calcium			Phase 1 (Start-up)		Phase 2 (Summer)		Phase 3 (Winter)		Phase 4 (Spring)	
Parameter		Unit	Aver.	Dev.	Aver.	Dev.	Aver.	Dev.	Aver.	Dev.
In	Ca_{total}	*mg/L*	2509	±420	2868	±170	2005	±429	2366	±847
	Ca_{added}		3338	±1478	3970	±774	3856	±1370	1551	±1061
	Ca_{sus} [1]		2377	±902	2778	±813	1877	±944	2104	±1115
	Ca_{sol}		132	±28	90	±21	128	±37	189	±50
	Ca^{2+}		<100		<100		<100		<100	
Out	Ca_{total}	*mg/L*	657	±160	692	±106	642	±119	596	±62
	Ca_{sus} [1]		467	±485	293	±65	291	±96	305	±146
	Ca_{sol}		190	±151	399	±28	351	±51	291	±109
	Ca^{2+}		188	±60	238	±32	226	±64	133	±23
Ca_{total} removal		%	88	±2	89	±1	88	±2	83	±3

[1]Calculated values

iii. Magnesium (EF)

Table S2.11. Average magnesium concentrations with variations over time in the influent and effluent and removal of cumulative phosphorus entering and leaving the reactor R_R for four operation phases.

R_R without calcium			Phase 1 (Start-up)		Phase 2 (Summer)		Phase 3 (Winter)		Phase 4 (Spring)	
Parameter		Unit	Aver.	Dev.	Aver.	Dev.	Aver.	Dev.	Aver.	Dev.
In	Mg_{tot}	*mg/L*	1233	±181	1412	±119	947	±229	1204	±346
	Mg_{sus} [1]		1219		1405		933		1188	
	Mg_{sol}		14	±24	7	±4	14	±7	16	±12
	Mg^{2+}		<100	±	<100	±	<100	±	<100	±
Out	Mg_{tot}	*mg/L*	174	±33	290	±202	289	±223	358	±273
	Mg_{sus} [1]		142		193		210		276	
	Mg_{sol}		32	±27	97	±29	79	±28	82	±54
	Mg^{2+}		<100	±	<100	±	<100	±	<100	±
Mg_{total} removal		%	86	±4	80	±3	70	±2	69	±4

[1]Calculated values

Table S2.12. Average magnesium concentrations with variations over time in the influent and effluent and removal of cumulative phosphorus entering and leaving the reactor R_R for four operation phases.

R_{Ca} with Calcium			Phase 1 (Start-up)		Phase 2 (Summer)		Phase 3 (Winter)		Phase 4 (Spring)	
Parameter		Unit	Aver.	Dev.	Aver.	Dev.	Aver.	Dev.	Aver.	Dev.
In	Mg_{tot}	*mg/L*	1282	±208	1437	±101	930	±242	995	±410
	Mg_{sus} [1]		1274		1430		917		972	
	Mg_{sol}		8	±5	7	±3	13	±6	23	±15
	Mg^{2+}		<100	±	<100	±	<100	±	<100	±
Out	Mg_{tot}	*mg/L*	121	±34	200	±52	189	±44	186	±47
	Mg_{sus} [1]		80		104		109		107	
	Mg_{sol}		41	±23	96	±11	80	±17	79	±37
	Mg^{2+}		<100	±	<100	±	<100	±	<100	±
Mg_{total} removal		%	90	±2	85	±1	78	±3	77	±3

[1]Calculated values

d. Particle size distribution

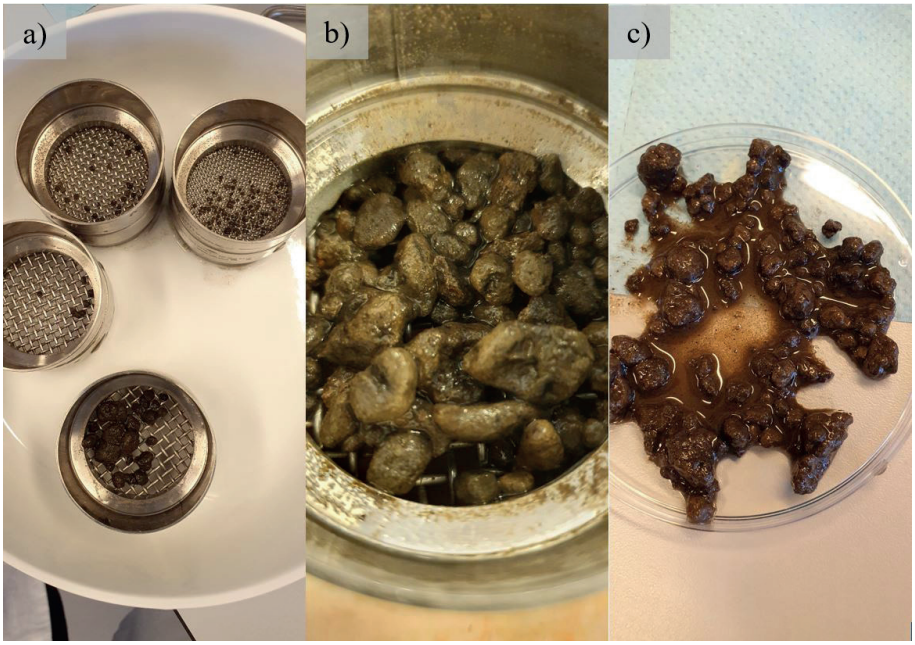

Fig. S2.2. Particle size distribution experiment with analytical sieves (a) of particles from the bottom of R_{Ca}. The >2.5 mm fraction shown in the sieve (b) and on a Petri dish (c).

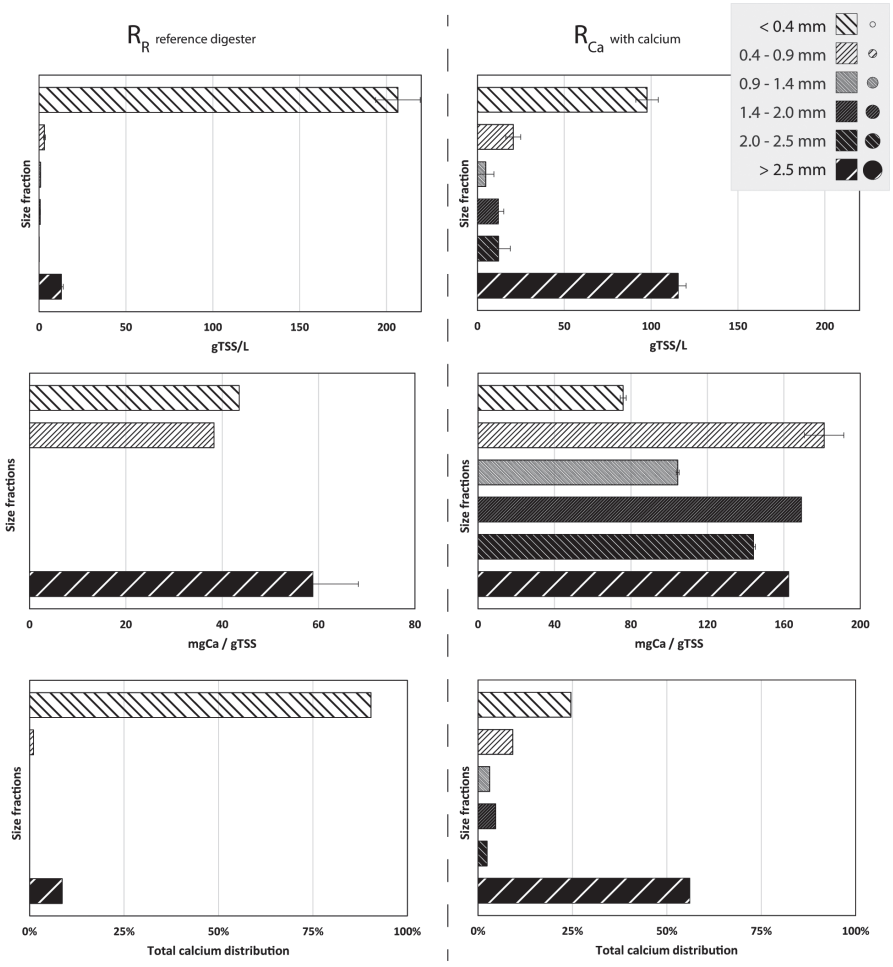

Fig. S2.3. Particle size distribution based on gTSS L^{-1} with the calcium concentration for each size fraction and the total calcium distribution based on the combination of abundancy of particle size fraction and its calcium concentration for R_R and R_{Ca}.

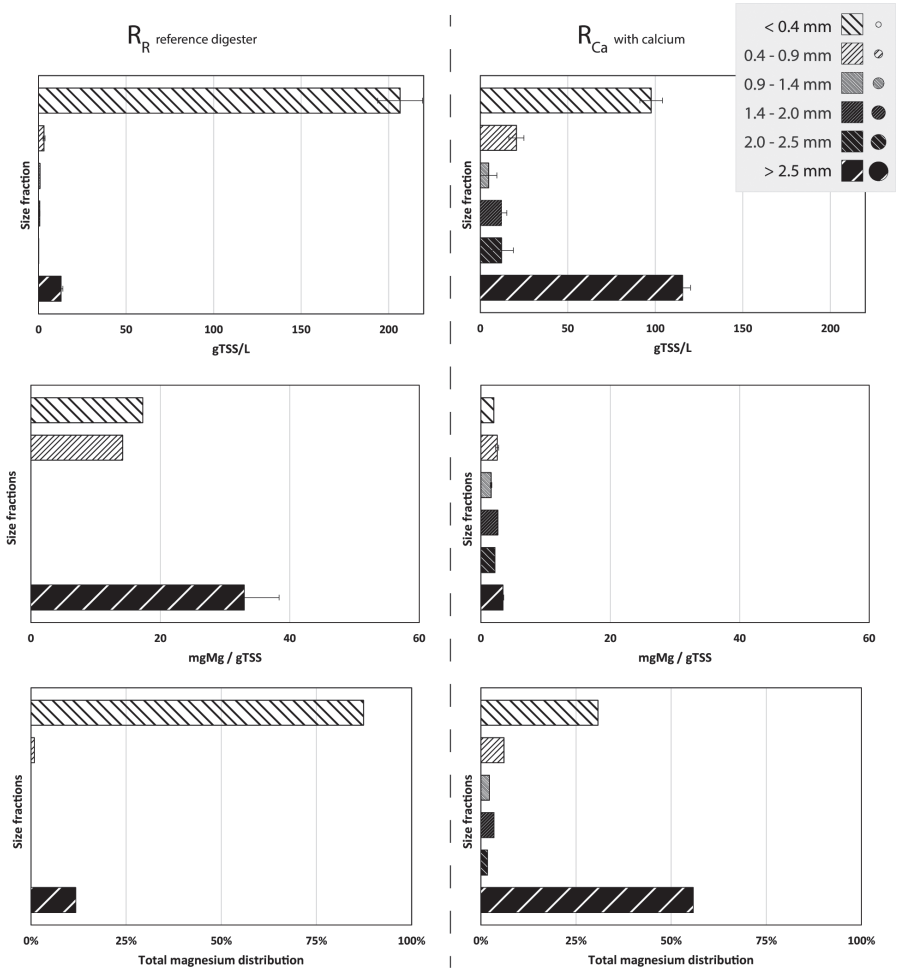

Fig. S2.4. Particle size distribution based on gTSS L^{-1} with the magnesium concentration for each size fraction and the total magnesium distribution based on the combination of abundancy of particle size fraction and its magnesium concentration for R_R and R_{Ca}.

e. SEM-EDX

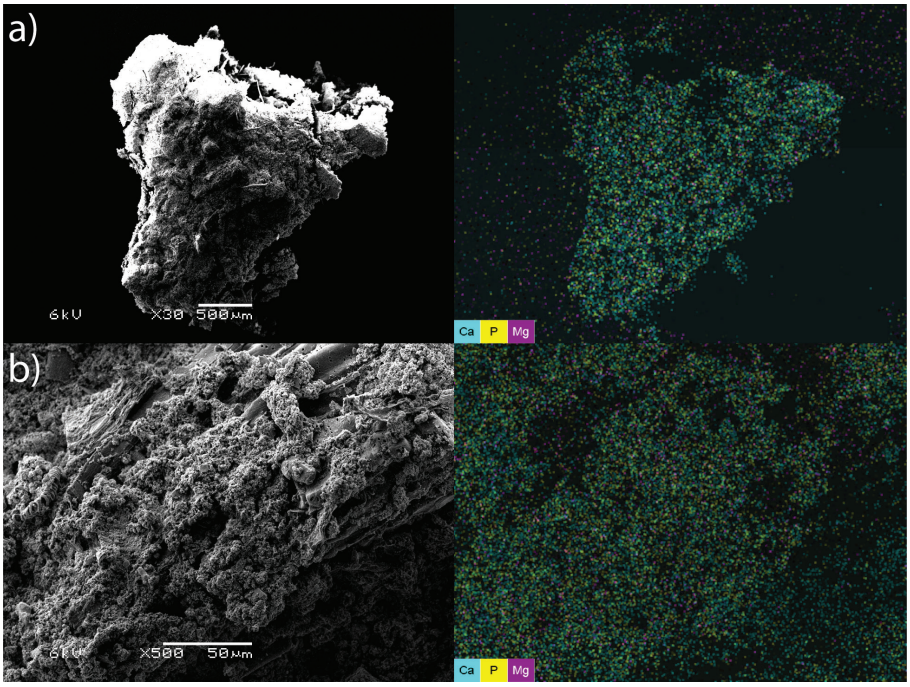

Fig. S2.5. SEM images of particles smaller than 0.4 mm in with EDX showing calcium as cyan, phosphorus as yellow and magnesium as purple in 30x magnification (a) and 500x magnification (b). The particles aggregated during the drying process but were individual particles in solution passing the sieve.

f. XRD

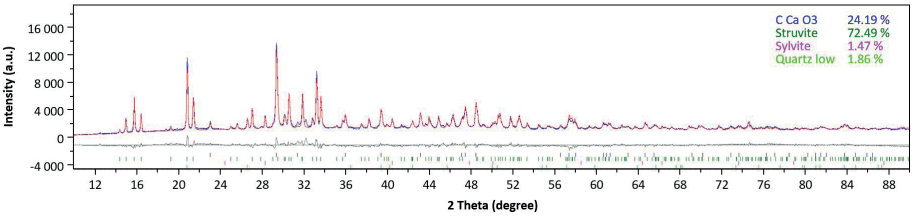

Fig. S2.6. XRD spectra of particles smaller than 0.4 mm from the bottom of R_R.

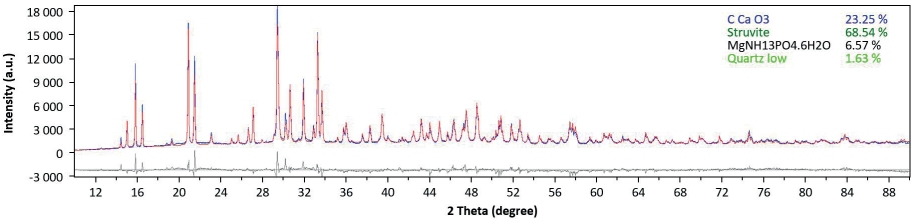

Fig. S2.7. XRD spectra of particles larger than 2.5 mm from the bottom of R_R.

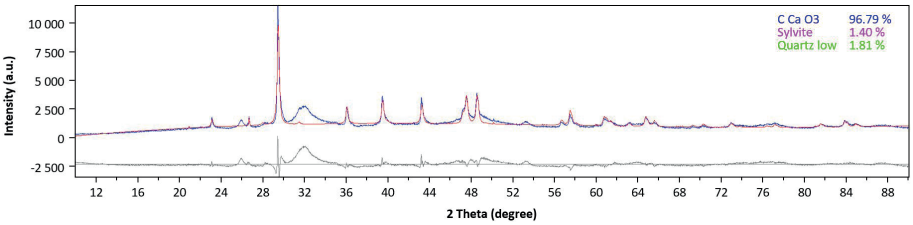

Fig. S2.8. XRD spectra of particles larger than 2.5 mm from the bottom of RCa. The unidentified peak theta angle 32 represents amorphous calcium phosphate.

g. TGA

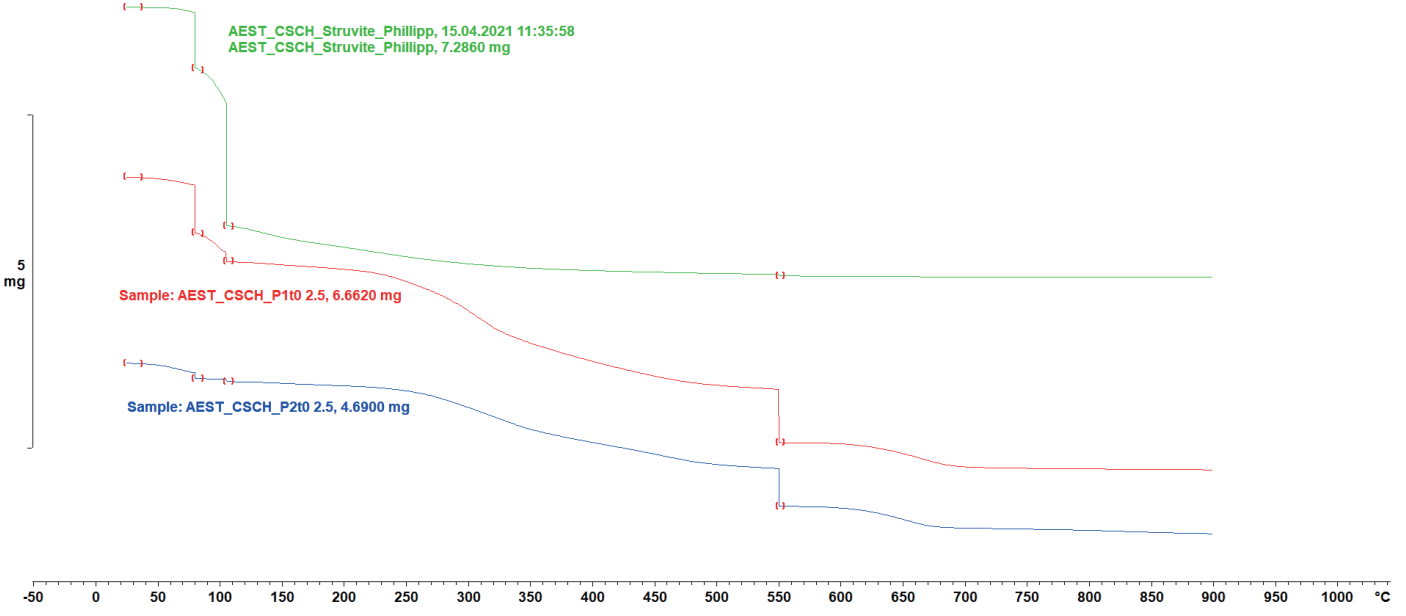

Fig. S2.9. Thermogravimetric analysis with struvite reference (green) and particles larger than 2.5 mm from R_R (red) and R_{Ca} (blue).

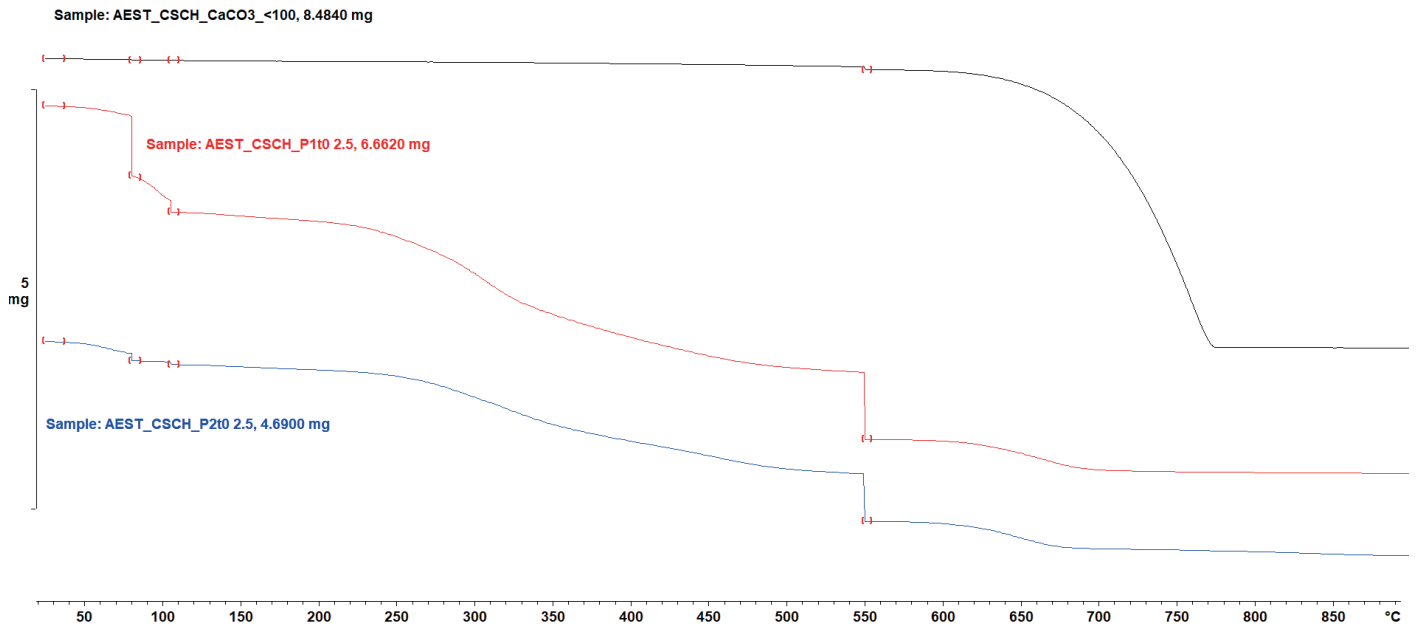

Fig. S2.10. Thermogravimetric analysis with calcium carbonate reference (black) and particles larger than 2.5 mm from R_R (red) and R_{Ca} (blue).

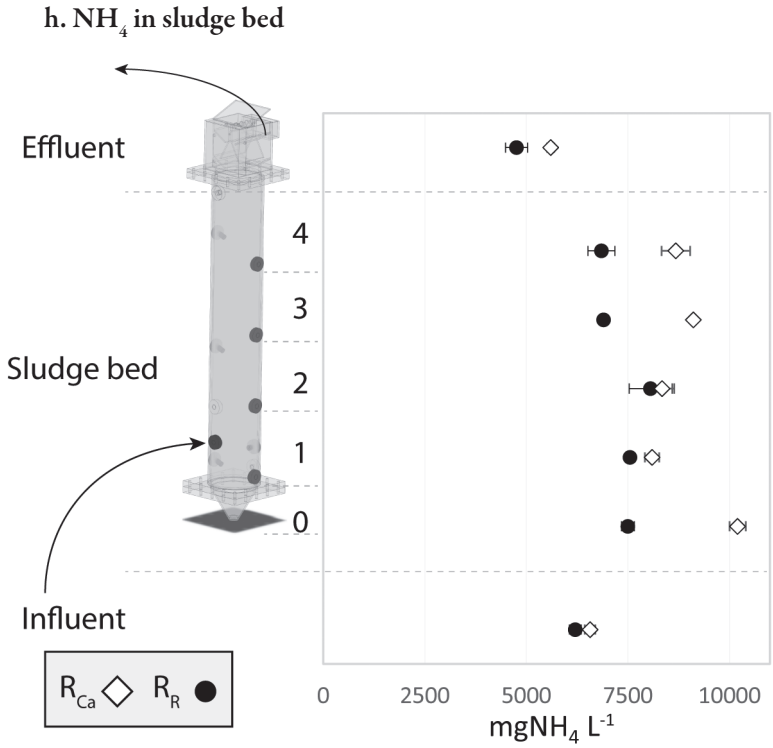

Fig. S2.11. NH4 concentration in the sludge beds of R_{Ca} and R_R at operation day 167.

i. Economic analyses

Table S.13

€20 per m^3_{manure} current costs for farmers
85% reduction with presented technology gives €3 per m^3_{manure}
Additional calcium needed for one m^3 costs about €3
Total costs are €6 instead of €20 per m^3, resulting in savings of €14.
3100 m^3_{manure} $year^{-1}$ of an averaged size farm gives €43K savings

B. Appendix Chapter 3

a. Treatment performance

Table S3.1. Average and deviation over time of organic loading rate (OLR), hydraulic retention time (HRT), solid retention time (SRT), TSS and COD_{tot} in- and effluent concentrations, cumulative TSS and COD_{tot} removal and methanization of COD_{tot} over four operation phases of R_R.

R_R without Calcium			Phase 1 (Start-up)		Phase 2 (Summer)		Phase 3 (Winter)		Phase 4 (Spring)	
Parameter		Unit	Aver.	Dev.	Aver.	Dev.	Aver.	Dev.	Aver.	Dev.
OLR		*gCOD/L*d*	1.3	±0.4	1.2	±0.5	0.9	±0.3	0.8	±0.4
HRT		*Days*	55	±12	57	±13	61	±9	65	±17
SRT			n.a.		123		197		224	
In	TSS	*g/L*	40	±3	39	±1	32	±5	38	±6
	COD_{tot}		70	±4	70	±2	54	±10	54	±9
Out	TSS		23	±6	22	±2	12	±7	15	±8
	COD_{tot}		47	±5	45	±3	31	±7	32	±7
TSS removal			46	±2	43	±2	63	±6	67	±5
COD_{tot} removal		*%*	33	±1	36	±2	44	±2	45	±2
Methanization			27		33		9		20	

Table S3.2. Average and deviation over time of organic loading rate (OLR), hydraulic retention time (HRT), solid retention time (SRT), TSS and COD_{tot} in- and effluent concentrations, cumulative TSS and COD_{tot} removal and methanization of COD_{tot} over four operation phases of R_{Ca}.

R_{Ca} with Calcium			Phase 1 (Start-up)		Phase 2 (Summer)		Phase 3 (Winter)		Phase 4 (Spring)	
Parameter		Unit	Aver.	Dev.	Aver.	Dev.	Aver.	Dev.	Aver.	Dev.
OLR		*gCOD/L*d*	1.2	±0.5	1.1	±0.2	0.7	±0.2	0.6	±0.2
HRT		*Days*	49	±11	57	±7	57	±3	60	±10
SRT			n.a.		252		406		450	
In	TSS	*g/L*	39	±3	38	±1	32	±4	41	±5
	COD_{tot}		69	±6	68	±2	54	±9	57	±7
Out	TSS		14	±7	10	±2	7	±3	11	±7
	COD_{tot}		36	±7	30	±3	23	±4	23	±3
TSS removal			57	±4	73	±4	78	±8	77	±7
COD_{tot} removal		*%*	41	±1	51	±2	54	±2	54	±3
Methanization			40		51		49		46	

Table S3.3. Average inorganic carbon (IC), ammonium (NH_4), and volatile fatty acids (VFA, acetate, propionate, and butyrate) concentrations with variations over time in the influent and effluent and cumulative removal of R_R for four operation phases.

R_R without Calcium			Phase 1 (Start-up)		Phase 2 (Summer)		Phase 3 (Winter)		Phase 4 (Spring)	
Parameter		Unit	Aver.	Dev.	Aver.	Dev.	Aver.	Dev.	Aver.	Dev.
In	IC	*g/L*	1.9	±0.2	2.0	±0.6	2.4	±0.7	2.1	±0.8
	NH_4		3.1	±0.2	3.2	±0.2	2.2	±0.7	3.1	±0.4
	VFA		13.1	±1.6	14.2	±0.8	7.8	±3.1	11.6	±3.4
Out	IC	*g/L*	2.3	±0.3	2.6	±0.3	2.4	±0.3	2.3	±0.3
	NH_4		2.4	±0.3	2.5	±0.2	2.1	±0.5	2.0	±0.3
	VFA		3.5	±1.9	1.9	±0.6	1.2	±0.7	0.3	±0.2
IC removal		%	-24	±4	-32	±5	-7	±6	-13	±5
NH_4 removal			23	±4	21	±5	6	±6	38	±3
VFA removal			71	±2	86	±2	81	±6	96	±3

Table S3.4. Average inorganic carbon (IC), ammonium (NH_4), and volatile fatty acids (VFA, acetate, propionate, and butyrate) concentrations with variations over time in the influent and effluent and cumulative removal of R_{Ca} for four operation phases.

R_{Ca} with Calcium			Phase 1 (Start-up)		Phase 2 (Summer)		Phase 3 (Winter)		Phase 4 (Spring)	
Parameter		Unit	Aver.	Dev.	Aver.	Dev.	Aver.	Dev.	Aver.	Dev.
In	IC	*g/L*	1.9	±0.5	2.1	±0.9	2.2	±0.6	1.7	±0.2
	NH_4		3.0	±0.3	3.3	±0.3	2.2	±0.6	3.0	±0.4
	VFA		12.2	±1.2	13.3	±2.4	7.9	±3.0	10.8	±3.5
Out	IC	*g/L*	2.5	±0.2	2.5	±0.2	2.1	±0.4	1.5	±0.1
	NH_4		2.1	±0.4	2.3	±0.1	1.9	±0.2	1.9	±0.3
	VFA		1.6	±1.7	0.2	±0.1	0.1	±0.1	0.1	±0.1
IC removal		%	-42	±6	-31	±6	-4	±8	3	±7
NH_4 removal			24	±4	25	±3	6	±5	28	±7
VFA removal			84	±2	98	±2	99	±3	99	±2

Table S3.5. Average and deviation over time of pH in the influent, effluent, and at three vertically distributed locations inside R_R over four operation phases.

R_R without calcium			Phase 1 (Start-up)		Phase 2 (Summer)		Phase 3 (Winter)		Phase 4 (Spring)	
Parameter		Unit	Mean	Dev.	Mean	Dev.	Mean	Dev.	Mean	Dev.
Effluent			8.4	±0.9	8.8	±0.0	8.9	±0.1	8.9	±0.3
Reactor	Top	*pH*	7.7	±0.1	7.9	±0.0	8.0	±0.0	8.1	±0.1
	Middle		7.8	±0.1	8.0	±0.0	8.0	±0.0	8.1	±0.1
	Bottom		7.7	±0.1	7.8	±0.0	7.9	±0.0	7.9	±0.1
Influent			7.7	±0.1	7.8	±0.1	8.1	±0.3	7.9	±0.4

Table S3.6. Average and deviation over time of pH in the influent, effluent, and at three vertically distributed locations inside R_{Ca} over four operation phases.

R_{Ca} with calcium			Phase 1 (Start-up)		Phase 2 (Summer)		Phase 3 (Winter)		Phase 4 (Spring)	
Position		Unit	Aver.	Dev.	Aver.	Dev.	Aver.	Dev.	Aver.	Dev.
Effluent			8.9	±0.1	9.0	±0.1	8.9	±0.1	9.0	±0.2
Reactor	Top	*pH*	7.7	±0.1	7.8	±0.0	7.9	±0.0	8.0	±0.1
	Middle		7.7	±0.0	7.8	±0.0	7.8	±0.0	7.8	±0.0
	Bottom		7.8	±0.1	7.9	±0.0	8.0	±0.0	8.1	±0.1
Influent			7.8	±0.1	7.8	±0.1	8.2	±0.3	7.6	±0.1

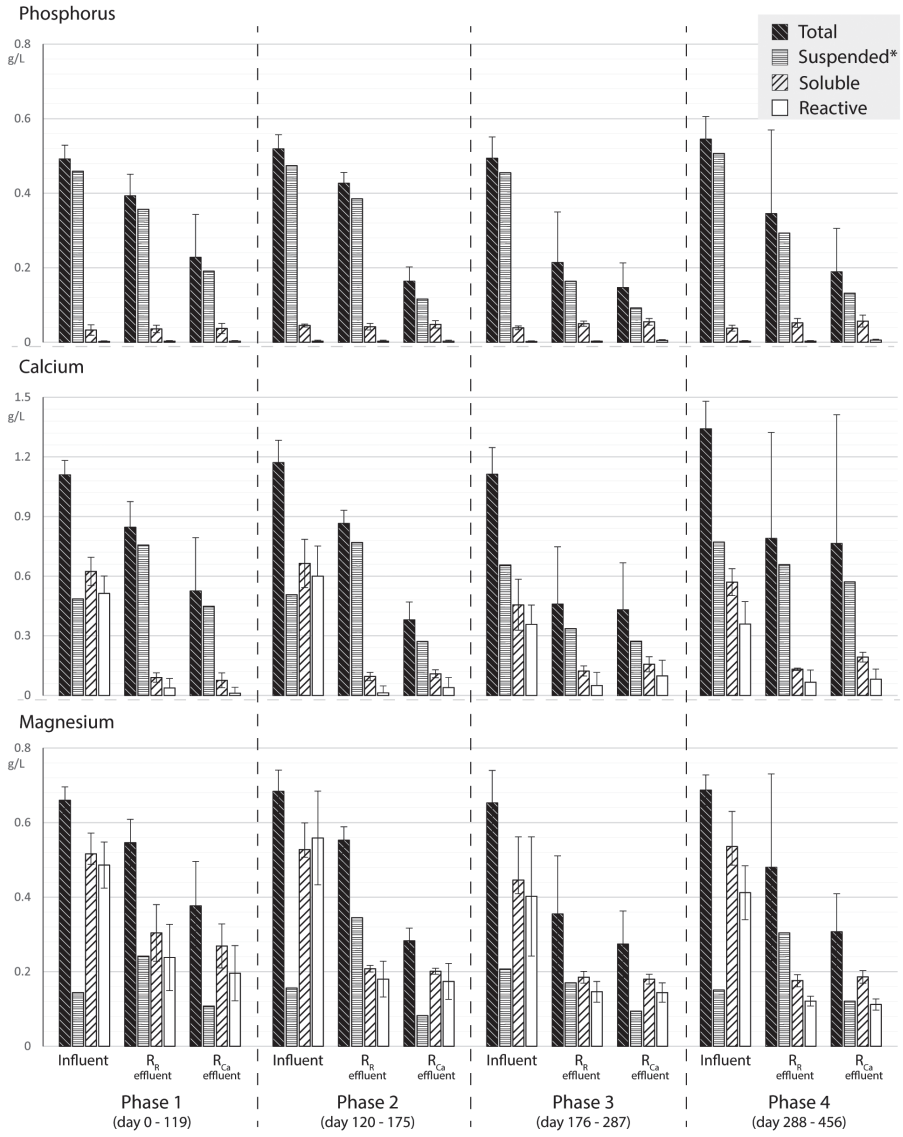

Fig. S3.1. Average influent, effluent of RR and effluent of RCa concentrations of phosphorus, calcium, and magnesium over four operational phases where error bars represent the fluctuation in a phase. The elements are represented in total (P_{tot}, Ca_{tot}, Mg_{tot}), suspended (P_{sus}, Ca_{sus}, Mg_{sus}), soluble (P_{sol}, Ca_{sol}, Mg_{sol}) and reactive (PO_4^{3-}-P, Ca^{2+}, Mg^{2+}). *The suspended fractions are calculated as the difference of total and soluble, but their variation is not shown because of the partly excessive size of the error bar due to the variation in the soluble fractions.

b. Sludge bed

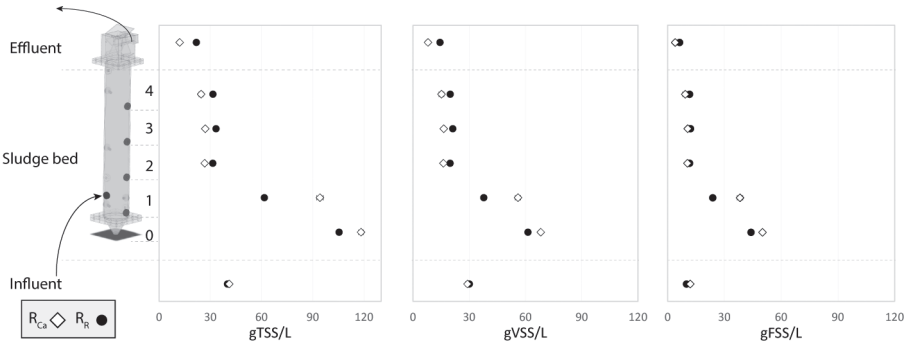

Fig. S3.2. The vertical distribution of TSS (Total suspended solids), VSS (Volatile suspended solids) and FSS (Fixed suspended solids, Ash) in the sludge bed of the UASB reactors R_R as reference and R_{Ca} with calcium addition together with the influent (bottom) and effluent (top) TSS and VSS concentrations at operation day 165 (Phase 2).

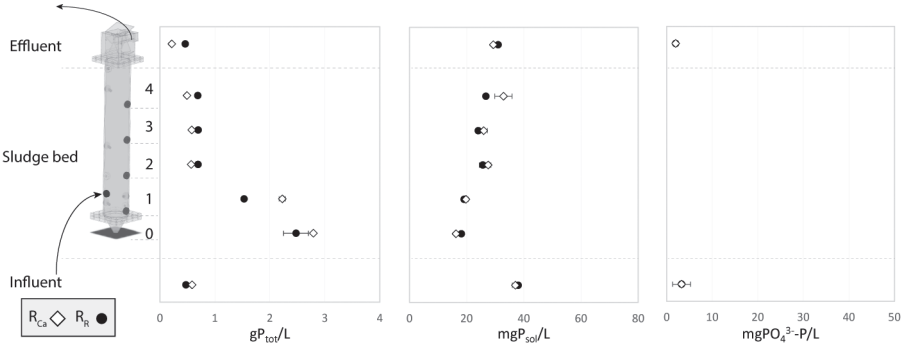

Fig. S3.3. The vertical distribution of total phosphorus (P_{tot}), soluble phosphorus (P_{sol}) and phosphorus as phosphate (PO_4^{3-}-P) in the sludge bed of the UASB reactors R_R as a reference and R_{Ca} with calcium addition together with the influent (bottom) and effluent (top) concentration at operation day 165 (Phase 2).

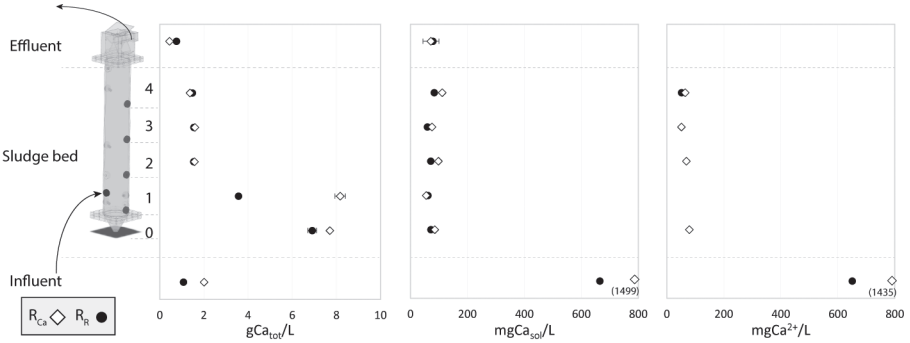

Fig. S3.4. The vertical distribution of total calcium (Ca_{tot}), soluble calcium (Ca_{sol}) and calcium ions (Ca^{2+}) in the sludge bed of the UASB reactors R_R as a reference and R_{Ca} with calcium addition together with the influent (bottom) and effluent (top) concentration at operation day 165 (Phase 2).

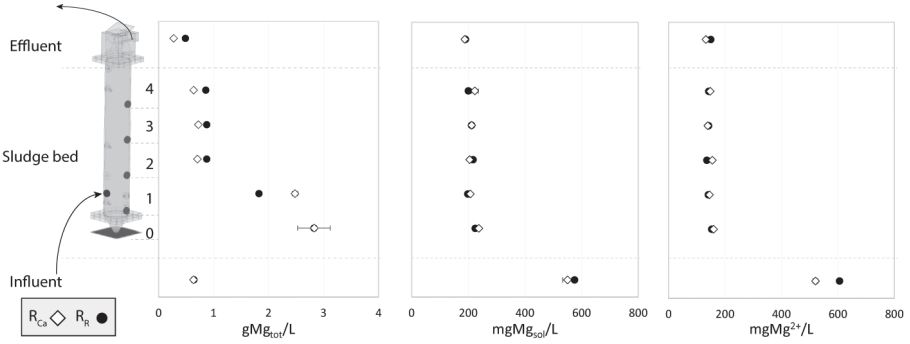

Fig. S3.5. The vertical distribution of total magnesium (Mg_{tot}), soluble magnesium (Mg_{sol}) and magnesium ion (Mg^{2+}) in the sludge bed of the UASB reactors R_R as a reference and R_{Ca} with calcium addition together with the influent (bottom) and effluent (top) concentration at operation day 165 (Phase 2).

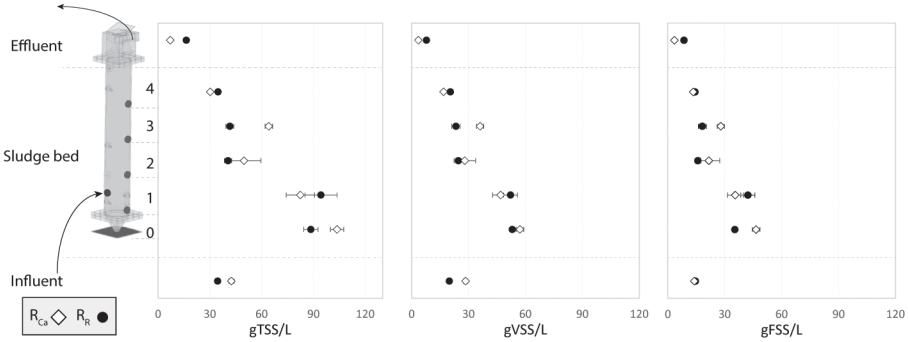

Fig. S3.6. The vertical distribution of TSS (Total suspended solids), VSS (Volatile suspended solids) and FSS (Fixed suspended solids, Ash) in the sludge bed of the UASB reactors R_R as reference and R_{Ca} with calcium addition together with the influent (bottom) and effluent (top) TSS and VSS concentrations at operation day 340 (Phase 4).

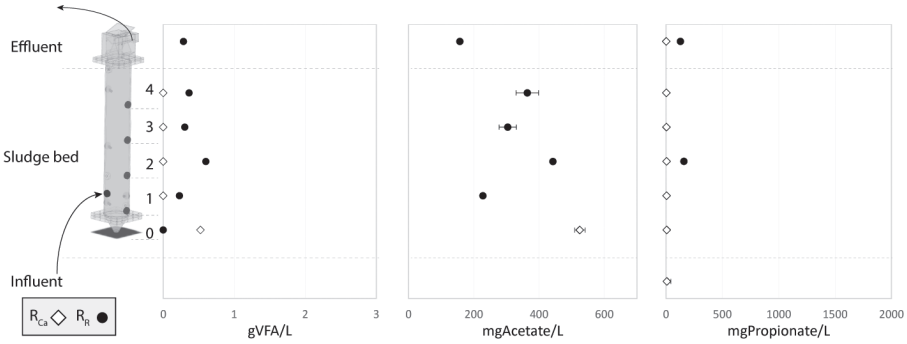

Fig. S3.7. The vertical distribution of VFA (Acetate, Propionate and Butyrate), Acetate and Propionate in the sludge bed of the UASB reactors R_R as reference and R_{Ca} with calcium addition together with the influent (bottom) and effluent (top) concentrations at operation day 340 (Phase 4).

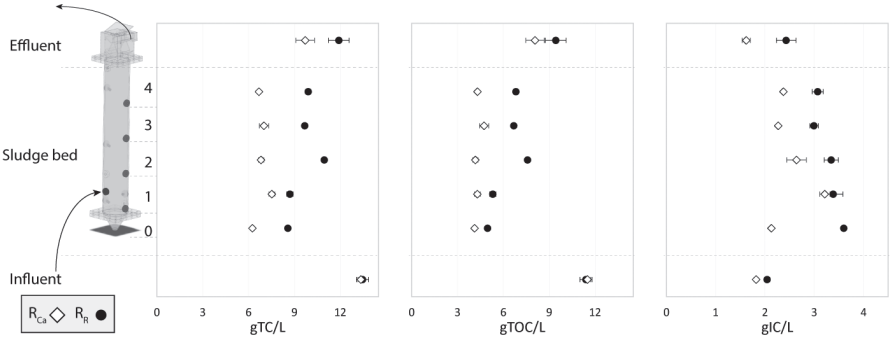

Fig. S3.8. The vertical distribution of total carbon (TC), total organic carbon (TOC) and inorganic carbon (IC) in the sludge bed of the UASB reactors R_R as a reference and R_{Ca} with calcium addition together with the influent (bottom) and effluent (top) concentration at operation day 340 (Phase 4).

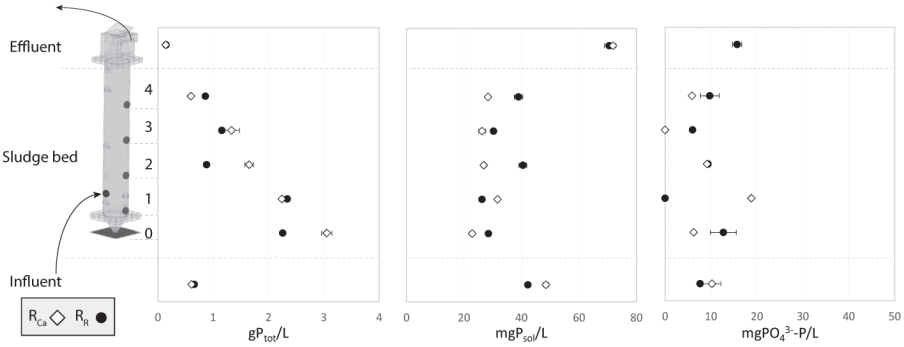

Fig. S3.9. The vertical distribution of total phosphorus (P_{tot}), soluble phosphorus (P_{sol}) and phosphorus as phosphate (PO_4^{3-}-P) in the sludge bed of the UASB reactors R_R as a reference and R_{Ca} with calcium addition together with the influent (bottom) and effluent (top) concentration at operation day 340 (Phase 4).

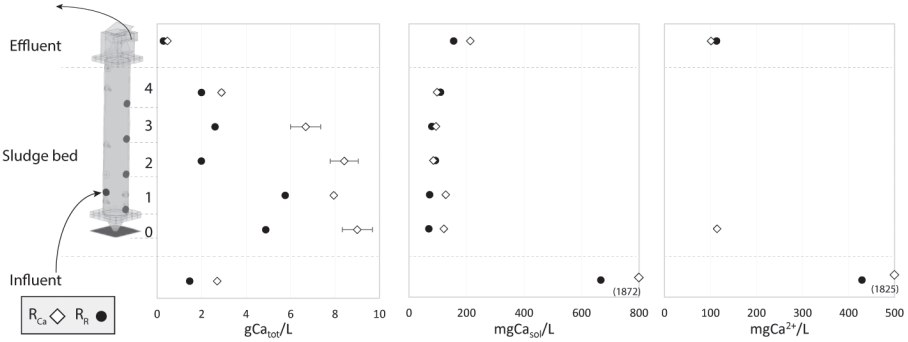

Fig. S3.10. The vertical distribution of total calcium (Ca_{tot}), soluble calcium (Ca_{sol}) and calcium ions (Ca^{2+}) in the sludge bed of the UASB reactors R_R as a reference and R_{Ca} with calcium addition together with the influent (bottom) and effluent (top) concentration at operation day 340 (Phase 4).

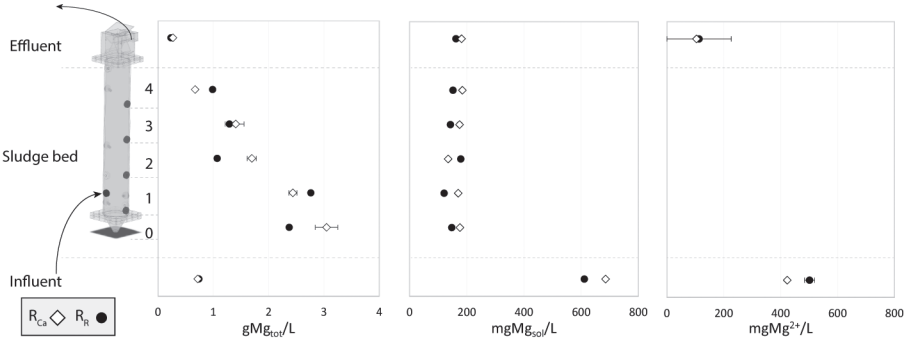

Fig. S3.11. The vertical distribution of total magnesium (Mg_{tot}), soluble magnesium (Mg_{sol}) and magnesium ion (Mg^{2+}) in the sludge bed of the UASB reactors R_R as a reference and R_{Ca} with calcium addition together with the influent (bottom) and effluent (top) concentration at operation day 340 (Phase 4).

SI

c. XRD

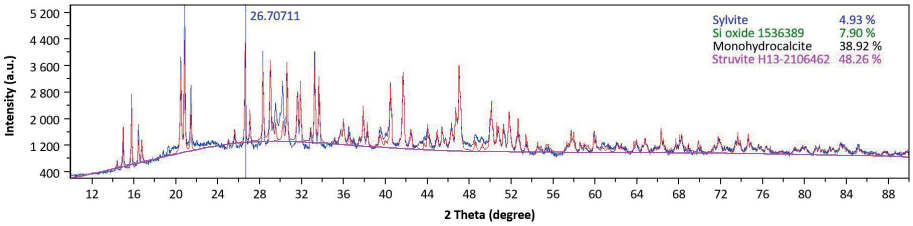

Fig. S3.12. Particles smaller than 0.4 mm from the bottom of R_R. Dominating crystalline phases are CaCO3, its precursors and struvite.

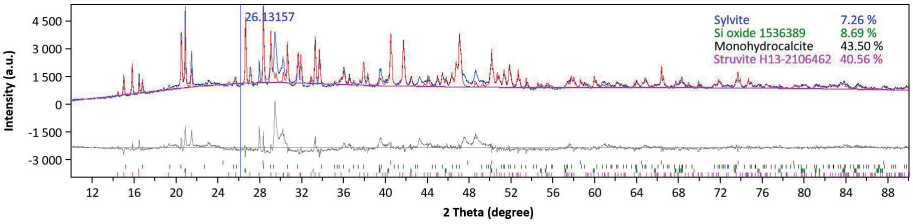

Fig. S3.13. Particles smaller than 0.4 mm from the bottom of R_{Ca}. Dominating crystalline phases are CaCO3 and struvite. The broadened unidentified peak at theta 30.5 might be an indication of ACP.

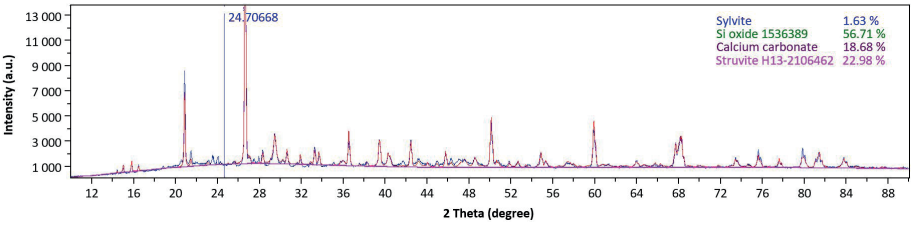

Fig. S3.14. XRD spectra of solid part from separated untreated dairy manure (Influent).

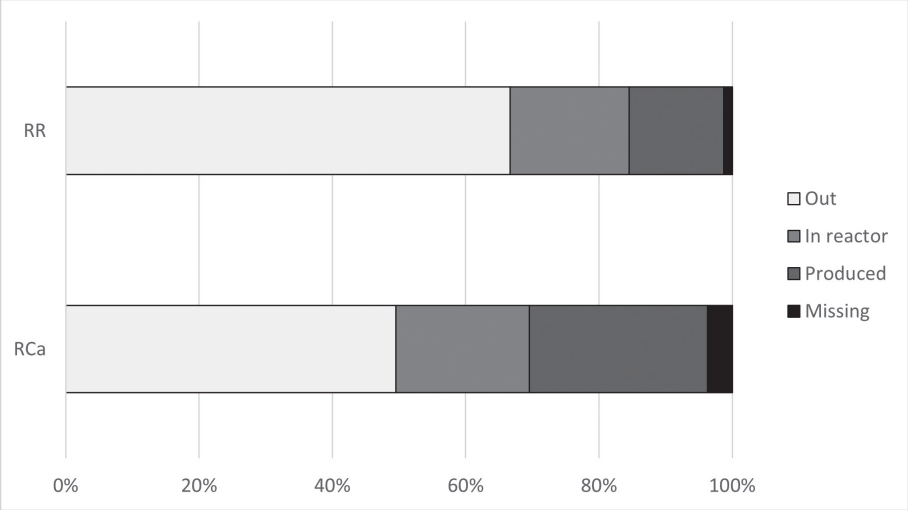

Fig. S3.15. Carbon balance over R_{Ca} (bottom) and R_R (top) based on grams carbon entering the reactor as measured TC and VSS, leaving the reactor based on TC and VSS, in the reactor based on TC and VSS and measured calcium assuming bound to calcite based on XRD and SEM measurements, and produced carbon as measured CO_2 and CH_4

C. Appendix Chapter 4

a. Solubilization of elements during acidification

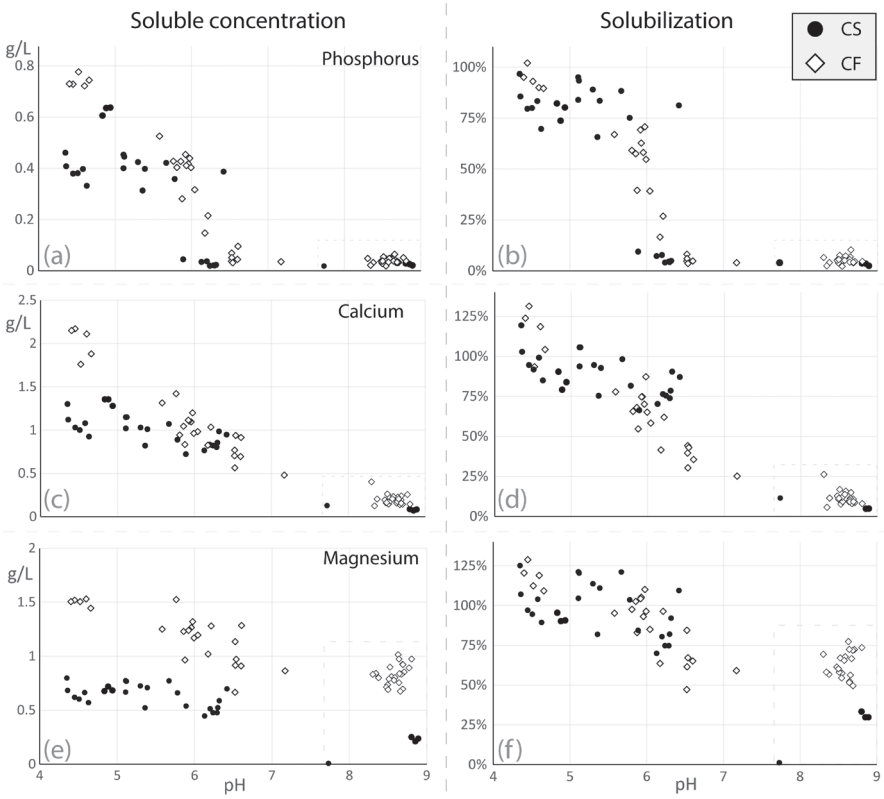

Fig. S4.1. The soluble concentrations (left side) and solubilization (right side) of phosphorus (a and b), calcium (c and d) and magnesium (e and f) of acidified manure and the influent (above pH 7.5).

b. SEM-EDX

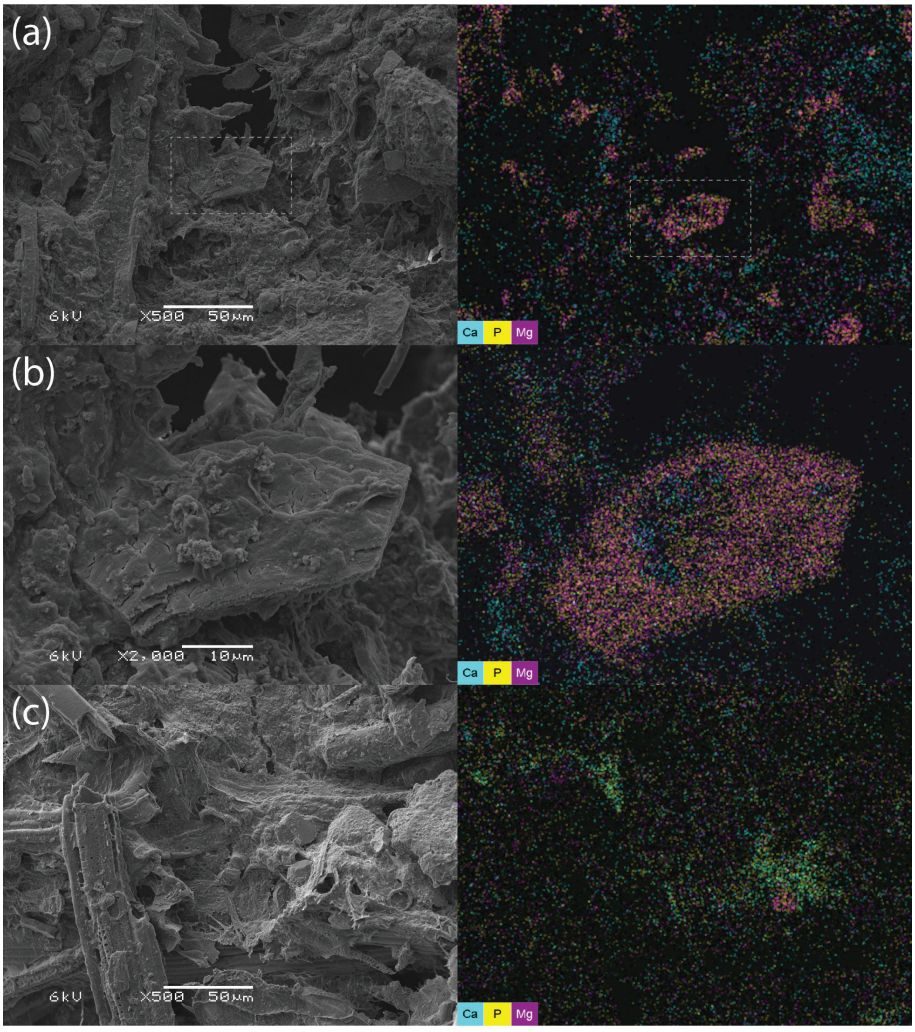

Fig. S4.2. SEM EDX images of (a) untreated cow feces, (b) a zoom in on a struvite crystal in cow feces with calcium carbonate on the surface of the struvite crystal and (c) acidified cow feces with less struvite crystals and some calcium phosphate. Note that the overlap of calcium (cyan) and phosphorus (yellow) appears as green and the overlap of magnesium (purple) and phosphorus (yellow) appears as orange.

c. XRD

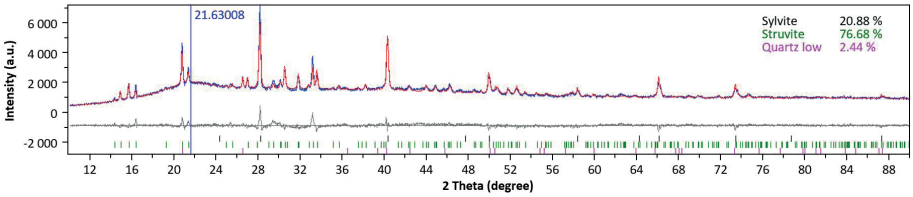

Fig. S4.3. XRD measurement of centrifuged cow feces solids.

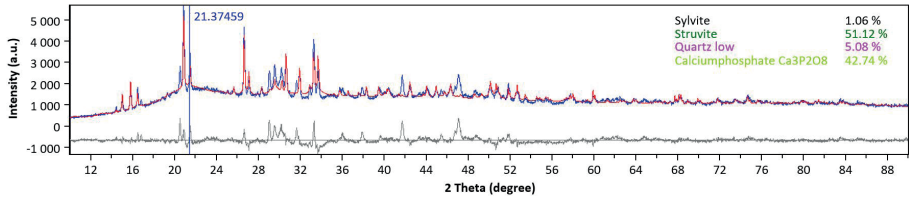

Fig. S4.4. XRD measurement of particles < 0.4 mm in diameter from tap 0 on day 34.

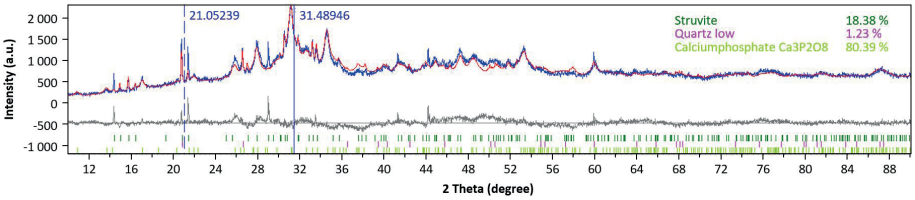

Fig. S4.5. XRD measurement of particles > 2.5 mm in diameter from tap 0 on day 34.

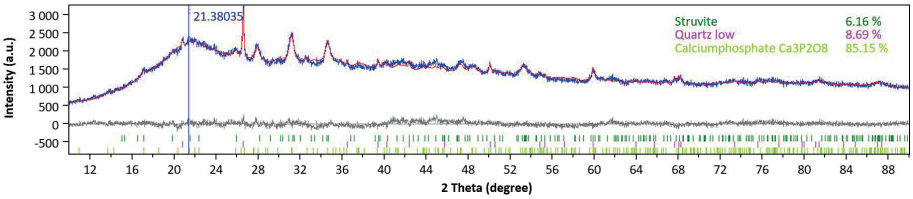

Fig. S4.6. XRD measurement of particles < 0.4 mm in diameter from tap 0 on day 181.

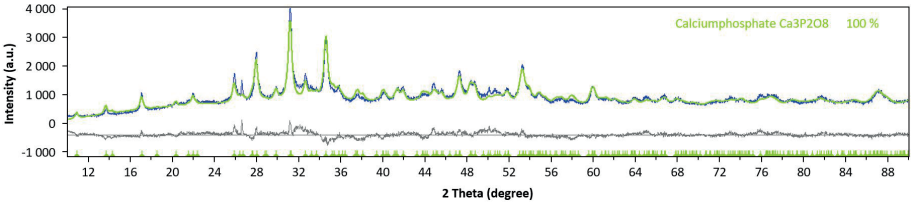

Fig. S4.7. XRD measurement of particles > 2.5 mm in diameter from tap 0 on day 181.

Table S4.1. Crystallinity percentage of samples analyzed with EVA

	% crystallinity - EVA
Cow feces solids	21%
Particles < 0.4 mm d34	23%
Particles > 2.5 mm d34	26%
Particles < 0.4 mm d181	13%
Particles > 2.5 mm d181	34%

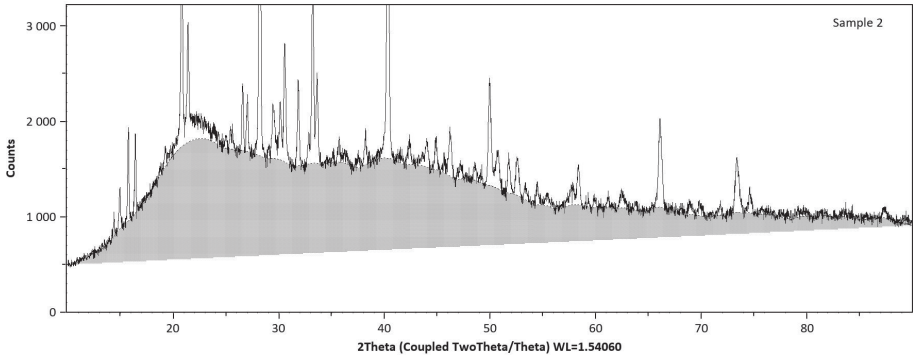

Fig. S4.8. Crystallinity calculation with EVA of centrifuged cow feces solids.

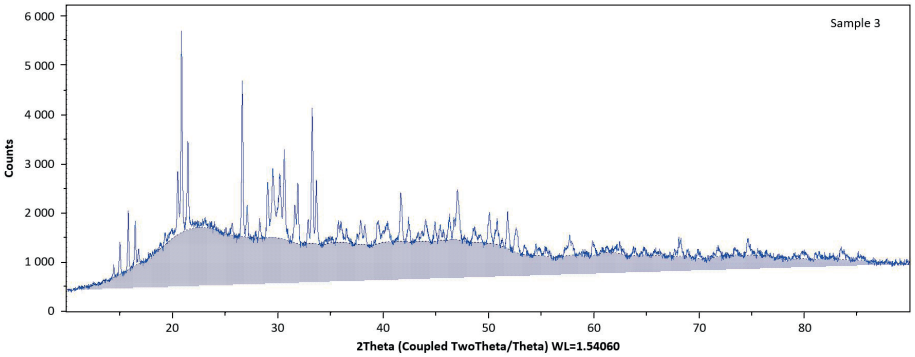

Fig. S4.9. Crystallinity calculation with EVA of particles < 0.4 mm in diameter from tap 0 on day 34.

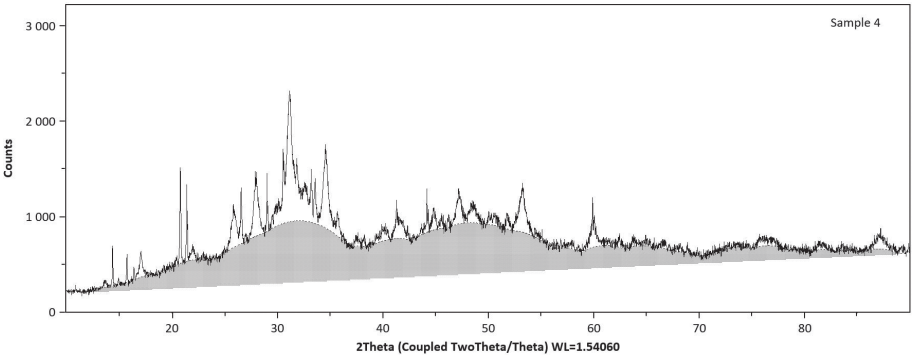

Fig. S4.10. Crystallinity calculation with EVA of particles > 2.5 mm in diameter from tap 0 on day 34.

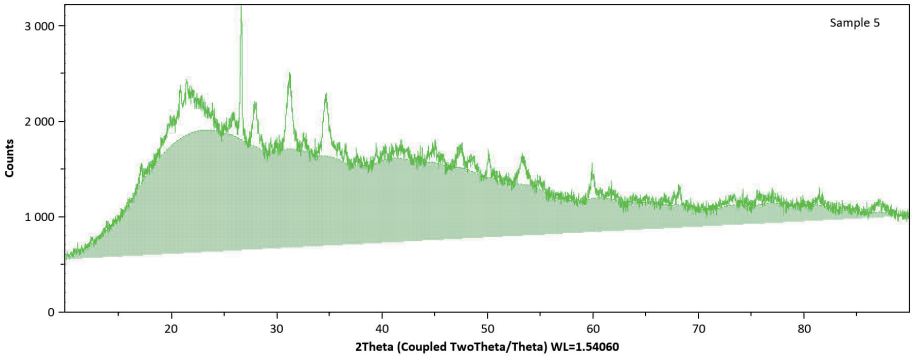

Fig. S4.11. Crystallinity calculation with EVA of particles < 0.4 mm in diameter from tap 0 on day 181.

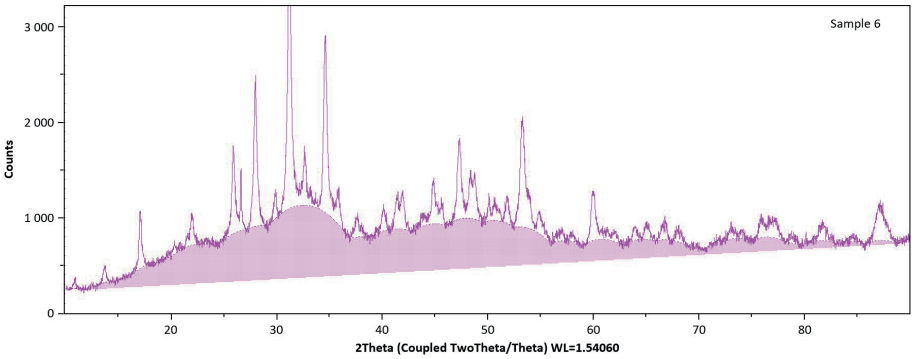

Fig. S4.12. Crystallinity calculation with EVA of particles > 2.5 mm in diameter from tap 0 on day 181.

D. Appendix Chapter 5

a. XRD

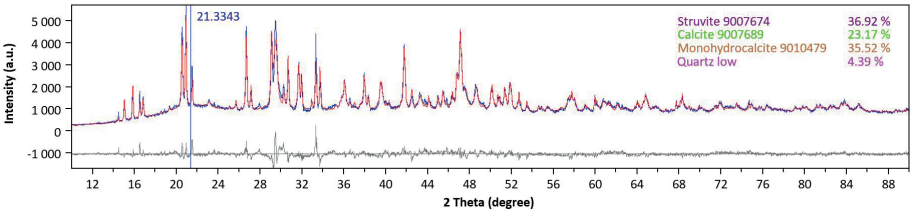

Fig. S5.1. XRD spectra of particles smaller than 0.4 mm from the bottom of R_{N2}.

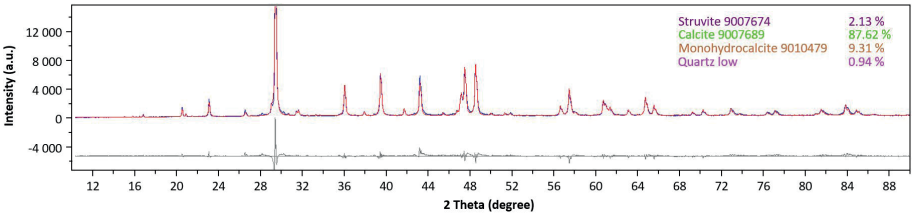

Fig. S5.2. XRD spectra of particles larger than 2.5 mm from the bottom of R_{N2}.

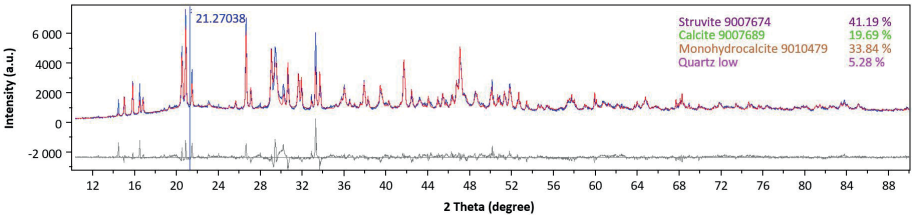

Fig. S5.3. XRD spectra of particles smaller than 0.4 mm from the bottom of R_{H2}.

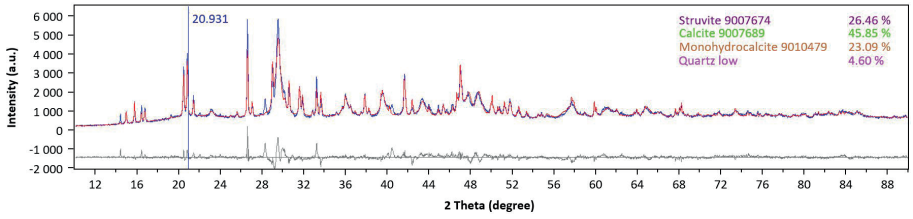

Fig. S5.4. XRD spectra of particles larger than 2.5 mm from the bottom of R_{H2}.

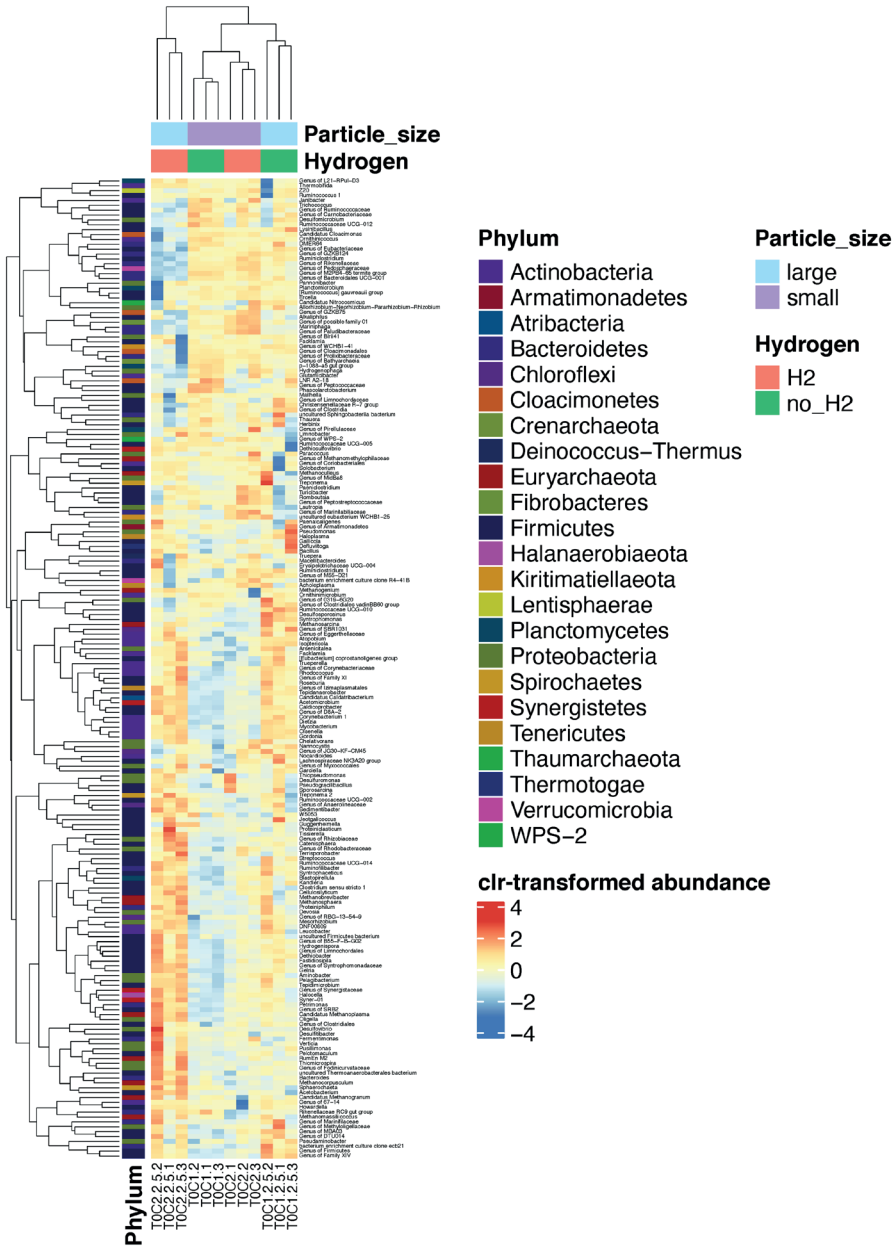

Fig. S5.5. Heatmap of microbial community analysis showing the relative microbial abundance in particles smaller than 0.4 mm and larger than 2.5 mm in R_{N2} and R_{H2}. This heatmap was used for making Fig. 5.5.

E. Appendix PHREEQC

Please find the PHREEQC scripts at DOI: 10.5281/zenodo.7867506.

List of Publications

Publications

In this thesis:

C. Schott, J.R. Cunha, R.D. van der Weijden, C. Buisman, **Phosphorus recovery from pig manure: Dissolution of struvite and formation of calcium phosphate granules during anaerobic digestion with calcium addition**, Chemical Engineering Journal (2022) 135406. DOI: 10.1016/j.cej.2022.135406.

C. Schott, J.R. Cunha, R.D. van der Weijden, C. Buisman, **Innovation in valorization of cow manure: Higher hydrolysis, methane production and increased phosphorus retention using UASB technology**, Chemical Engineering Journal (2022) 140294. DOI: 10.1016/j.cej.2022.140294.

C. Schott, L. Yan, U. Gimbutyte, J.R. Cunha, R.D. van der Weijden, C. Buisman, **Enabling efficient phosphorus recovery from cow manure: Liberation of phosphorus through acidification and recovery of phosphorus as calcium phosphate granules**, Chemical Engineering Journal 460 (2023) 141695. DOI: 10.1016/j.cej.2023.141695.

Beyond this thesis:

J.R. Cunha, C. Schott, R.D. van der Weijden, L.H. Leal, G. Zeeman, C. Buisman, **Calcium addition to increase the production of phosphate granules in anaerobic treatment of black water**, Water Research 130 (2018) 333-342. https://doi.org/10.1016/j.watres.2017.12.012.

J.R. Cunha, C. Schott, R.D. van der Weijden, L.H. Leal, G. Zeeman, C. Buisman, **Recovery of calcium phosphate granules from black water using a hybrid upflow anaerobic sludge bed and gas-lift reactor**, Environmental Research 178 (2019) 108671. https://doi.org/10.1016/j.envres.2019.108671.

J.R. Cunha, C. Schott, R.D. van der Weijden, L.H. Leal, G. Zeeman, C. Buisman, **Calcium phosphate granules recovered from black water treatment: A sustainable substitute for mined phosphorus in soil fertilization**, Resources, Conservation and Recycling 158 (2020) 104791. https://doi.org/10.1016/j.resconrec.2020.104791.

S. Georg, C. Schott, J.R. Capitao, T. Sleutels, P. Kuntke, A. ter Heijne, C. Buisman, **Bio-electrochemical degradability of prospective wastewaters to determine their ammonium recovery potential**, Sustainable Energy Technologies and Assessments 47 (2021) 101423, https://doi.org/10.1016/j.seta.2021.101423

G. Macedo, C. Schott, Y. van der Zee, L. Hernandez-Leal, P. van der Maas, H. Schmitt, **Thermophilic anaerobic digestion of cattle and swine manure removed Escherichia coli, but not sulfitereducing Clostridia or antimicrobial resistance genes**, Chapter in doctoral thesis (2021), https://doi.org/10.33540/860

T. Prot and C. Schott, E. Fleury, A.I. Dugulan, R. Hendrikx, R.D. van der Weijden, J.R. Cunha, L. Korving, C. Buisman, M.C.M van Loosdrecht, **Formation of vivianite in iron-amended pig manure and its subsequent magnetic recovery**, Chapter in doctoral thesis (2021), https://doi.org/10.4233/uuid:3d31068b-259a-4798-8723-be755cc15d23

Patent

C. Schott, R.D. van der Weijden, J.R. Cunha, C. Buisman, **Method, system and stable for phosphate recovery from a waste stream**, NL 2024746, 2021, WO/2021/150112, 2021 and 20230059525, 2023

Acknowledgments

Looking back at four years full of manure and amazing people. My journey at Wetsus and in Leeuwarden started even earlier and many people contributed with chats, science, sports, humor and many laughs to make it a great time. I want to thank everybody for their active, passive, intentional and unintentional contributions to my experience.

Thank you to my supervisor team, Ricardo, Renata and Cees! You had a lot of trust in me and supported me in shaping my ideas and research skills. Ricardo, you were my first contact at Wetsus when finishing my bachelor studies and we clicked immediately. Working and doing research with you throughout the years felt like solving puzzles with a friend. Our shared curiosity for technology and science paired with our competitive spirit made it a great experience working and spending time together. Renata, your level of understanding and depth in science made working with you a humbling experience for me. I could only get a glimpse at your knowledge, and it inspired me to go back to the fundamentals and strengthen my knowledge. I also very much appreciated our talks about current events and politics and your trust in our capability to have impact with our research. Cees, I admire your sharpness and ability to get to the essence of a point in technology, science and life. This combined with your vision on the bigger picture motivated and keeps on motivating me. I am very happy that I could and can continue learning from and working with you. Your genuine will to do good is contagious and inspiring to me.

Thank you to my students, Ao, Nike, Alon, Aisha, Ambra, Marrit, Ugne, Jiahui, Ana, Garry, Gautier, Liwen, Yixin, Rok and Steven! We brought cubic meters of manure to Wetsus and treated it. I had lots of fun working with you all and learned a lot from it. Thank you for your determination and all the laughter during the hours of sampling, analyzing and lots of cleaning. I really enjoyed the time we spent together. I hope we all get to meet again!

Thank you to the analytical team, Jelmer, Mieke, Marianne, Jan Willem and Lisette. You knew my samples by heart and endured the countryside fragrances I brought to the lab. Pieter, Cristina and Aga, thank you for going through the microbial community analyses with me. Thank you to the technical team, Wim, Jan, JJ, Harm, Wiebe, Johan and Ernst. You helped me with many technical difficulties and helped me implement and improving all my ideas. Ernst and Jan, you helped me through

the messiest and dirtiest experiences of my Ph.D. (and probably life). Thanks a lot!

Thank you to the soil theme for all the nice discussions and the insights into agriculture. Your practical perspectives and details led to more tangible research and gave clear purpose. In that regard, special thanks to Sietze and Karst from Oosterhof Holman. You introduced me to Fryslân and Friesian outside Wetsus, local agriculture and endless amounts of coffee. Valentina, thank you for your pragmatic input and making me keep the goal in sight. I appreciate you sharing your perspective with me and making me reflect. Yujia and Vania, soil power! Lourens, Marija and Mithat good luck!

Thank you to Johannes, Cees, Jan and Bert for steering Wetsus. Bert, your input to research in all disciplines seems effortless and I appreciate your help with my project. Thanks to the team keeping Wetsus up and running in the secretary office, HR, finances and the canteen. Roely and Jannie, thanks for organizing the many vaccinations. Nynke, Anke and Alexander, thank you for dealing with all the contracts and always finding a solution. Gerben, Catharina and Karin, thank you for all the excellent sandwiches, soups and chats.

Thank you to Wetsus Academy Lucia, Nelleke, Henk, Tom, Caroline and Miriam for all the things I learned, and I could teach later. Thanks to my own class and, especially, Qingdian, Paraschos, Gerhardus, Laurens, Nandini and Advait. Seriously looking forward to a reunion with all of you!

Thank you to my office mates Mariana, Paulina Steffen, Stan, Nimmy, Maarten, Karine, Talie, Alicia, Edward, Kevin, Jessica, Pamela and Marija for the chats, fun and dinners. Thank you to my new office Roel, Doekle, Michel, Olga and Maarten for welcoming me warmly, practicing Dutch with me and many inspiring talks.

Thank you to the football, ping pong, squash and volleyball players, board game players, party animals, travelers and more! In that regard, thanks to Martin "Keule" Futterlieb, Jaap, Filipe, Cesar, Felipe, Hector, Aziz, João, Sara, Amanda, Carlos and Jan dG. Louis, with you the ping pong competition in Wetsus was at its best. Mirvahid, I hope we get to play more ping pong. Mu, Aurora hunting with you is great and padel too. Maarten, thank you for all the board games, the excellent rule explanations and wanting to play Root. Gonçalo, Dr. Jekyll and Mr. Hide, thanks for "boosting" our spirits and calmly explaining microbiology to me the next moment.

Alex and Vinise, great to get to know you. Looking forward to more. Angel, thanks for the cinema visits, football, stand up comedy and more. Also, thanks for your gesture at Markies. Carlo, thanks for your determination and endurance. I hope our next project goes through and with less pain for you. Rebeca, I am happy you are coming back. Wokke, thanks for speaking the cutest German to me. Ruizhe, you are one of a kind. Thank you for being a good friend and spending many hours talking, talking, and talking. I hope to visit you in Switzerland soon! Qingdian, masters, Ph.D., what are we going to do next? Thanks for the many talks, dinners, games and so much more and sorry for the CO_2 pollution in the lab. I am glad we can defend and celebrate together.

Thank you to my paranymphs Ragne and Thomas. Thomas, we met on my first day at Wetsus and soon became flat mates. I have many good memories of game nights, parties and much more with you. Thank you for welcoming me twice to Alsace and for importing and introducing me to the most terrible smells. It made my Ph.D. easier. I hope for much more to come! Ragne, you are the funniest person I know. Your humor makes my German soul jump. You were and are a huge support to me. Thank you for collecting manure with me, introducing me to drinking tea and liking my pancakes. At this point, you seem to start liking anything I produce in the kitchen.

Vielen Dank an meine Familie! Ich kann mich immer auf euch verlassen. Ihr habt mir alles mitgegeben um eine Doktorarbeit und noch viel mehr zu bewerkstelligen.

About the Author

Chris Schott was born in Kusel in the southwest of Germany. He went to school in Osnabrück in the northwest of Germany, where he focused on physical sciences. While visting a job fair for high school graduates, the expertise of Dutch universities in water technology sparked his interest. After visiting an open day in Enschede, his choice was clear to study chemical engineering with a focus on water technology in the Netherlands. His internships at MPS Aqua (Today Marel) and Wetsus made him wanting to continue studying water technology. His masters' studies for a joint degree in water technology at Wageningen University, Twente University, and Groningen University got him enthusiastic about novel and sustainable resource recovery technologies. This led to the Ph.D. studies resulting in this thesis.

Chris currently continues researching and implementing the findings from this thesis with Wetsus and Oosterhof Holman. His goal is to close nutrient loops and recover energy from animal manure and human excreta, reducing the use of natural resources and increasing the reusability of secondary resources.

Netherlands Research School for the
Socio-Economic and Natural Sciences of the Environment

D I P L O M A

for specialised PhD training

The Netherlands research school for the
Socio-Economic and Natural Sciences of the Environment
(SENSE) declares that

Christopher Schott

born on 19 September 1993 in Ruthweiler, Germany

has successfully fulfilled all requirements of the
educational PhD programme of SENSE.

Wageningen, 2 June 2023

Chair of the SENSE board

Prof. dr. Martin Wassen

The SENSE Director

Prof. Philipp Pattberg

The SENSE Research School has been accredited by the Royal Netherlands Academy of Arts and Sciences (KNAW)

KONINKLIJKE NEDERLANDSE
AKADEMIE VAN WETENSCHAPPEN

The SENSE Research School declares that **Christopher Schott** has successfully fulfilled all requirements of the educational PhD programme of SENSE with a work load of 34.5 EC, including the following activities:

SENSE PhD Courses

- Environmental research in context (2018)
- Research in context activity: 'A2 - Organizing science communication event' (2019)

Other PhD and Advanced MSc Courses

- Bridging across cultural differences, Wageningen Graduate Schools (2018)
- Talents course & Presentation course, Wetsus (2019)
- Communication Styles, How Company (2019)
- Crystallisation Science and Engineering, University of Leeds (2019)
- Scientific Writing, Wageningen Graduate Schools (2020)
- Pre-treatment Workshop, University of Michigan (2022)
- Better BMP: How to Accurately Measure Biochemical Methane Potential, University of Michigan (2022)
- Career Perspectives, Wageningen Graduate Schools (2022)

Impact activities

- WaterCampus Business Development Course (2021)
- European water campus business challenge (2022)

Management and Didactic Skills Training

- Organizing a stakeholder meeting - Boeren bijeenkomst (2022)
- Supervising eight MSc students with and 6 BSc students with thesis (2019–2022)
- Teaching in the MSc course 'Biological Wastewater Treatment" of Water technology' (2019–2022)

Oral Presentations

- *Phosphorus recovery from dung.* Wetsus - European water technology week (EWTW), 09–10 October 2018, Leeuwarden, Netherlands
- *Circular use of phosphorus From cow and pig manure enabled by a single anaerobic bioreactor.* Wetsus congress, 07–08 October 2019, Leeuwarden, Netherlands
- *Calcium phosphate granulation from pig manure: Simultaneous nutrient recovery and anaerobic digestion*. IWA 17th Anaerobic digestion conference- University of Michigan, 19–22 June2022, Ann Arbor, Michigan, USA
- *Thermophilic anaerobic digestion (TAD) of black water.* IWA 17th Anaerobic digestion conference, University of Michigan, 19–22 June 2022, Ann Arbor, Michigan, USA

SENSE coordinator PhD education

Dr. ir. Peter Vermeulen

This work was performed in the cooperation framework of Wetsus, *European Centre of Excellence for Sustainable Water Technology*. Wetsus is co-funded by the Dutch Ministry of Economic Affairs and Ministry of Infrastructure and Environment, the Province of Fryslân, and the Northern Netherlands Provinces (www.wetsus.eu). The author would like to thank Oosterhof Holman for insights into the practical application and all the members of the research theme "Soil" for financial support and fruitful discussion.

Financial support from Wageningen University and Wetsus for printing this thesis is gratefully acknowledged.

About the cover: Agriculture evolved from manual work with small yields to the Green Revolution with artificial fertilizers and big yields, but with resource waste and pollution. The future is focused on circular agriculture and technology to reduce waste while maintaining productivity.

Layout: Publiss | www.publiss.nl
Cover design: Publiss | www.publiss.nl
Printed by: Ridderprint | www.ridderprint.nl


P
P
P